Methods for the Characterisation of Hybrid Energy Storage System for Independently Powered Trains

Dena Servatian

A thesis submitted to

the University of Birmingham

for the degree of

DOCTOR OF PHILOSOPHY

Department of Electronic, Electrical and Systems Engineering

College of Engineering and Physical Sciences

University of Birmingham, UK

March 2020

Abstract

The UK has set a new target for reducing carbon emissions by 57% by 2030 and 80% by 2050 compared to the carbon emission level in 1990. In the UK, transport contributes to a quarter of the overall carbon emissions. Although the railway is considered one of the most environmentally-friendly modes of mechanised transport, it should be ensured that the railway sector plays its role in this new target and that its share of carbon emissions is reduced. Currently, about 29% of the UK's fleet is diesel-only, and phasing out these types of trains by 2040 is part of the Carbon Emission Reduction plan. In order to reach this goal, either railway lines should be electrified or on-board energy storage systems should be installed above the trains. While electrification appears to be an efficient and clean method, it is time-consuming and initial costs are high. Installing on-board Energy Storage Systems (ESSs) including batteries, supercapacitors or fuel cells is a zero-emission and cost-effective approach to phasing out the remaining diesel trains in the UK and, consequently, contributing to the Carbon Emission Reduction plan. This thesis aims to propose an on-board ESS for independently powered trains where the ESS supplies all the energy required for the train traction.

This thesis begins with a review on the previous researches on Hybrid Energy Storage Systems (HESSs) including batteries and supercapacitors in power applications and specifically in the railway sector. It reviews the reasons for employing an HESS and the sizing methods. Following this, the gap in sizing and charging an HESS for an independently-powered train is discussed and the hypothesis is developed.

The first phase of this thesis analyses the use of batteries and supercapacitors together in an HESS in order to evaluate the efficiency of integrating these two energy storage devices in

Abstract

terms of the weight and volume of the HESS. Various scenarios with different configuration of batteries and supercapacitors are considered to provide the required energy and power demand in the traction. Hence, the total size of the HESSs and performance of the sized HESSs in all scenarios are compared. Furthermore, it considers the influence of the energy density and power density of the battery and supercapacitor on the total size of the HESS. This phase also evaluates the effect of the C-rate of the battery on the total size of the HESS as well on the performance of the battery.

In the second phase of this thesis, an HESS including batteries and supercapacitors is sized optimally by employing the Frequency Analysis method. The objective function of the optimisation is to minimise the weight and volume of the HESS based on the power profile, where decreasing the weight of the on-board HESS decreases the mass of the train and consequently, the energy consumption. Low-pass and high-pass filters with optimal cut-off frequencies (achieved by Brute Force optimisation) are employed to split the journey into the low frequency and high frequency parts of the load so that batteries are in charge of supplying the low-frequency parts and supercapacitors can provide power to the high-frequency parts. Furthermore, this phase proposes the use of batteries to act as the energy supply and charge supercapacitors during the journey in order to meet the energy and power demand.

The two phases are applied to two case studies in order to validate the results. The first case study is a diesel line from Bidston Station to Shotton Station in Liverpool where the on-board HESS can be installed above the Electrical Multiple Unit (EMU) running on this line to provide the energy required for the return journey. The second one is a tram line in Edinburgh where the installed on-board HESS could be a substitute for overhead electrification. These journeys

Abstract

are simulated in Single Train Simulator (STS) in MATLAB in order to achieve some precious data such as energy consumption and peak power requirement.

The key findings of this thesis are that the integration of batteries and supercapacitors in an HESS is an efficient choice for independently powered trains the HESS can be optimally sized using Frequency Analysis method and supercapacitors can be charged by batteries during the journey.

Acknowledgement

I would like to express my sincere gratitude to my supervisors, Prof. Clive Roberts and Dr. Stuart Hillmansen, for their precious guidance and encouragement during my PhD studies. Their enthusiasm in carrying out research and their care for students inspired me to pursue my research in this team and their extensive knowledge in my educational life alongside their care and support in my personal life helped me to carry out research with ease of mind.

I am extremely thankful to Dr. Rob Ellis and Dr. Ning Zhao who consistently offered me their invaluable know-how and appreciable guidance as well as their great inspiration. I am also grateful to Dr. Zhongbei Tian and Dr. Mani Entezami for sharing their worthy experience and advice to support me during my research studies. Furthermore, I would like to thank all staff and student members of Birmingham Centre for Railway Research and Education (BCRRE) for their kind help.

Finally, I would like to give my appreciation to my family and friends for their constant support and patience. Especially, I would like to thank my beloved parents who supported me from thousands of kilometres away and gave me love and encouragement every day.

Table of Contents

Table of Contents

Table of Contents

Table of Contents

List of Figures

List of Figures

List of Figures

List of Figures

List of Figures

List of Figures

List of Figures

List of Figures

List of Tables

List of Tables

List of Acronyms

Term	Explanation / Meaning / Definition
EDLC	Electric Double Layer Capacitor
EMU	Electrical Multiple Unit
ESS	Energy Storage System
EV	Electric Vehicle
FFT	Fast Fourier Transform
GA	Genetic Algorithm
HESS	Hybrid Energy Storage System
Li-ion	Lithium-ion
Li-poly	Lithium-polymer
LTO	Lithium Titanate
MTS	Multi Train Simulator
NbTi	Niobium Titanium
OLE	Overhead Line Equipment
PSO	Particle Swarm Optimisation
PV	Photovoltaic
RES	Renewable Energy Resource
SC	Supercapacitor
SCADA	Supervisory Control and data Acquisition
SMES	Superconducting Magnetic Energy Storage
SoC	State of Charge
STEC	Simulation of Train Energy Consumption
STS	Single Train Simulator
UC	Ultracapacitor

Chapter 1
Introduction

1.1. Background

In recent decades, sustainable transportation has received a great deal of attention worldwide. The necessity to reduce CO_2 emissions form transport has led many countries to adopt different strategies and long-term plans; the EU supports the policy of cutting CO_2 emissions from transport [1]. In 2016, the share of transport in making CO_2 emissions in the EU was about 25% [2]. The EU has set an agreement to reduce CO_2 emissions from transport by 30%, compared to the 1990 base year, by 2030 [1], [3]. Although the railway has a share of over 8.5% of transport, it contributes less than 1.5% to the total transport CO_2 emissions and, compared to other modes of transport, the railway is already recognised as a low-producing sector for CO_2 emissions [3], [4]. However, the rail sector as a mode of transport can play a key role in reducing environmental impacts and should be able to demonstrate that it can contribute to the global move to cut transport emissions [4].

In the UK, as part of the decarbonisation strategy in the rail sector, diesel trains are going to be phased out by 2040. Currently about 29% of the trains in the UK are diesel-only and this leads to a significant amount of CO_2 emissions [5]. For a full-scale phase-out, one solution could be electrification. Electrifying railway lines began in the late 1800s in the UK and the early 1900s worldwide, and it became popular as a friendly mode of transport due to advantages such as high efficiency, low air pollution and heavy load and mass transit capabilities [6], [7]. However, electrifying the whole network is time-consuming and initial costs are very high [8]. Moreover,

although it appears that an electrified railway is a 100% CO_2 emission-free mode of transport, but still a part of the electricity used in the electrified network is generated by fossil fuels [9].

An alternative solution for phasing out diesel-only trains could be installing an on-board Energy Storage System (ESS) on trains, making them independently powered [8]. An on-board ESS could be capable of providing all the energy required for traction so that no additional diesel or electricity is required. These independently powered trains are able to run on both diesel and electrified lines, where the ESS on the train can be charged by braking energy or overhead wires while running on an electrified rail, or it can be charged at stations by different energy resources and then use the saved energy when it runs on diesel rails [10]. Compared to electrification, independently powered trains have lower carbon-emissions (from generating electricity to charging ESS and then moving the train) which is a significant advantage contributing to the eco-friendliness of the rail industry. Furthermore, these newly innovated trains can be more economical than electrification [11].

Since the early 21st century, rail companies have started introducing ESSs and Hybrid Energy Storage Systems (HESS) for light rail vehicles in order to contribute to the power supply. These ESSs/HESSs include battery, supercapacitor, flywheel or a combination of these energy storage devices and have been able to provide power for catenary-free parts of the routes where electrification was not either economical or safe [12], [13], [14], [15], [16], [17], [18], [19], [20]. The first battery-powered tram in the UK was opened to the public in 2017 in Birmingham [17], [21]. In recent years, rail companies have started working on prototypes with on-board ESSs/HESSs which are able to provide the power required for the whole journey. These ESSs/HESSs can fully replace the overhead electrification system and are able to overhaul current light rail power systems. In the UK, the first and only modern battery-powered train in the railway network began its first trial passenger service in January 2015 as part of a research

project carried out by NetworkRail in partnership with Bombardier, Abellio Greater Anglia, FutureRailway and the Department for Transport. This trial was carried out on a 25 kV/50 Hz electrified line in Essex on the Manningtree–Harwich branch [10], [11], [22].

From the literature, it can be seen that integrating the battery and supercapacitor in an HESS in a rail system has become more popular recently, as an HESS allows for better performance and a more flexible system compared to a single energy storage device [19], [23], [24], [25], [26], [27], [28], [29], [30], [31], [32]. However, developing an HESS increases the complexity of the architecture and sizing an HESS is not straightforward [33], [34]. Hence, optimal sizing is one of the most significant parts of developing an HESS. Sizing the HESS optimally, which can be executed by utilising various methods, reduces costs, decreases weight and volume, reduces energy consumption, increases the lifespan of the devices and improves efficiency [27], [35], [36], [37], [38], [39], [40]. Regarding charging the HESS, researchers have proposed methods such as charging via overhead lines, in charging stations, substations or passenger stations, charging by regenerative braking energy or by emerging Wireless Power Transfer [18], [19] [24], [27], [28], [29], [41], [42].

This thesis aims to introduce a novel approach to sizing an HESS including batteries and supercapacitors for rail vehicles where the HESS is in charge of supplying the energy required for the whole journey. Moreover, this thesis proposes an innovative method to make batteries play as the main energy supply in order to charge supercapacitors. The methods considered contribute significantly to a decrease in CO_2 emissions, energy consumption and cost.

1.2. Objectives

In order to reach the abovementioned goals, the following objectives need to be addressed:

- A review of the literature on previous sizing and charging methods is required. Previous studies have to be assessed and compared; after analysing the literature, a clear and detailed research plan can be identified.
- It is essential to model train movement and traction power supply in order to understand railway system requirements. Simulation software needs to be employed in order that various parameters of the traction such as energy consumption, peak power requirement, journey time, etc. can be identified.
- Utilising batteries and supercapacitors together in an HESS should be evaluated. It is crucial to observe the effectiveness of integrating these two energy storage devices and to validate the advantages of this combination over single ESSs.
- Different optimisation methods should be discussed and evaluated for the proposed strategies. Optimum-decision approaches contribute to decreased energy consumption and costs.
- Applications have to be considered to apply the methodologies on. Theoretical studies based on simulations show proper and efficient results, but it is crucial to apply methodologies into real-world applications to validate the results obtained and demonstrate the feasibility of the proposed strategies.

1.3. Thesis Structure

This thesis will address the facets presented below for the sake of railway system optimisation regarding CO2 emissions, energy consumption and cost.

Chapter 1 presents the background of the current situation in railway networks. The principal research purpose of this thesis is developed in this chapter, which is optimising the railway

system in terms of CO_2 emissions, energy consumption and cost by optimal sizing of an HESS and optimal charging approaches.

Chapter 2 reviews the literature on HESSs for railway system. After a brief review of train movement, traction power supplies and traction drives, ESSs/HESSs, different sizing methods and existing approaches to charging ESSs/HESSs are identified in this chapter. The methods are analysed and after discovering the gap, the hypothesis of this thesis is developed.

Chapter 3 discusses the methodologies employed in this thesis in order to reach the objectives. First, it is shown how the train movement is simulated. Following this, the integration of batteries and supercapacitors in an HESS is evaluated. Then, the optimal sizing and charging methods are presented.

Chapter 4 applies the methodologies to a real-world application. Evaluation, sizing and charging strategies are applied to a diesel train line; the data for the chosen case study are based on a diesel line in Liverpool. The results are validated in this chapter.

Chapter 5 proves the validation of the proposed strategies by demonstrating another case study. All considered methodologies (evaluation, sizing and charging methods) are applied to a suburban tram line; the data used are from a tram line in Edinburgh.

Chapter 6 discusses the results obtained from Chapter 4 and Chapter 5. The results obtained from evaluation of batteries and supercapacitors together in an HESS, optimal sizing of the HESS and, finally, getting batteries to charge supercapacitors in both case studies are discussed.

Chapter 7 summarises the conclusions and contributions of this thesis. The hypothesis is validated according to the results. Additionally, future work is also described.

Chapter 2
Literature Review

2.1. Introduction

In the last decade, employing ESSs/HESSs in railway networks has been popular within the railway industry. ESSs/HESSs have been introduced to rail systems to support in different aspects such as recovering regenerative braking energy, acting as a back-up for the energy source, providing the main energy supply, etc. [41], [42]. Research has indicated that compared to an ESS, using an HESS increases system performance and flexibility [19], [23], [24], [25], [26], [27], [28], [29], [30], [31]. Different energy storage devices have been used in HESSs in railway networks and various sizing methods have been introduced by researchers [24], [25], [26], [27], [35], [37], [38], [39], [40]. Charging the HESS is also of importance and researchers have discussed diverse energy suppliers to charge the energy storage devices in HESSs [18], [19], [24], [27], [28], [29], [41], [42].

This chapter first talks about railway traction power systems. Both DC and AC power supplies and traction drives are discussed. Following this, different types of ESSs as well as the energy storage devices commonly used in railway networks are presented. HESSs are then discussed and different sizing methods to size them are described. Moreover, previous researches which have used the mentioned sizing methods are reviewed. Finally, the gap in sizing and charging HESSs for railway systems is identified and the hypothesis is developed.

2.2. Fundamentals of Train Performance

Railway systems play a key role in both urban and suburban transportation networks. This is mostly because of this mode of transport's benefits of such as being more economical and producing less pollution and noise production compared to other modes. Railway vehicles are characterised by different parameters which determine the nature of the traction load and its performance [41], [43], [44], [45].

2.2.1. Train Performance

Energy supplied to a train is used to accelerate it in linear motion as well as rotating components (wheels or motor armatures) in rotary motion, in order to conquer both electrical and mechanical power losses. Friction resistance to motion or to do work in moving the mass of the train uphill can be considered as mechanical loss, and the loss from motors and drives can be considered as electrical loss. The amount of energy that a train uses is dependent on the type of railway network. In urban rail systems, spacing between stations is short and the energy most required is that needed to accelerate the train, whereas in high-speed railways, the energy consumed to overcome the resistance to motion between stations is the greatest. Figure 2.2.1 presents the forces on a train:

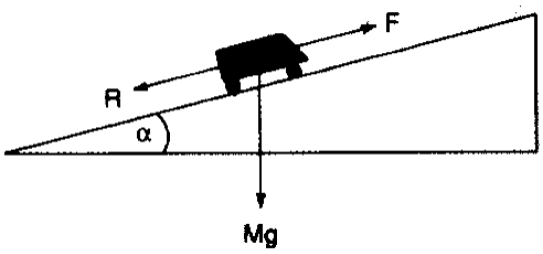

Figure 2.2.1. Forces on train, produced by R.J. Hill [46]

The equation of motion which can be used for train motion can be defined as:

$$M' \frac{d^2 s}{dt^2} + Mg \sin \alpha = F - R \tag{2.2.1}$$

Where M' is the effective mass including rotary allowance, s is the instant distance of the train, t is the dependent element time, M is the tare mass, g is the gravitational acceleration, α is the slope angle, F is the tractive force and R is the resistance [46], [47].

In order for the train to move, the torque of the motor needs to be transferred to the wheel/rail interface as tractive force. This force, which is called adhesion, is the friction force between the wheels and rail. The values of the adhesion force on each driven axle is:

$$F = \mu Mg \tag{2.2.2}$$

where μ is the friction coefficient between 0 and 1 and Mg represents the axle load.

R in the equation of motion is the resistance to motion and is the result of the internal forces (in the train) and the external forces (due to the interaction between vehicle and track). R can be expressed as:

$$R = (A + Bv)M + Cv^2 + Mg\alpha + \frac{DMg}{r} \tag{2.2.3}$$

A, B, C and D are coefficients. V is the velocity, M is the mass and r is the track radius [46], [48]. $(A + Bv)M$ indicates the internal rolling resistance and the vehicle–track interface resistance. The second term, Cv^2, is aerodynamic resistance and can be defined as normal pressure drag or surface friction. $Mg\alpha$ presents the alignment (track) resistance which is the sum of the gradient and curvature components. The last term, $\frac{DMg}{r}$, happens due to track curvature.

Returning to the equation of motion, it can be deduced that motor torque is capable of accelerating the train after overcoming the abovementioned resistances. Figure 2.2.2 indicates the characteristics that the most economical drive needs to have:

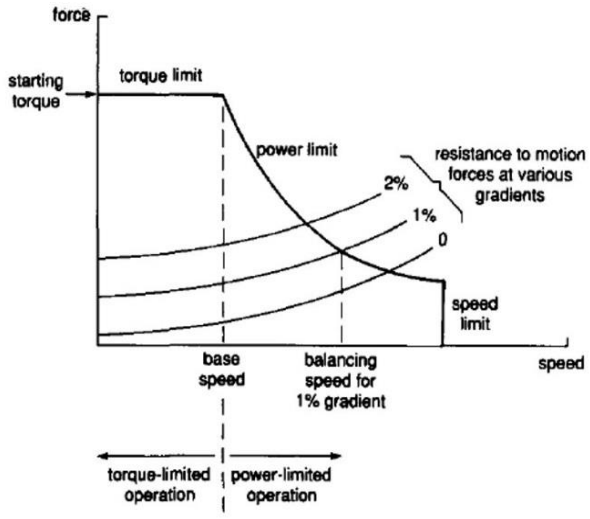

Figure 2.2.2. Traction force vs speed characteristics in traction, produced by R.J. Hill [46]

As seen in the Figure 2.2.2, initial torque is limited by traction motor current rating requirements. Therefore, the maximum tractive envelope, which is a function of speed, becomes consistent with constant power operation. A balancing speed can consequently be achieved should the maximum power be set by the controller and, at this point, tractive effort becomes equal to the sum of gradient forces and vehicle resistance. In balancing speed, acceleration is zero [46].

2.2.2. Train Movement

The entire journey of a train between two stations can be decomposed into four steps [49], [50]. The typical running behaviour of a train can be predicted according to some constraints, such as speed limitations or length and rolling stock characteristics [49]. This speed profile is indicated in Figure 2.2.3:

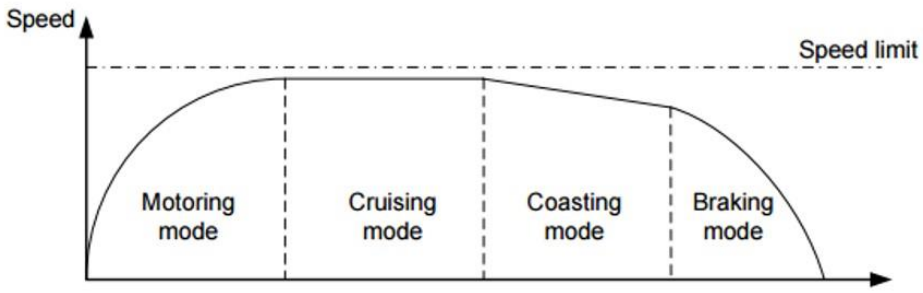

Figure 2.2.3. Speed profile of a train over a section between two stations, produced by Ning Zhao [51]

2.2.2.1. Acceleration

During acceleration, which is called motoring or powering too, power is applied to the train when climbing a hill in order to overcome the effects of gravity. Moreover, Power is used to conquer dynamic resistance in order to accelerate the train and obtain the required acceleration rate [52], [53].

In the acceleration mode, if F_{tr} is traction force, F_{grad} is gradient force on train movement and F_{resist} is resistance to train movement:

$$F_{grad} + F_{resist} < F_{tr} < F_{max} \tag{2.2.4}$$

If K_v is the coasting factor which equals $\frac{V_{c-min}}{V_{c-max}}$ (V_{c-min} and V_{c-max} are minimum and maximum coasting speed, respectively), traction force for this mode can be expressed as:

$$F_{tr} = K_v \times F_{max} \tag{2.2.5}$$

And the total force to move the train is:

$$F_{total} = F_{tr} - F_{grad} - F_{resist} \tag{2.2.6}$$

Train acceleration is a_{tr} and in acceleration mode is presented as:

$$a_{tr} = \frac{F_{total}}{m_{tr}} \tag{2.2.7}$$

where m_{tr} is the effective mass of the train. Effective mass of the train considers rotary allowance and is the train mass plus the mass of rotating wheels.

Train current is another parameter which is considered for different modes of train. In acceleration mode, this parameter is expressed as:

$$I_{tr} = I_{max} \times \frac{F_{tr}}{F_{max}} = I_{max} \times K_f \tag{2.2.8}$$

where K_f is the traction force factor.

Finally, electric power in acceleration can be obtained:

$$P_e = I_{tr} \times U_{tr} \tag{2.2.9}$$

where U_{tr} is the average voltage on the conductor shoe.

By integrating the electric power, energy consumption can be achieved [52].

2.2.2.2. Cruising

In cruising mode, there is no acceleration and the train moves with a constant speed [49], [53]. In this mode, both tractive force and acceleration are zero [51].

$$F_{total} = 0 \tag{2.2.10}$$

$$a_{tr} = \frac{F_{total}}{m_{tr}} = 0 \tag{2.2.11}$$

2.2.2.3.Coasting

Coasting mode is a phase during which no power is required and the train moves by the forces of dynamic resistance and the active component of gravity (inertia) [52]. Due to deceleration in coasting, speed decreases and energy can be saved as it does not depend on power [50], [52]. Should the coasting mode happen early in the journey, more energy can be saved. However, this results in an increase in the journey time [49].

Since the train does not need power in this mode and thus traction force (F_{tr}) is zero, total force in coasting mode can be expressed as:

$$F_{total} = -(F_{grad} + F_{resist}) \tag{2.2.12}$$

And the train acceleration is:

$$a_{tr} = \frac{F_{total}}{m_{tr}} \tag{2.2.13}$$

In coasting mode, train current is zero, which results in zero train power. Hence, no energy is consumed in this mode [46].

2.2.2.4. Braking

In braking mode, speed is reduced in order for the train to either meet the speed limits or stop at a station [52]. In this mode, resistance to the train's advance and the service braking force are combined [50], [53].

For braking, if K_{br} is the deceleration factor, the braking force will be:

$$F_{br} = K_{br} \times F_{br-max} \tag{2.2.14}$$

And total force can be achieved by:

$$F_{total} = -(F_{br} + F_{grad} + F_{resist}) \tag{2.2.15}$$

In this mode, train deceleration is expressed as:

$$a_{br} = \frac{F_{total}}{m_{tr}} \tag{2.2.16}$$

In braking, the train current is negative and can be presented as:

$$I_{tr} = -I_{max} \times \frac{F_{br}}{F_{max}} = -I_{max} \times K_{br} \tag{2.2.17}$$

Finally, the power can be obtained:

$$P_e = I_{tr} \times U_{tr} \tag{2.2.18}$$

In braking, because electric power is negative, energy can be produced if the motor is used as a generator [52].

2.2.3. Train Simulation

In different engineering disciplines, simulation is the definition of reconstruction and representation of reality in a virtual procedure. Railway Engineering is no exception as simulation plays a crucial role in railway networks and train operations. Simulation increases comprehension of the railway system environment as well as creating assumptions and predictions [54]. Furthermore, simulation contributes to more efficient performance analysis, as well as checking future timetables, avoiding disturbance , assessing interaction and consequently cost saving [55]. Various universities and institutions have developed methods

and software for simulating train behaviour. While developing simulation software and tools for railway networks, one the most remarkable objectives is to calculate/estimate the energy consumption of a train. In the early days, FORTRAN language was used in order to simulate train traction. Gradually, C++ replaced FORTRAN. Nowadays, most researches carried out to simulate railway networks and calculate train energy consumption are performed in applications such as MATLAB. In spite of the benefits and convenience of computer programs and software for simulating train behaviour, there are drawbacks to these methods such as non-portable executable files and computational inefficiency [56].

The Single Train Simulator (STS), developed by Dr Stuart Hillmansen at the University of Birmingham in the UK, is one the programs employed to simulate train traction. This software is able to assess the effects of different driving styles for various railway vehicles and is suitable for simulating a range of propulsion packages [57]. The Multi Train Simulator (MTS), which is the improved version of STS, was developed using object-oriented methods and modular structure design. This program can provide single train simulation, multi-train traction calculation and timetable analysis [58].

Simulation of Train Energy Consumption (STEC) is another railway simulator, which was developed by Johan Öberg (MiW Konsult AB) for the Royal Institute of Technology in Sweden (KTH). The essential objective of this software, which is Microsoft Excel-based, is to calculate the energy consumption and running times when both vehicle and route are defined with different parameters. Flexibility and a practical interface are two key advantages of this software [59]. OpenTrack is another train simulation program which was started as a research project at the Swiss Federal Institute of Technology. This simulator is object-oriented and the most significant advantage of this program is its ability to offer interfaces to general data formats (ASCII and XML) as well railway-specific formats (PROTIN and FBS) [60]. The

Railway Total Simulator, developed by Hitachi, has the capability to predict train energy consumption and traffic volumes. This program allows a wide range of simulations to be carried out by dividing the whole railway system into subsystems. These subsystems include rolling stock, traffic control system, signalling system and supply system [61].

All the above-mentioned simulators have different advantages and can be employed for different railway applications. However, STS is amongst the most popular simulators for simulating train behaviour as it is user-friendly, simple and flexible; moreover, it uses MATLAB to run. This program takes the data of the route (gradient, speed limits, driving styles, distance between stations) and of the vehicle running on the route (physical, mechanical and electrical properties) and sends this information to the simulator. Various outputs are acquired after simulation, such as total energy consumption, total journey time and peak power demands during the journey [57].

2.3. Railway Traction Power Systems

In an electrical railway network, power is transmitted from the power supply to the electric vehicle through conductor systems. Based on the application and the required features, the power is transmitted in AC or DC and is converted to be used in an AC or DC traction drive [62], [63].

2.3.1. Power Supply

In general, in modern railway systems, urban lines and high-speed railways mostly use AC power supplies. There are several reasons for this; for instance, higher voltages can be transmitted in AC which reduces transmission loss for long distances. Moreover, AC systems

have higher efficiency. DC power supplies are usually employed for suburban and light railways due to their lower voltage, less prone to failure and less electromagnetic interference, which all decrease risks to public in suburban areas [64].

2.3.1.1. DC Power Supplies

Depending on the size and demand of the railway network, the electrical supply which is fed to the railway network is normally 132, 66 or 33kV. The electricity is then stepped down by transformers to a medium voltage of 33, 22 or 11kV. This medium voltage feeds the whole railway network and is transferred to the substations. In each DC traction substation, there are transformers and rectifiers to convert 11kV AC to 600, 750, 1500 or 3000V DC. Regarding economics, the substation positions depend on the voltage: a higher voltage requires a greater distance. It is suggested to have 2–4 km between substations for 600V; 4–6km for 750V; 8–13km for 1500V; and 20–30km for 3000V [62], [64], [65]. By considering the power and the number of trains on the network, the exact distance between substations can be determined [64], [66]. Figure 2.3.1 indicates a typical DC supply arrangement in a railway system.

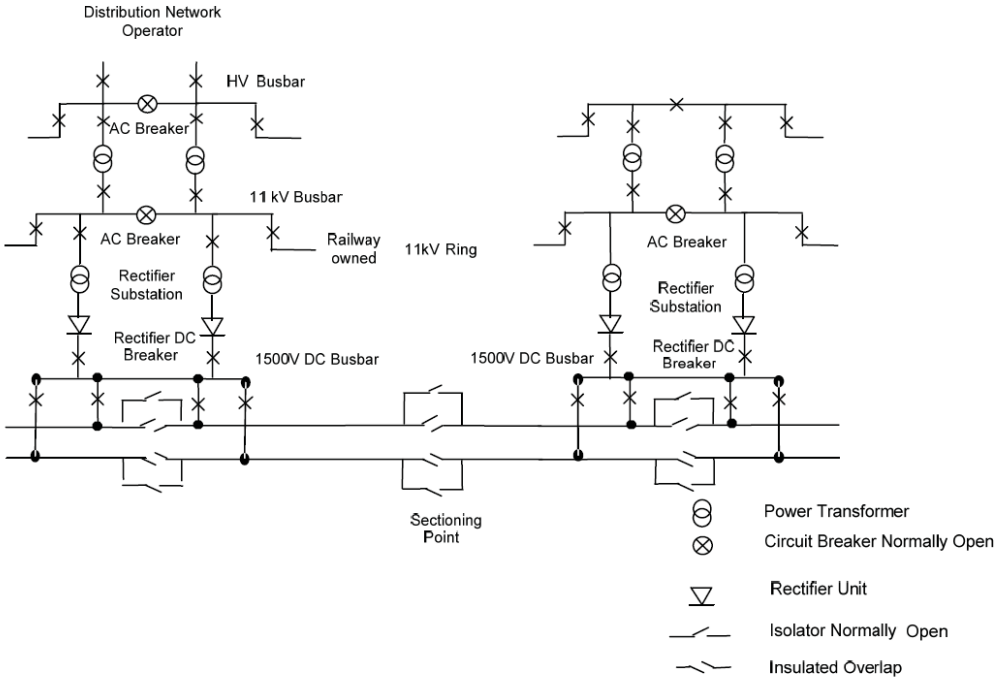

Figure 2.3.1. A typical DC supply arrangement in a railway system, produced by R.D. White [62]

In a DC supply system, current is transmitted to the vehicle through an overhead line, or through third rails by pantographs/shoes. This current usually returns using running rails. However, some railway systems, such as London Underground, use an additional insulated conductor to return the current in order to prevent the effects of stray current [64], [65].

2.3.1.2. AC Power Supplies

System Voltage 15kV, 16.7Hz

One of the typical supply systems for railway networks is 15kV, 16.7Hz (50/3Hz). A railway electrification system with this voltage and frequency is employed in countries such as Switzerland, Germany, Sweden and Austria. In Austria, Switzerland and some parts of Germany, there are power grids which produce single-phase AC current at a frequency of 16.7 HZ. The voltages which are produced in these power grids are from 110kV in Germany and

Austria and 132kV in Switzerland. In Germany, for instance, the energy is taken from the national power grid at 110kV, 50Hz and, by the use of AC/AC converters or rotary machines, is transformed to 55–0–55kV AC or 66–0–66kV AC at 16.7Hz. The zero point is connected to the earth, giving each part of the single-phase AC power line a voltage of either 55 or 66kV. In Sweden, Norway and other parts of Germany, there is no special single-phase power grid. The electricity is directly taken from the three phase 110V at 50Hz, transformed to low-frequency single-phase. For both systems, the energy is converted into 15kV AC at the substations [63].

System Voltage 25kV, 50Hz

The incoming energy for a 25kV, 50Hz supply system, which is specifically designed for rail systems, is typically 132, 275 or 400kV. This energy is transmitted to two feeder stations (to increase the degree of security) which have transformers, switchgear metering systems and communication, and Supervisory Control and data Acquisition (SCADA) monitoring. In feeder stations, the energy is converted to 25kV AC and is fed to the overhead lines [63]. This AC system is employed in the UK.

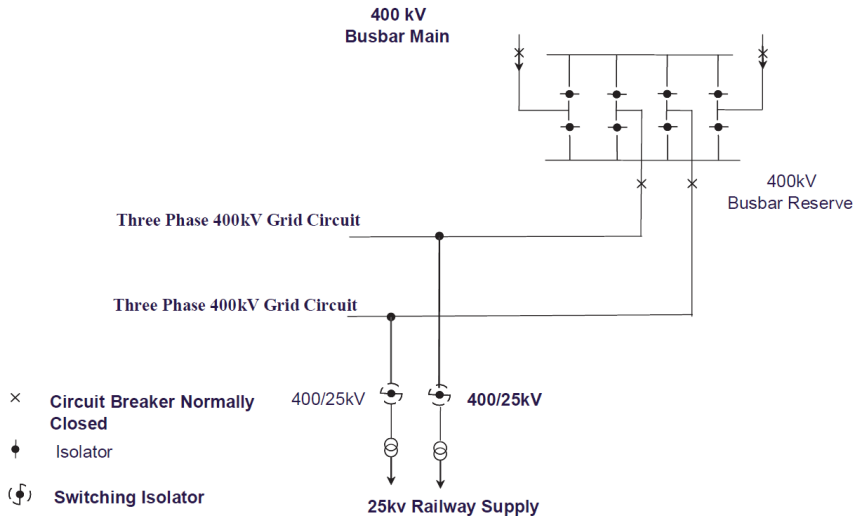

Figure 2.3.2. A typical 25kV, 50Hz AC supply arrangement in a railway system produced by R.D. White [63]

2.3.2. Traction Drive

In railway systems, regardless of DC or AC supply, both DC and AC traction drives are employed. Both electric motors take the energy from either DC or AC supply after proper conversions and transform the electrical energy into mechanical energy to send to the wheels.

2.3.2.1. DC Traction Drives

Since they were originated, DC motors have been controlled by various voltage supplies. In the early days, the output voltage was controlled by series resistances. The device used, called a camshaft controller, is still in use for some light railways. Modern control systems in DC motors take advantage of a DC–DC chopper converter with variable input–variable output voltages.

Figure 2.3.3 shows a schematic of a typical chopper circuit for a DC traction drive.

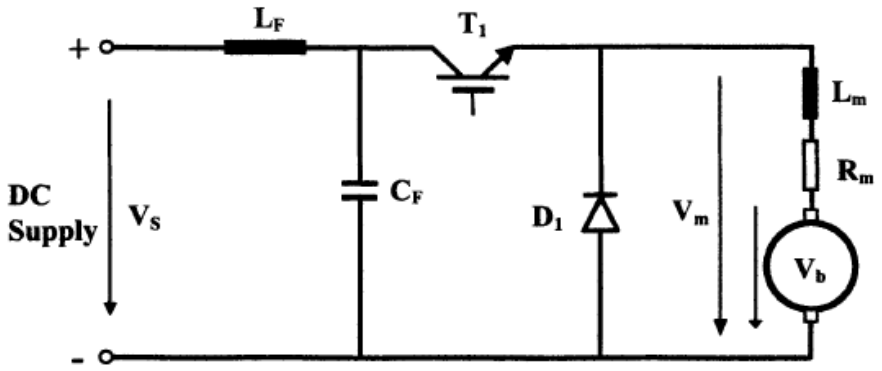

Figure 2.3.3. A typical chopper control circuit in a DC motor, produced by F. Schmid and C.J. Goodman [66]

In order to meet the driving speed, a closed loop control is used to achieve the required armature or field current [64], [66].

2.3.2.2. AC Traction Drives

Nowadays, modern railway systems around the globe are moving towards the use of AC traction drives. This is due to advantages such as low maintenance requirements for AC motors and, more important, an increase in power density due to elimination of commutators [64], [67]. The major drawbacks of these types of motors is their complexity due to the power electronic converters required to supply variable voltage and frequency. The controllers in old AC motors were Gate Turn-off Thyristors (GTO) with operating frequencies between 200 and 300Hz. These controllers have now been replaced by Insulated Gate Bipolar Transistors (IGBT) which have a higher frequency range, voltage and current. Figure 2.3.4 indicates the circuit of a typical AC motor drive [64], [66].

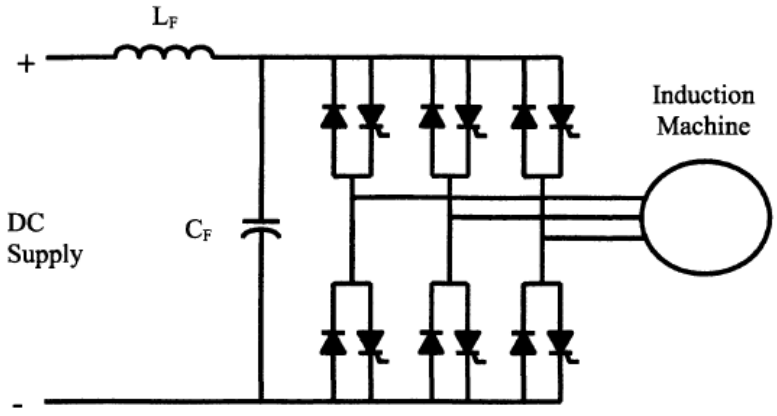

Figure 2.3.4. A typical control circuit in an AC motor, produced by F. Schmid and C.J. Goodman [66]

2.4. Energy Storage System

An ESS is a technology with the ability to absorb energy, store it for a period of time and then dispatch it [68]. ESSs can be employed to manage different characteristics of electricity, such as hourly changes in the price of electricity and power demand [69]. Each ESS has three main parts; the first is an energy storage device which is used to store electricity, such as batteries,

supercapacitors, flywheels, etc. A power converter which controls the input/output electrical flows is the second part of an ESS. Due to the various input and output conditions under which ESSs work, power converters, which are based on power electronic devices, manage the energy flow in a bidirectional way and ensure suitable performance of the ESS. Finally, there should be a power flow controller to optimise the operation of the ESS. These controllers manage the charge/discharge process with regard to the State of Charge (SoC) or the network voltage [41], [70]. ESSs can be classified according to the form of energy used. The categories into which these systems are classified are: mechanical, electrical, chemical, electrochemical and thermal ESSs [69].

In railway transport, motors have the capability to act as generators during braking. In this procedure, kinetic energy is converted into electricity in a process known as dynamic braking. In rheostatic braking, regenerated electricity is dissipated in banks of variable resistors and the process of reusing this electricity for the railway transport itself is called regenerative braking [41]. After the development of power electronic devices in recent decades, regenerative braking seems an effective and optimistic solution for reducing energy consumption in electrified urban transport systems [41], [70]. The excess energy recovered from regenerative braking of a vehicle can be employed to supply the auxiliary functions of the vehicle itself or can be used for the other vehicles in the same network after being returned to the power supply. Research has shown that the energy consumption in urban rail systems can be reduced by between 10% and 45% by using regenerative braking. Urban rail systems use 2% of the electricity generated in the UK [161]. The amount of energy recovered is dependent on several factors such as track gradient. ESSs are outstanding new technologies to store the energy obtained from regenerative braking and increase the efficiency of energy consumption in railway systems.

Moreover, ESSs have been recently recognised as a contributor to supply power to railway systems. They are able to provide power for the catenary-free parts of routes. For routes where it is not cost-effective or there is difficulty in electrifying the line, introducing trains equipped with on-board ESSs appears to be an efficient method to replace the diesel trains. Moreover, this avoids the visual pollution of the catenary, for example when the train passes a historical building [12], [13], [14], [15], [16], [17], [71].

Choosing a suitable and efficient ESS for each application depends on the given characteristics and requirements of that application but, generally speaking, an ESS to be utilised for a railway application should have high power peaks of charge/discharge (in the range of 0.1 to 10MW), low weight and volume (especially for on-board applications), a high number of life cycles (between 100,000 and 300,000 cycles) and intermediate energy capacity [41]. Batteries, supercapacitors, flywheels, Superconducting Magnetic Energy Storages (SMES) and fuel cells are common energy storage systems employed in railway applications [41], [70].

2.4.1. Different Types of Energy Storage System

There are two types of ESS which can be implemented for railway networks: the first one is a stationary or trackside ESS which is installed along the track or at the substation level; the second kind, an on-board or mobile ESS, is implemented on board the train and forms a series-hybrid electric topology in the case of using the network as the main energy source [41], [70].

2.4.1.1. Wayside Energy Storage Systems

Wayside energy storage systems are implemented in existing substations or at particular places where there are more line voltage variations (for example, near to stations). Not only can wayside ESSs reduce the whole energy demand of the system, but they also have the ability to

stabilise the voltage at weak points of the network. Wayside devices help to shave peaks of energy consumption during acceleration, which results in decreased resistive losses and energy costs in the supply line. There is no need to have additional substations for voltage drop compensations when using these types of ESS. Compared to on-board systems, wayside ESSs do not require additional space and mass on the vehicle and, consequently, no additional traction energy is consumed while employing a wayside solution [41]. Being capable of recovering braking energy from several braking vehicles at the same time is another advantage of stationary solutions; on-board solutions do not have this ability.

Variability of traffic conditions is a significant factor to be considered when designing a wayside ESS. It is also essential to carry out a fine-tuned analysis in order to optimise the capacity of a wayside system. In recent research, diverse optimisation procedures have employed various techniques to reach an optimised size for wayside ESSs [41], [70].

There is a wide range of storage technologies which are suitable for employment in wayside operations. Using supercapacitors in wayside ESSs contributes greatly to voltage stabilisation and peak shaving. Flywheels, with similar power characteristics to supercapacitors with higher energy densities, are another type of storage device suitable for wayside systems. An SMES system with fast response seems to be an efficient storage device, but its high cost and complexity mean that it is not currently used in many applications [41], [72].

Several researches can be found in the scientific literature on wayside ESSs for urban rail systems. Most researchers have preferred to choose supercapacitors as storage devices for wayside applications. However, there have been some studies on employment of flywheels and batteries for these ESSs [41], [70], [72].

2.4.1.2. On-board Energy Storage Systems

Employing an on-board ESS benefits the railway system in different ways: similar to the use of a wayside ESS, power peak demand can be shaved during acceleration by using an on-board ESS. There can also be a certain degree of power autonomy in catenary-free applications or depot operations when using an on-board ESS which is a significant benefit of these types of ESSs. Moreover, voltage drops can be limited, which consequently results in higher traffic density without additional modification. On-board storage systems operate at higher efficiencies than wayside ESSs because of the absence of line losses. When using an on-board ESS for electric trains, 20–30% of the energy can be saved. Due to the independent control of traffic conditions, it is easier to manage recovered energy in on-board ESSs than when using wayside storages. If properly sized, on-board systems are capable of storing the whole braking energy.

In order to utilise an on-board ESS efficiently, as for wayside applications, a sizing optimisation analysis should be carried out to prevent oversizing (which results in increased weight and volume) or undersizing (which leads to energy waste) of the storage system. To control these types of ESS, various parameters such as network voltage, vehicle speed, traction power and SoC have to be considered [18], [41], [70].

Due to the weight and volume limitations of on-board ESSs, there are only a few types of energy storage device which are applicable for on-board solutions. Supercapacitors are currently the best option to be employed for on-board systems due to their low cost, long lifetime, fast response and high power density. Supercapacitors have low energy density; in cases where high energy density is required for an on-board application, batteries, which are capable of providing

higher energy densities, can be used. Due to operability and safety issues, flywheels and SMESs are not recommended for on-board applications.

With regard to recent studies on recovering braking energy with on-board energy storage systems, the majority of researchers have worked on supercapacitor technology, indicating that supercapacitors are the most appropriate option to employ for on-board solutions. In contrast, only a few studies have been carried out regarding on-board solutions with batteries and flywheels to recover regenerative braking energy. It should be noted that batteries have been the preferred type of storage device in long-distance catenary-free operations. Hybrid ESSs have hardly been studied in urban rail applications and there has been no research on SMES operation for on-board ESS [24], [41].

2.4.2. Different Energy Storage Devices

2.4.2.1. Batteries

Batteries are the most common type of energy storage devices in ESSs and have the widest range of applications amongst all storage devices. A battery is composed of a certain amount of cells (with a certain voltage and current), each of which consists of two different electrodes (one positive and one negative) immersed in an electrolyte, and a separator. Energy in a battery is delivered through reversible electrochemical charge/discharge reactions in cells [41], [73], [74]. A battery cell is shown in Figure 2.4.1:

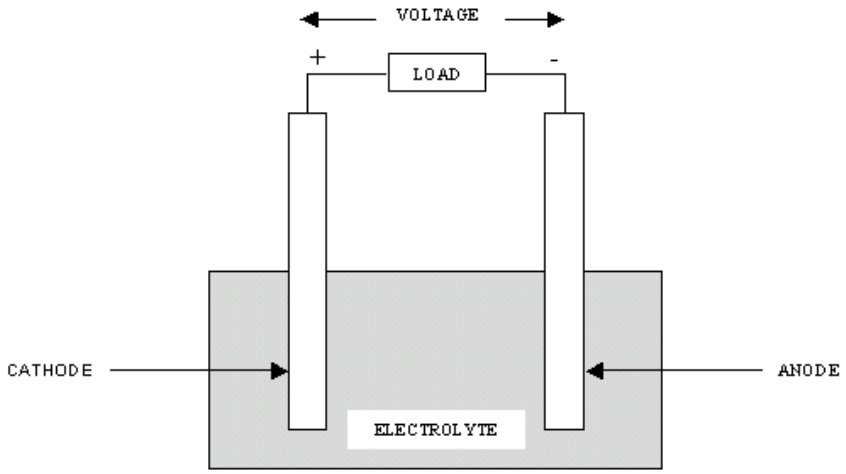

Figure 2.4.1. Schematic of a battery [73]

There are two types of cell: the first type is called a primary cell which is not rechargeable and has to be replaced after depletion of reactants. The second type, the secondary cell, is rechargeable and reactants can be restored until they reach their full charge state, provided a DC charging source is utilised. To be able to use batteries in an ESS and accommodate regenerative braking energy, batteries consisting of secondary cells should be chosen [73], [75].

The rating of a battery is stated in terms of its nominal voltage (V) and ampere-hour (Ah) capacity; the performance of a battery can be described by these two parameters. As stated above, each cell in a battery produces voltage, and the nominal voltage of the whole battery is based on the sum of the nominal voltages of cells connected in series [73], [74]. Ah capacity is the amount of current that a fully charged battery can deliver in a certain amount of time (before the voltage drops below a specific limit) at a given temperature.

The rate of discharge of a battery (C-rate) is a battery feature specifying the amount of current that can be delivered in 1 hour in a certain voltage range [74], [76]. SoC is also a notable characteristic of batteries; it describes the percentage of battery capacity relative to the capacity of a fully charged battery. In other words, SoC defines the battery capacity remaining in the

battery with regard to its maximum capacity [73], [77]. In general, to calculate the SoC, the current is integrated to determine the change in battery capacity over time [77].

In terms of the advantages of employing batteries in different applications, the high energy density of batteries is the most significant advantage of this type of storage device. Batteries are safer than other types of energy storage devices regarding performance, they are easy to use and have minimal environmental impacts. Employing batteries contributes to load smoothing and peak lopping, which leads to remarkable savings in energy and cost [78]. They can also provide a rapid response to meet the demands of applications [79], [80]. On the other hand, due to the chemical reactions in batteries, the maximum current which can be pumped into or drawn out of a battery is limited. This results in typical batteries having a low power density compared to some energy storage devices such as supercapacitors [81].

Batteries can be classified into different types based on their electrode material. In railway applications, commonly used batteries are lead-based (lead–acid), nickel-based (nickel–cadmium and nickel–metal hybrid), lithium-based (lithium-ion and lithium-poly) and sodium-based (sodium–sulphur and sodium–nickel chloride or ZEBRA). Amongst all these types, lithium-based batteries have a relatively higher energy density, power density, lifetime and efficiency. Moreover, they have a lower self-discharge rate compared to other types of batteries. Although the biggest disadvantage of lithium-based batteries is their high initial cost, their great advantages contribute significantly to the reduction of the total energy consumption and, consequently, the total cost. The high manufacturing cost, thus, can be compensated. Considering these factors, lithium-based batteries are the most appropriate energy storage devices to be employed in an ESS in a railway system [41].

In addition to the above-mentioned advantages of lithium-based batteries, their low maintenance requirements, absence of memory effects and smaller weight and volume (compared to other battery types) are other positive characteristics of these batteries. Furthermore, for applications requiring rapid frequent switching back and forth between charge and discharge conditions, lithium-based batteries are the most efficient type. However, it should be noted that while using lithium-based batteries, there should be a battery management system in order to maintain the SoC, temperature and voltage within a secure range of operation [41], [82], [83], [84], [85], [86], [87].

There is a wide range of batteries with electrodes which are made from lithium, but Lithium-ion (Li-ion) and Lithium-polymer (Li-poly) are the major types in this battery category. Li-ion batteries have much longer life cycles, are able to operate in middle temperature ranges, have fewer limitations on the charge/discharge current and no organic electrolyte (organic electrolytes are volatile and inflammable) [41], [85], [87], [162]. Therefore, it appears that Li-ion batteries are more efficient and appropriate for utilise in railway applications. Amongst the different types of Li-ion batteries, Lithium Titanate (LTO) appears to be efficient due to its higher power density compared to the other types [88], [89].

2.4.2.2. Supercapacitors

Supercapacitors (SC) or Ultracapacitors (UC) are subcategories of electrochemical capacitors and are popular types of energy storage device employed in various electrical systems, especially in electrified railway applications. Supercapacitors have a higher capacitance compared to normal electrostatic capacitors. A supercapacitor is built up of two electrodes, a separator and an electrolyte, and the energy is stored by charge transfer at the boundary between the electrolyte and electrodes. There is a membrane between the two electrodes in order to allow

charged ions to move and prevent electronic contact. In a supercapacitor, the size of ions, the level of voltage level decomposition and the surface area of the electrodes are three factors influencing the amount of stored energy [90]. Figure 2.4.2 indicates a schematic of a supercapacitor.

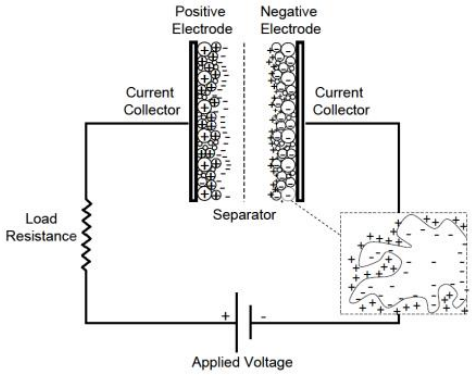

Figure 2.4.2. Schematic of a supercapacitor [91]

Since supercapacitors are a type of capacitor, they are ruled by the same basic principles as conventional capacitors. As for capacitors, supercapacitors can be rated by their capacitance (C) and their nominal voltage (V). Capacitance can be defined as the ratio of stored charge (Q) to applied voltage (V). Capacitance is proportional to the surface area of electrodes (A) and the distance between electrodes (D) where dielectric constant ($\varepsilon_0 \varepsilon_r$) is considered as well.

The energy density and power density of supercapacitors are important attributes to consider when choosing them as storage devices for different applications. Compared to conventional capacitors, supercapacitors have a much larger surface area and a shorter distance between electrodes; therefore, their energy density and capacitance are higher than those of common capacitors [90], [91]. As discussed in Section 2.4.1.2, supercapacitors are the preferred and most suitable type of energy storage device for storing regenerative braking energy in both wayside and on-board applications for electrical railway systems [41]. In order to store the

maximum braking energy of a train while using supercapacitors, there should be a power flow controller to control the level of SOC [70].

The most notable advantage of supercapacitors is their high power density which easily benefits the network in dealing with peak power demands and, consequently, decreasing voltage drops. These types of energy storage device have a very high efficiency within one charging/discharging cycle (around 95%), which is due to their low internal resistance. Another advantage of employing supercapacitors is that it is easy to measure their SOC by using terminal voltage as their voltage is much more correlated with SoC compared to electrochemical cells. The electrostatic nature of these types of energy storage devices helps them benefit from a long life of about 1 million charging/discharging cycles. Low heating losses are another advantage of supercapacitors. The long life of these capacitors with little degradation makes them environmentally friendly, safer than other types of energy storage devices such as flywheels and Superconducting Magnetic Energy Storage and reversible (high rate of electron transfer) [70], [90], [92]. In contrast, low energy density is the most notable disadvantage of supercapacitors. These devices have low voltage and, to reach the required voltage level specified for each application, many cells have to be put in series. Therefore, there should be a voltage balancing system controlling the individual voltage of each cell in order to protect it from overvoltage. Significant self-discharge, rapid voltage drop and spark hazard (when shorted) are other drawbacks of supercapacitors, which must considered when choosing them to be employed in an application [90], [92].

There are diverse materials used for supercapacitor electrodes and electrolytes. Materials used to build electrodes are carbon, metal oxide and conducting polymer; electrolyte material can be organic, aqueous or solid. The most significant classification by which supercapacitors are categorised is electrolyte type. Electric Double Layer Capacitor (EDLC) or Symmetric,

Pseudocapacitor or Asymmetric, Composite and Hybrid are different types of supercapacitors [90], [91]. EDLCs, which store energy electrostatically, use carbon for both electrodes, and a double layer of charge is used store electricity. There is no transfer of charge between electrode and electrolyte [91], [93].

2.4.2.3. Flywheels

Flywheels or mechanical batteries are electromechanical storage devices that store the kinetic energy in a rotor. The energy stored in the rotor is proportional to the inertia of the rotor and the square of its rotational speed. The rotor of a flywheel is connected to an electrical machine which has the ability to operate as either a generator or a motor. In the charging process, the electrical machine functions as a motor. In this mode, the electrical supply increases the rotational speed of the flywheel to enhance the kinetic energy. On the other hand, the electrical machine becomes a generator in the discharging process when the energy stored in the flywheel is released [41], [94]. Figure 2.4.3 shows a schematic of a flywheel.

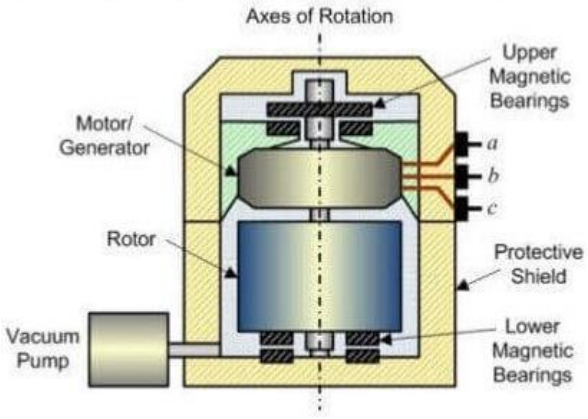

Figure 2.4.3. Schematic of a flywheel [95]

The advantages of flywheels are their high efficiency, fast charge/discharge process, strong instantaneous power, low maintenance and long life. However, flywheesl are not considered an

efficient type of energy storage device for use in railway applications. When employing flywheels, there is a potential risk of explosive shattering if there is a failure. Moreover, flywheels are relatively heavy and they also have a high self-discharge rate [41], [94].

2.4.2.4. Superconducting Magnetic Energy Storages

SMESs store electric energy in a magnetic field which is generated by a direct current flowing through a coil. This coil, which is contained in a cryostat or dewar consisting of a vacuum vessel and a liquid vessel, is cryogenically cooled by refrigeration below its superconducting critical temperature. Because of the nearly zero resistance of the superconducting Niobium Titanium (NbTi) cables, the current circulates indefinitely in the coil. In the discharging mode, the DC potential is removed to release the energy [41], [96]. Figure 2.4.4 shows a schematic of an SMES.

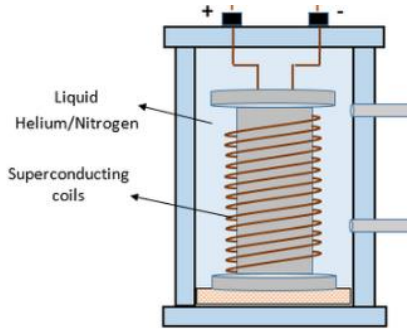

Figure 2.4.4. Schematic of a SMES [97]

SMESs have a number of advantages such as high energy density efficiency and fast response. They also have a very long life cycle. In contrast, they have high initial and maintenance costs due to refrigeration and they generate very strong magnetic fields which can easily interfere with railway systems such as signalling and telecommunication [41], [96].

2.4.2.5. Fuel Cells

In a fuel cell, chemical energy is converted to electric energy though an oxidation reduction (redox) between the fuel (hydrogen) and oxidant (oxygen). This process is the reverse of electrolysis in which electricity separates hydrogen and oxygen. A fuel cell includes three main components: a cathode, an anode and an electrolyte sandwiched between the two. Oxygen flows past the cathode from the air and the fuel gas which contains hydrogen flows through the anode. Hydrogen ions that are positively charged pass though the electrolyte membrane and react with oxygen to form water. Electrons that are generated by this electrochemical reaction flow from the anode to an external load and then to the cathode again, which consequently generates power. Fuel cells differ by electrolyte type: alkaline, phosphoric acid, molten carbonate, proton exchange membrane, microbial, and solid oxide fuel cells are various types known by the type the electrolyte they have [98], [99]. Figure 2.4.5 shows a schematic of a fuel cell.

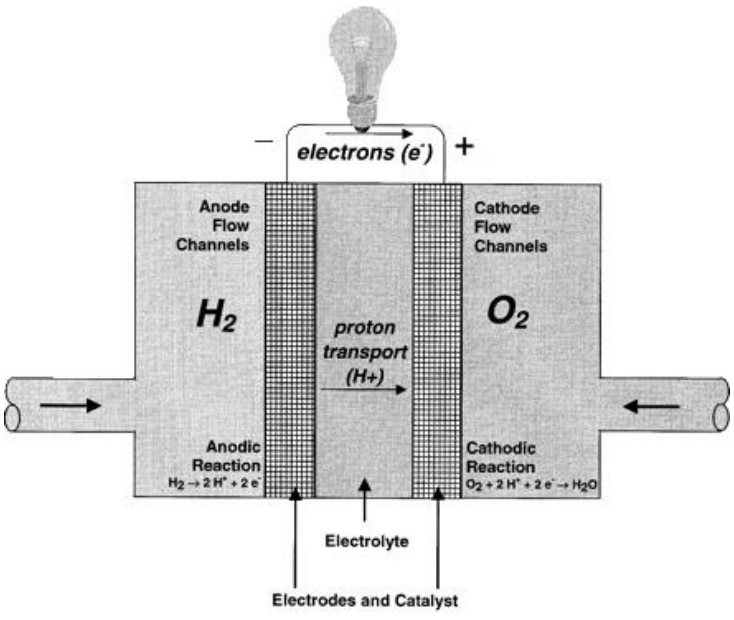

Figure 2.4.5. Schematic of a fuel cell [100]

Fuel cells are new type of energy storage device in railway systems and researchers are working on prototypes to make use of fuel cells for on-board applications [101], [102]. Fuel cells appear to be decent energy storage devices for contributing to the power supply. They have advantages such as high reliability, efficiency and flexibility and low production of noise and CO_2 emission. However, it should be noted that hydrogen is still expensive (about £10-£15 per kg in the UK) to produce and is not widely available; there is lack of infrastructure supporting the distribution of hydrogen, and a major part of the currently available fuel cell technologies are in the prototype stage and have not yet been validated [98], [99], [102], [103], [104], [163]. Moreover, compared to batteries, the current hydrogen fuel cell technologies have lower efficiency and in order to produce the hydrogen (in electrolysis process) to fuel them, more CO2 emissions are produced [101].

2.4.3. Hybrid Energy Storage Systems

An HESS is a type of ESS in which two or more energy storage devices are combined in order to obtain the best features of each type, overcome drawbacks and improve the efficiency of the storage system [105], [106].

In general, the integration of batteries and supercapacitors in an HESS has attracted the attentions of researchers in various applications due to the complementary characteristics of these two energy storage devices. The integration of batteries and supercapacitors has been proposed in various applications such as microgrids, PV applications, wind applications, Electric Vehicles (EV), aircraft, wireless sensor networks, uninterruptable power supplies, excursion ships, Wave Energy Converters, Rubber- Tire Gantry Cranes, Plug-in Electric City Bus, etc. [35], [38], [107], [108], [109], [110], [111], [112], [113], [114], [115].

In these applications, HESSs including batteries and supercapacitors have been introduced for various reasons such as taking advantage of the positive features of both devices simultaneously, increasing battery life by not causing severe damage, avoiding an oversized storage system, enhancing the overall performance of the HESS, decreasing the total cost, improving the balance between generation and demand, and absorbing regenerated power [35], [38], [107], [108], [109], [110], [111], [113], [114], [116].

In railway applications, the combination of batteries and supercapacitors, in particular, seems to be an efficient solution for on-board energy storages, especially in catenary-free operations. There has been research proposing this integration in railway applications and work has been carried out on designing, sizing, controlling and charging these HESSs [18], [19], [20], [23], [24], [25], [26], [27], [28], [29], [32], [117]. As mentioned above, flywheels and SMESs are not suggested to be used for on-board ESS in railway applications due to operability, safety and economic issues. Moreover, fuel cell technologies are still not fully available and the costs are high. Batteries and supercapacitors are safer, more functional, more environmentally friendly (not contributing to air, noise and land pollution and helping to conserve resources such as water and energy) and more cost-effective. The integration of batteries with a high energy density to supply the energy required for the journey, and supercapacitors with high power density to meet the stringent power requirements during acceleration and braking means an HESS meets both energy and power requirements [19], [23], [32], [41], [105], [118], [119]. Making batteries to meet the high power requirements in the mentioned modes leads to an oversized system and, moreover, decreases battery life. Due to the high cost of supercapacitors, using solely them in a storage system results in a highly expensive system [23], [25], [26], [27]. Therefore, combining batteries and supercapacitors in an HESS benefits railway application to a great extent. The result of this combination is basically dependent on the way in which batteries and

supercapacitors are interconnected and controlled and how the strengths and weaknesses of each type are utilised and avoided, respectively [105].

Fundamentally, one of the most critical factors to consider while designing an HESS for a rail system is the size (both weight and volume) of the HESS. An HESS installed on a train adds to the mass of the train and therefore increases the energy consumption and costs. Moreover, there is usually limited space on a train to install the HESS [24], [27], [28], [29].

2.4.4. Sizing Methods for HESS

In order to size HESSs, there are various sizing methods that can be employed. These methods can be classified into three groups: 1) Constrain-based or Generic methods, 2) Optimisation-based or Heuristic methods, and 3) Frequency-based methods [120], [121].

Various applications, including railway ones, have employed these methods to size HESSs including batteries and supercapacitors, with different objectives.

2.4.4.1. Constraint-based Methods

Constraint-based or Generic sizing methods size the HESS generally based on constraints. These constraints can be various parameters; the ones most used in research are specific energy/power and voltage/current limits which are either requirements of the application or characteristics of each energy storage device.

Several researches have been carried out on power applications in order to size HESSs including batteries and supercapacitors. [36] considered the voltage limits of the application and the specific energy of the storage device in sizing an HESS for EV applications. In [40], the energy requirement for the application and the voltage limits of the supercapacitor were considered for

wind turbines. Historical power values were used in [110] in a PV-based wireless sensor network considering the battery voltage limit. In [111], the energy and power requirements of an uninterruptable power supplies system were considered. [112] considered the current and voltage limits of the application and the storage devices as well as the energy capacity of both devices for an electric excursion ship. The energy and power requirements of the system were used when sizing the HESS for a Wave Energy Converter in [113]. In [122], both the energy requirement and voltage limits for the application were considered for another EV-related sizing study.

Regarding Constraint-based sizing methods in railway-related research, the voltage limits of the battery and supercapacitor as well as the line voltage were used in [28] to size an HESS for urban rail transit. [29] carried out a sizing procedure for urban rail as well, based on the required regenerative braking energy.

2.4.4.2. Optimisation-based Methods

In an Optimisation-based or Heuristic method, an optimisation algorithm is employed to size the HESSs. These algorithms are applied with different objective functions; the one most used is the reduction of costs.

With regard to Heuristic methods carried out in the literature to size batteries and supercapacitors in an HESS, [115] used a Particle Swarm Algorithm (PSO) to size an HESS for Plug-in Electric City Bus in order to minimise the energy storage costs. Multi-objective optimisations were developed in [123] and [124] for EV applications to minimise the total size and cost of the HESS and maximise the life cycle of batteries. [125] proposed an optimal capacity determination model with the objective function of minimum annual cost for a wind application. An HESS was sized optimally in [126] with the objective function of total cost

minimisation using PSO for a PV application. Again, for another PV application, an HESS was sized in [127] using Bacteria Foraging Optimisation to minimise the total costs. An updated Differential Evolution (DE) was introduced in [128] to size an HESS for renewable energy resources considering the target of total cost minimisation.

In railway applications, [25] and [26] have presented Linear Programming and a multi-period optimal power flow problem formulation, respectively, for electric railways. For HESSs installed on trams, [27] and [32] used a Genetic Algorithm (GA) and PSO, respectively; the objective function in [27] was minimising operation costs and in [32] it was decreasing weight and cost as well as prolonging battery life. [129] proposed a GA for DC rail transit with the objective function of minimising operation costs.

2.4.4.3. Frequency-based Methods

Both constraint- and optimisation-based approaches are executed in the time domain. Frequency-based methods carry out the sizing procedure in the frequency domain. Power is decomposed amongst the energy storage devices by applying low-pass, band-pass or high-pass filters where each device needs to supply the low-, middle-, or high-frequency parts of the load [33], [35], [38]. Amongst the three sizing approaches, for both generic and heuristic methods which are carried out in the time domain, numerous scenarios need to be explored and a large amount of computations need to be implemented in order to obtain reliable results. On the other hand, frequency-domain methods require a small amount of computations and ,furthermore, precise and credible results can be acquired with fast operations [121], [130].

Regarding the non-railway researches that have been carried out to size HESSs including batteries and supercapacitors in the frequency domain, [33] proposed a filter-based approach in an EV application in order to minimise the installation and running costs. Two band-pass filters

were employed in [35] in a frequency-based approach to size an HESS in an isolated system with high wind generation. In [38], a frequency approach employing two low-pass filters was adopted to minimise the size of the HESS installed on an aircraft. Spectrum analysis and Discrete Fourier Transform (DFT) were proposed in [130] and [131], respectively, to size an HESS for wind turbines. [132] considered frequency analysis using low- and high-pass filters to size an HESS for renewable energies to minimise the total annual cost. Again for renewable energy applications, a Role Dividing Strategy via an Empirical Wavelet Transform was used in [133], employing band-pass and low-pass filters to size an HESS. [134] and [135] employed Fast Fourier Transform (FFT) and DFT, respectively, to size HESSs in PV applications, with the objective function of cost minimisation for [134].

In some of these methods, there have been objectives sought while using frequency-based methods. In these researches, optimisation tools were proposed as well in order to determine the optimal cut-off frequencies for the filters to reach the required objectives. As mentioned above, these objectives were cost or size minimisation.

In the literature, some researches have applied frequency analysis to HESSs including batteries and supercapacitors not to size the HESS, but as a controller to manage the energy split between the battery pack and supercapacitor pack that have been sized already. [136], [137] and [138] used this approach for EV applications, and [139] used it for urban rail transit.

Fast Fourier Transform

The Fast Fourier Transform (FFT) is a type of Fourier Transform which is widely used in various applications in engineering. This method is used to transform a function of time into a function of frequency, or in other words, transform signals from time domain to frequency domain. In a Discrete Fourier transform (DFT), a finite sequence of equally-spaced samples of

a signal in time domain is transformed into a sequence of equally-spaced samples in frequency domain with the same length. FFT is an effective algorithm of DFT which removes duplicated terms and the calculating time is decreased from N^2 to $NLog_2N$; where N is the number of samples of the discrete signal. This results in dramatic decrease in calculation time compared to DTF. In FFT algorithm, every discrete Fourier with N samples can be divided into the two Fourier transforms, each with N/2 samples. The first Fourier transform includes even samples and the second one includes odd samples. FFT uses large number of samples without decreasing the speed of transformation procedure. FFT produces the exact result as DFT, but in a faster operation [174], [175], [176].

In this project, due to fast and accurate response, FFT method is used to transform the signals from time domain to frequency domain.

2.5.Optimisation Methods in Railway Applications

As a whole, optimisation plays a key role in engineering, economics and related fields. In engineering, optimisation is the process of an idea improvement. Optimisation can be defined as a process of finding the best feasible solution to a single- or multi- dimensional problem by an objective function or a performance index within a given time and in a pre-determined search space. In an optimisation, the problem needs to be formulated and the required output is obtained through adjusting inputs or characteristics by use of a mathematical procedure. Inputs are parameters, the mathematical procedure is called the objective function, fitness function or cost function and the outputs are objective, fitness or cost. [51], [164].

In recent decades, several optimisation techniques have been developed with different characteristics and their own advantages and disadvantages and they have been applied to

different sectors. Railway sector has not been an exception and diverse optimisation techniques have been widely employed for various purposes such as optimising time, cost or energy. Optimisation methods can be generally categorised into two groups: meta-heuristic or approximate methods and deterministic or exact methods.

2.5.1. Meta-heuristic Optimisation Methods

Meta-heuristic or approximate optimisation methods were developed to sample a set of solutions for optimisation problems with large search space which were difficult to be fully sampled. Since then, meta-heuristic methods have become popular and have been widely used in various fields. These types of optimisation approaches do not guarantee to obtain the most optimal solution, but when there is imperfect/incomplete data and/or limited computation capacity, they provide sufficiently good results with low computational efforts. Thus, meta-heuristic optimisation methods are more efficient compared to other methods when it comes to addressing problems by exploring a high dimensional search space [165], [166], [167], [168].

The first set of popular meta-heuristic methods that have been employed for railway applications are Evolution- or population-based solutions such as Genetic Algorithm, Harmony Search Algorithm, Evolutionary Programming and Simulated Annealing. The next set of meta-heuristic methods are subcategory of swarm-based algorithms including Particle Swarm Algorithm, Ant Colony Optimisation and Bacteria Foraging Algorithm [51], [165], [166], [167], [168].

2.5.2. Deterministic Optimisation Methods

Deterministic or exact optimisation methods analyse all possible solutions in order to choose the most optimal one. Compared to metaheuristic methods, deterministic methods provide a

more straightforward approach and more importantly, achieving the most optimal solutions within instance dependent run time is guaranteed. The biggest drawbacks of these types of optimisation solutions are that they involve a great amount of computation and they are more time-consuming compared to meta-heuristic approaches [51], [64], [167].

Various deterministic optimisation techniques have been employed in railway applications, where the most used ones and Brute Force Optimisation, Dynamic Programming and Integer/Fuzzy Linear Programming [51], [64], [167], [169], [170].

Considering the advantages and disadvantages of meta-heuristic and deterministic methods and the objective of this project, deterministic optimisation approaches are chosen to be used for this project. The main reason for this decision is due to the capability of deterministic methods in choosing the most optimal solution, which directly affects the sizing procedure of the HESS, its final size and hence, the energy consumption of the train. Although deterministic methods are time-consuming and need complicated computation, the optimisations proposed for this project will be used only once in the design during the sizing process of the HESS and there is no need to employ fast or real time optimisation approaches.

Amongst different mentioned deterministic methods, Brute Force Optimisation will be used due to its efficiency and higher applicability for this project. In Brute Force Optimisation, which is known as exhaustive search, the searching process includes the enumeration of all possible candidate solutions in solution domain that can be given to the problem and evaluation of candidate satisfaction in meeting the problem. Normally, Brute Force is directly based on the statement of a problem and the definitions of involved concepts for that problem. As any deterministic optimisation method, Brute Force finds optimum solutions [51], [64], [169], [170].

2.6. Economic Aspects of Battery Systems Vs. Electrification

As part of the decarbonisation strategy established in the UK in phasing out all diesel trains by 2040, Network Rail has established technology deployment recommendations to achieve traction decarbonisation by phasing out unelectrified railway. Unsurprisingly, the capital and ongoing costs required for each of the proposed recommendations is remarkable. The upfront capital investment and ongoing operational costs associated with the infrastructure and rolling stock as well as disruption dis-benefit during construction for the recommendations are as below:

- Infrastructure capital and renewal costs;
- Infrastructure maintenance costs;
- Disruption during construction disbenefits;
- Rolling stock maintenance costs;
- Rolling stock fuel costs;
- Rolling stock lease costs; and,
- NR maintenance costs.

However, costs and benefits for traction decarbonisation strategy will be broadly balanced over a ninety-year appraisal period. Figure 2.6.1 indicates the benefits, costs and Net Present Value (NPV) of traction decarbonisation strategy over a ninety-year period which is produced by Network Rail [171].

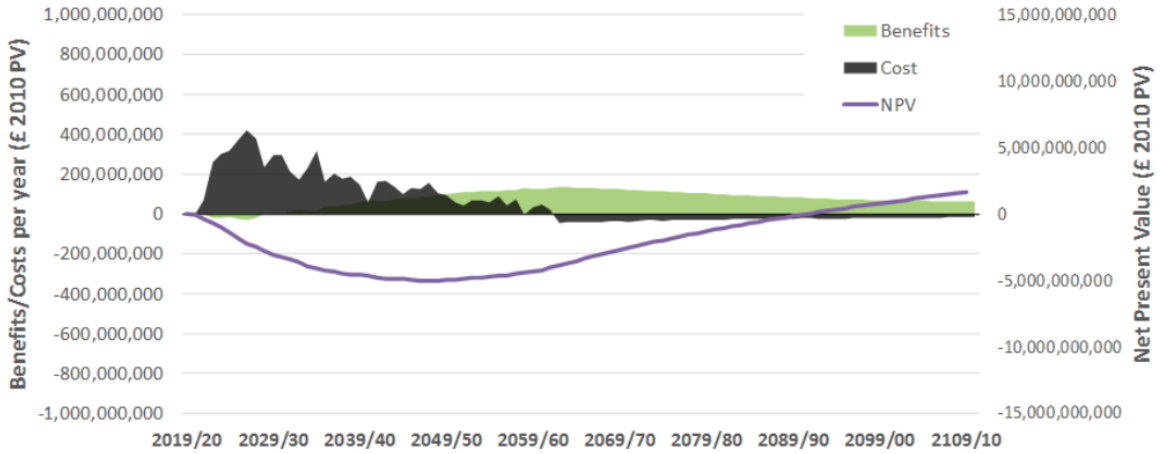

Figure 2.6.1. Benefits, costs and NPV of traction decarbonisation strategy over a ninety-year period, produced by Network Rail [171]

Amongst the proposed solutions, there are recommendations for 13,000 Single Track Kilometres (STK) of electrification and 800 STK of battery train deployment. In the current recommendation, the deployment of batteries is less than electrification. This is due to the novelty and on-going research being associated with this technology. Moreover, most train operating companies currently expect autonomously-powered mainline trains to store adequate energy to be able to complete a whole day of operation as a minimum. With the current available battery technology, this target is difficult to achieve. However, researches carried out in Network Rail and RSSB claim that battery technology is a rapidly developing field, reducing cost and increasing power and energy capacities. Hence, in Traction Decarbonisation Strategy proposed by Network Rail, it is recommended that battery train operations commence to ensure the development of standards, gaining whole-system operational experience, and learning lessons. This will lead to embedding best practice as part of the required longer-term introduction of these units.

Currently there is a fundamental economic difference between the capital costs and maintenance costs of electrification and battery systems. Electrification involves relatively high one-off or long-lived initial costs but very low marginal costs for the train services which use it. Conversely, battery traction involves a relatively lower capital cost but higher on-going operational costs [171], [172].

Regarding electrification, in general capital costs span from £1m/STK to £2.5m/STK. For the electrification recommendation in Traction Decarbonisation Strategy, the total capital investment is predicted between £18bn and £26bn (2020 prices) for infrastructure. Analysis suggests the capital cost of the rolling stock required to fulfil the recommendation is likely to be between £15bn-£17bn (2020 prices) with freight locomotives an additional £3bn-£4bn (2020 prices). This results in a combined capital cost of £36bn-£47bn (2020 prices). Operation cost savings for the proposed electrification system recommendation have been estimated to be in the range of £12bn-£17bn (2020 prices) over the ninety-year period [171].

With regard to battery train system, Table 2.6.1 indicates the cost of different components of an on-board battery storage system [173].

Table 2.6.1. Cost components of on-board battery storage systems [173]

System	Component	Description	Capital Cost	Maintenance Cost/year
Delivery	Grid Connection	• Grid connection • Metering	£210/kW	0.3% of Capital Cost
	Conversion	• Converter (AC to DC)	£250/kW	5% of Capital Cost

Storage	Battery System	• Modules • Enclosures • Heating, Ventilating and Air Conditioning (HVAC)	£296/kW	2% of Capital Cost
	Power Electronics	• Invertor • Battery Management System (BMS)	£11.5/kW	-
	Primary Substation connection	• Install 1 connection	£40,000	-
	Civils	• Foundation for battery package	£42.5/kW	1.9% of Capital Cost
End-use	Electrification Infrastructure	• Catenary • Gantry	£1,125,000/STK	-

Obviously, the key component of an on-board battery system is the battery storage system which has the capital cost of £296/kW for 2020. However, the suite of publications demonstrates cost reduction for battery storage over time. Table 2.6.2 indicates the capital and Operation and Maintenance (O&M) costs of battery storage system from 2020 to 2050 for every decade, produced by RSSB, where the projections in the table are based on the low, medium, and highest values (on a normalised basis) [173].

Table 2.6.2. Capital investment cost of battery storage system from 2020 to 2050, produced by RSSB [173]

		Unit	2020	2030	2040	2050
Capital Investment Costs	Default	£/kWh	296	168	144	120
	Low	£/kWh	280	104	80	64
	High	£/kWh	304	240	208	176
O&M Costs	-	% Capex	2.0	2.0	2.0	2.0

2.7. Hypothesis Development

As seen in the literature, due to the complementary characteristics of batteries and supercapacitors, their integration has attracted the attention of researchers to employ it in numerous power applications, including railways. As mentioned in the literature, one of the biggest advantages of this combination is to take advantage of the high energy density of batteries and the high energy density of supercapacitors. Furthermore, it has been stated in the literature that combining batteries and supercapacitors leads to a decrease in the size of the HESS. However, for HESSs installed on board in railway applications, there has been no unified research indicating the relevance of these two facts and the influence of the mentioned characteristics of these two energy storage devices on the decrease in the total size. Moreover, the effects of the battery C-rate on the total size of an HESS installed on board in a railway application is an area that has not been so far considered in research.

Regarding sizing an HESS including batteries and supercapacitors, the literature indicated that a great number of researches have been executed in various applications using Generic, Heuristic or Frequency-based methods. In rail systems, although Generic and Heuristic methods have been deployed in a number of researches to size HESSs including batteries and supercapacitors, there has not been any research on sizing on-board HESSs with batteries and

supercapacitors using Frequency-based methods and with the objective function of size minimisation along with an optimisation method.

In the literature, researchers have indicated different methods for charging HESSs including batteries and supercapacitors. Most of these methods propose charging by the grid, either at stations or by overhead lines. However, there is a gap in employing one energy storage device to charge the other one during the journey.

Considering the objectives of decreasing energy consumption, cost and CO_2 emissions, the hypothesis proposed in this thesis is as follows: Batteries and supercapacitors can integrate to form an effective energy storage system to meet both energy and power required by independently powered trains. There is a crucial need for optimal sizing of batteries and supercapacitors and Frequency Analysis method is a proper method to reach this goal. Moreover, batteries can be employed to charge supercapacitors during the journey. In order to fulfil the hypothesis, a simulation tool is required to model the HESS and the energy hub as well as the sizing and optimisation procedures. Modelling the whole performance of the HESS should be considered jointly. The applicability of the proposed approaches should be demonstrated based on the case studies.

2.8. Summary

In this chapter, first, the fundamentals of train performance and railway traction power system were discussed. The basics of train performance and movement as well as the simulation tools used to trace train behaviour were studied. Moreover, AC and DC traction power supplies and drives were reviewed. Then, the ESSs and their different types were described as well as the

energy storage devices employed in railway networks. HESSs including batteries and supercapacitors were studied and sizing methods used to size HESSs were discussed.

This chapter reviewed the literature on integrating batteries and supercapacitors in an HESS in various power applications, including railways. This chapter studied the benefits of this integration as well as the sizing approaches used for this combination for all applications. In addition to this, the charging methods proposed by researchers specifically for railway applications were studied. By analysing the prior literature, a hypothesis was developed for this thesis in order to evaluate the use of batteries and supercapacitors in an HESS for independently powered trains, size the HESS using FFT and Brute Force optimisation and employing batteries to charge supercapacitors.

Chapter 3
Methodology

3.1. Introduction

In order to design an HESS for an independently-powered train, there are numerous methods that can be employed in each stage of the design procedure. From choosing proper energy storage devices to selecting optimal methods for sizing and charging an HESS, a great number of methods exist which have their own advantages and disadvantages. Hence, choosing a decent method for each stage of the design is essential and challenging. A method needs to be chosen based upon the function of the application, performance and maintenance requirements, objective priorities, operation constraints and costs as the design requirements and procedure will be different when aiming at different goals [27], [41], [112].

In this chapter, first, various scenarios are proposed to evaluate the combination of batteries and supercapacitors as the selected energy storage devices to understand whether this combination leads to a more efficient HESS to support train traction. Furthermore, indication of how to assess the performance of the HESS for the chosen scenarios is given. Following this, the Frequency Analysis method, the approach chosen for sizing the HESS optimally, is discussed. It is shown how the battery pack and supercapacitor pack can be sized using this method, and evaluation of performance of the sized HESS is discussed as well. This chapter finally discusses how battery pack can be used as an energy supply to charge supercapacitor pack during the journey. For the proposed methods in this project, different validation approaches will be proposed in order to validate the methods.

3.2. Evaluation of an HESS Including Batteries and Supercapacitors

As discussed in Chapter 2, employing an HESS including batteries and supercapacitors for rail systems has become popular in recent decade for various reasons. It was said that one of the main reasons for employing batteries and supercapacitors together in an HESS was to decrease the size of the HESS. Thus, in this project, the main goal of proposing battery + supercapacitor for the storage system to be installed above the train is reducing the size of the storage system which, in turn, leads to a reduction in the total mass of the train and consequently decreases the total energy consumption and cost. Hence, this phase of the project firstly indicates whether it is more efficient to use a battery + supercapacitor HESS rather than a battery-only or supercapacitor-only ESS according to the weight and volume of the storage system. In the literature, it was expressed that integrating batteries and supercapacitors in an HESS could result in getting advantage of the high energy density of the batteries and the high power density of supercapacitors simultaneously. Hence, in this phase it is shown how the energy densities and power densities of the batteries and supercapacitors influence the total size of the HESS. Finally, this phase of the project assesses the change in the total size of the HESS when the C-rate of the batteries changes.

As mentioned in Section 2.4, each ESS/HESS has three parts: energy storage device, convertors and controllers. This project focuses on the key part of the HESS which is energy storage device. Hence, this project only considers the weight and volume of this part, which is battery modules and supercapacitor modules, and ignores the weights and volumes of other parts in the HESS.

3.2.1. Calculation of the Number of Modules

In order to compare the weight and volume of a battery + supercapacitor HESS with the weight and volume of a battery-only or supercapacitor-only ESS, the storage systems need to be sized. 3.2.1The first step in sizing is to determine the total energy and the peak power demands that should be met by the HESS.

3.2.1.1. Total Energy Demand and Peak power Demand

As mentioned in Chapter 2, both ESSs and HESSs should be sized in such a way to meet both the energy demand and peak power demand for the required train journey. Simulation helps to obtain the required information. In order to simulate the traction in Single Train Simulator (STS), the simulator chosen for this project, route data and vehicle specifications need to be entered as expressed in Chapter 2. For this project, the HESS is sized for one return journey. In other words, it is expected that the HESS is sized in such a way to be capable of providing enough energy and power for the train for one return journey. The generation rate in STS is 85%, which is the efficiency from the energy supply (HESS in this case) to the energy transferred to the wheels. Hence, no additional efficiency rate is considered for transferring energy between the HESS and the wheels of the train. Regenerative braking energy (regen energy) is considered in this project; it is absorbed by the HESS in braking modes with the regeneration rate of 50%. Due to the energy densities and power densities of the battery and supercapacitor, it is expected that the battery will play the main role in supplying the energy required during cruising modes, and the supercapacitor is mostly in charge of meeting the peak power demand in acceleration modes. By achieving energy and peak power requirements, they should be split between the battery pack and supercapacitor pack and therefore the number of

battery modules and supercapacitor modules in the HESS needed to provide the required energy and power can be calculated.

3.2.1.2. Sizing the Battery Pack

The number of battery modules can be determined when the energy and power that the battery pack needs to supply during the journey are known. The number of battery modules needed to provide the energy requirement and the number of battery modules to support the peak power demand are calculated separately, and the greater number is chosen as the final number of battery modules.

- **Calculation regarding energy demand**

To start the calculation, the highest energy that a single battery module can supply should be determined:

$$E_{Bat}^{Mod} = C_{Bat}^{Mod} \times V_{Bat}^{Mod}(Max) \tag{3.2.1}$$

where C_{Bat}^{Mod} is the capacity of the battery module in Ampere-hours (Ah) and $V_{Bat}^{Mod}(Max)$ is the maximum voltage of the battery module in Volts (V). Now the number of battery modules required to provide the energy requirement can be calculated:

$$N_{Bat}^{E} = \frac{E_{Bat}^{Req}}{E_{Bat}^{Mod} \times [SOC_{Bat}(Max) - SOC_{Bat}(Min)]} \tag{3.2.2}$$

where E_{Bat}^{Req} expresses the energy required from the battery pack to supply in Watt-hours (Wh). The SOC of the battery presents the current capacity of the battery as a percentage of the maximum capacity that can be stored in the battery. In these calculations, $SOC_{Bat-Max}$ is the maximum percentage of the energy that can be saved in a battery module and $SOC_{Bat-Min}$ is

the amount of energy that cannot be used. This is due to the internal impedance of the batteries where some part of the energy is dissipated within cells and is lost as heat. Thus, $SOC_{Bat}(Max) - SOC_{Bat}(Min)$ conveys the useful amount of energy that can used and in other words, it is the efficiency of the battery module. For this project, $SOC_{Bat}(Max)$ is considered to be 100% and $SOC_{Bat}(Min)$ is considered to be 20% which makes the efficiency of a battery module 80%. By knowing the number of battery modules in the battery pack, the weight and volume of the battery pack can be determined:

$$Wei_{Bat}^{E} = N_{Bat}^{E} \times Wei_{Bat}^{Mod} \tag{3.2.3}$$

$$Vol_{Bat}^{E} = N_{Bat}^{E} \times Vol_{Bat}^{Mod} \tag{3.2.4}$$

where Wei_{Bat}^{Mod} and Vol_{Bat}^{Mod} are the weight and volume of a single battery module in Kilograms (kg) and cubic metres (m^3), respectively.

- **Calculation regarding power demand**

In order to calculate the number of battery modules required for the peak power demand, the discharging power for each battery module should be calculated:

$$P_{Bat}^{Mod} = I_{Bat}^{Mod} \times V_{Bat}^{Mod}(Max) \tag{3.2.5}$$

where I_{Bat}^{Mod} is the typical discharging current of the battery module in Amperes (A) obtained by:

$$I_{Bat}^{Mod} = \frac{C_{Bat}^{Mod}}{T} \tag{3.2.6}$$

and T is the time in Hours (h). Now the number of battery modules needed to meet the peak power demand can be obtained:

$$N_{Bat}^{P} = \frac{P_{Bat}^{eq}}{P_{Bat}^{Mod} \times [SOC_{Bat}(Max) - SOC_{Bat}(Min)]} \quad (3.2.7)$$

where P_{Bat}^{Req} is the peak power that the battery pack needs to meet in Watts (*W*). The weight and volume of the battery pack sized regarding the power demand can be achieved using the equations below [27], [38], [77]:

$$Wei_{Bat}^{P} = N_{Bat}^{P} \times Wei_{Bat}^{Mod} \quad (3.2.8)$$

$$Vol_{Bat}^{P} = N_{Bat}^{P} \times Vol_{Bat}^{Mod} \quad (3.2.9)$$

3.2.1.3. Sizing the Supercapacitor Pack

As for the batteries, the supercapacitor pack needs to be sized regarding energy demand and power demand separately, and the greater number of modules is chosen at the end. By determining the energy and power that the supercapacitor pack needs to provide, the number of supercapacitor modules can be calculated.

- **Calculation regarding energy demand**

Using the same process as for sizing the battery pack, the amount of energy that can be stored in a single supercapacitor module should be calculated first:

$$E_{SC}^{Mod} = \frac{1}{2} \times C_{SC}^{Mod} \times [V_{SC}^{Mod}(Max)]^2 \quad (3.2.10)$$

where C_{SC}^{Mod} is the capacity of the supercapacitor module in Farads (*F*) and $V_{SC}^{Mod}(Max)$ is the maximum voltage of the module in Volts (*V*). Now the number of supercapacitor modules required to meet the energy demand can be calculated:

$$N_{SC}^{E} = \frac{E_{SC}^{Re}}{E_{SC}^{Mod} \times [1 - [SOC_{SC}(Max) - SOC_{SC}(Min)]^2]} \quad (3.2.11)$$

where E_{SC}^{Req} is the energy requirement that the supercapacitor pack needs to provide in Watt-hours (Wh). As for the battery, $SOC_{SC}(Max)$ is considered to be 100% and $SOC_{SC}(Min)$ is considered to be 20%, making the total efficiency of the supercapacitor module 80%. Then the total weight and volume of the supercapacitor pack which is sized regarding energy demand can be determined:

$$Wei_{SC}^{E} = N_{SC}^{E} \times Wei_{SC}^{Mod} \quad (3.2.12)$$

$$Vol_{SC}^{E} = N_{SC}^{E} \times Vol_{SC}^{Mod} \quad (3.2.13)$$

where Wei_{SC}^{Mod} is the weight in Kilograms (kg) and Vol_{SC}^{Mod} is the volume in Cubic-metres (m^3) for a single supercapacitor module.

- **Calculation regarding power demand**

The procedure to determine the weight and volume of a supercapacitor pack regarding power demand is the same as for batteries. The discharging power that each supercapacitor module is able to provide can be obtained as below:

$$P_{SC}^{Mod} = I_{SC}^{Mod} \times V_{SC}^{Mod}(Max) \quad (3.2.14)$$

where I_{SC}^{Mod} is the typical discharging current of the supercapacitor module in Amperes (A). This power is the typical discharging power of the supercapacitor considering the supercapacitor's allowed discharging current.

Following this, the number of supercapacitor modules required to meet the required peak power demand can be determined:

$$N_{SC}^{P} = \frac{P_{SC}^{Re}}{P_{SC}^{Mod}} \tag{3.2.16}$$

where P_{SC}^{Req} is the peak power in Watt (W) that should be met by the supercapacitor pack. Finally, the weight and volume of the supercapacitor pack can be achieved:

$$Wei_{SC}^{P} = N_{SC}^{P} \times Wei_{SC}^{Mod} \tag{3.2.17}$$

$$Vol_{SC}^{P} = N_{SC}^{P} \times Vol_{SC}^{Mod} \tag{3.2.18}$$

Finally, the total weight and volume of the HESS regarding either the energy demand or the power demand can be obtained as below [37], [38], [116]:

$$Wei_{HESS} = Wei_{Bat} + Wei_{SC} \tag{3.2.19}$$

$$Vol_{HESS} = Vol_{Bat} + Vol_{SC} \tag{3.2.20}$$

3.2.2. Tests for Evaluation

Now that the procedure for calculating the number of modules for both the battery pack and supercapacitor pack is determined, it is possible to size a battery-only ESS, supercapacitor-only ESS and an HESS including batteries and supercapacitors in order to compare their weights and volumes and, moreover, to evaluate the influence of the energy density and power density of both devices on the total size of the storage system.

3.2.2.1. Size and Influence Evaluation

- **Case 1: Energy Demand and Power Demand Separately**

In the first case, energy demand and power demand are considered separately. Battery-only, supercapacitor-only and hybrid storage systems should be sized in such a way to provide the total energy required from the storage system. Five scenarios can be considered in order to size the storage system, as indicated in Table 3.2.1. Scenario 1 is the battery-only storage system where all the required energy is provided by the battery. Scenario 5 is the supercapacitor-only storage system where supercapacitor is in charge of meeting the whole energy demand.

Table 3.2.1. Five scenarios to meet the energy demand

Scenario	Storage device	Energy supply percentage
Scenario 1	Bat	100%
	SC	0%
Scenario 2	Bat	75%
	SC	25%
Scenario 3	Bat	50%
	SC	50%
Scenario 4	Bat	25%
	SC	75%
Scenario 5	Bat	0%
	SC	100%

In Scenarios 2-4, which are hybrid storage systems, different supply percentages are considered for the battery and supercapacitor to meet the energy requirement in order to observe the effects of the energy density of both battery and supercapacitor on the total size of the HESS. For instance, in Scenario 2, 75% of the total energy demand is to be supplied by the battery pack and 25% of the total energy demand is to be met by the supercapacitor pack. When the total energy requirement is known from the simulation, this amount of energy can be split between the battery and supercapacitor for each scenario according to the considered percentages and the weight and volume of the storage systems can be calculated using the procedures stated in Sections 3.2.1.2 and 3.2.1.3. Therefore, it can be decided which storage system has the lowest

weight and volume regarding energy requirement and moreover, the influence of the energy densities of both battery and supercapacitor can be assessed.

The same process can be executed for meeting the peak power demand. Five scenarios can be considered; in each scenario, the battery and supercapacitor are responsible for meeting different percentages of the peak power demand. These scenarios are indicated in Table 3.2.2. Here, the sizes of the storage systems can be compared regarding power, and the influence of the power densities of both devices on the total size of the storage system can be evaluated.

Table 3.2.2. Five scenarios to meet the peak power demand

Scenario	Storage device	Peak power supply percentage
Scenario 1	Bat	100%
	SC	0%
Scenario 2	Bat	75%
	SC	25%
Scenario 3	Bat	50%
	SC	50%
Scenario 4	Bat	25%
	SC	75%
Scenario 5	Bat	0%
	SC	100%

Although the methods mentioned give a generic opportunity to compare the sizes of battery-only/supercapacitor-only ESSs with HESSs including both battery and supercapacitor, and also help to evaluate the effects of the energy density and power density of both devices on the total size of the storage system, they cannot be referred to as an adequate validation for this project. In train traction, both energy demand and peak power demand should be met simultaneously during the journey and hence the ESS/HESS should be sized in order to provide both energy and peak power properly. Therefore, there should be scenarios where both energy demand and peak power demand are considered together to size the storage system.

- **Case 2: Energy Demand and Power Demand Together**

In order to have scenarios considering both energy demand and peak power demand, the above-mentioned scenarios can be considered together. The five scenarios regarding energy demand can be combined with the five scenarios regarding peak power demand, and twenty five scenarios can be obtained. In this case, all combinations to meet both energy demand and peak power demand simultaneously are considered and as a result, the proximity of validation of the incoming results is increased. Table 3.2.3 indicates these 25 scenarios.

Table 3.2.3. Twenty-five scenarios to meet energy demand and peak power demand simultaneously

Scenario	Storage device	Energy supply percentage	Peak power supply percentage
Scenario 1	Bat	100%	100%
	SC	0%	0%
Scenario 2	Bat	100%	75%
	SC	0%	25%
Scenario 3	Bat	100%	50%
	SC	0%	50%
Scenario 4	Bat	100%	25%
	SC	0%	75%
Scenario 5	Bat	100%	0%
	SC	0%	100%
Scenario 6	Bat	75%	100%
	SC	25%	0%
Scenario 7	Bat	75%	75%
	SC	25%	25%
Scenario 8	Bat	75%	50%
	SC	25%	50%
Scenario 9	Bat	75%	25%
	SC	25%	75%
Scenario 10	Bat	75%	0%
	SC	25%	100%
Scenario 11	Bat	50%	100%
	SC	50%	0%
Scenario 12	Bat	50%	75%
	SC	50%	25%
Scenario 13	Bat	50%	50%
	SC	50%	50%
Scenario 14	Bat	50%	25%
	SC	50%	75%
Scenario 15	Bat	50%	0%
	SC	50%	100%
Scenario 16	Bat	25%	100%
	SC	75%	0%
Scenario 17	Bat	25%	75%
	SC	75%	25%
Scenario 18	Bat	25%	50%
	SC	75%	50%
Scenario 19	Bat	25%	25%
	SC	75%	75%
Scenario 20	Bat	25%	0%
	SC	75%	100%

Scenario 21	Bat	0%	100%
	SC	100%	0%
Scenario 22	Bat	0%	75%
	SC	100%	25%
Scenario 23	Bat	0%	50%
	SC	100%	50%
Scenario 24	Bat	0%	25%
	SC	100%	75%
Scenario 25	Bat	0%	0%
	SC	100%	100%

Regarding the battery, in each scenario the percentage of the required energy that the battery pack needs to supply is different to the percentage of the peak power demand that it is in charge of supplying. In other words, the battery pack should supply a given percentage of the energy demand and it is responsible for supplying a different percentage of the peak power demand. In Scenario 2, for instance, the battery pack should supply all the required energy, but it is responsible for meeting 75% of the required peak power, and the rest should be met by the supercapacitor pack. It is the same for the supercapacitor pack where different numbers of modules are achieved for this pack to meet the energy demand and the peak power demand. Hence, in each scenario for either battery pack or supercapacitor pack, the higher number of modules is considered to be on the safe side and to be ensured that both energy demand and peak power demand, to be provided by either battery pack or supercapacitor pack, are met properly.

$$N_{Bat} = Max(N_{Bat}^{E}, N_{Bat}^{P}) \tag{3.2.21}$$

$$N_{SC} = Max(N_{SC}^{E}, N_{SC}^{P}) \tag{3.2.22}$$

After choosing the higher number of modules, by using the equations mentioned in Sections 3.2.1.2 and 3.2.1.3, the weight and volume of either battery pack or supercapacitor pack can be calculated accordingly; following this, the total weight and volume of the HESS can be determined.

Scenario 1 is the battery-only storage system, Scenario 25 is the supercapacitor-only storage system and Scenarios 2–24 are HESSs with different percentages of energy and power supply for battery and supercapacitor. By taking this measure, ESSs can be compared to HESSs regarding weight and volume and the influence of the energy and power densities of the chosen storage devices can be assessed considering both energy demand and peak power demand at the same time. Therefore, the validation process is more precise.

3.2.2.2. C-rate of the Battery

As mentioned in Section 2.4.2.1, the C-rate of a battery is a measurement of the rate at which the battery discharges according to its maximum capacity. The C-rate states the discharge current of batteries. When a battery is discharged at 1 C-rate, it becomes fully empty in an hour. When it is said that the C-rate of a battery has increased, it means that the battery is discharged at a higher current and hence, it is able to deliver energy in a shorter period of time. In other words, the specific power of the battery increases [77]. While increasing the C-rate of the battery increases the specific power that it can provide, it makes battery discharge in a shorter time and moreover, it decreases the battery's life time [24], [41], [77], [140].

The C-rate of the battery is an important factor when sizing a battery pack and consequently, sizing an HESS including battery and supercapacitor since it directly affects the specific power that a battery module can provide to be able to meet the power demand. In order to assess the effects of the C-rate of the battery on the total size of the HESS and also on the performance of the battery, a different approach is used to size the HESS in which the C-rate of the battery is considered.

Firstly, the energy that a battery module can provide and then the number of battery modules required to meet the total energy demand should be determined:

$$E_{Bat}^{Mod} = C_{Ba}^{Mod} \times V_{Bat}^{Mod}(Max) \tag{3.2.23}$$

$$N_{Bat} = \frac{E_{Bat}^{Req}}{E_{Bat}^{Mod} \times [SOC_{Bat}(Max) - SOC_{Bat}(Min)]} \tag{3.2.24}$$

Then, the power that each battery module is able to provide, considering the C-rate, can be determined:

$$P_{Bat}^{Mod} = \text{Crate} \times I_{Bat}^{Mod} \times V_{Bat}^{Mod}(Max) \tag{3.2.25}$$

Now the maximum power that the number of battery modules obtained from Equation (3.2.24) is able to provide can be calculated:

$$P_{Bat}^{Req} = N_{Bat} \times P_{Bat}^{Mod} \times [SOC_{Bat}(Max) - SOC_{Bat}(Min)] \tag{3.2.26}$$

The rest of the peak power demand can be supplied by the supercapacitor pack:

$$P_{SC}^{Req} = P_{Req} - P_{Bat}^{Req} \tag{3.2.27}$$

and the number of supercapacitor modules can be determined based on the power required from the supercapacitor pack:

$$N_{SC} = \frac{P_{SC}^{Req}}{P_{SC}^{Mod}} \tag{3.2.28}$$

where

$$P_{SC}^{Mod} = I_{SC}^{Mod} \times V_{SC}^{Mod}(Max) \tag{3.2.29}$$

The weights and volumes of the battery pack and the supercapacitor pack can be obtained as below:

$$Wei_{Bat} = N_{Bat} \times Wei_{Bat}^{Mod} \quad (3.2.30)$$

$$Vol_{Bat} = N_{Bat} \times Vol_{Bat}^{Mod} \quad (3.2.31)$$

$$Wei_{SC} = N_{SC} \times Wei_{SC}^{Mod} \quad (3.2.32)$$

$$Vol_{SC} = N_{SC} \times Vol_{SC}^{Mod} \quad (3.2.33)$$

Finally, the total size of the HESS can be determined:

$$Wei_{HESS} = Wei_{Bat} + Wei_{SC} \quad (3.2.34)$$

$$Vol_{HESS} = Vol_{Bat} + Vol_{SC} \quad (3.2.35)$$

By Increasing the C-rate of the battery, the change in the total size of the HESS can be observed.

3.2.3. Methodology Validation

The next step is to validate the proposed methodology. In order to achieve this, the performance of the sized HESS needs to be observed and assessed. Methods were proposed in the last section to determine the number of battery modules and supercapacitor modules by knowing the required energy demand and power demand that each pack needs to meet. However, this does not determine how this sized HESS behaves in providing the required energy and power demand during the journey. The performance of the sized HESS needs to be tracked in order to validate its ability to meet the demands and therefore, validate the proposed sizing method.

3.2.3.1. Supplying the Required Energy and Power

The first validation method is to be ensured that the sized HESS is able to meet the required energy and power. Hence, all 25 scenarios are simulated in STS in order to observe and compare their performances in supplying the required energy and power. Below are the factors considered for the HESS when employed during the journey:

- Battery pack and supercapacitor pack meet the total energy demand and power demand regarding their energy and power limit.

- Regarding the rate of charge/discharge, for the first assessment where C-rate is not a variable factor, it is considered that the battery pack is not charged/discharged at more than its 1 C-rate. According to the literature, charging batteries in higher C-rates make them discharge quicker and frequency charge/discharge harms batteries and shortens their lifetime. With regard to the supercapacitor pack, it is charged/discharged at its typical power.

- Regarding regenerative braking energy, in general it is considered that regen energy is absorbed by the supercapacitor pack during braking as a supercapacitor has a high power density than a battery and is capable of absorbing more regen energy than battery. However, if the SOC of the battery goes below 50%, the regen energy is to be absorbed by the battery pack. This is because the battery plays the main role in providing the energy demand during the journey. The regeneration rate is determined as 0.5.

- In scenarios where either the battery pack or supercapacitor pack is sized based on only energy demand or power demand, the pack will not be able to meet the required demands during the journey. Hence, the pack becomes empty earlier than expected and will not be

able to provide its share of the supply. The general solution in these scenarios is to use the other storage device to compensate and meet the requirements in lieu of the empty device. This is feasible only if the other device has an adequate amount of energy stored. Furthermore, other measures can be taken to make the HESS perform properly in these scenarios. The measures can be increasing the number of modules, or getting the other device to act as an energy supply and charge that device before becoming empty. The latter method will be discussed in detail in Section 3.3.4.

By simulating the train traction, where the required energy and power demands are to be met by the HESS, it can be observed how the HESS supplies the train during the journey and the capability of the HESS to meet the required energy and power demand can be seen. This will validate the proposed methodology in sizing an HESS. Moreover, this simulation will indicate the necessity of considering both energy demand and power demand in determining the number of battery and supercapacitor modules; if a sized HESS does not work properly in a scenario due this essential matter, the simulation will make this clear. Thus, the proposed validation process validates this necessity as well.

3.2.3.2. SOC of the HESS

Another approach for validating the sizing procedure is to observe the changes in the HESS's SOC during the journey. The SOCs of both the battery pack and supercapacitor pack can be tracked, which makes it possible to see how both packs behave in different modes of the journey. Simulating the SOC of the HESS indicates how the battery pack and supercapacitor pack discharge in acceleration and cruising modes and how they charge from regen energy during braking modes. By tracking the stored energy in both the battery pack and supercapacitor

pack during the journey, it is possible to evaluate whether both packs have been sized properly to meet the traction requirements and hence, the proposed sizing methodology will be validated.

3.3. Sizing the HESS in the Frequency Domain

After evaluating the integration of battery and supercapacitor in an HESS and proposing methods to calculate the number of battery and supercapacitor modules, the HESS needs to be sized optimally. Although 25 possible combinations of battery and supercapacitor were considered in Section 3.2, they were proposed based on mathematical calculations only and for validation purposes. The HESS needs to be sized optimally in order to minimise its size, which minimises the total mass of the train and hence decreases the total energy consumption of the train during the journey.

As mentioned in Chapter 2, an optimal sizing method in the frequency domain was chosen for this project due to the small amount of computations and fast and credible results. This section proposes a method to size the HESS optimally in the frequency domain using FFT and Brute Force optimisation with the objective function of weight and volume minimisation. As in Section 3.2, the performance of the sized HESS during the journey is evaluated to validate the use of FFT alongside Brute Force Optimisation in sizing an HESS.

The same as the previous part, this project only considers the weight and volume of battery modules and supercapacitor modules in the HESS and the weight and volume of other parts are not considered.

3.3.1. Frequency Analysis Method

In order to start sizing the HESS using the Frequency Analysis, the first step is to design filters. In this project, both low-pass and high-pass filters are employed. In general, there are two types of digital filter: Finite Impulse Response (FIR) and Infinite Impulse Response (IIR). An FIR filter has a finite duration. Another name for these types of filters is 'non-recursive' filter which means that the filter takes only input values for calculation. An FIR has linear phase characteristics. In order to obtain precise results while using an FIR, the order number should be high. A higher order increases the amount and time of calculation. An IIR filter, which has infinite duration, is a recursive filter where in addition to input values, previous output values are also considered. This enhances the sensitivity of the filter. An IIR has non-linear phase characteristics and requires a lower order than an FIR in order to have the same performance as a high-order FIR. In this project, an IIR filter is chosen due to less and faster computation and more sensitivity. There are different types of IIR filters: Butterworth, Chebyshev I, Chebyshev II, Bessel and Elliptic filters. In this project, a Butterworth filter is used because it has very low ripples in the pass band and stop band [141], [142], [143], [144]. However, although Butterworth filter is called a maximally flat filter and has the lowest ripples among all IIR filters, overshoots/undershoots can happen. This is because Butterworth filter is underdamped and therefore, overshoots and undershoots happen whenever there is a rapid transition in the data, such as acceleration and braking modes in both case studies for this project [143], [145], [146].

A proper cut-off frequency should be determined for both filters. Various cut-off frequencies can lead to different low pass-filtered and high pass-filtered results, different energy and power demands that the battery pack and supercapacitor pack need to meet, different numbers of

modules for both battery pack and supercapacitor pack and, eventually, different sizes for the HESS. Therefore, it is crucial to determine optimal cut-off frequencies for both filters.

After designing the filters, they are ready to be applied to the load. As in Section 3.2, first the train traction needs to be simulated in STS. In this phase, the Power/Frequency result is of interest. Both low-pass and high-pass filters need to be applied to this result in order to split the power demand into low-frequency parts and high-frequency parts. The low-frequency parts of the demand are to be supplied by the battery pack because of its low power density; for high-frequency parts of the demand, the supercapacitor is in charge of supply because of its high power density. It is obvious that the power demand determined from the simulation is in the time domain. In order to apply the filters, the power demand needs to be in the frequency domain. Hence, with the help of an FFT, the Power/Time result is transformed into Power/Frequency. This is executed with the FFT function in MATLAB. The result is then transformed back into time domain. The power split is indicated in Figure 3.3.1

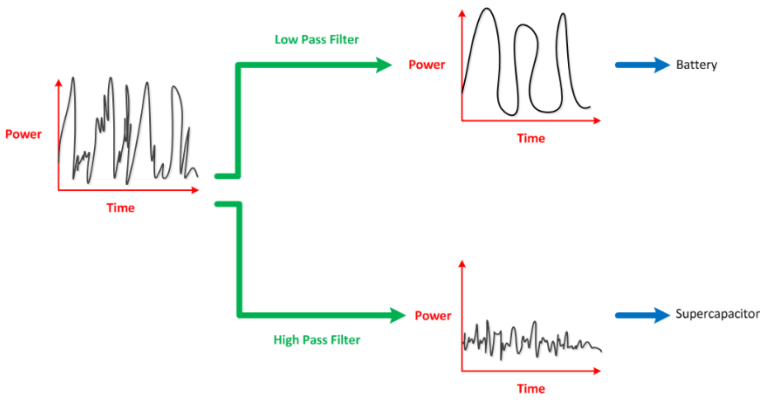

Figure 3.3.1. Power split using low-pass filter and high-pass filter

3.3.1.1. Sizing the Battery Pack Using a Low-Pass Filter

Now the designed low pass filter can be applied into the Power/Frequency result, and the low pass-filtered Power/Frequency is obtained. This result is then transformed back into the time domain. The power demand which needs to be supplied by the battery pack is obtained by:

$$P_{Bat}^{Req} = Max[Max[P(t)_{Low}], Min[P(t)_{Low}]] \tag{3.3.1}$$

where $P(t)_{Low}$ is the low pass-filtered power demand in the time domain, $Max[P(t)_{Low}]$ is the maximum discharging power and $Min[P(t)_{Low}]$ is the maximum charging power of the low pass-filtered power demand.

Then, Equations (3.2.5) to (3.2.7) can be used in order to determine the number of battery modules regarding peak power demand. Now the number of battery modules regarding the energy demand should be determined. To achieve this, the energy demand of the low frequency parts of the power demand should be obtained first. By integrating the low pass-filtered Power/Time result, the low pass-filtered Energy/Time can be determined by:

$$E(t)_{Low} = \int_0^t P(t)_{Low} \tag{3.3.2}$$

and the energy demand which the battery pack is in charge of supplying can be determined by:

$$E_{Bat}^{Req} = Max[E(t)_{Low}] - Min[E(t)_{Low}] \tag{3.3.3}$$

where $Max[E(t)_{Low}] - Min[E(t)_{Low}]$ expresses the energy variation over the whole journey. The energy capacity of the battery pack should be able to meet the difference between the maximum energy and the minimum energy.

By using Equations (3.2.1) and (3.2.2), the number of battery modules regarding the energy demand can be determined. As mentioned before, after calculating the number of modules regarding energy demand and peak power demand, the higher number of modules needs to be chosen to be on the safe side and to be ensured that both demands are met properly. Hence, according to Equation (3.2.21), the higher number of modules is determined. Due to the high energy density and low power density of battery, it is expected that the higher number of modules is the number of modules regarding power demand. Finally, the weight and volume of the battery pack can be determined by employing Equations (3.2.30) and (3.2.31) [37], [116].

3.3.1.2. Sizing the Supercapacitor Pack Using a High-Pass Filter

Now the designed high-pass filter is applied to the Power/Frequency power demand (obtained by FFT) in order to achieve the high pass-filtered result. Again, this result which is in the frequency domain is transformed into the time domain. As for the low pass-filtered result, the power demand that should be supplied this time by the supercapacitor pack is obtained by:

$$P_{SC}^{Req} = Max[Max\left[P(t)_{High}\right], Min\left[P(t)_{High}\right]] \tag{3.3.4}$$

where $P(t)_{High}$ represents the high pass-filtered power demand in the time domain and $Max\left[P(t)_{High}\right]$ and $Min[P(t)_{Low}]$ are the maximum discharging power and the maximum charging power of the high pass-filtered power demand, respectively. Equations (3.2.14) and (3.2.16) can be used to calculate the number of supercapacitor modules regarding peak power demand. As for the procedure used to size the battery pack, integrating the high pass-filtered Power/Time result can lead to Energy/Time:

$$E(t)_{High} = \int_0^t P(\quad)_{High} \tag{3.3.5}$$

And the energy requirement that should be met by the supercapacitor pack is obtained by:

$$E_{SC}^{Req} = Max\left[E(t)_{High}\right] - Min[E(t)_{High}] \tag{3.3.6}$$

Equations (3.2.10) and (3.2.11) can be used to calculate the number of supercapacitor modules regarding energy demand, and Equation (3.2.22) determines the final number of supercapacitor modules. Due to the high power density and low energy density of supercapacitors, it is expected that the higher number of modules is the number of modules regarding energy demand. Eventually, the weight and volume of the supercapacitor pack can be acquired by employing Equations (3.2.32) and (3.2.33).

Now, by knowing the sizes of both the battery pack and supercapacitor pack, the total size of the HESS can be obtained using Equations (3.2.34) and (3.2.35).

3.3.2. Choosing an Optimal Cut-off Frequency and Sizing the HESS

As mentioned previously, the most crucial part in sizing an HESS using the Frequency Analysis method is to use an optimal cut-off frequency for both the low-pass filter and high-pass filter since this affects the weight and volume of the HESS. In order to find the optimal cut-off frequency/frequencies, an optimisation method can be employed. As mentioned in Section 2.5.2, for this project Brute Force Optimisation is chosen where all possible cut-off frequencies and their respective weights and volumes are considered in order to find the cut-off frequency/frequencies that results in the lowest weight and volume of the HESS. Brute Force is built in MATLAB.

To start the optimisation procedure, a suitable range needs to be determined for the cut-off frequencies. The Sample frequency is 1Hz. In filters, the Nyquist frequency is the frequency at which any result sampled beyond this frequency is distorted and signals are reconstructed. The Nyquist frequency is half of the Sample frequency, which is 0.5Hz in this project. Hence, the upper limit of the cut-off frequency range is considered to be 0.5Hz. For the lower limit, 1μHz is considered. Moreover, the step is considered to be 1μHz, which makes 500,000 iterations.

For the first iteration, a 1μHz cut-off frequency is considered for both the low-pass filter and high pass-filter, and all the procedures explained in Section 3.3.1.1 for sizing the battery pack and Section 3.3.1.2 for sizing the supercapacitor pack are executed. At the end of this iteration, the total weight and volume of the HESS are achieved for a 1μHz cut-off frequency. Then, the whole procedure is carried out in the second iteration, for a 2μHz cut-off frequency, and again the total size of the HESS is obtained. This is repeated to the last iteration, a 0.5Hz cut-off frequency. The total weight and volume of the HESS achieved in each iteration is saved and eventually, the minimum weight and volume of the HESS among 500,000 iterations are chosen, which leads to the optimum cut-off frequency for the filters. It should be noted that since there are two different parameters to find the minimum amount for, weight and volume, two different optimal cut-off frequencies might be achieved at the end. A decision needs to be made should this happens and only one optimal cut-off frequency should be chosen for designing the filters and sizing the HESS. Figure 3.3.2 indicates the proposed Frequency Analysis method a Brute Force optimisation procedure for finding optimal cut-off frequency for the filters.

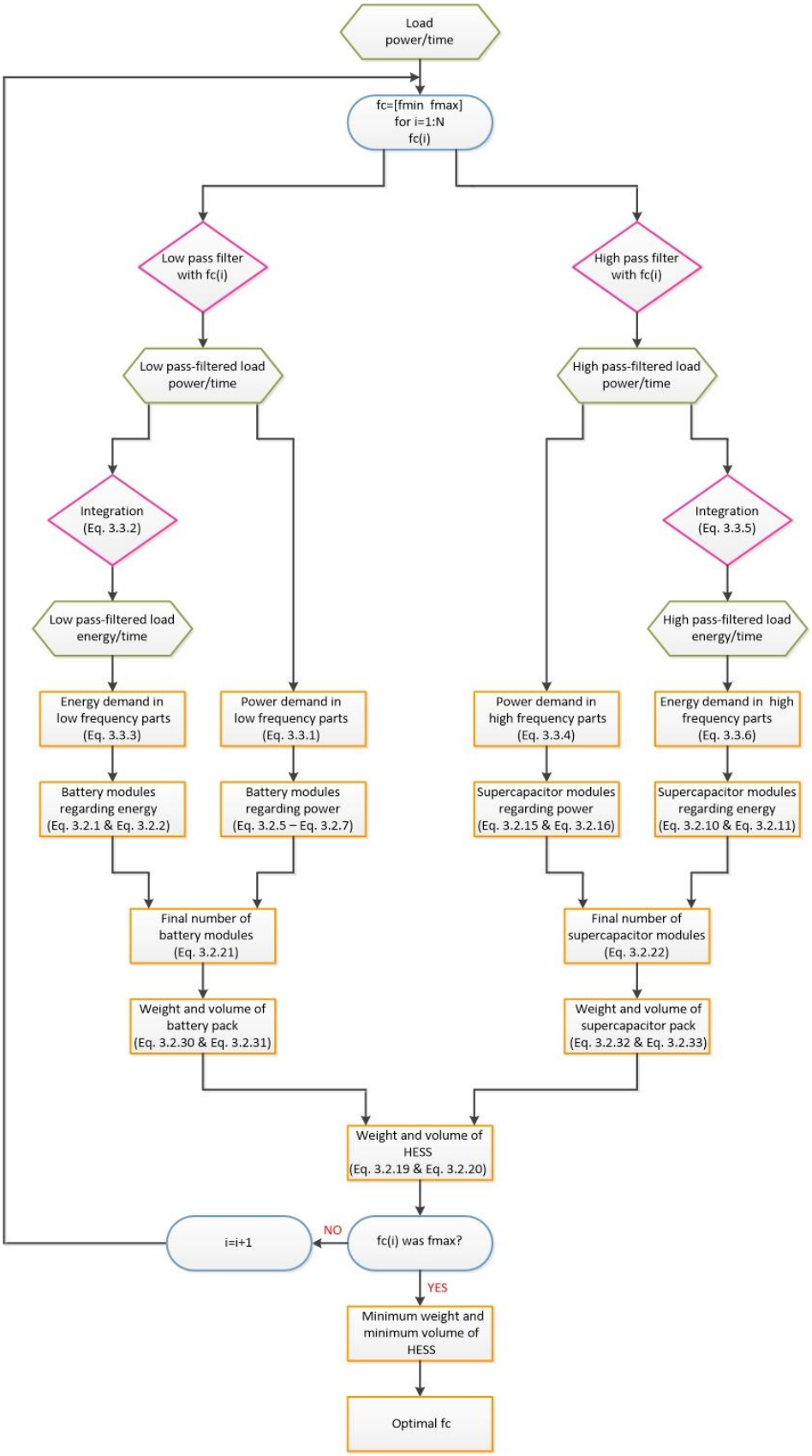

Figure 3.3.2. Brute force optimisation to find the optimal cut-off frequency

3.3.3. C-rate Constraint in Energy-based and Power-based Calculations

In power-based calculations, the power requirement and the device's specific power are the bases of determining the number of modules. This automatically considers the allowable discharging power of the energy storage device and C-rate constraint is generally considered in these calculations. As mentioned in Sections 3.3.1.1, it is expected that the final number of batteries is determined based on the power demand calculations and hence, the C-rate constraint is met while determining the number of battery modules.

On the other hand, due to the nature of energy-based calculations, these calculations only focus on the total energy requirement that the energy storage device needs to meet, and the device's specific energy is the base parameter for the device considered to determine the final number of modules disregard the device's typical discharging power. If the device's typical discharging power is of a great importance in discharging procedure, there is a risk that the energy-based sized pack discharges higher than its typical discharging power during the journey, becomes empty earlier than expected and consequently, is not able to meet the required energy and power.

As mentioned in Section 3.3.1.2, it is expected that the final number of supercapacitors is determined based on the energy demand calculations. In order to check if the sized supercapacitor pack discharges within the limit of its typical discharging power during the journey, the C-rate constraint can be imposed on the energy based-sized supercapacitor pack after determining the final number of supercapacitors from the high pass-filtered energy result. If the sized supercapacitor pack is not able to meet the required energy and power demand for which it was responsible after considering the C-rate constraint, this means the already sized

supercapacitor pack discharges at higher C-rates than allowed which makes it become empty earlier than expected.

By increasing the number of supercapacitors, the power capability of the supercapacitor pack increases and hence, the supercapacitors do not need to discharge higher than their typical discharging power. This in turn will help the supercapacitor pack to be able to meet the required energy and power demand.

3.3.4. Employing Battery Pack as an Energy Supplier

Due to the high energy density of batteries and their ability to save greater amount of energy compared to supercapacitors, these energy storage devices can be employed to act as an active energy supplier during the journey and charge supercapacitors. By charging supercapacitors in intervals or continuously during the journey, the supercapacitor pack does not need to be accurately sized to meet the total required energy and power demand that it is responsible for as it can receive a part of the required energy during the journey by the battery pack. This will lead to a decreased number of supercapacitor modules and hence, a decreased size of the HESS.

In order for the batteries to charge supercapacitors during the journey, optimisation methods can be defined and applied. Inputs can be used to reach the defined objective functions considering constraints and criteria. Table 3.3.1 indicates requirements for optimisation methods to charge supercapacitors by batteries. Fixed inputs are the total energy and power requirements and also characteristics of batteries and supercapacitors. Numbers of batteries and supercapacitors can be controlled and hence, are considered as variable inputs. Moreover, the discharging power of batteries to charge supercapacitors is a variable input. Different objective functions can be considered, but according to the main objectives of this project, the objective function here is to minimise the total size of the HESS. The most important constraint in the

optimisation procedure is for the HESS to be able to meet the total energy and power requirements. Moreover, the SOC of the battery pack or supercapacitor pack are other constraints that might be needed. Various criteria can be considered for the optimisation methods, such as charging supercapacitors based on the mode of traction (acceleration, coasting, cruising and braking), charging based on the energy left in the supercapacitors, or charging based on journey time.

Table 3.3.1. Requirements for optimising battery charging supercapacitors

Fixed Input	Variable Input	Objective Function	Constraint	Criteria
$E_{Tot}^{Req}, P_{Tot}^{Req}$				Charging based on the mode of traction
$E_{Bat}^{Mod}, P_{Bat}^{Mod}$	N_{Bat}		Meeting $E_{Tot}^{Req}, P_{Tot}^{Req}$	
Wei_{Bat}, Vol_{Bat}	N_{SC}	Minimising Wei_{HESS}, Vol_{HESS}	SOC_{Bat}	Charging based on SOC_{SC}
$E_{SC}^{Mod}, P_{SC}^{Mod}$	P_{Bat}^{Dis}		SOC_{SC}	Charging based on journey time
Wei_{SC}, Vol_{SC}				

In this project, the charging method is proposed as a further analysis in frequency domain sizing procedure and is dependent on the results achieved from the Frequency Domain analysis. Hence, the charging procedure is applied to the HESS which is already sized using the Frequency Analysis method.

Two charging criteria are considered for this project and for each criteria, two scenarios are proposed. The criteria and associated scenarios are set out as below:

1. Charging based on SOC of the supercapacitor pack:
    a) Battery pack charging supercapacitor pack whenever SOC of the supercapacitor pack goes below 1%,
    b) Battery pack charging supercapacitor pack whenever SOC of the supercapacitor pack goes below 100%.
2. Charging based on the mode of traction:
    a) Battery pack charging supercapacitor pack only in acceleration modes,
    b) Battery pack charging supercapacitor pack only in cruising modes.

Brute Force optimisation will be applied to all four scenarios with the objective function of minimising the total size of the HESS. For the optimisation process, the fixed inputs stated in Table 3.3.1 stay fixed. Since the battery pack will act as the energy supply to charge the supercapacitor pack during the journey, the number of battery modules is considered as fixed inputs. The number of supercapacitor modules is considered as the variable input which needs to be optimised in order to achieve the objective of the optimisation method. Moreover, since the C-rate of the battery has been considered as a significant factor throughout the whole project and it is important not to discharge batteries higher than their 1 C-rate, the discharging power of the batteries to charge supercapacitors is considered fixed at 1 C-rate for the charging procedures. Two constraints need to be considered for this optimisation problem. The first one is for the HESS to be able to meet the total energy and power demand, and the second one is for the supercapacitor pack's minimum SOC which should be between 0 and 1 and it should not become 0. This means the number of supercapacitor modules need to decrease as much as

the HESS is still able to meet the required energy and power demand without making the supercapacitor pack empty during the journey.

3.3.5. Methodology Validation

As in the first phase of this project, the Evaluation Phase, this phase needs validation as well. General and specific validation methods are introduced for this phase in order to validate the proposed Frequency Analysis method.

3.3.5.1. Brute Force Optimisation Validation

As mentioned in Section 3.3.2, the most crucial part of the proposed Frequency Analysis method is to find out the most optimal cut-off frequency for the filters. Brute Force optimisation is considered to achieve this goal. In order to validate this optimisation method, the results for all iterations achieved from the optimisation method need to be analysed. The figures indicating the cut-off frequency versus the total weight and volume of the HESS will be analysed to see whether the determined optimal cut-off frequency results in the minimum weight and volume of the HESS.

Brute Force optimisation proposed for charging procedure will be validated as well. The figures showing the number of supercapacitor modules versus the minimum SOC of the supercapacitor pack during the journey will be analysed to validate the results.

3.3.5.2. FFT+Filters Validation

In order to size the HESS in frequency domain, FFT and low pass and high pass filters are the bases of the proposed method. After validating the proposed Brute Force optimisation method for finding the most optimal cut-off frequency/frequencies for the filters, then the designed

filters need to be validated. The filtered results will be added in order to see whether the initial results before filtering can be obtained. This will indicate whether the FTT method works well and if the filters are designed properly. The low pass-filtered Power/Time result can be added to the high pass-filtered Power/Time result to obtain the very first Power/Time result and moreover, the low pass-filtered Energy/Time can be added to the high pass-filtered Energy/Time result to see whether the unfiltered Energy/Time result can be achieved. By achieving the initial results, proposed FFT method and designed filters can be validated.

3.3.5.3. Sizing in Frequency Domain Validation

The performance of the sized HESS should be assessed to validate the whole Frequency Analysis method chosen for optimal sizing of the HESS. The validation methods are the same as those used for the first phase of this project. As mentioned in Section, it should be seen whether the sized HESS is able to meet the energy demand and the power demand during the journey. All considerations mentioned in Section 3.2.3 are considered here as well. Following this, the SOCs of both the battery pack and supercapacitor pack are tracked in order to observe the rate of changes of the stored energies in both packs. The chosen Frequency Analysis method will be validated if the sized HESS performs properly in meeting the total energy and power demand. This validation might indicate that choosing the higher number of modules for both packs may lead to some energy being left in either pack at the end of the journey. Therefore, other methods will be proposed in order to decrease the size of the HESS.

3.4. Summary

This chapter discussed the methodology used in this project. Two phases were considered to reach the aim of the project and the approaches proposed in each phase were discussed.

The objective of the first phase was to evaluate the use of battery and supercapacitor together in an on-board HESS. After proposing calculations for sizing the battery pack and supercapacitor pack regarding energy demand and power demand, evaluation tests were introduced. Five scenarios, considering the energy demand and the power demand separately, and then 25 scenarios, considering the energy demand and the power demand simultaneously, were introduced to compare the weight and volume of the HESS with battery-only and supercapacitor-only ESSs. Moreover, scenarios were introduced to assess the influence of the energy density and power density of both the battery pack and supercapacitor pack on the total size of the HESS. Assessing the effect of a change in the C-rate of the battery on the total size of the HESS was another test proposed in the first phase. Validation methods were introduced to assess the proposed methods.

In the second phase, the Frequency Analysis method was proposed to size the HESS. Low-pass and high-pass filters were proposed to split the power demand into low-frequency and high-frequency parts, where battery was chosen as the storage device to support the low-frequency parts and supercapacitor to support the high-frequency parts of the demand. Brute Force was also proposed as an optimisation method to determine the optimal cut-off frequency for both filters. Following this, imposing C-rate constraint on energy based-sized supercapacitor pack was proposed. Moreover, it was proposed to use batteries as active energy suppliers in order to charge supercapacitors during the journey. In order to validate the proposed methodology in this phase, validation procedures were introduced.

These mentioned methodologies will be applied to the case studies in Chapter 4 and Chapter 5 in order to validate the chosen approaches.

Chapter 4
Case Study 1: Non-electrified Line

4.1. Introduction

In this chapter, in order to validate the methodology introduced in Chapter 3, the proposed approaches are applied to a case study. As mentioned in Chapter 1, the main idea of introducing an HESS installed on a train is to provide the required energy and power for the whole journey without the support of electrification. Hence, the applications that this idea is most beneficial for are non-electrified lines. By installing the HESS above a train running on a non-electrified line, which is assumed to be a diesel line, CO_2 emissions can be cut dramatically due to the phasing out of diesel trains. Moreover, there is no need to electrify the line.

For the case study, an existing non-electrified line in the UK is considered; the data used for the route and vehicle running on this route are based on a railway line in Liverpool. In this chapter, first, it is seen whether it is efficient to integrate the battery and supercapacitor in an HESS to be installed above a train running on this line. Following this, a proper HESS is sized using the Frequency Analysis method and Brute Force optimization to be installed above the train running on the line. Then, scenarios will be proposed to use batteries to charge supercapacitors during the journey.

4.2.Case Study Familiarisation

4.2.1.Route Data

For this case study, the timetable considered is the real timetable for the existing journeys of a diesel train on a non-electrified line. This route is close to two electrified routes and shares its first station with one of those routes. There are six stations on this route with a whole length of 23.33km, which makes the return journey 46.66km. The speed limit is different in different parts of the route and the maximum speed is 80km/h. The route is fairly smooth and hence the gradient is considered zero for the whole route. Dwell time is 30 seconds for all stations. Table 4.2.1 indicates the route data of this case study.

Table 4.2.1. Route data of Case study 1

Parameter	Amount
Stations	6
Distance (km)	23.33
Maximum Speed (km/h)	80
Gradient	~0
Dwell time (s)	30

4.2.2. Vehicle Data

The current vehicle running on this line is a diesel engine; if an HESS needs to be installed on this train, it would be costly as it would need upgrading to become an electrified train. Hence, it is assumed that the HESS is installed on the electrified trains running on the electrified lines close to this line and. When the train runs on those electrified lines, it is supplied by the

electrification system, and when it enters this non-electrified route, it uses the energy stores in the HESS.

The trains running on the mentioned electrified lines are British Rail Class 507/508 (BR C507/508), which are DC-powered Electrical Multiple Units (EMU). This train is indicated in Figure 4.2.1.

Figure 4.2.1. British Rail Class 507/508

There are three cars in each EMU and one driving motor at each end of the train (cars 1 and 3). Each driving motor (car) has four series wound motors and one camshaft driven rheostat controller. The key properties of C507/508 are indicated in Table 4.2.2.

Table 4.2.2. Vehicle data of Case study 1

Property	**Data**
Car	3
Car dimensions ($L \times W \times H$)	19.8 × 3.85 × 8.82 m
Seats	232 on all except 192 on class 508/1
Laden weight (t)	121. 9
Series motors	8
Train output (kW)	8 × 85

Rated power (kW)	656
Maximum power (kW)	1200
Maximum speed (mph)	75
Davis coefficients	A = 0.00186, B = 0.2179, C = 16.62
Brakes	Rheostat and West code
Number of notches	5

4.2.3.Traction Simulation

By knowing the route data and vehicle data of the case study, it can be simulated in STS. Figure 4.2.2 indicates the gradient and velocity profile of the route, which were entered as inputs for the simulation.

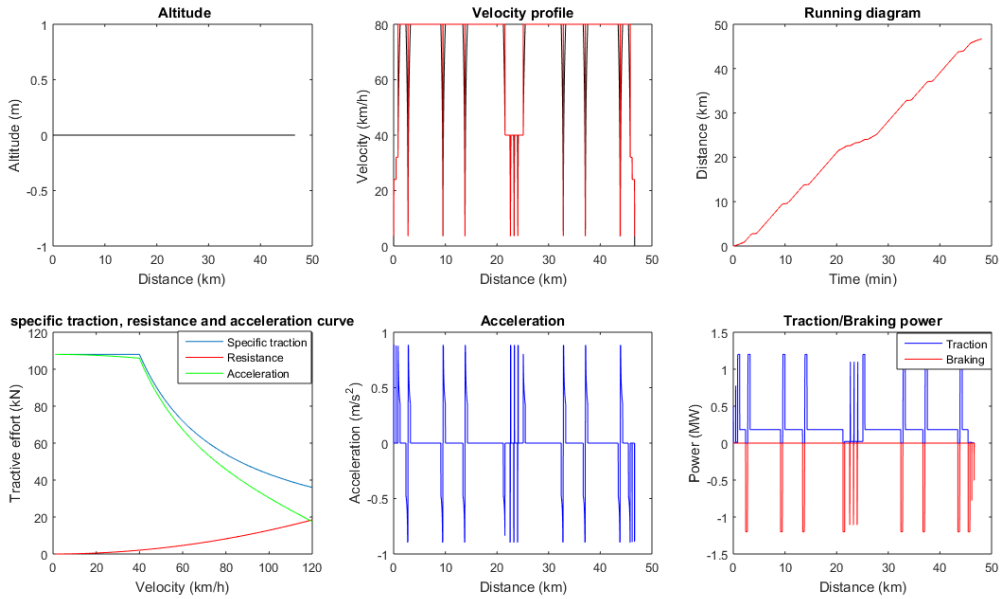

Figure 4.2.2. Altitude, Velocity profile, Running diagram, Specific traction, resistance and acceleration, Acceleration and Traction/Braking power of the simulated route

In the upper left figure, it can be seen that the altitude is zero for the whole journey. The changes in the velocity during the journey are shown in the upper middle figure, showing the maximum of 80km/h. The upper right figure indicates time versus distance, indicating the total journey time of 48.1 minutes. The tractive effort versus velocity is indicated in the bottom left figure for specific traction, resistance and acceleration. The changes in acceleration during the journey are shown in the bottom middle figure. One of the key results required for sizing the HESS, as mentioned before, is the peak power requirement which is indicated in the bottom right. This figure indicates traction and braking power versus distance, and it can be seen that the peak charging and discharging power is 1.2MW. Figure 4.2.3 is a closer look at this figure. It can be seen that the total journey time is 2886 seconds (48.1 minutes). Green dots indicate the stations in the return journey.

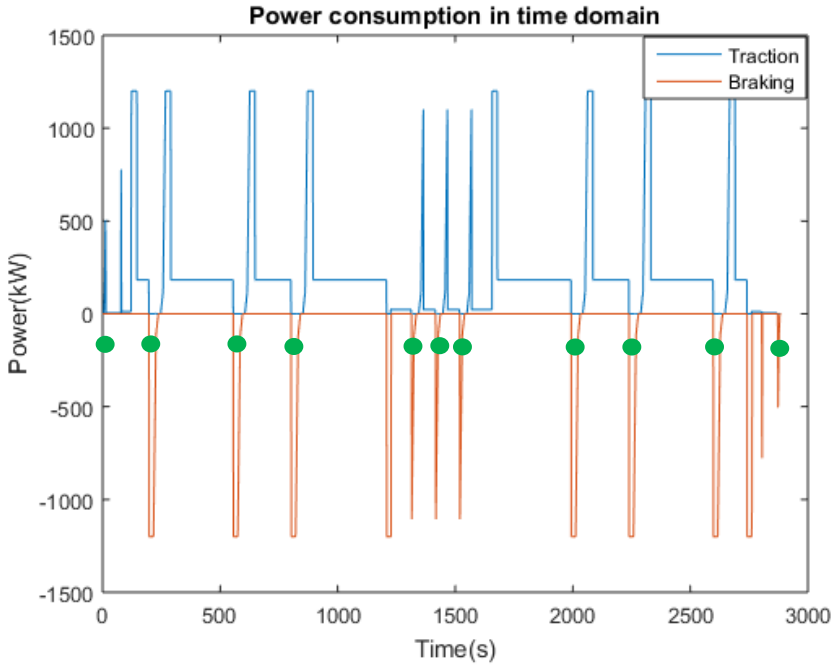

Figure 4.2.3. Power consumption in the time domain

The Traction line indicates acceleration and cruising modes and the Braking line indicates the braking modes during the journey. Another parameter required to size the HESS is the energy

consumption required for the whole journey; this is indicated in Figure 4.2.4, where it can be seen that the total energy which should be provided by the HESS is 154.6kWh. It is seen that the regenerative braking energy is absorbed in the braking modes, every time the train brakes. The total power demand and energy demand that should be provided by the HESS become 1200kW and 154.6kWh, respectively.

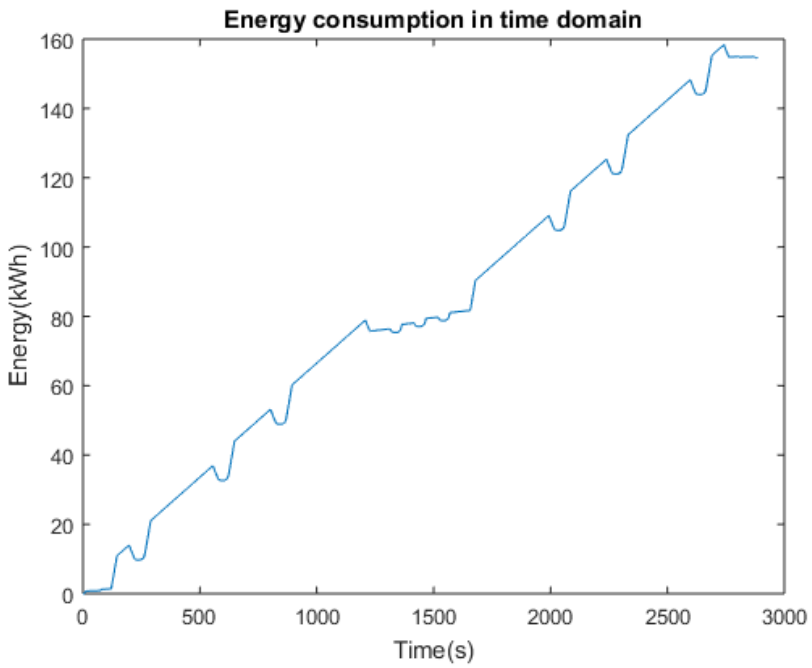

Figure 4.2.4. Energy consumption in time domain

4.3. Applying the "Evaluation" Phase to the Case Study

In order to start the evaluation of integrating battery and supercapacitor, based on Section 3.2.2.1, Case 1 with five scenarios for both energy demand and power demand is applied to the case study to determine the total weight and volume of the HESS. For these tests, the characteristics of 24V 60Ah Altairnano battery modules (which are LTO batteries) and 125V Heavy Transportation Maxwell supercapacitor Modules (which are EDLCs) are considered.

The characteristics of the considered battery and supercapacitor modules are indicated in Table 4.3.1 and

Table *4.3.2* [154], [155].

Table 4.3.1. Characteristics of 24V 60Ah Altairnano battery module

Parameter	**Amount**
Voltage range (V)	17-27.5
Capacity (minimum/typical) (Ah)	65/67.4
Typical discharge energy (wh)	1450
Energy density (wh/l)	108
Specific energy (wh/kg)	51.8
Peak power (discharge/charge (w)	22600/36300
Power density (discharge/charge) (w/l)	1682/2704
Specific power (discharge/charge) (wh/kg)	806/1296
Weight (kg)	28
Volume (m^3)	0.0147
Cycle life (at 25˚C)	>25000

Table 4.3.2. Characteristics of 125V Heavy Transportation Maxwell supercapacitor module

Parameter	**Amount**
Voltage (rated/maximum) (V)	125/136
Capacity (rated) (F)	63
Stored energy (wh)	140
Specific energy (wh/kg)	2.3
Typical discharging current (A)	100
Weight (kg)	61
Volume (m^3)	0.0054
Cycle life (at 25˚C)	1000000

The numbers of battery modules and supercapacitor modules are calculated in each scenario based on the required energy or power. Then, the weight and volume of the battery pack and supercapacitor pack and, finally, the total weight and volume are determined. Figure 4.3.1 indicates the total weight and volume of the HESS where only energy demand is considered. As said in Chapter 3, from Scenario 1 to Scenario 5, the number of battery modules required to provide the total energy demand decrease and the number of supercapacitors increases. It is obvious that from Scenario 1 to Scenario 5, the total weight and total volume of the HESS increase. It can be seen that every time the battery pack provides 25% less of the total energy required and the supercapacitor pack provides 25% more of the total energy required, the total weight of the HESS increases by about 40t and its volume increases by about 3.2m^3. Scenario 1 is the battery-only scenario and Scenario 5 is the supercapacitor-only Scenario, and it is visible that to support the energy demand, it is better to have a battery-only ESS to have the lowest

weight and volume. The supercapacitor-only scenario has the biggest size when it comes to the energy demand. Figure 4.3.2 indicates the weight and volume of the HESS in five scenarios to meet the power demand. Again, from Scenario 1 to Scenario 5, the number of battery modules decreases and the number of supercapacitor modules increases. From the figures, it can be seen that from Scenario 1 to Scenario 5, the total weight and total volume of the HESS decrease. From one scenario to another, every time, the weight and volume of the HESS decrease by 4.3t and 2.86m^3, respectively. Again, Scenario 1 is the battery-only scenario and Scenario 5 is the supercapacitor-only one and it can be seen that for the power demand, the supercapacitor-only scenario results in the smallest size and using only batteries as energy storage devices results in the highest weight and volume.

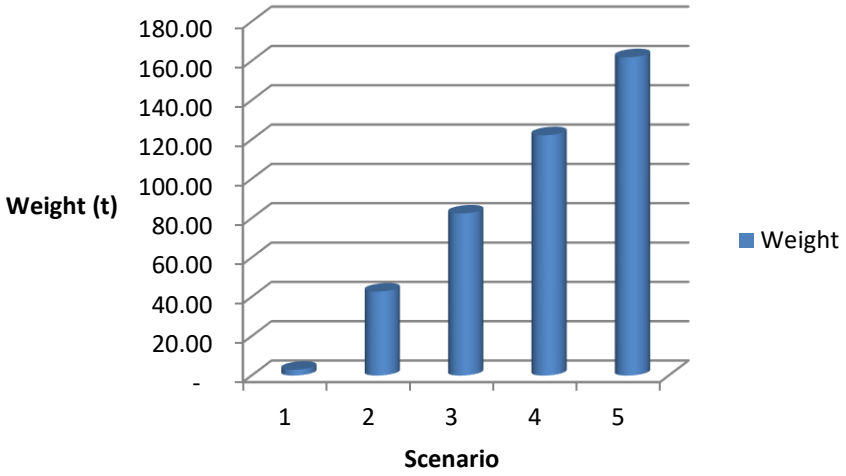

(a)

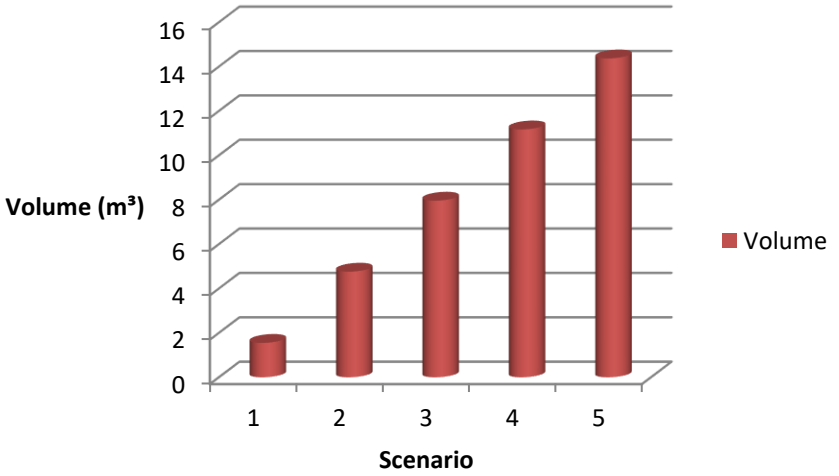

(b)

Figure 4.3.1. (a) Total weight of the HESS for 5 scenarios to meet the energy demand, (b) total volume of the HESS for 5 scenarios to meet the energy demand

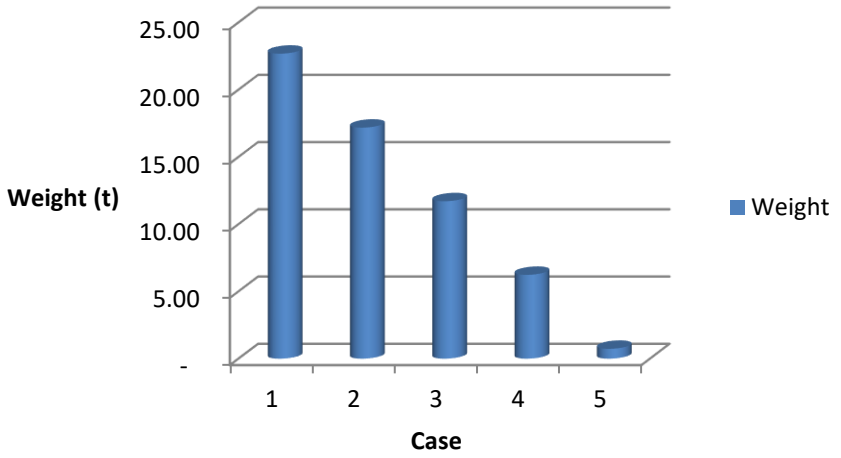

(a)

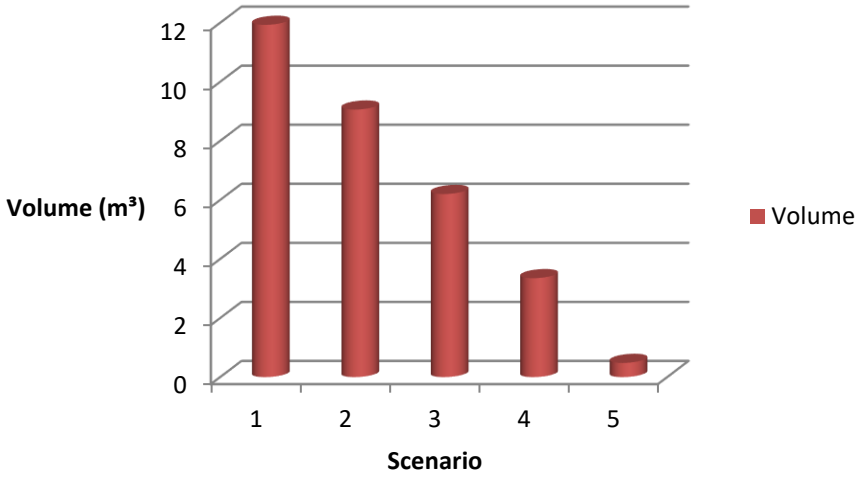

(b)

Figure 4.3.2. (a) Total weight of the HESS for 5 scenarios to meet the power demand, (b) total volume of the HESS for 5 scenarios to meet the power demand

Now, these two cases combine to form 25 scenarios. Regarding the procedure mentioned in 3.2.2.1, the numbers of battery modules and supercapacitor modules are determined. After choosing the higher numbers of modules, the weight and volume of each pack and, finally, the total size of the HESS are calculated in each scenario. Figure 4.3.3 indicates the total weight and volume of the HESS in all 25 scenarios. As scenarios go from Group A to Group E, the

energy percentage that the battery pack needs to supply decreases and the energy percentage that the supercapacitor pack has to provide increases. The power demand percentage for each storage pack stays unchanged. It can be seen that from Groups A to E, as the battery pack has to provide a lower amount of energy and the supercapacitor pack is in charge of supplying more energy, the total weight and volume of the HESS increase. Every time the battery pack provides 25% less and the supercapacitor pack provides 25% more energy, the total weight and volume of the HESS increase by about 40t and about 3.2m^3. Now in each individual group, from the first scenario to the fifth one, the energy demand stays the same and the power demand percentage that the battery pack and supercapacitor pack need to supply change. From the figure, it can be observed that both weight and volume have decreased. Every time the battery pack is responsible for providing 25% less of the power demand and the supercapacitor pack is responsible for providing 25% more of the demand, the total weight and volume of the HESS decrease by about 4.3t and 2.86m^3. From the figures, it can be seen that both the lowest weight and lowest volume happen in Scenario 5, in which the battery pack is in charge of supplying the total energy demand and the supercapacitor pack is responsible for supplying the total power demand. On the other hand, the highest weight and volume happen in Scenario 21, in which all the energy demand and all the power demand are expected to be supplied by the supercapacitor pack and battery pack, respectively.

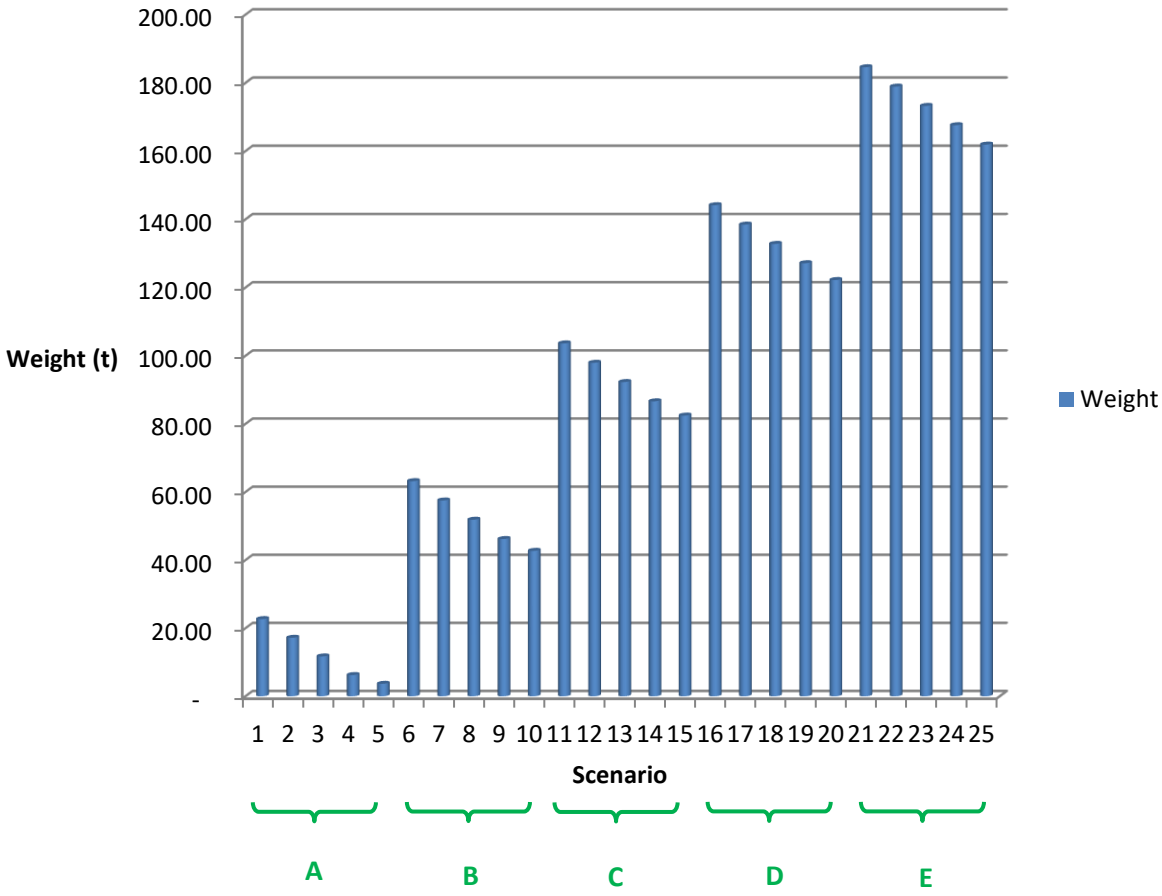
200.00
180.00
160.00
140.00
120.00
100.00
80.00
60.00
40.00
20.00
-
Weight (t)
1 2 3 4 5 6 7 8 9 10 11 12 13 14 15 16 17 18 19 20 21 22 23 24 25
Scenario
A
B
C
D
E
Weight

(a)

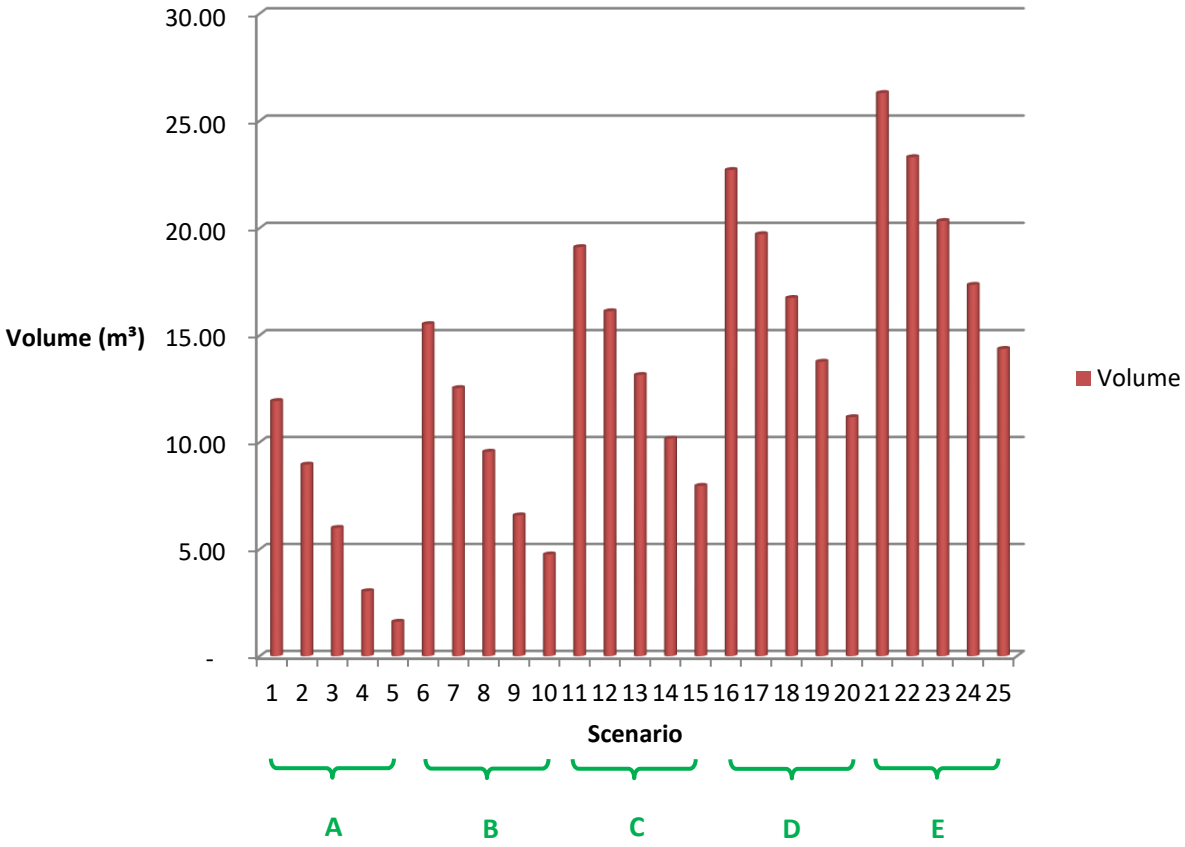

(b)

Figure 4.3.3. (a) Total weight of the HESS for 25 scenarios,
(b) total volume of the HESS for 25 scenarios

In order to assess the performance of the sized HESS, Scenario 2 is chosen as an example. As mentioned in 3.2.2.1, in this scenario, the whole energy demand is supplied by the battery pack; in terms of the power demand, 75% of the peak power required is supplied by the battery pack and 25% is provided by the supercapacitor pack.

Table *4.3.3* indicates the number of battery and supercapacitor modules as well as the sizes of the battery pack, supercapacitor pack and the HESS.

Table 4.3.3. Results of sizing HESS in Scenario 2

	Battery pack	Supercapacitor pack
Energy-based module number	105	0
Power-based module number	607	23
Higher number of modules	607	23
Power supply (kW)	900.1	299.9
Weight (t)	17	1.403
Total weight of the HESS (t)	18.4	
Volume (m^3)	8.94	0.12
Total volume of the HESS (m^3)	9.06	

Figure 4.3.4 indicates how the battery pack and supercapacitor pack in the sized HESS supply the power demand of the train during the whole journey. From the figure, it can be deduced that the acceleration modes are the modes that both the battery pack and supercapacitor pack should work together to provide the required power. The power required in cruising modes is 182.5kW, which is within the battery pack power limit, and the battery pack is in charge of meeting the power demand in these modes. In cruising modes, everything is as expected, but it can be seen that in the acceleration modes the simulation does not correspond to the calculations. In the acceleration modes, because the supercapacitor pack is not able to provide the 299.9kW for which it is responsible, the battery pack is forced to go beyond its power limit (900.1kW) and discharge more than its 1 C-rate. This makes the battery pack able to compensate for the supercapacitor pack and, consequently, help the HESS to meet the 1200kW power demand.

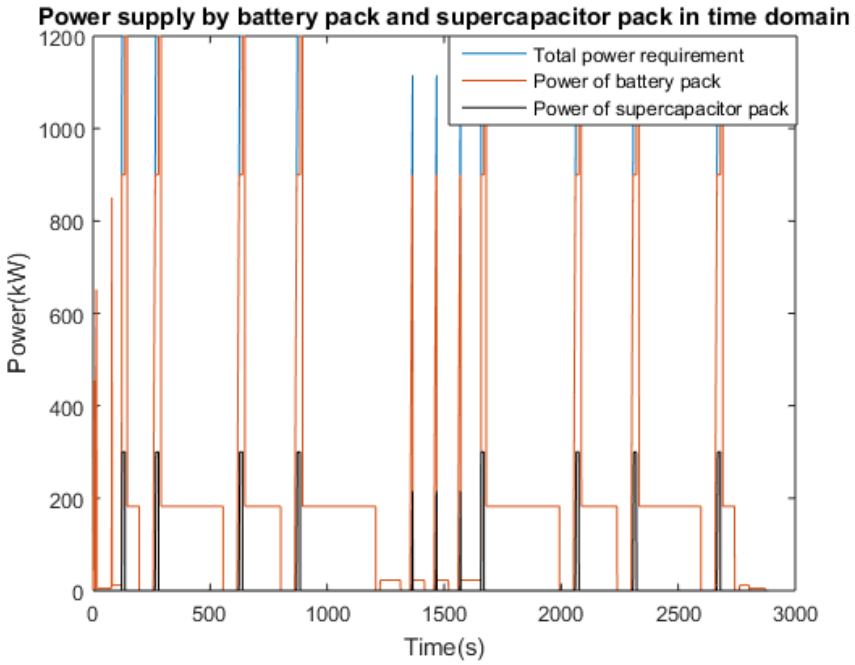

Figure 4.3.4. HESS supplying power demand in time domain for Scenario 2

Looking at the acceleration mode in the second station, which happens in 122s to 146s, it can be observed that the supercapacitor pack starts to supply the power, but it stops supplying before the end of the acceleration mode, in 136s, and the battery pack has to take over until the end of the acceleration modes. As mentioned before, the supercapacitor pack absorbs all the regenerative braking energy in braking modes, unless the SOC of the battery pack is less than 50%. Therefore, the supercapacitor pack becomes full during braking modes, but again it does not have enough energy to meet the power demand percentage which it is in charge of supplying during the next acceleration mode. This happens until the end of the journey. Figure 4.3.5 shows how both the battery pack and supercapacitor pack discharge to support the train traction during the journey.

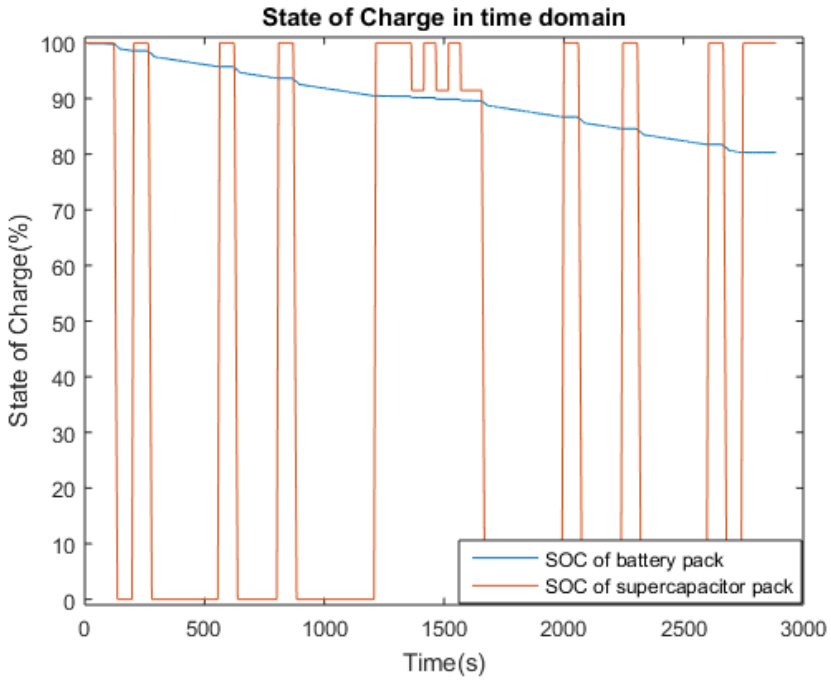

Figure 4.3.5. SOC changes of battery pack and supercapacitor pack in time domain for Scenario 2

For the acceleration at second station, the discharging procedure for both packs starts in 122s. The supercapacitor pack becomes fully empty in 14 seconds and from 136s, the battery pack discharges more (with a higher slope in the figure) to compensate for the supercapacitor pack until the end of the acceleration mode. In cruising mode, the battery pack is the only pack discharging and it discharges gradually at its 1 C-rate. When the train enters braking mode, all the regen energy is absorbed by the supercapacitor pack and it becomes full again. This happens until the end of the journey. It is seen that at the end of the journey, the supercapacitor pack is full; because it charges with regen energy from the last braking mode at the end of the journey. Regarding the battery pack, 80.28% of stored energy in the battery pack is left unused.

The sized supercapacitor pack is not able to perform as expected in this scenario as the number of supercapacitor modules is considered based on the power demand only. The supercapacitor pack should be able to meet the required power, but it does not have the energy required to do so. In order to tackle this problem, the first solution was for the battery pack to discharge more

than its 1 C-rate and compensate for the supercapacitor pack. Another solution is to increase the number of supercapacitor modules until the supercapacitor pack is able to meet the required percentage of the power demand. In Scenario 2, if 19 supercapacitor modules are added to the previous three modules to make it 42 supercapacitor modules in total, the supercapacitor pack is able to meet the required power demand. Figure 4.3.6 indicates how the HESS supplies the power demand during the journey when 19 supercapacitor modules are added.

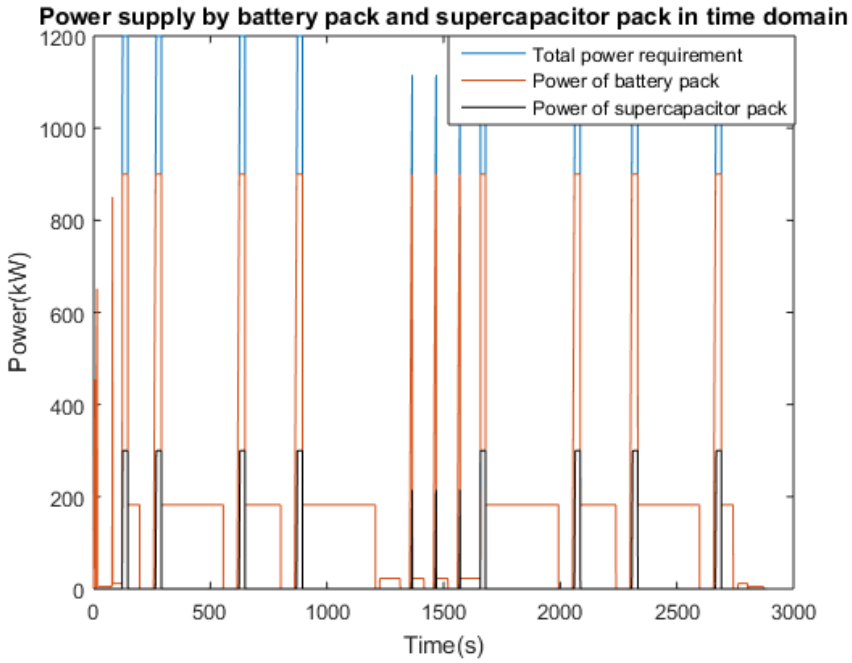

Figure 4.3.6. HESS supplying power demand in time domain for Scenario 2, increased number of supercapacitor modules

It is seen that the supercapacitor pack is now able to meet the percentage of the power demand for which it is responsible for, and it has enough energy to meet the required power in acceleration modes until the end of the journey. Moreover, it can be observed that the battery pack has met the power demand within its power limit and is not forced to discharge more than 900.1kW. The SOC changes of the both packs after adding supercapacitor modules is shown in Figure 4.3.7.

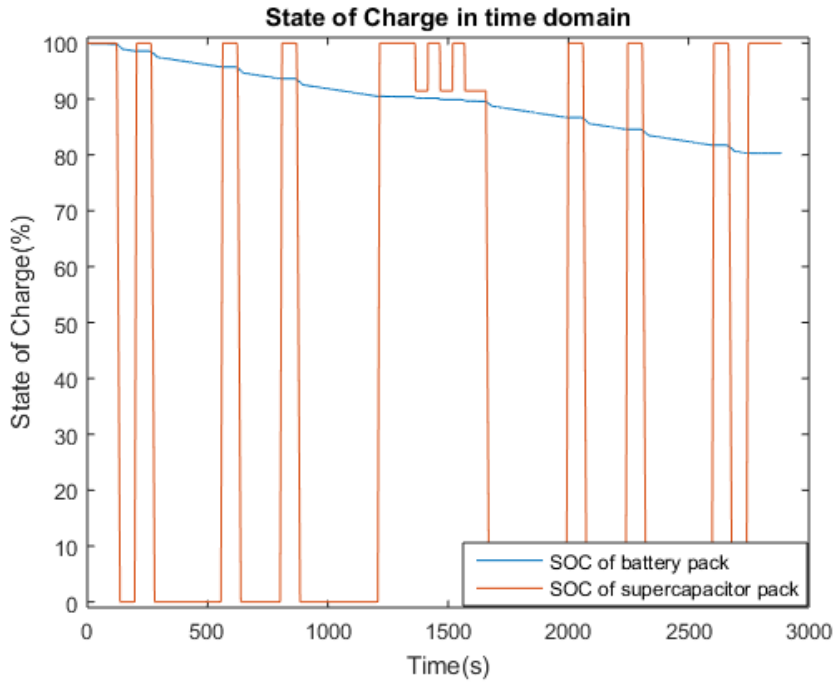

Figure 4.3.7. SOC changes of battery pack and supercapacitor pack in time domain for Scenario 2, increased number of supercapacitor modules

The supercapacitor pack fully charges by the regen energy in braking modes and uses that energy for accelerations, but its SOC never goes below 3.32%. This is because now there are more supercapacitor modules to be charged by the regen energy and the supercapacitor pack has enough energy to meet the required power demand. The battery pack uses 18.82% of its stored energy and, at the end of the journey, 81.18% of the stored energy in the battery pack stays unused. Compared to the previous solution, when the battery pack had to discharge more than its 1 C-rate, where 80.28% of the stored energy was left in the battery pack at the end of the journey, it can be deduced that battery uses 0.9% of its stored energy (8.1kWh) to compensate for the supercapacitor pack.

Increasing the number of supercapacitor modules solves the problem, but it not an efficient method. Adding supercapacitor modules increases the total weight and volume of the HESS by 1.15t and 0.7m^3, and increased weight of the HESS in turn adds to total mass of the train by

1.15t and consequently, increases the total energy consumption of the train. Another solution could be getting the battery pack to charge the supercapacitor pack at its 1 C-rate whenever the supercapacitor pack's SOC goes below 1%. When the supercapacitor pack's SOC goes below 1% in the acceleration mode, the battery pack starts charging the supercapacitor pack and at the same time, the supercapacitor can meet the power demand until the end of the acceleration mode. Figure 4.3.8 indicates how both the battery pack and supercapacitor pack do their duties properly and supply the power demand.

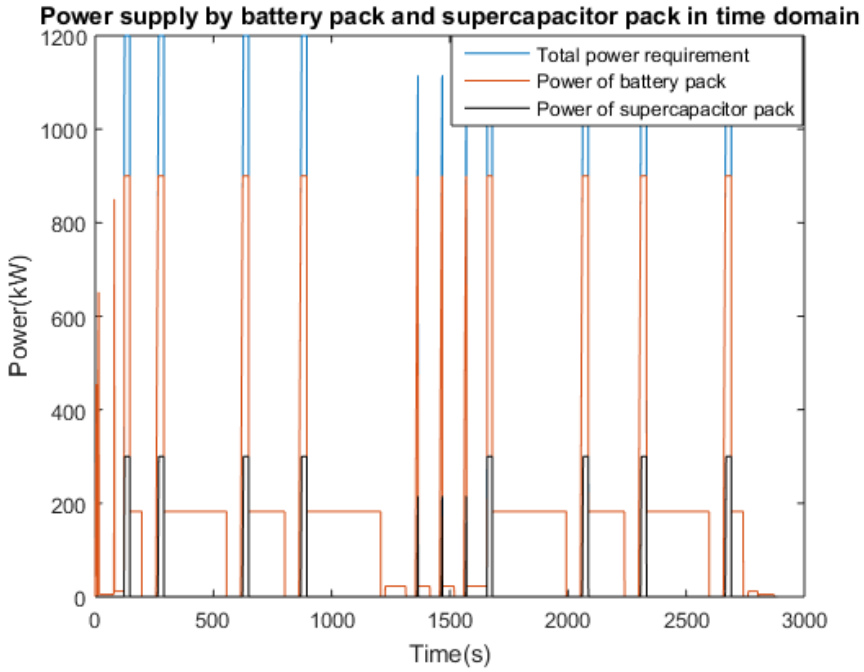

Figure 4.3.8. HESS supplying power demand in time domain for Scenario 2, battery pack charging supercapacitor pack

The interesting part of this solution is to see how both packs discharge during the journey. Figure 4.3.9 indicates the discharging procedures for both battery pack and supercapacitor pack when the battery pack charges the supercapacitor pack. Figure 4.3.10 indicates a closer look at the charging procedure.

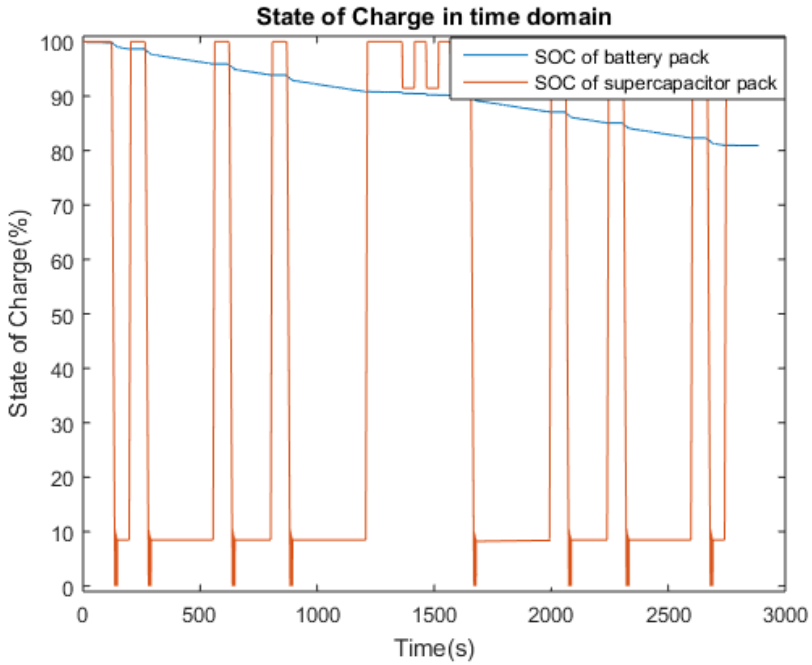

Figure 4.3.9. SOC changes of battery pack and supercapacitor pack in time domain for Scenario 2, battery pack charging supercapacitor pack

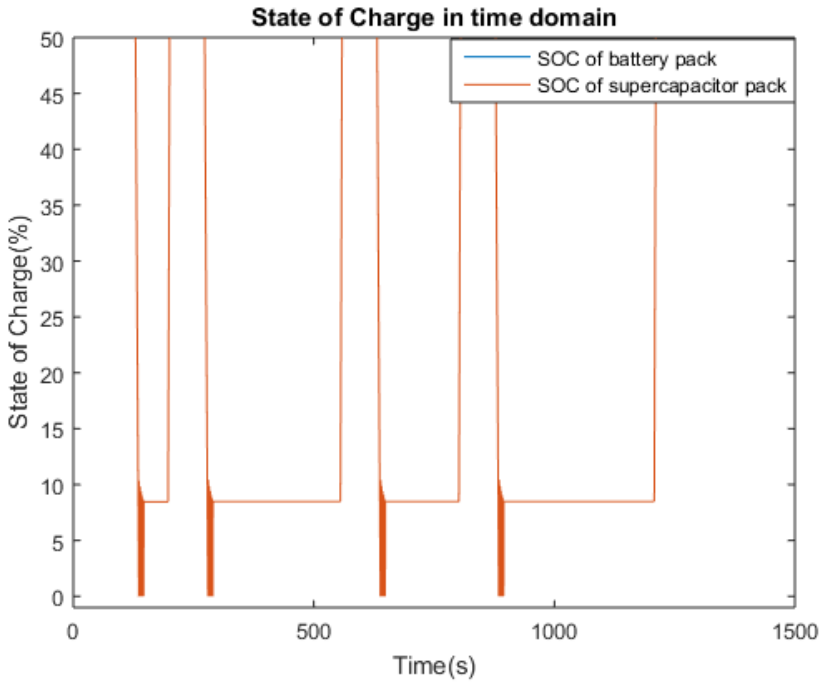

Figure 4.3.10. Closer look of SOC changes of battery pack and supercapacitor pack in time domain for Scenario 2, battery pack charging supercapacitor pack

It can be seen that both packs start to discharge in 122s as the first acceleration mode starts. The supercapacitor pack's SOC goes below 1% at 136s and from this point until 146s, the end of the acceleration mode, the battery pack discharges to meet the power demand and to charge the supercapacitor pack. From 136s to 146s, the supercapacitor pack absorbs energy from the battery pack and discharges to meet the power demand. It is seen that at the end of the acceleration mode, 146s, the energy stored in the supercapacitor pack is 1.5%. The supercapacitor charges by regen energy in the braking mode and this procedure continues until the end of the journey. At the end of the journey, the battery pack has 80.93% of its stored energy left. This means the battery pack uses 0.25% of its stored energy (2.2kWh) to charge the supercapacitor pack. This is 0.65% (5.8kW) less than in the solution when it was compensating for the supercapacitor pack.

This problem that the supercapacitor pack is not able to meet the required power demand happens in scenarios 2, 3, 4, 5, 10, 15 and 20. Figure 4.3.11 compares the weight and volume of the total HESS for 25 scenarios for three proposed solutions: adding supercapacitor modules, battery pack compensating for supercapacitor pack and battery pack charging supercapacitor pack. For normal scenarios, where the supercapacitor pack behaves as expected, there is no need to add to the supercapacitor modules and the size of the HESS is the same for all three solutions. The scenarios with unexpected results, where solutions were proposed, are indicated with green circles. It is obvious that the weight and volume of the HESS are greater when supercapacitors are added compared to the solutions where no additional module is added and the battery pack either compensates for or charges the supercapacitor pack. It is seen that Scenario 5 has the biggest size difference between the proposed solutions. In this scenario, regarding weight, it is 60.75t for the adding supercapacitors solution and 5.4t for battery compensating/charging solutions. In terms of the volume, it is 6.93m^3 for adding

supercapacitors solution and 0.49m^3 for battery compensating/charging solutions. Orange line indicates the laden mass of the train.

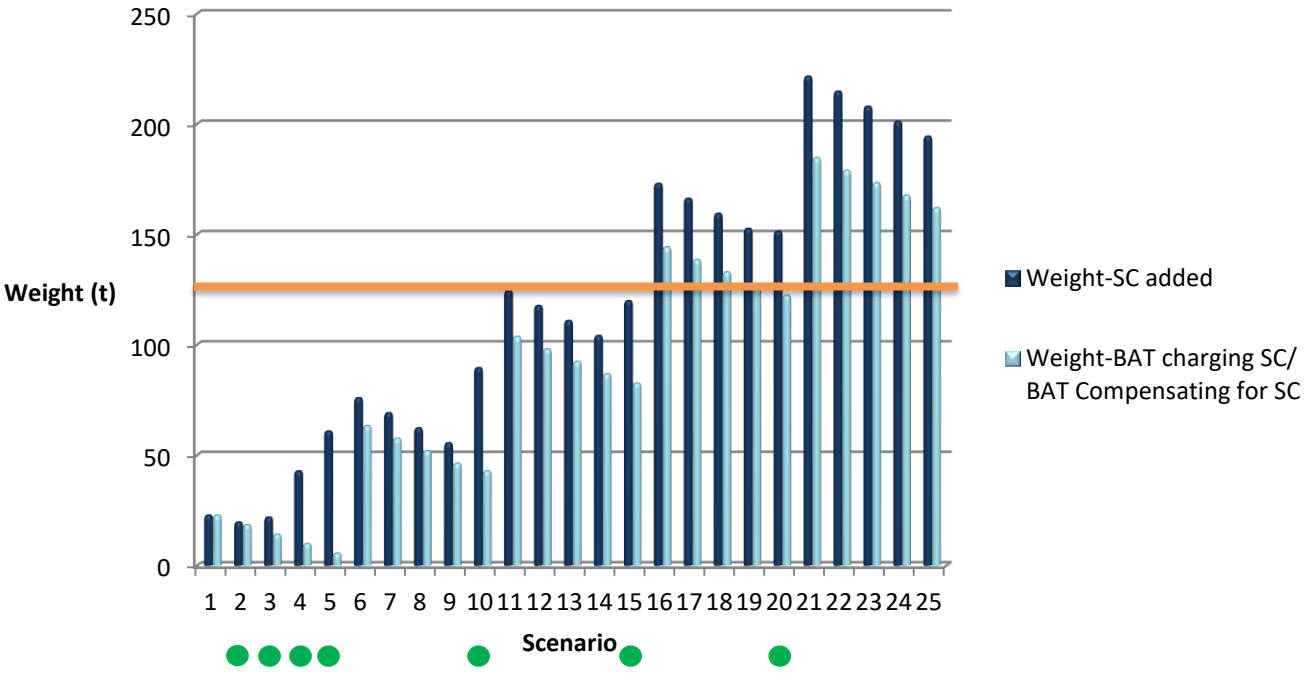

(a)

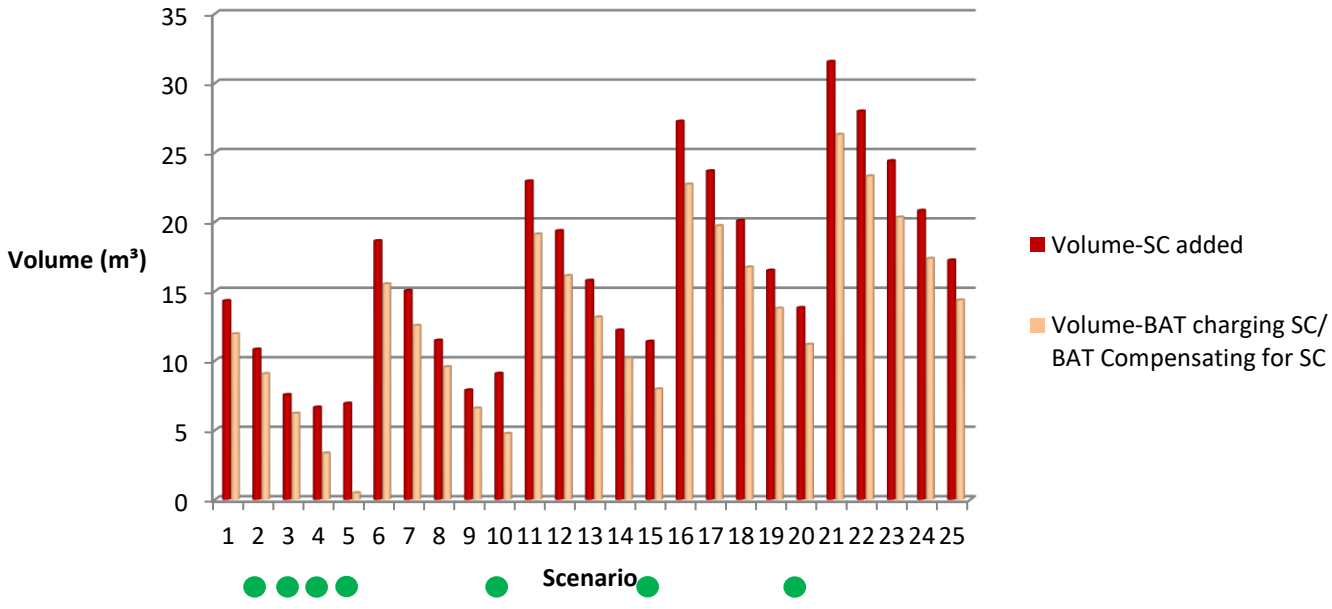

(b)

Figure 4.3.11. (a) Total weight of the HESS for 25 scenarios for 3 solutions,
(b) Total volume of the HESS for 25 scenarios for 3 solutions

Now the effects of a change of the C-rate of the battery on the total size of the HESS are assessed. As mentioned in Section 3.2.2.2, the C-rate of the battery modules is increased from 1 to 5 and by using the approach mentioned, the number of battery modules and supercapacitor modules, their weights and volumes and finally the total size of the HESS are achieved. Figure 4.3.12 indicates both total weight and total volume of the HESS for C-rates 1, 2, 3, 4 and 5.

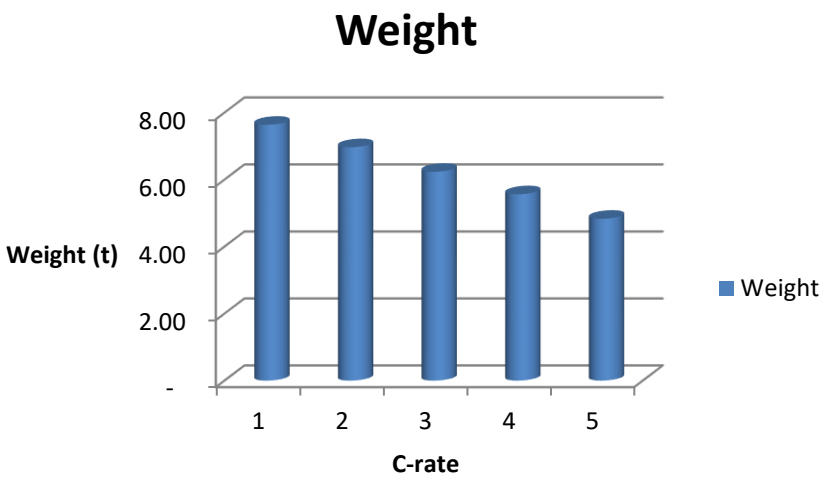

(a)

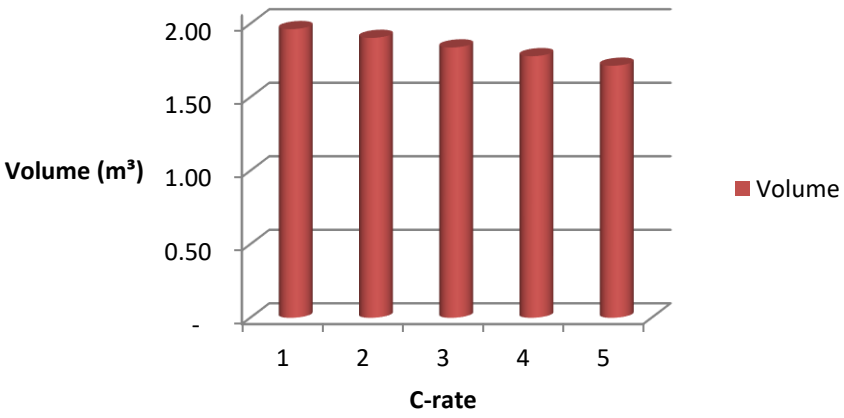

(b)

Figure 4.3.12. (a) Total weight of the HESS for C-rates from 1 to 5
(b) total volume of the HESS for C-rates from 1 to 5

It can be seen that both the weight and volume of the HESS decrease gradually as the C-rate of the battery pack increases. Regarding the total weight of the HESS, every time that one supercapacitor module is removed, the total weight is decreased by 0.061t (61kg). Regarding the total volume of the HESS, every time that there is one less supercapacitor module in the supercapacitor pack, the total volume is decreased by 0.0054m^3 (5400cm^3).

Table 4.3.4 indicates the number of battery and supercapacitor modules in each pack and also the power limit that each pack can provide.

Table 4.3.4. Power limit of battery and supercapacitor packs for C-rates from 1 to 5

C-rate	Number of battery modules	Power limit of battery pack (kW)	Number of supercapacitor modules	Power limit of supercapacitor pack (kW)
1	105	155.7	77	1044.3
2	105	311.4	66	888.6
3	105	467.1	54	732.9
4	105	622.8	43	577.2
5	105	778.5	31	421.5

From the table, it can be seen that the number of battery modules stay unchanged, but by increasing the C-rate of the battery pack, the battery pack is able to provide more power. Hence, the number of supercapacitor modules and consequently, the power demand that the supercapacitor pack needs to meet decreases.

Since the supercapacitor pack is sized based on the power demand only, it is expected that it does not have enough energy to meet the required power demand. This is indicated in Figure 4.3.13 for 1 C-rate.

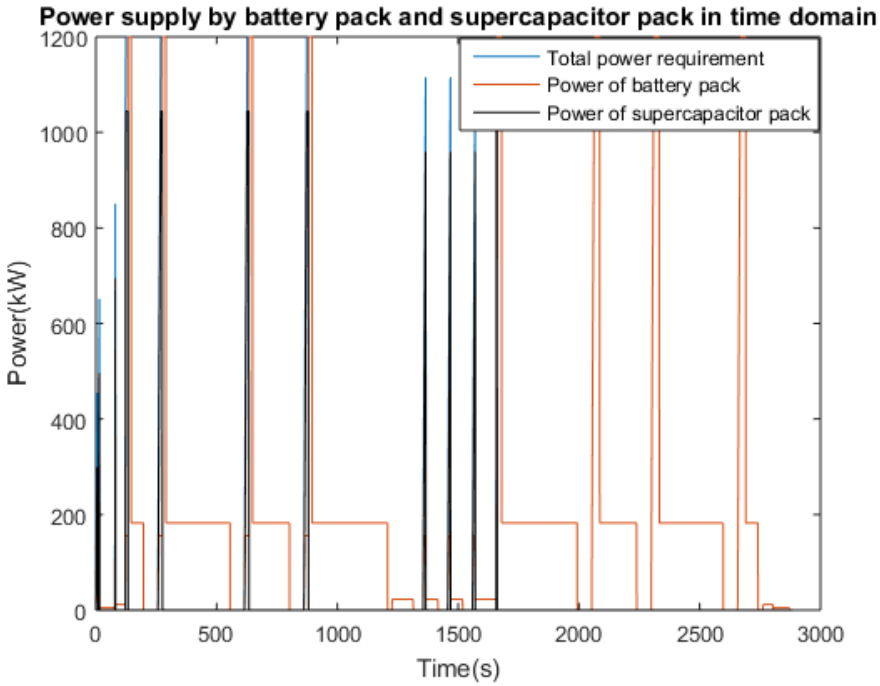

Figure 4.3.13. HESS supplying power demand in time domain for 1 C-rate

The change of the SOC in both the battery pack and supercapacitor pack is indicated in Figure 4.3.14.

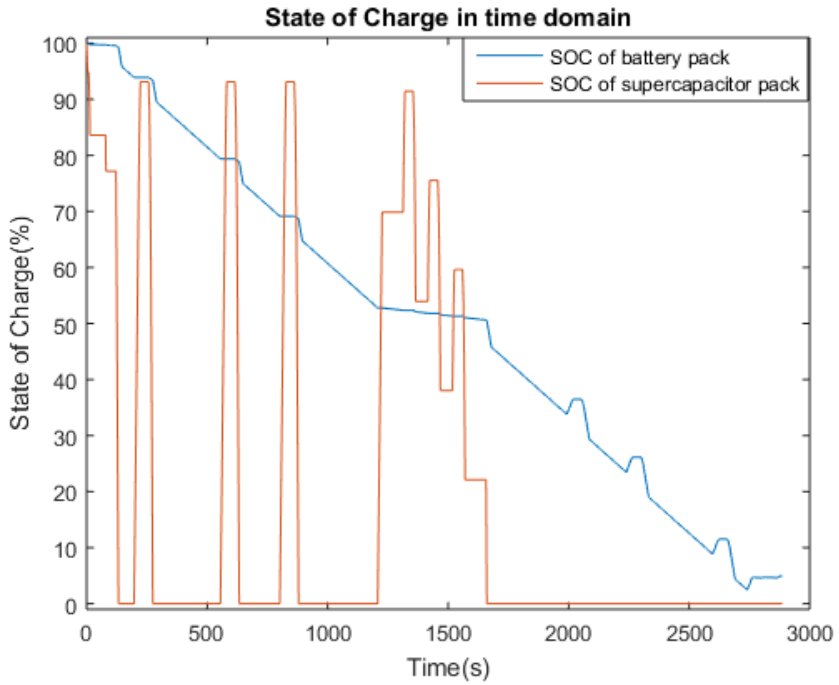

Figure 4.3.14. SOC changes of battery pack and supercapacitor pack in time domain for 1 C-rate

It can be seen that the supercapacitor pack becomes empty in the return journey and because the battery pack has discharged more than its power limit to compensate for the supercapacitor pack, its SOC drops below 50%. Therefore, the battery pack absorbs regen energy in braking modes and the supercapacitor pack stays empty until the end of the journey. At the end of the journey, 4.95% of the energy stored in the battery pack is left unused.

This happens for all five scenarios considered above, from 1 C-rate to 5 C-rate. As shown in previous tests, the battery pack can be used as a source to charge the supercapacitor pack whenever the supercapacitor pack is about to become empty and continues charging until the end of that mode.

Figure 4.3.15 shows the HESS in each scenario meets the total power demand and how both the battery pack and supercapacitor pack can meet the specific power demand which they are responsible for, without discharging more than their power limits. It can be seen that from 1 C-

rate to 5 C-rate, the power limit of the battery pack increases and the power demand that the supercapacitor pack has to provide decreases. Scenario 1 is the only scenario where the supercapacitor pack helps to meet the power demand in cruising modes too.

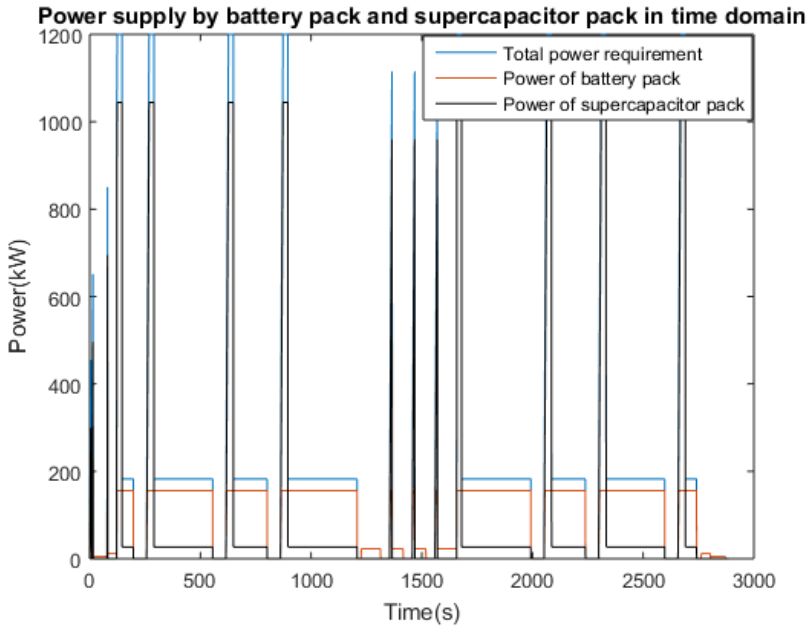

(a)

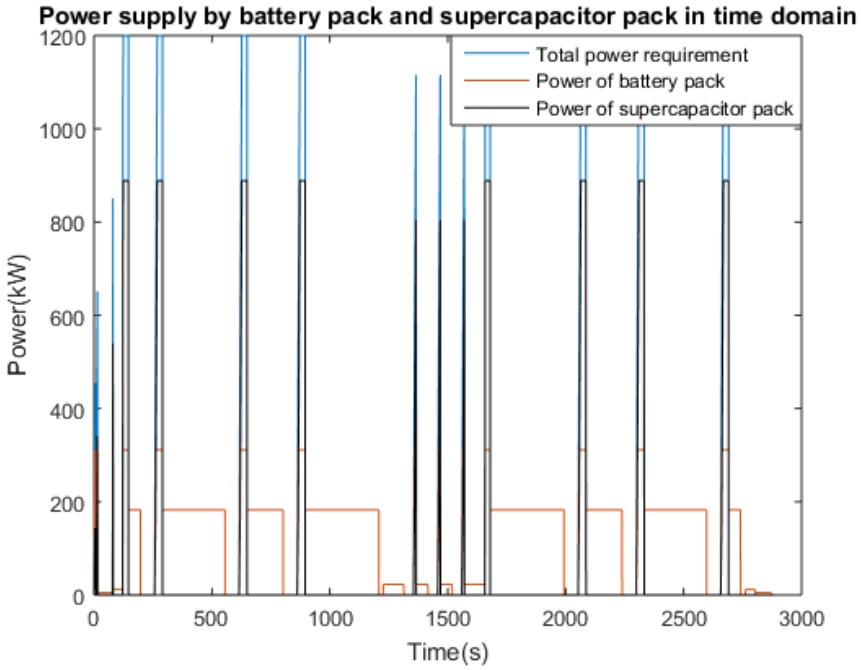

(b)

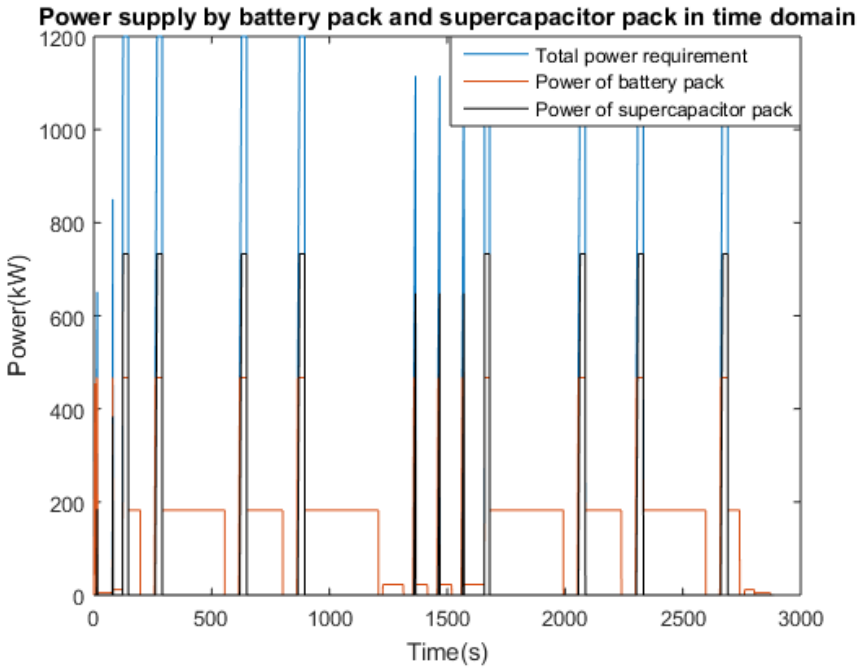
Power supply by battery pack and supercapacitor pack in time domain
Total power requirement
Power of battery pack
Power of supercapacitor pack
Power(kW)
Time(s)
0
200
400
600
800
1000
1200
0
500
1000
1500
2000
2500
3000

(c)

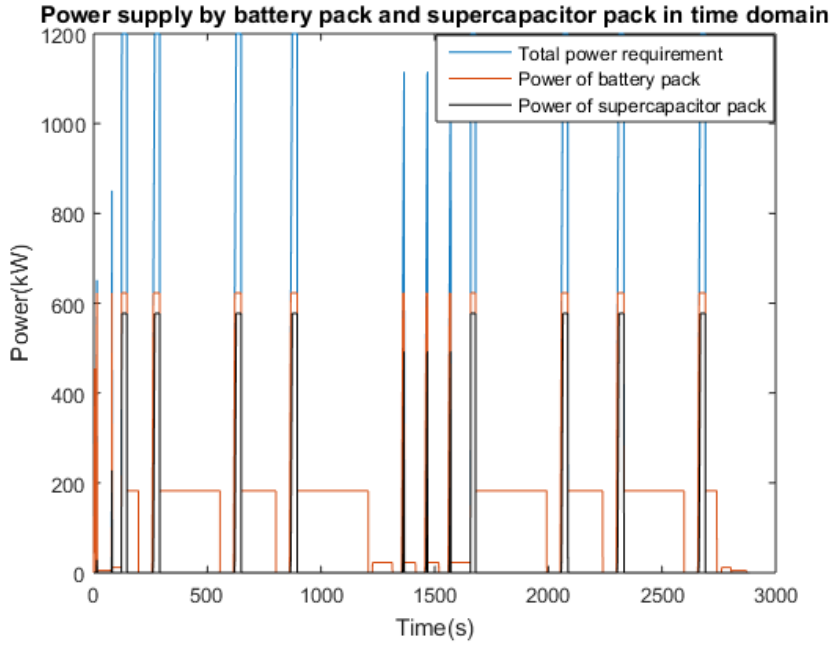
Power supply by battery pack and supercapacitor pack in time domain
Total power requirement
Power of battery pack
Power of supercapacitor pack
Power(kW)
Time(s)
0
200
400
600
800
1000
1200
0
500
1000
1500
2000
2500
3000

(d)

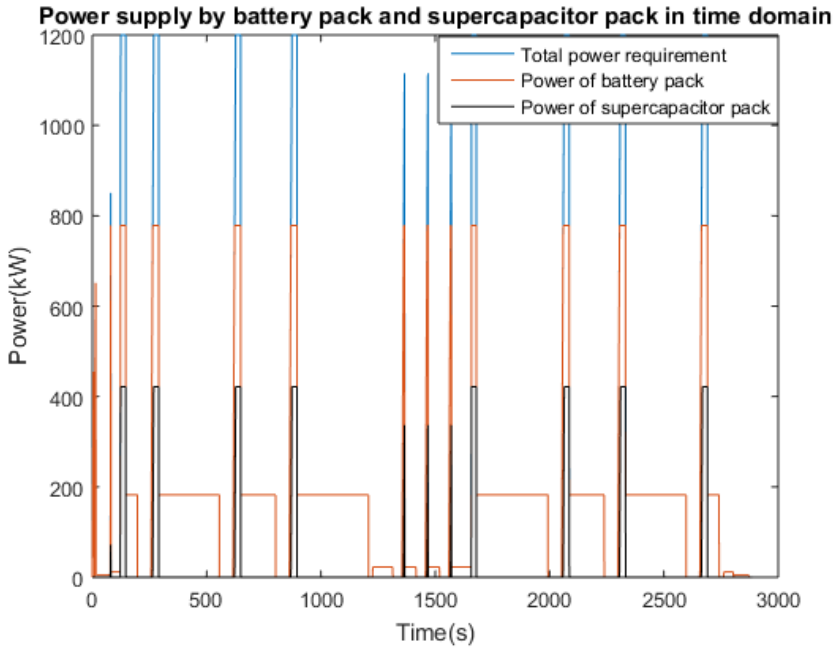

(e)

Figure 4.3.15. HESS supplying power demand in time domain for (a) 1 C-rate
(b) 2 C-rate
(c) 3 C-rate
(d) 4 C-rate
(e) 5 C-rate

One of the most important results of this test is the change in the SOC of the battery pack in different C-rates. Figure 4.3.16 shows how the battery pack discharges with C-rates 1 to 5 during the journey. From the figure, it can be seen that by increasing the C-rate of the battery pack, the battery pack discharges more quickly and, at the end of the journey, less energy is left in this pack. The figure shows that for all C-rates, whenever the SOC of the battery pack goes lower than 50%, the battery pack charges by regen energy in braking modes. By comparing the SOC figures for 1 C-rate in compensating mode and charging mode, again it can be seen that the battery uses less energy to charge the supercapacitor pack than when compensating to meet the power demand instead of the supercapacitor pack. It should be noted that for all figures indicating the SOC of batteries and supercapacitors, 0 means 20% of the energy left in the pack and is the energy that cannot be used.

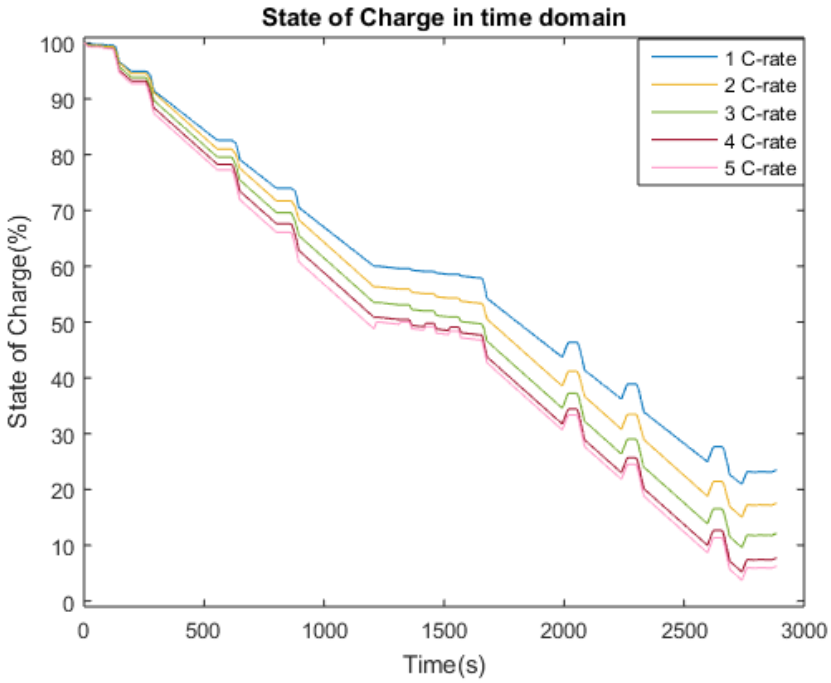

Figure 4.3.16. SOC change of battery pack in time domain for C-rates 1 to 5

Figure 4.3.17 shows the change in the SOC of both the battery pack and supercapacitor pack in all 5 C-rates. A closer look at the charging procedure for final three stations is indicated as well.

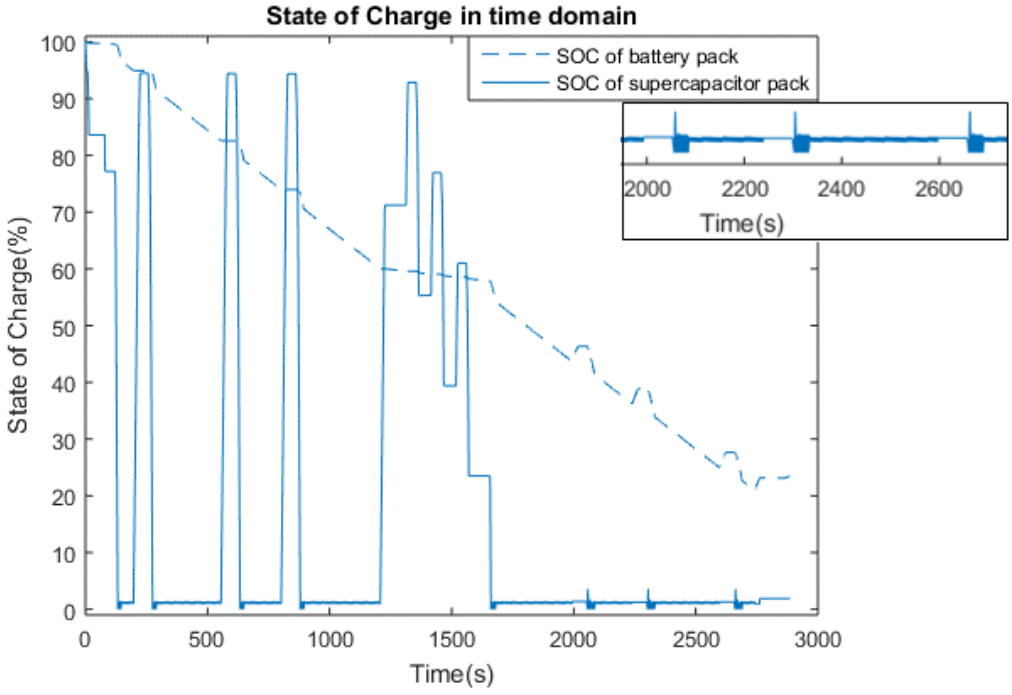

(a)

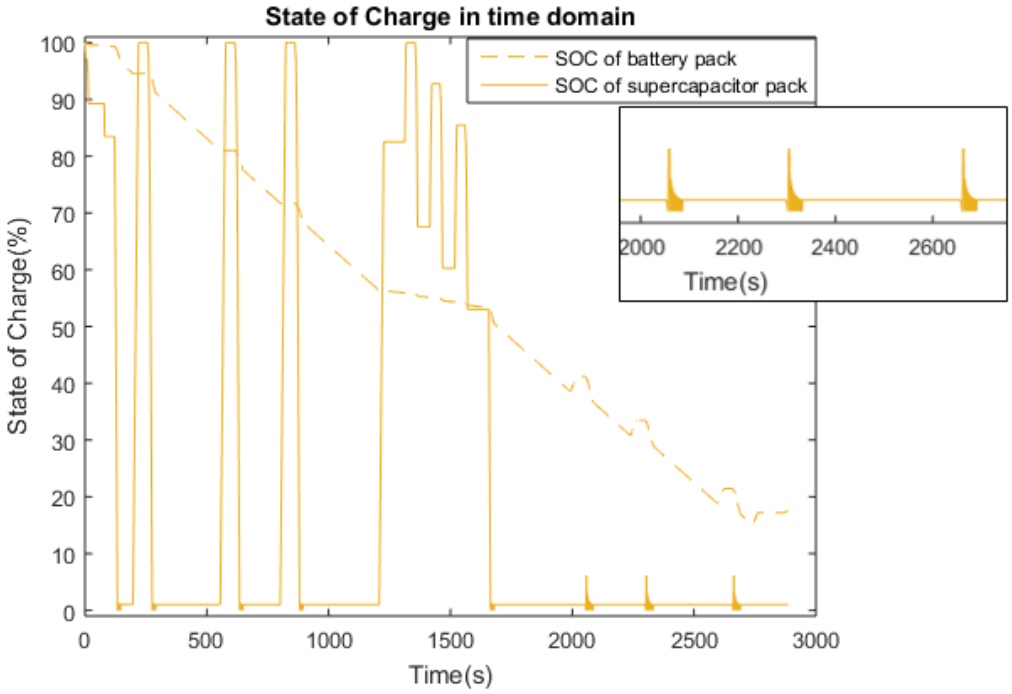
State of Charge in time domain
SOC of battery pack
SOC of supercapacitor pack
State of Charge(%)
Time(s)
0
10
20
30
40
50
60
70
80
90
100
0
500
1000
1500
2000
2500
3000
2000
2200
2400
2600
Time(s)

(b)

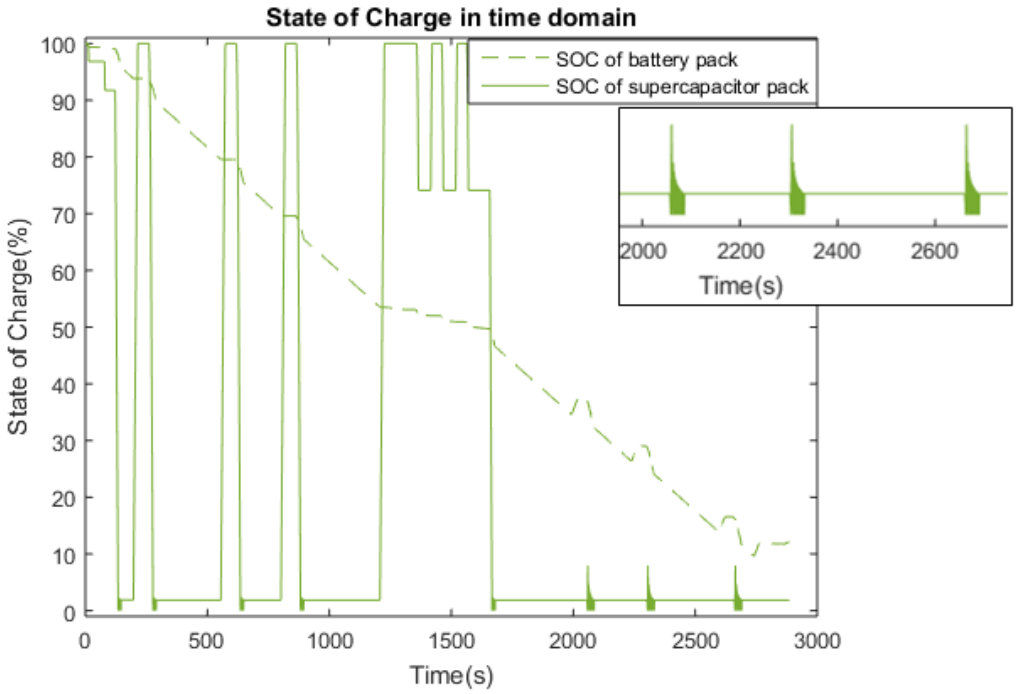
State of Charge in time domain
SOC of battery pack
SOC of supercapacitor pack
State of Charge(%)
Time(s)
0
10
20
30
40
50
60
70
80
90
100
0
500
1000
1500
2000
2500
3000
2000
2200
2400
2600
Time(s)

(c)

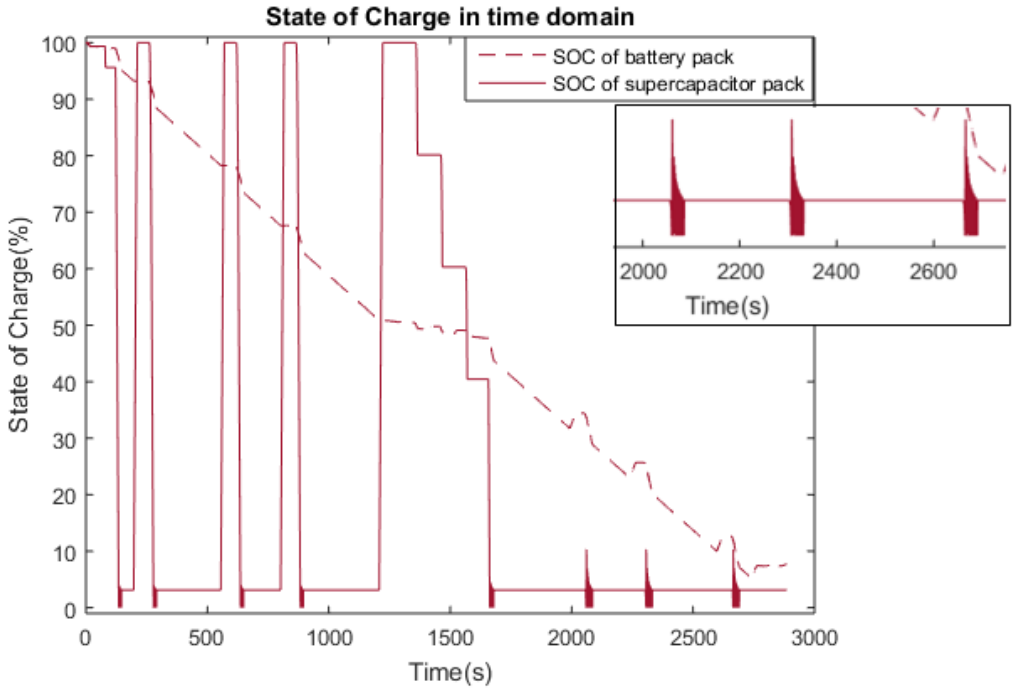

(d)

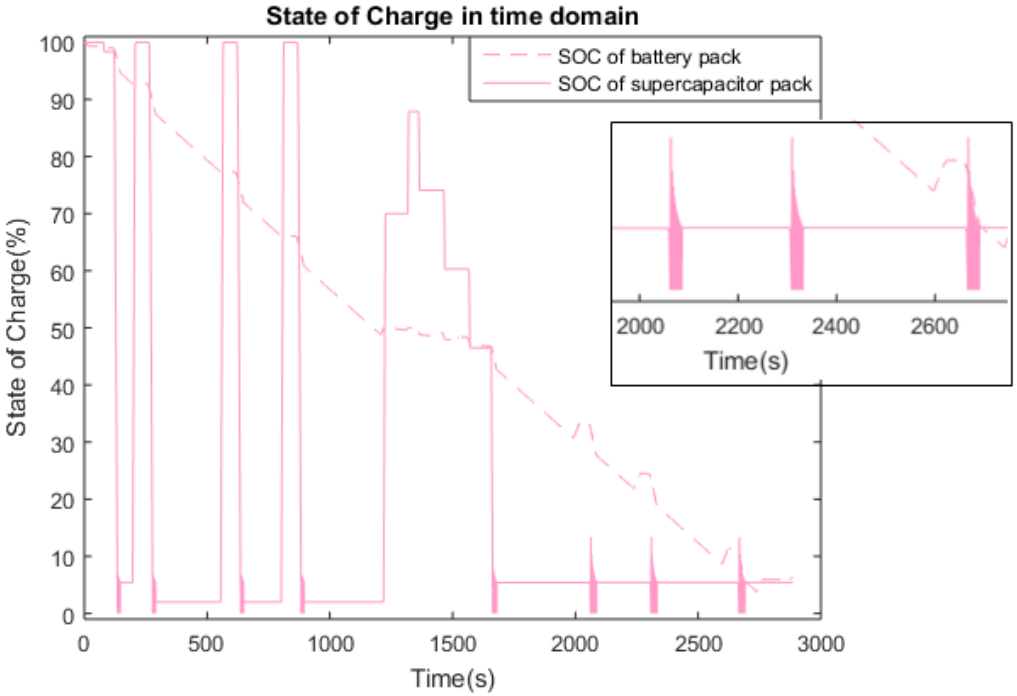

(e)

Figure 4.3.17. SOC changes of battery pack and supercapacitor pack in time domain for (a) 1 C-rate
(b) 2 C-rate
(c) 3 C-rate
(d) 4 C-rate
(e) 5 C-rate

The figures show that the battery pack charges the supercapacitor pack whenever the supercapacitor pack is about to become empty (when its SOC goes below 1%). This happens in acceleration and cruising modes for 1 C-rate and only in acceleration modes at 2 to 5 C-rates. Again, it is seen that by increasing the C-rate of the battery pack, the SOC of this pack reaches 50% more quickly and starts absorbing regen energy earlier. As a result, from the figures it can be observed that from 1 C-rate to 5 C-rate, the supercapacitor pack stops absorbing regen energy at an earlier stage during the journey.

4.4. Applying the 'Sizing' Phase to the Case Study

In the previous section, it was seen that integrating the battery and supercapacitor decreases the total size of the storage system to be installed above the train and, moreover, that due to the different characteristics of battery and supercapacitor, it is essential to size the HESS optimally to minimise its weight and volume. In this phase, the Frequency Analysis method as well as Brute Force optimization is used to size an HESS including Altairnano battery modules and Maxwell supercapacitor modules for the chosen case study.

As mentioned in Section 3.3.2, in order to design low-pass and high-pass filters, an optimal cut-off frequency should be determined. By using Brute Force Optimisation, with the frequency range from 1μHz to 0.5Hz, and the procedure explained in Section 3.3, optimal cut-off frequencies are achieved.

Figure 4.4.1 indicates the achieved results from Brute Force Optimisation, where the cut-off frequency is indicated versus weight and volume.

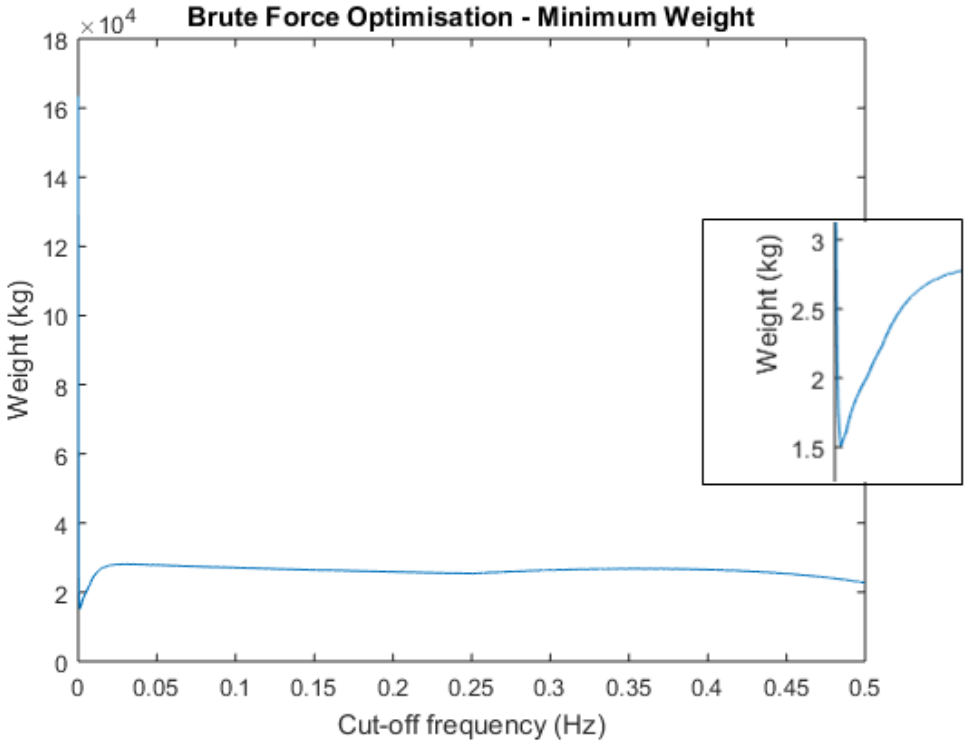

(a)

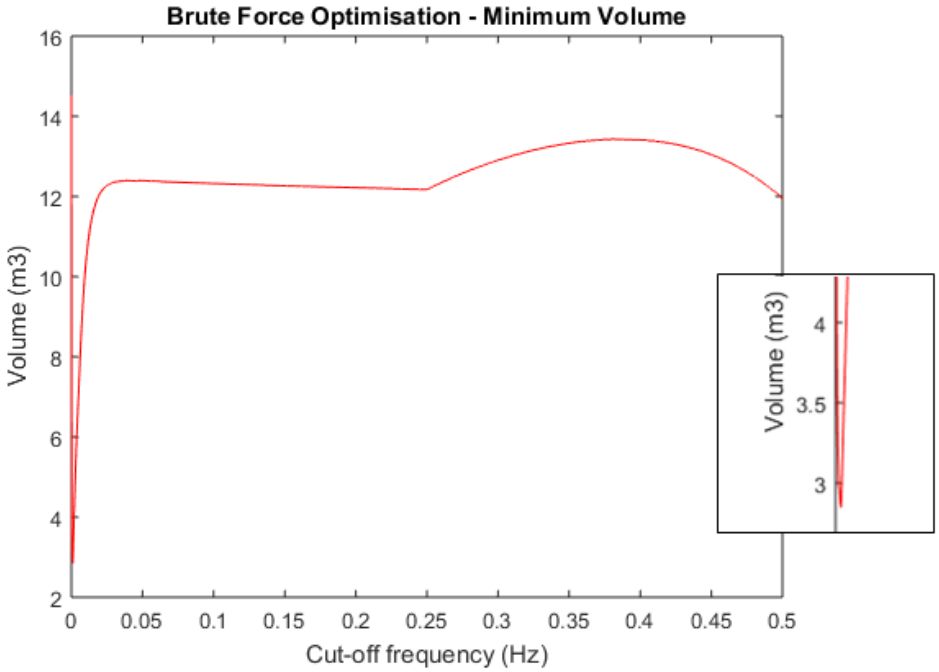

(b)

Figure 4.4.1. Brute Force Optimisation results to achieve minimum (a) weight and (b) volume

As expected, two optimal cut-off frequencies are achieved to have minimum weight and minimum volume. Table 4.4.1 indicates the achieved optimal cut-off frequencies and respective weights and volumes.

Table 4.4.1. Optimal cut-off frequencies

Cut-off frequency (μHz)	Total weight (t)	Total volume (m^3)
992–996	15.09	2.87
934–953	15.095	2.85

Since only one cut-off frequency needs to be considered for the filters, the cut-off frequency based on total weight is chosen as the weight of the HESS affects the mass of the train and then the total energy consumption. This results in a total weight and volume of 15.09t and 2.87m^3. Now both low pass and high pass filters can be built with a cut-off frequency of 992 μHz.

Figure 4.4.2 indicates the power demand for the whole journey in the frequency domain, and Figure 4.4.3 shows how this demand is filtered by a low-pass filter. It can be seen that frequencies higher than 992μHz are attenuated. Figure 4.4.4 indicates the low pass-filtered power demand in the time domain and based on the approach proposed in Section 3.3.1, the power demand required from the battery pack is 185kW.

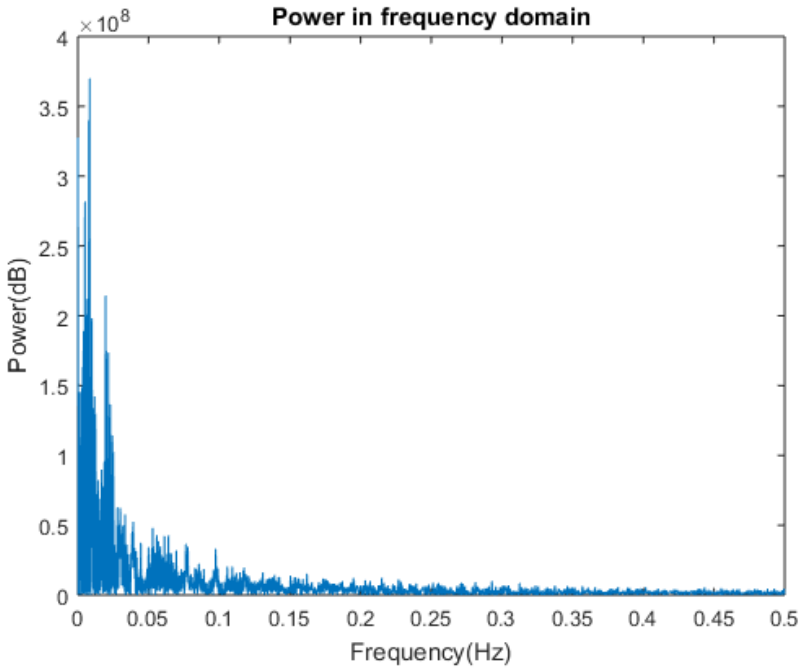

Figure 4.4.2. Power demand in frequency domain

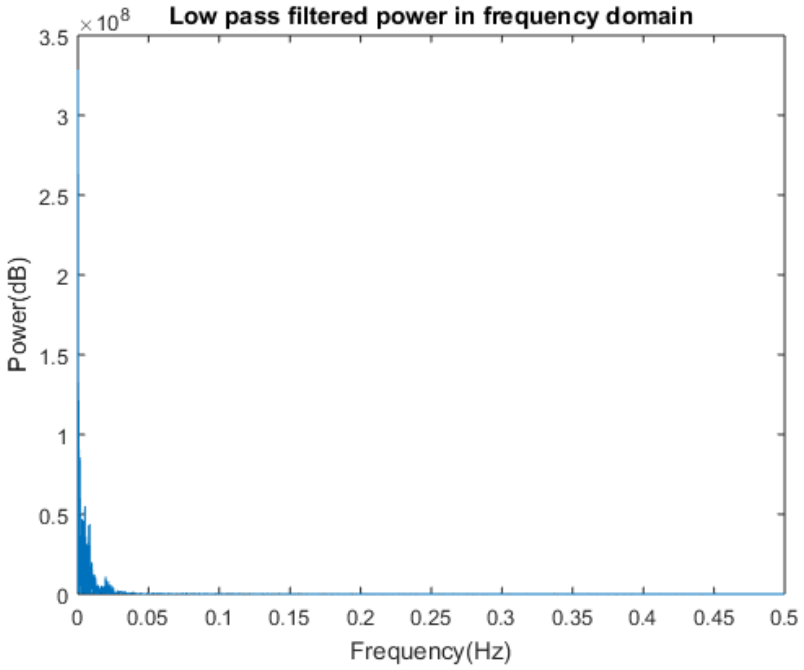

Figure 4.4.3. Low pass-filtered power demand in frequency domain

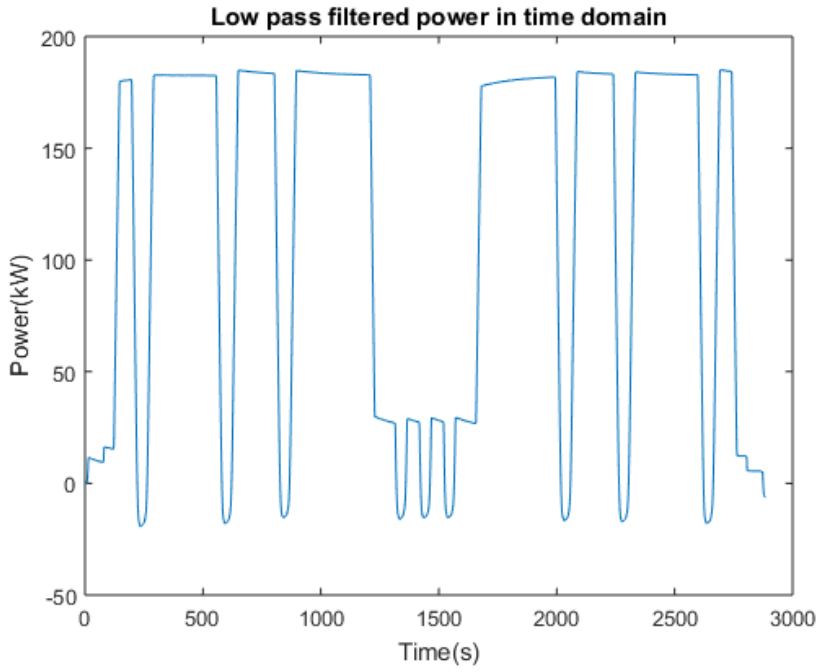

Figure 4.4.4. Low pass-filtered power demand in time domain

Using integration, the low pass-filtered energy requirement which should be supplied by the battery pack can be determined. This is indicated in Figure 4.4.5 and, based on Section 3.3.1, the battery pack should be sized in a way to provide 153.5kWh.

Now, by knowing the power and energy required from the battery pack, this pack can be sized. Table 4.4.2 indicates the number of battery modules calculated based on the energy demand and power demand: 125 battery modules are required to meet the power demand and 104 battery modules are required to meet the energy demand; 125 modules is chosen as the final number of battery modules and then, the weight and volume of the battery pack are determined.

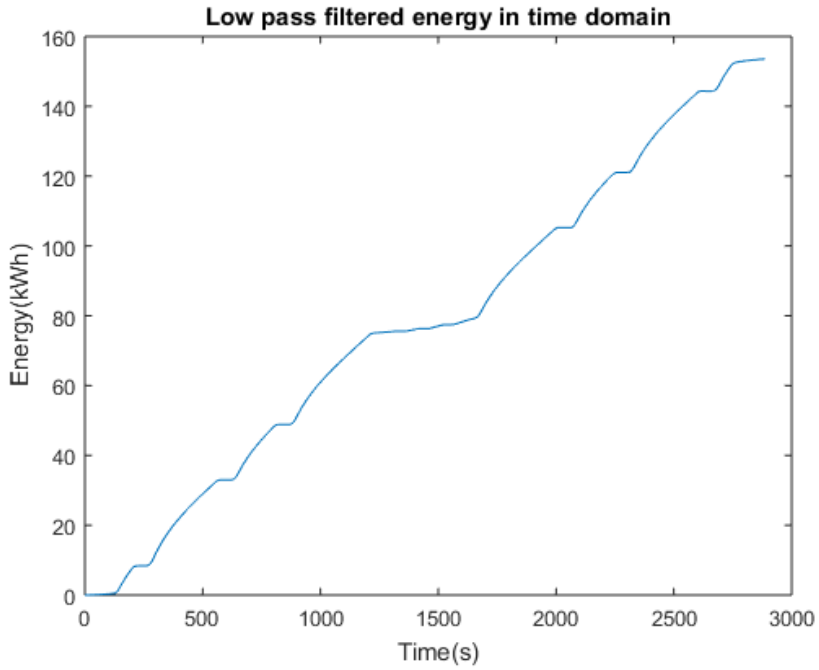

Figure 4.4.5. Low pass-filtered energy demand in time domain

Table 4.4.2. Sized battery pack

Power demand from battery pack (kW)	185
Power-based module number	125
Energy demand from battery pack (kWh)	153.5
Energy-based module number	104
Higher number of modules	125
Weight (t)	3.5
Volume (m^3)	1.84

Now the supercapacitor pack should be sized. This time, the designed high-pass filter with a cut-off frequency of 992μHz is applied to the total power demand of the case study. Figure 4.4.6 and Figure 4.4.7 indicate the high pass-filtered power demand in the frequency and time

domains, respectively. By looking at Figure 4.4.7 and according to Section 3.3.1, the highest power demand required from the supercapacitor pack is 1378kW.

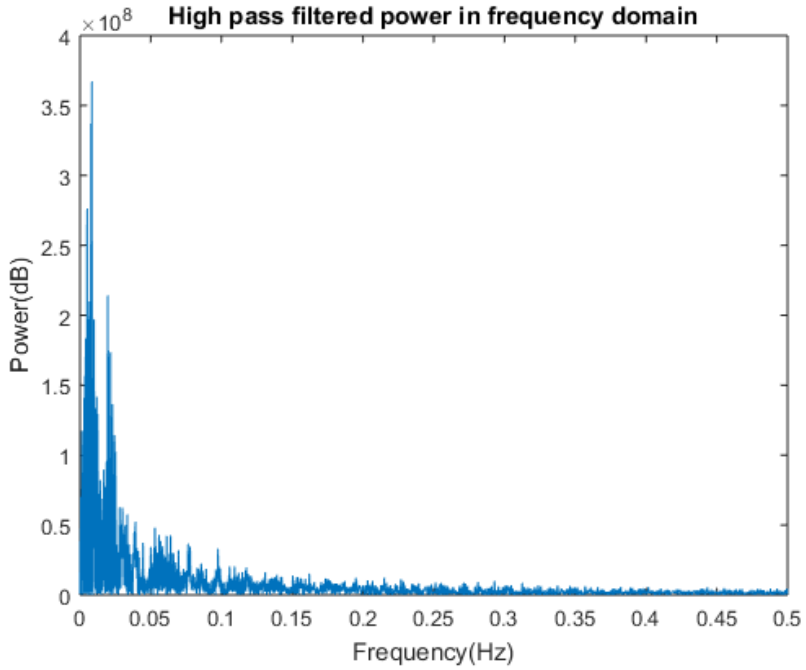

Figure 4.4.6. High pass-filtered power demand in frequency domain

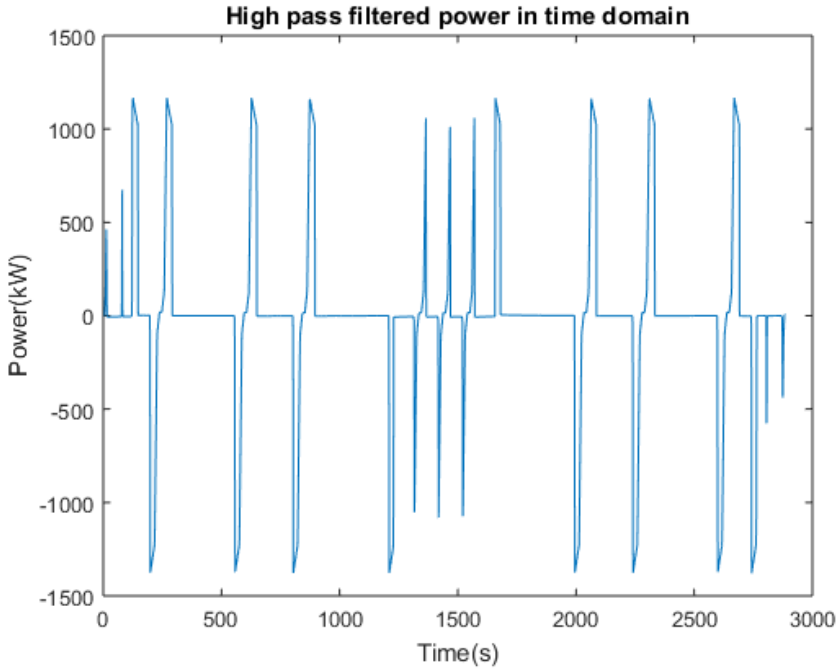

Figure 4.4.7. High pass-filtered power demand in time domain

In order to determine the high pass-filtered energy consumption, high pass-filtered Power/Time is integrated and Figure 4.4.8 is obtained. According to the method mentioned in Section 3.3.1, the total energy achieved from the high pass-filtered Energy/Time which should be supplied by the supercapacitor is 11.1kWh.

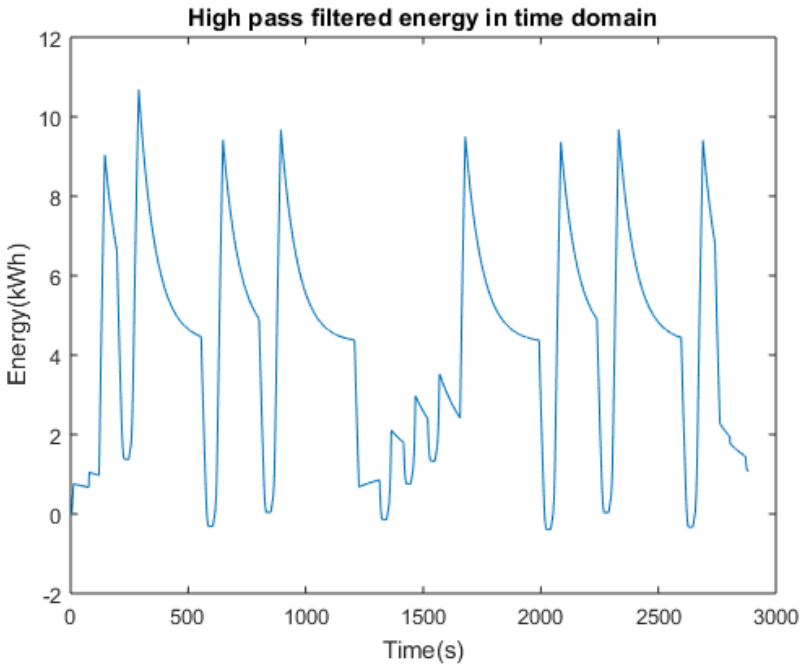

Figure 4.4.8. High pass-filtered energy demand in time domain

Table 4.4.3 indicates the energy and power required from the supercapacitor pack, and the number of supercapacitor modules is calculated based on those demands: 102 and 190 supercapacitor modules are required to meet the power demand and energy demand, respectively. The higher number of modules is the energy-based one and hence this number is chosen as the final number. Following this, the weight and volume of the supercapacitor pack can be obtained.

Table 4.4.3. Sized supercapacitor pack

Power demand from supercapacitor pack (kW)	1378
Power-based module number	102
Energy demand from supercapacitor pack (kWh)	11.1
Energy-based module number	190
Higher number of modules	190
Weight (t)	11.59
Volume (m^3)	1.03

As mentioned in the optimisation procedure to find the optimal cut-off frequency, this combination (125 battery modules and 190 supercapacitor modules) makes the total weight and volume of the HESS 15.09t and 2.87m^3, respectively.

Figure 4.4.9 indicates the total power demand as well as the low pass-filtered and high pass-filtered power demands together and Figure 4.4.10 shows the total, low pass-filtered and high pass-filtered energy demands together.

In order to check whether the filters have performed properly, the achieved Power/Time results from both low-pass and high-pass filters are added, which is shown in Figure 4.4.11. Moreover, the obtained Energy/Time results from both filters are added, which is shown in Figure 4.4.12. Regarding power, it can be seen that the figure is exactly the total power demand of the case study, with maximum charging and discharging power of 1200kW. With regard to energy, the figure is exactly the same as the total energy requirement of the case study, with total energy consumption of 154.6kWh.

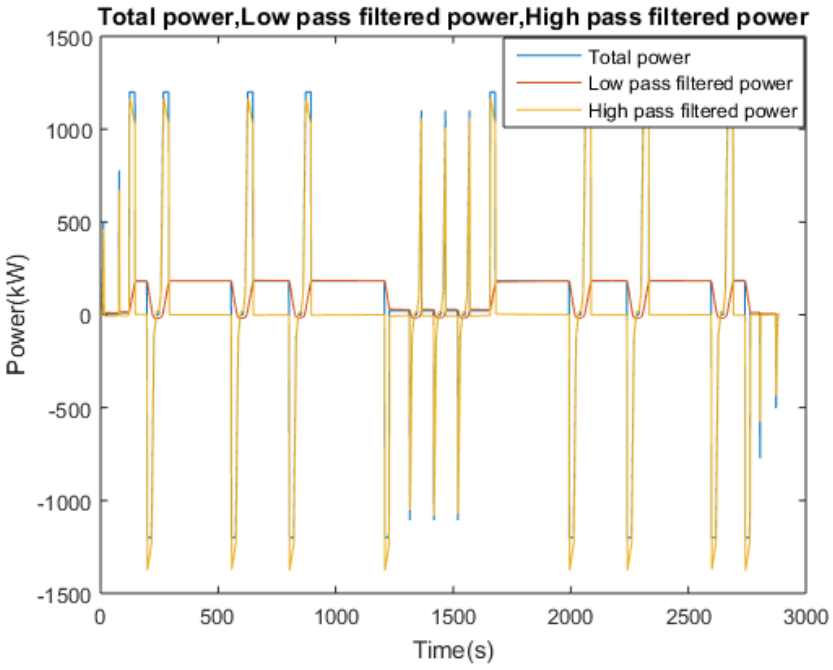

Figure 4.4.9. Total power demand, Low pass-filtered power demand and high pass-filtered power demand in time domain

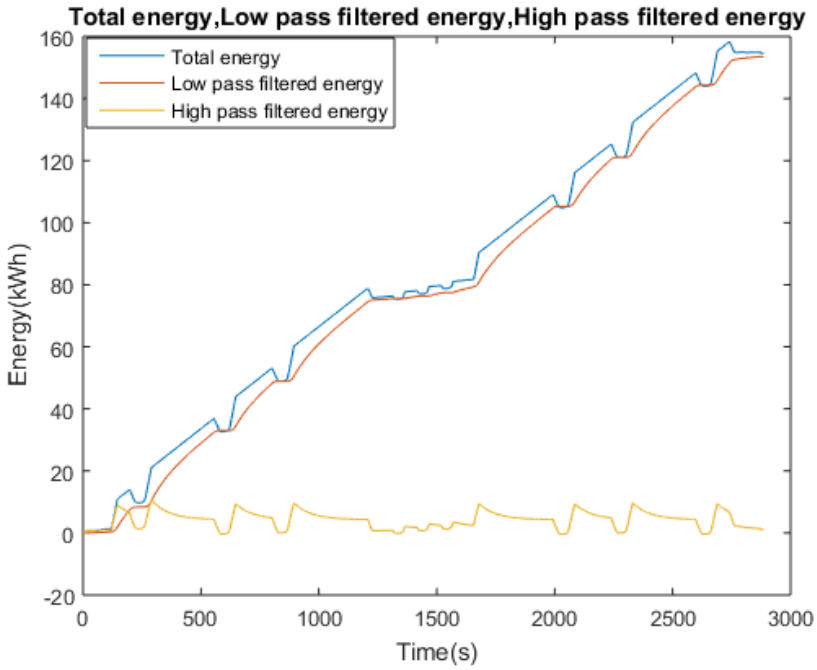

Figure 4.4.10. Total energy demand, Low pass-filtered energy demand and high pass-filtered energy demand in time domain

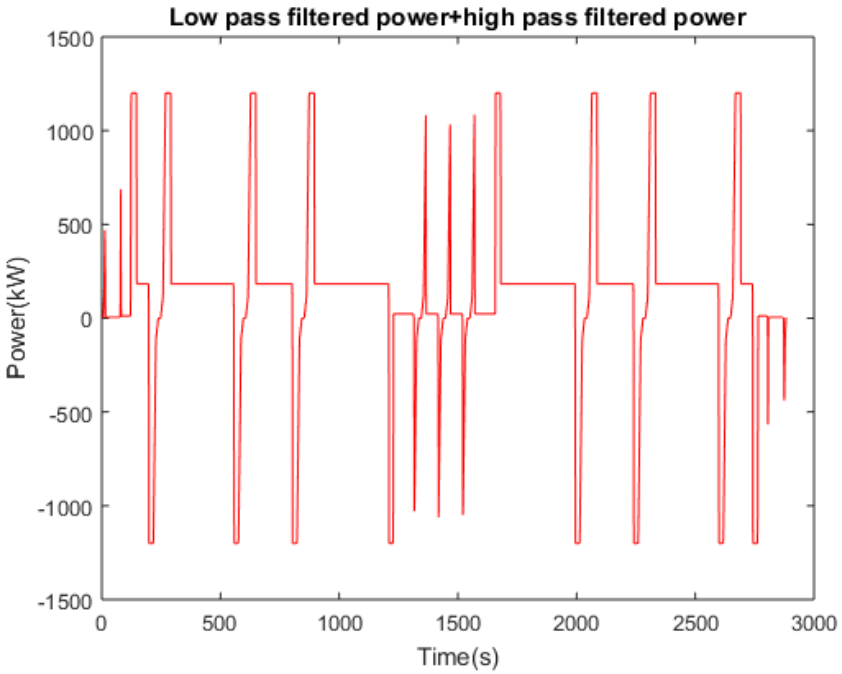

Figure 4.4.11. Sum of low pass-filtered and high pass-filtered power demands

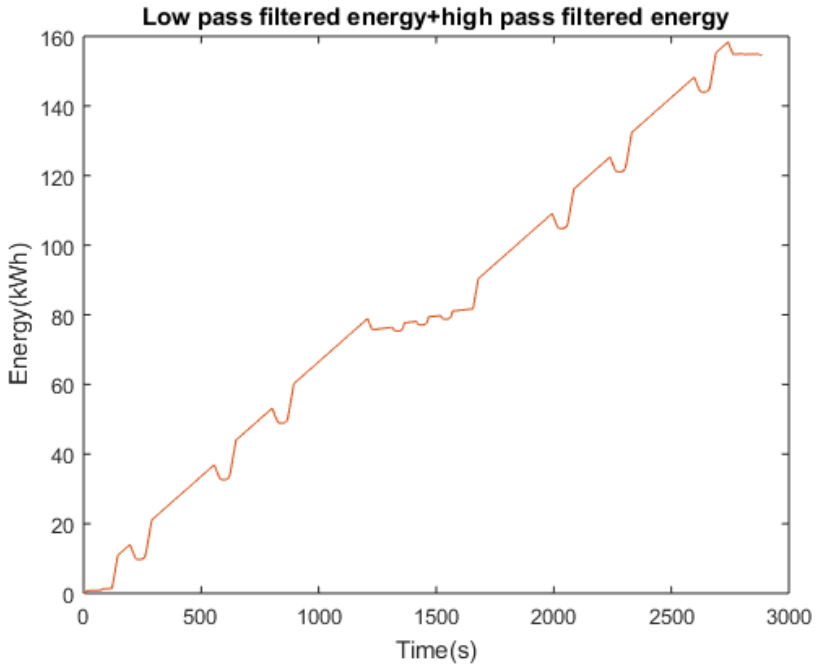

Figure 4.4.12. Sum of low pass-filtered and high pass-filtered energy demands

As it was expected, the higher number of supercapacitor modules is the energy-based number and as mentioned in Section 3.3.3, discharging power is not included in energy-based calculations. Hence, the C-rate constraint can now be imposed on the determined supercapacitor pack in order to see whether the pack has to discharge higher than its typical discharging power during the journey and whether the sized supercapacitor pack is able to meet the required energy and power demand after imposing the C-rate constraint. Figure 4.4.13 indicates how the sized HESS performs in meeting the power demand after imposing C-rate constraint on the supercapacitor pack.

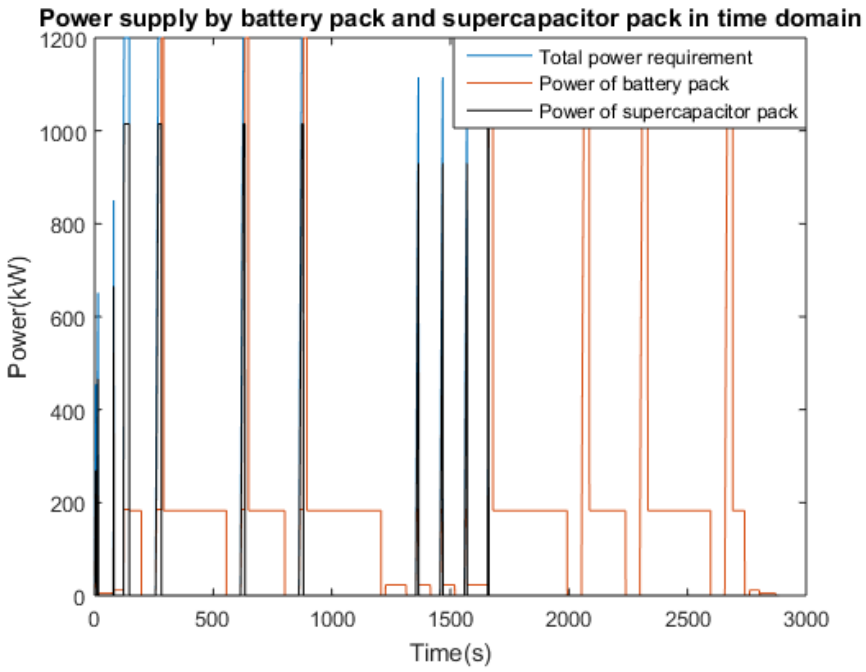

Figure 4.4.13. HESS supplying power demand in time domain
after imposing C-rate constraint

It can be seen that after imposing the C-rate constraint, the sized supercapacitor pack including 190 supercapacitors does not have enough energy to meet the required power demand which was responsible for. This means the supercapacitor pack discharges higher than its typical discharging power after imposing the C-rate constraint and it becomes empty earlier than

expected. The figure indicates that the battery pack is forced to compensate instead of the supercapacitor pack. Figure 4.4.14 indicates how both battery pack and supercapacitor pack discharge during the journey. It can be seen that the supercapacitor becomes fully empty from 1661s and stays empty until the end of the journey.

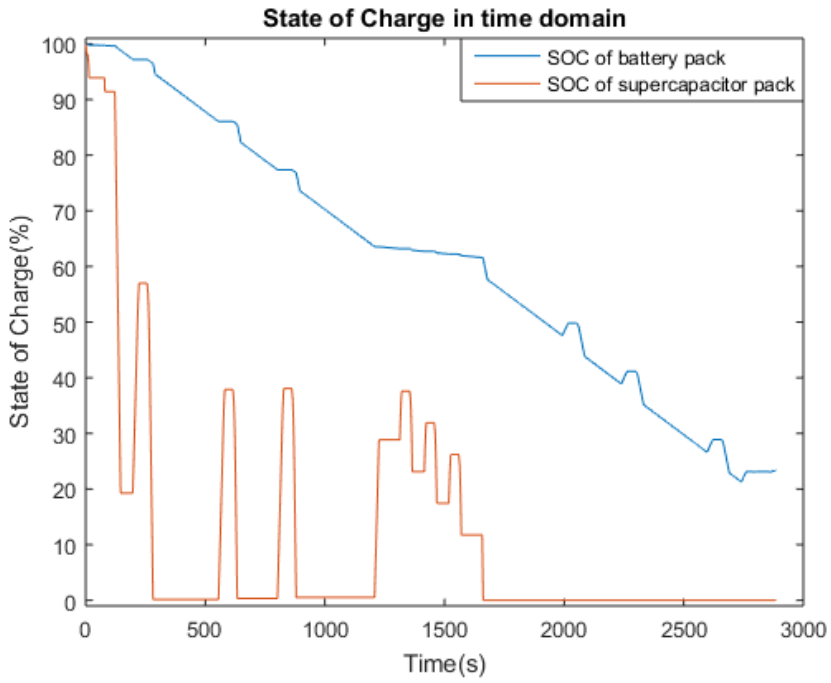

Figure 4.4.14. SOC changes of battery pack and supercapacitor pack in time domain after imposing C-rate constraint

Now, the number of supercapacitors need to increase in order to be ensured that there are adequate number of supercapacitors discharging not beyond the typical discharging power. By increasing the number of supercapacitor modules to 855, there will be enough supercapacitors which don't discharge above 13.6 kW.

Figure 4.4.15 indicates how this newly-sized HESS including 125 batteries and 855 supercapacitors supply the power demand during the journey.

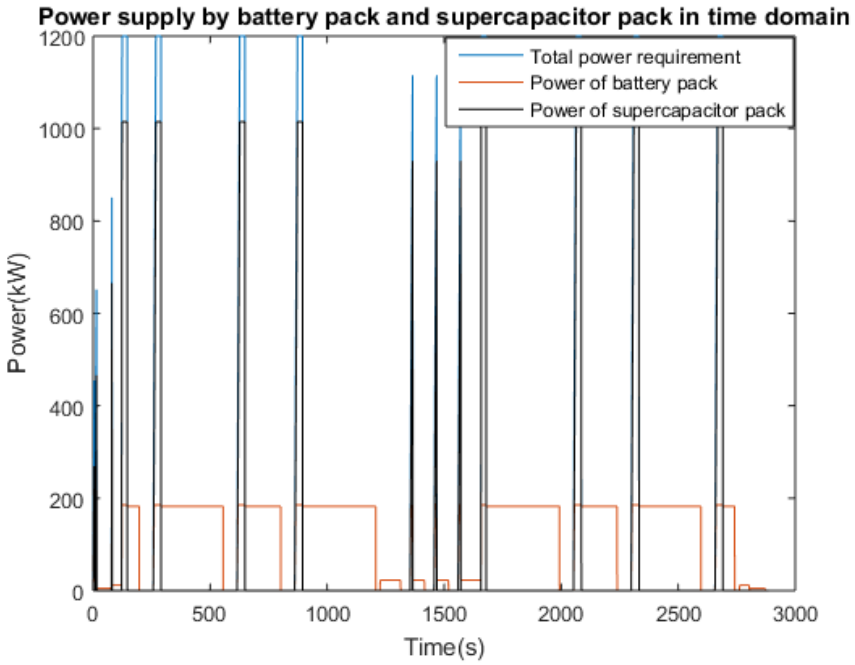

Figure 4.4.15. HESS supplying power demand in time domain

with increased number of supercapacitor modules

One hundred and twenty five battery modules can provide 185.3kW, and this is the power limit of the battery pack. It can be seen that the battery pack meets the low-frequency parts of the power demand (cruising modes and a part of the acceleration mode) and the supercapacitor pack supports the high-frequency parts of the power demand, in acceleration modes. This figure indicates that now the supercapacitor pack including 855 modules has adequate energy to meet the power demand for which it is responsible until the end of the journey, and the battery pack does not have to discharge more than its 1 C-rate to compensate for the supercapacitor pack.

Figure 4.4.16 indicates how both packs charge and discharge during the journey. Regarding the supercapacitor pack, it is seen that only 0.79% of its energy remains at the end of the journey; 44.02% of the battery pack's stored energy is left unused.

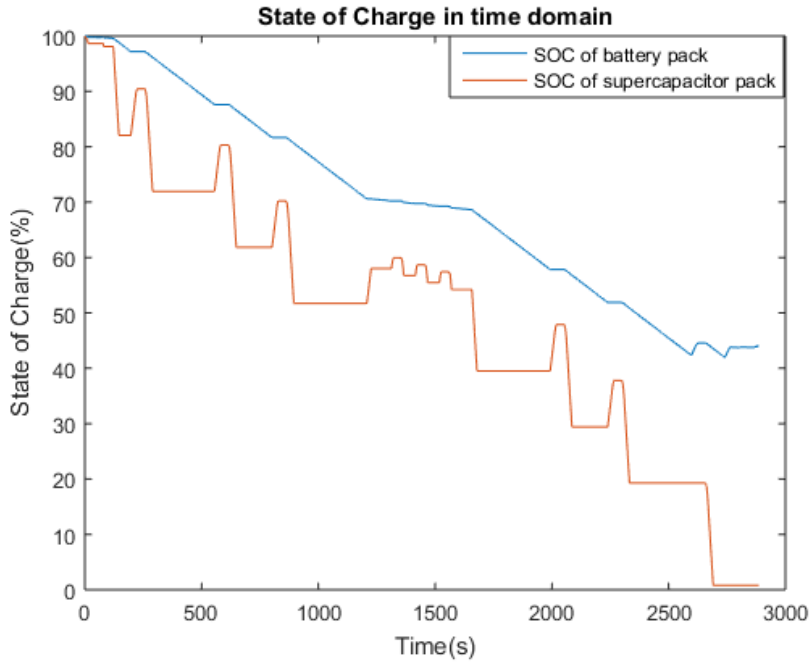

Figure 4.4.16. SOC changes of battery pack and supercapacitor pack in time domain with increased number of supercapacitor modules

By imposing the C-rate constraint to the supercapacitor pack, there are 125 battery modules and 855 supercapacitor modules in the HESS, which makes the total weight and volume of the HESS 55.65 t and 6.45 m^3.

Now the battery pack can be used as an energy supplier to charge the supercapacitor pack during the journey. As mentioned in Section 3.3.4, two criteria are considered for the charging procedure and two scenarios are proposed for each criteria. The first criteria is to get the batteries to charge the supercapacitors based on the energy left in the supercapacitor pack. The first scenario for this criteria is for the battery pack to charge the supercapacitor pack whenever the supercapacitor pack's SOC falls below 1%. Brute Force optimisation is applied to the already sized HESS including 125 batteries and 855 supercapacitors to minimise the number of supercapacitor modules and hence, minimise the size of the HESS. The range of search for the number of supercapacitor modules in the optimisation is between 1 and 855. The number of

supercapacitor modules can decrease as much as the minimum SOC of the supercapacitor pack does not become 0 and also, the HESS is able to meet the required energy and power. Figure 4.4.17 indicates the result of the Brute Force optimisation, where the number of supercapacitor modules are indicated versus the minimum SOC of the supercapacitor pack during the journey.

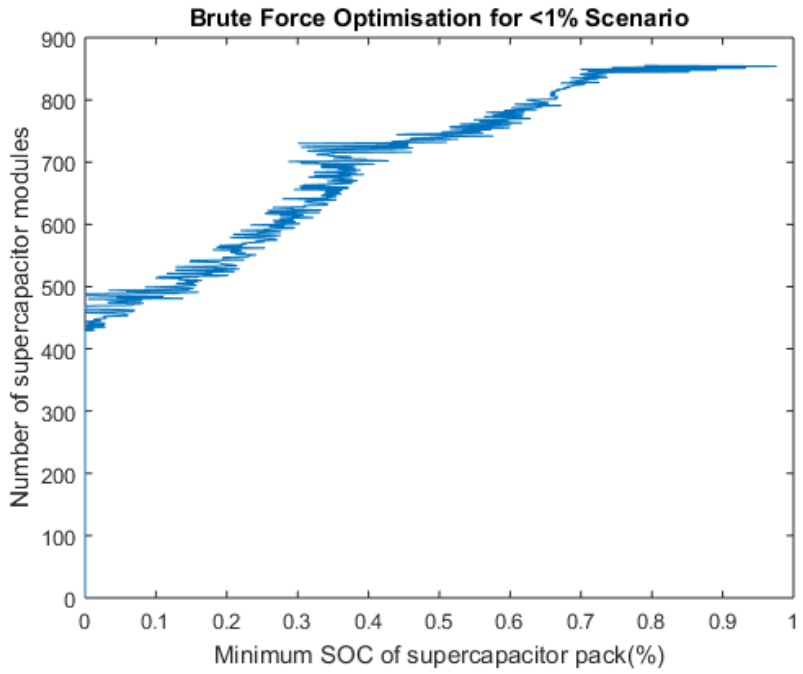

Figure 4.4.17. Brute Force Optimisation for Supercapacitor SOC <1% Scenario

From the figure, it can be seen that the minimum number of supercapacitors without making the SOC of the supercapacitor pack become 0 is 430. With 430 number of supercapacitor modules, the minimum SOC of the supercapacitor pack during the journey is 0.01%. With 429 supercapacitor modules, the SOC becomes 0 and this not desired. Hence, the optimal number of the supercapacitor modules for this scenario is considered 430. Figure 4.4.18 and Figure 4.4.19 indicate how the HESS including 129 battery modules and 430 supercapacitor modules perform during the journey.

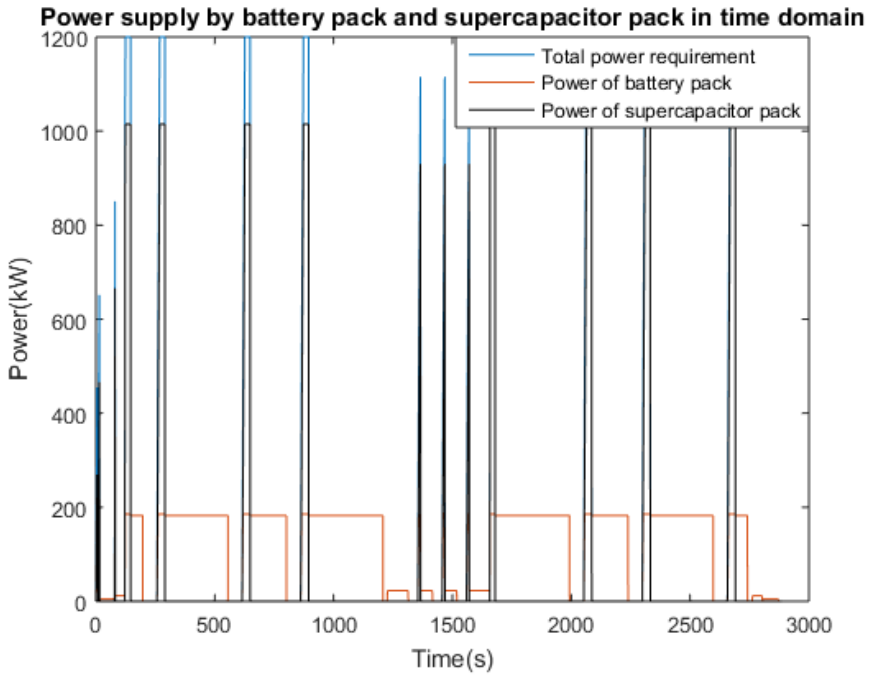

Figure 4.4.18. HESS supplying power demand in time domain,
battery pack charging supercapacitor pack for Supercapacitor SOC <1% Scenario

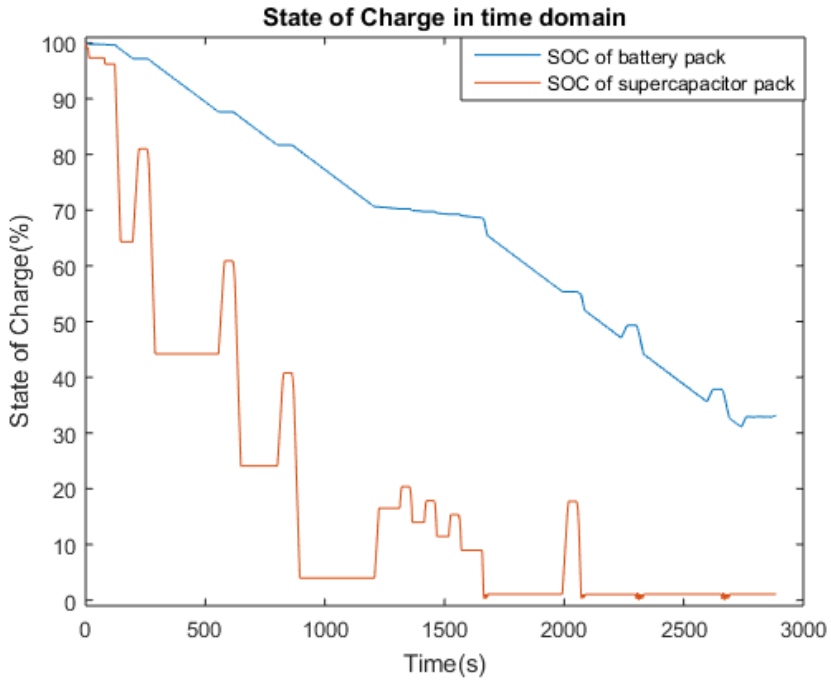

Figure 4.4.19. SOC changes of battery pack and supercapacitor pack in time domain,
battery pack charging supercapacitor pack for Supercapacitor SOC <1% Scenario

Figure 4.4.18 shows that the sized HESS is capable of meeting the energy and power demand and from Figure 4.4.19, it can be seen that the battery packs charges the supercapacitor pack whenever its SOC goes below 1%. This happens in acceleration modes in the return journey. The energy left at the battery pack at the end of the journey is 33.14%. With 125 battery modules and 430 supercapacitor modules in the HESS, the total weight and volume of the HESS can decrease to 29.73t and 4.15m^3, respectively.

The second charging scenario in this criteria needs to be considered, which is charging whenever the supercapacitor pack's SOC goes below 100%. Figure 4.4.20 indicates the result of Brute Force optimisation for this scenario, where 5 number of supercapacitor modules is the minimum number without making the SOC of the supercapacitor pack become 0. Figure 4.4.21 shows how the sized HESS with 125 battery modules and 5 supercapacitor modules meets the energy and power demand during the journey and in Figure 4.4.22, the change of the SOC of both packs can be seen, where the minimum SOC of the supercapacitor pack during the journey is 0.01% and the energy left at the battery pack at the end of the journey is 14.29%. The figure shows that the battery pack charges the supercapacitor pack whenever the supercapacitor pack's SOC falls below 100%. This happens in both cruising and acceleration modes.

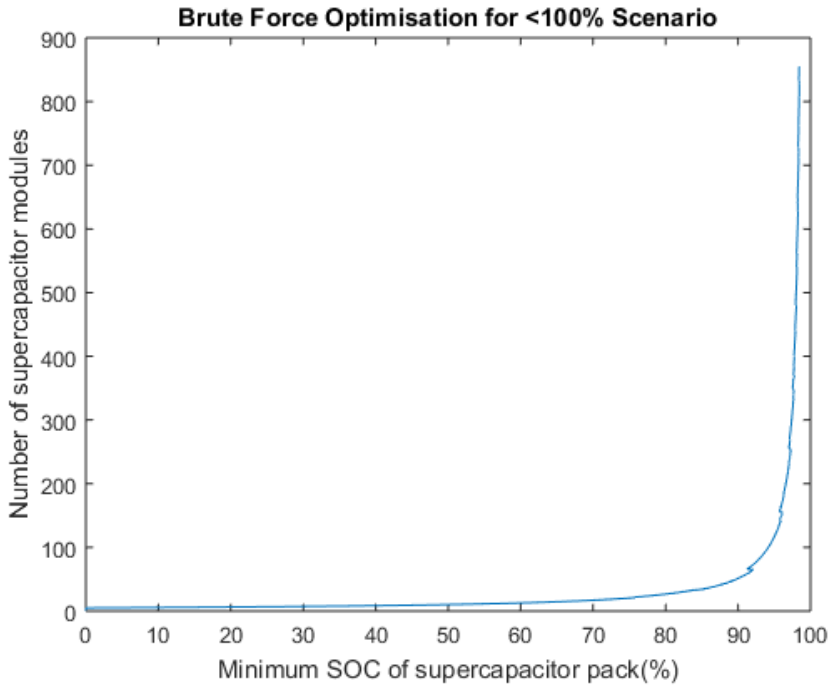

Figure 4.4.20. Brute Force Optimisation for Supercapacitor SOC <100% Scenario

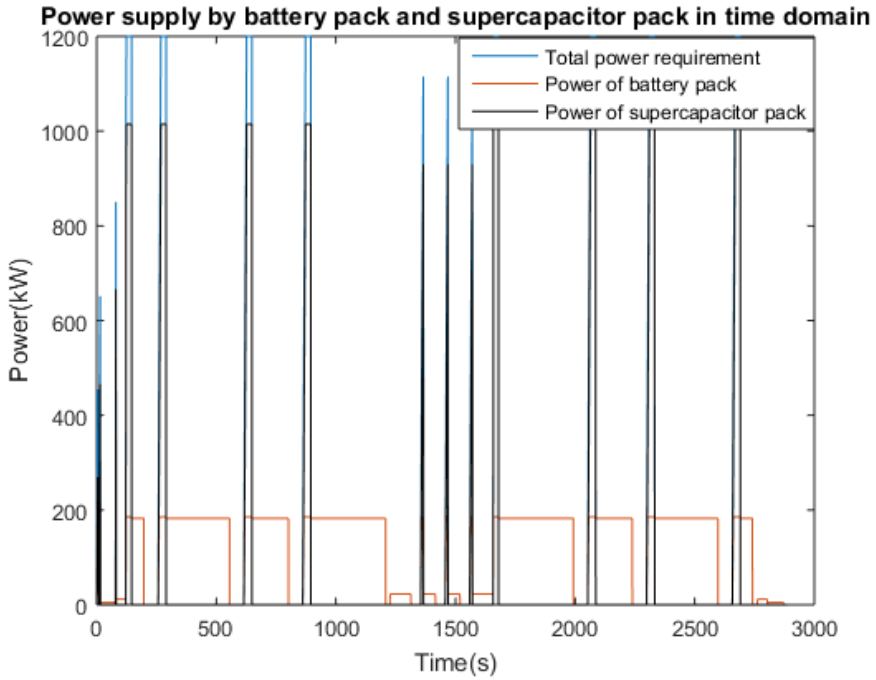

Figure 4.4.21. HESS supplying power demand in time domain,
battery pack charging supercapacitor pack for Supercapacitor SOC <100% Scenario

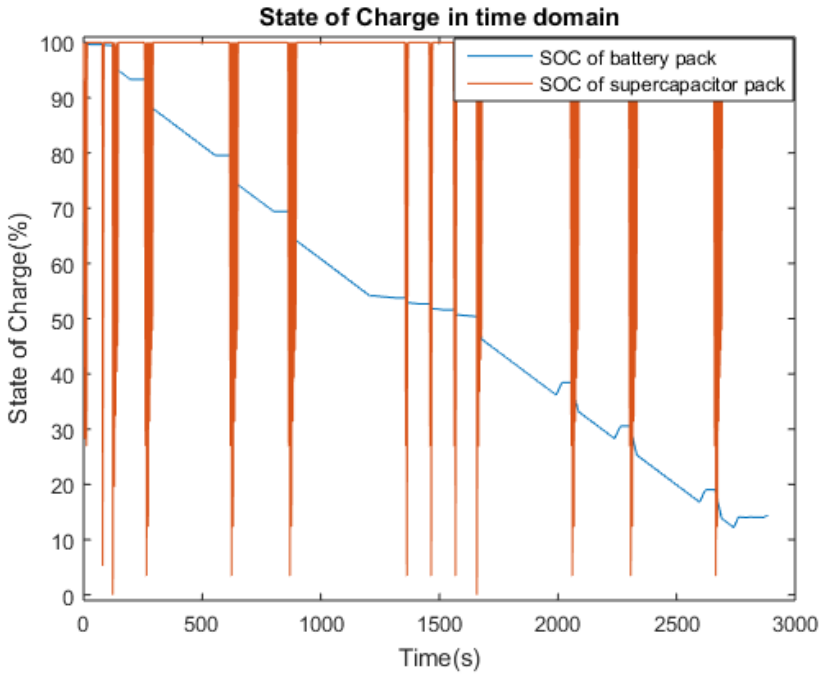

Figure 4.4.22. SOC changes of battery pack and supercapacitor pack in time domain, battery pack charging supercapacitor pack for Supercapacitor SOC <100% Scenario

The size of the HESS including 125 battery modules and 5 supercapacitor modules is 3.8t and 1.85m^3.

The next criteria to have the battery pack to size the supercapacitor pack is charging based on the mode of traction, where the first scenario in this criteria is to have the charging procedure in cruising modes during the journey. Figure 4.4.23 indicates the result of the used Brute Force optimisation applied to this scenario, which indicates that with 159 supercapacitor modules, the minimum SOC of the supercapacitor pack during the journey 0.37%. Decreasing this number to 158 makes the minimum SOC of the supercapacitor pack become 0; hence, 159 is chosen as the most optimal number in this scenario for the supercapacitor modules. Figure 4.4.24 and Figure 4.4.25 indicate the performance of the HESS including 125 battery modules and 159 supercapacitor modules; where the HESS is fully able to meet the required energy and power and energy left at the end of the journey for the battery pack is 12.98%.

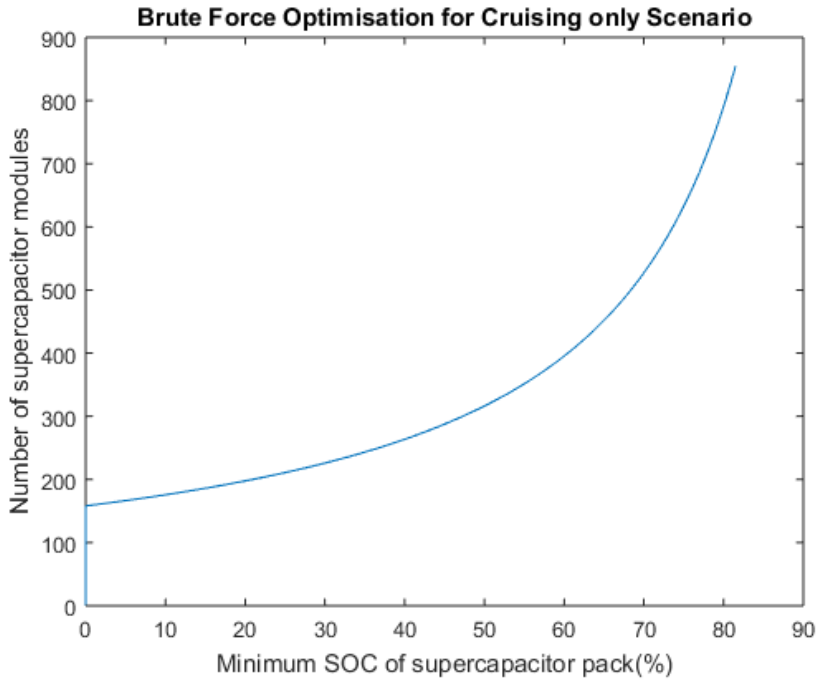

Figure 4.4.23. Brute Force Optimisation for Cruising Scenario

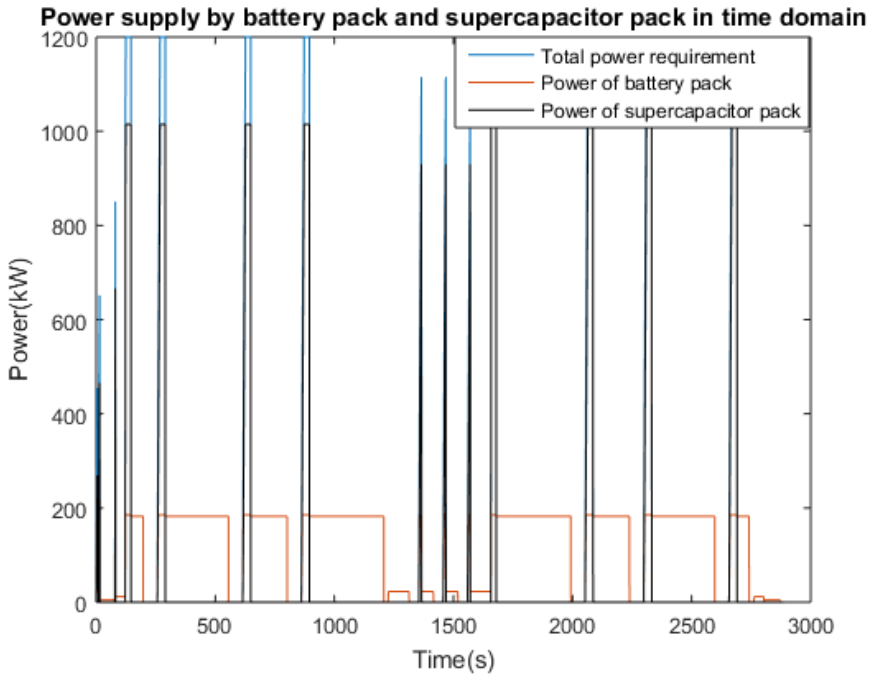

Figure 4.4.24. HESS supplying power demand in time domain,
battery pack charging supercapacitor pack for Cruising Scenario

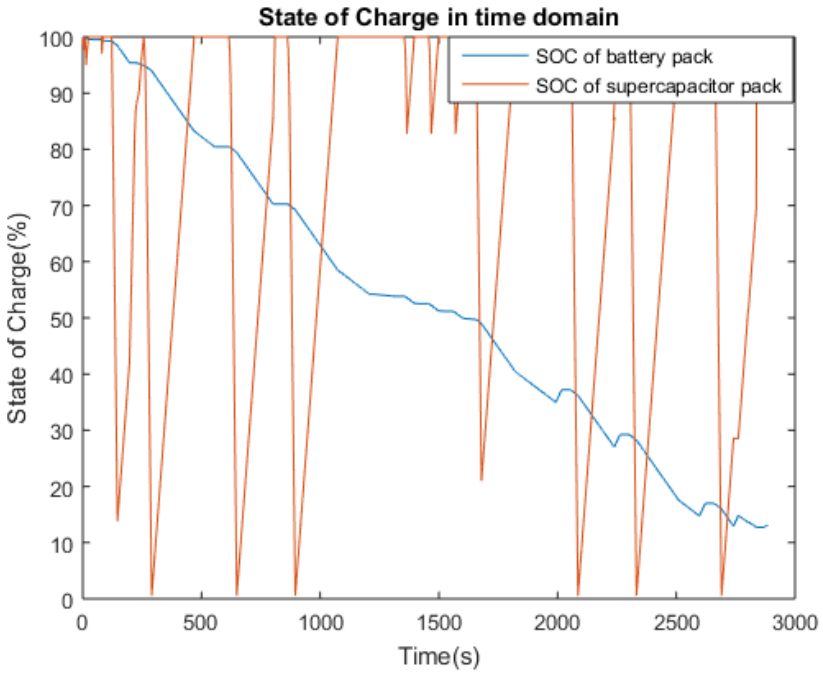

Figure 4.4.25. SOC changes of battery pack and supercapacitor pack in time domain, battery pack charging supercapacitor pack for Cruising Scenario

From Figure 4.4.25 it can be seen that the battery pack charges the supercapacitor pack in cruising modes until the supercapacitor becomes full in that mode. The total weight and volume of the optimal HESS in this scenario including 125 battery modules and 159 supercapacitor modules is 13.2t and 2.69m^3, respectively.

The final scenario is to get the battery pack to charge the supercapacitor pack only in acceleration modes. Figure 4.4.26 indicates the results achieved from Brute Force optimisation for this scenario. It can be seen that the optimal number of supercapacitor modules in this scenario is 17, where the minimum SOC of the supercapacitor pack is 0.01%. Figure 4.4.27 indicates how the HESS with 125 battery modules and 17 supercapacitor modules meets the energy and power demands. The change of the SOC of both packs can be seen in Figure 4.4.28.

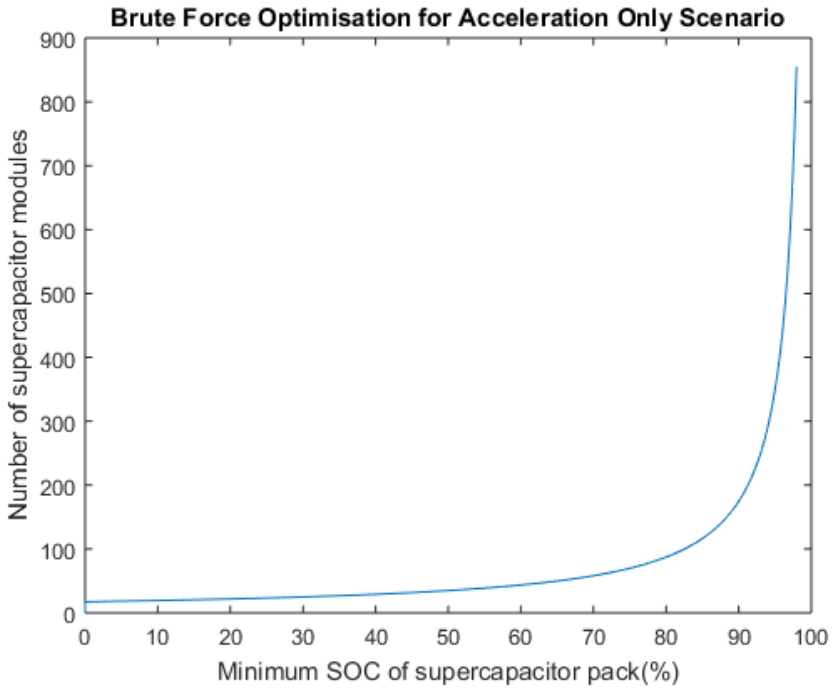

Figure 4.4.26. Brute Force Optimisation for Acceleration Scenario

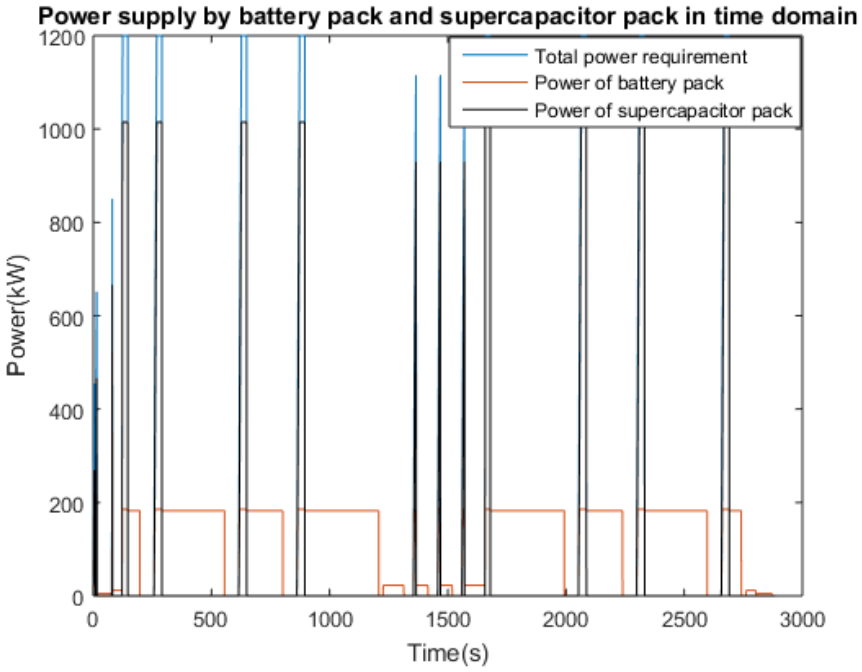

Figure 4.4.27. HESS supplying power demand in time domain,
battery pack charging supercapacitor pack for Acceleration Scenario

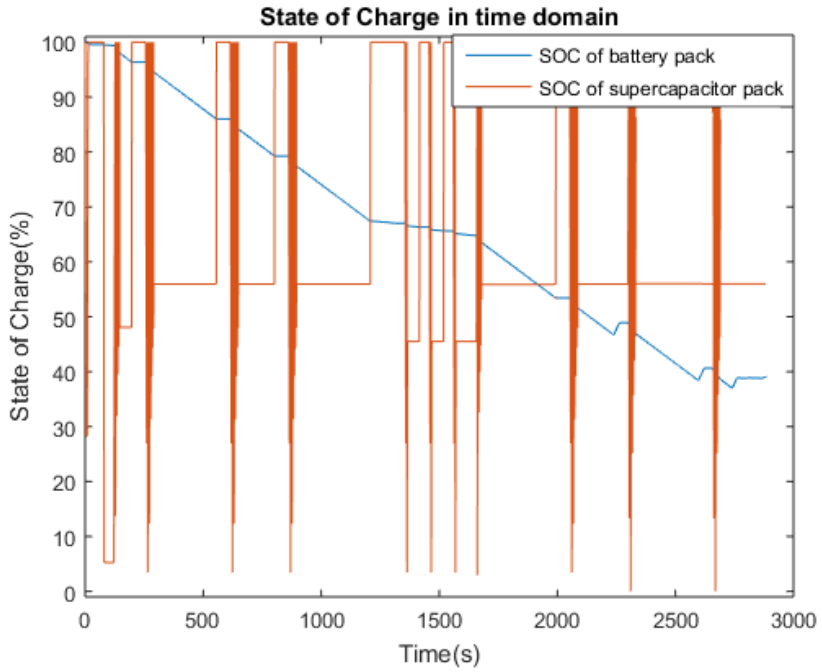

Figure 4.4.28. SOC changes of battery pack and supercapacitor pack in time domain, battery pack charging supercapacitor pack for Acceleration Scenario

Figure 4.4.28 indicates that the supercapacitor pack is only charged in acceleration modes and that is the only mode where the supercapacitor is used. The energy left at the battery pack at the end of the journey is 39.08%.

Now the sized HESSs in this phase need to be compared with each other and also with the battery-only and supercapacitor-only scenarios. Table 4.4.4 compares the weights and volumes of the battery-only and supercapacitor-only ESSs, optimised HESSs in normal modes with and without C-rate constraints and optimal HESSs when the battery pack charges the supercapacitor pack. The table indicates the total number of battery and supercapacitor modules in each scenario as well as the total weight and volume of the storage system. It can be observed from the table that four optimised HESSs have lower weights and volumes compared to battery-only and supercapacitor-only ESSs; however, the optimised HESSs when there is C-rate constraint and when the battery pack charges the supercapacitor pack in SOC<1% Scenario have higher

sizes than the battery-only scenario. The highest weight and volume are for the supercapacitor-only scenario, 161.89t and 14.33m^3, respectively, and the lowest are for the HESS in which the battery pack charges the supercapacitor pack in SOC<100% Scenario, with a total weight of 3.8t and volume of 1.86m^3. Amongst four proposed charging scenarios, charging when the supercapacitor pack's SOC goes below 100%, resulted in the lowest number of supercapacitor modules and consequently, the lowest size of the HESS. On the other hand, the biggest size of the optimal HESS with charging scenario was for the one when the battery pack charged the supercapacitor pack when the supercapacitor pack's SOC goes below 1%.

The most remarkable comparison that can be made for the mentioned eight scenarios is the total energy consumed by the train and the peak power demand after adding the weight of the sized storage system to the mass of the train. Figure 4.4.29 and Figure 4.4.30 indicate the total energy consumption and peak power demand before and after adding the HESS to the mass of the train. It is clear that the greater weight of the on-board storage system adds more to the total mass of the train and consequently results in more energy being required for the traction. The initial energy consumption before adding the on-board storage system was 154.6kWh. Amongst the mentioned eight scenarios, the scenario where the battery pack charged the supercapacitor pack with SOC<100% had the lowest weight of the HESS and hence, resulted in the lowest energy consumption increase, 1.2kWh, which is 0.77% increase compared to the initial energy consumption. On the other hand, the supercapacitor-only scenario with the highest weight of storage system increased the energy consumption to 209.6kWh, which is 35.57% increase. The figures show that change in the mas of the train does not have any impact on the peak power demand as this parameter is considered fixed for the vehicle running on the specified route. Total energy consumption and peak power demand for each scenario as well as the increased percentage in energy/power is included in Table 4.4.4. Both energy consumption and peak

power demand figures indicate that increasing the energy consumption results in the increased journey time and the more the energy consumption increases, the more the journey time increases.

Table 4.4.4. Comparing battery-only ESS, supercapacitor-only ESS and optimised HESSs

	Battery-only ESS	Supercapacitor-only ESS	Optimised HESS (no C-rate constraint)	Optimised HESS (with C-rate constraint)	Optimised HESS (charging: SOC<1% Scenario)	Optimised HESS (charging: SOC<100% Scenario)	Optimised HESS (charging: in cruising only Scenario)	Optimised HESS (charging: in acceleration only Scenario)
Number of battery modules	810	-	125		125	125	125	125
Number of supercapacitor modules	-	2654	190	855	430	5	159	17
Total weight (t)	22.68	161.89	15.09	55.65	29.73	3.8	13.2	4.54
Total volume (m^3)	11.91	14.33	2.87	6.45	4.16	1.86	2.7	1.93
Total energy consumption after adding storage system (kWh)	162	209.6	159.2	173.4	164.8	155.8	158.2	155.9
Increased energy consumption (%)	4.78	35.57	2.98	12.16	6.59	0.77	2.32	0.84
Peak power demand after	1200	1200	1200	1200	1200	1200	1200	1200

adding storage system (kW)								
Increased peak power demand (%)	0	0	0	0	0	0	0	0

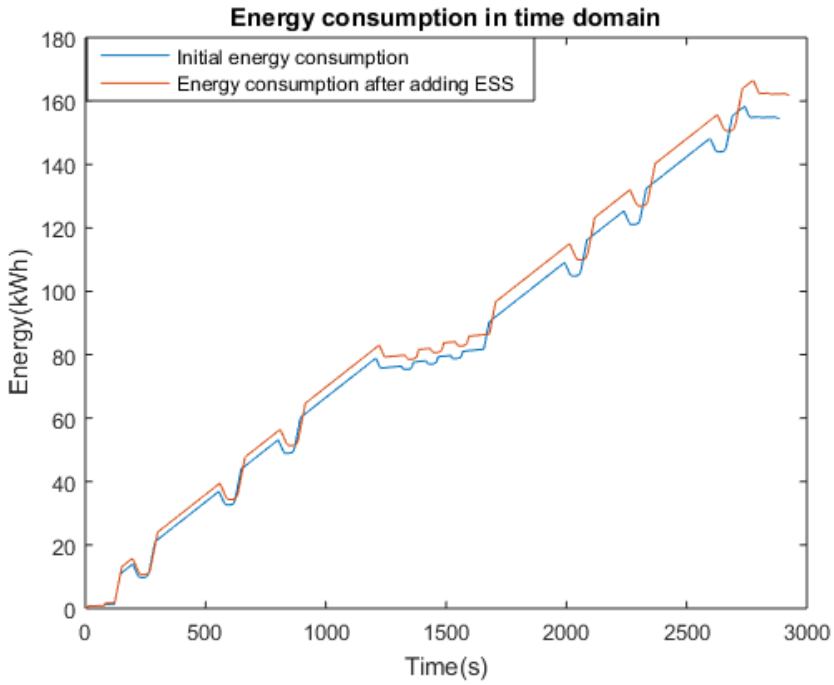

(a)

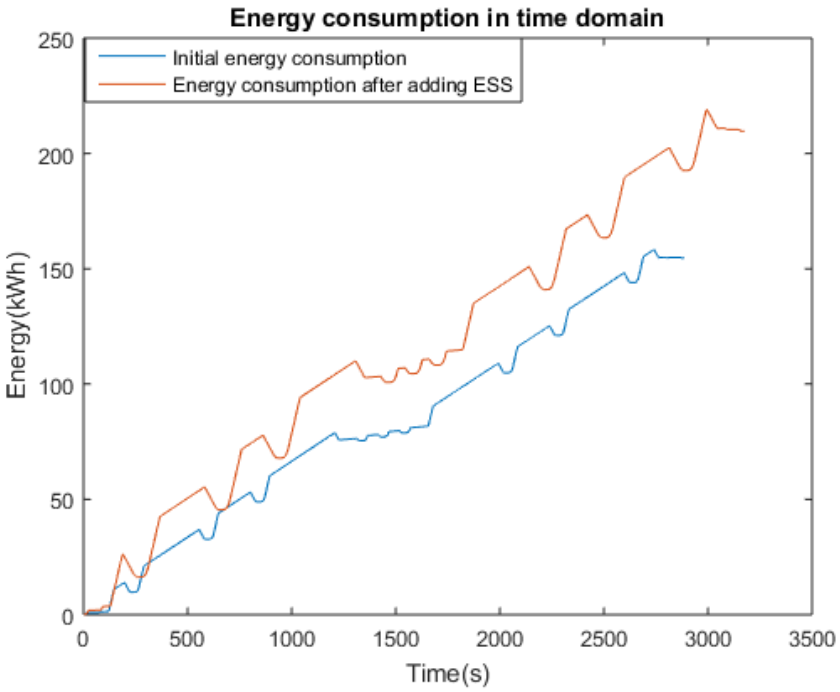
Energy consumption in time domain
Initial energy consumption
Energy consumption after adding ESS
Energy(kWh)
Time(s)
0
50
100
150
200
250
0
500
1000
1500
2000
2500
3000
3500

(b)

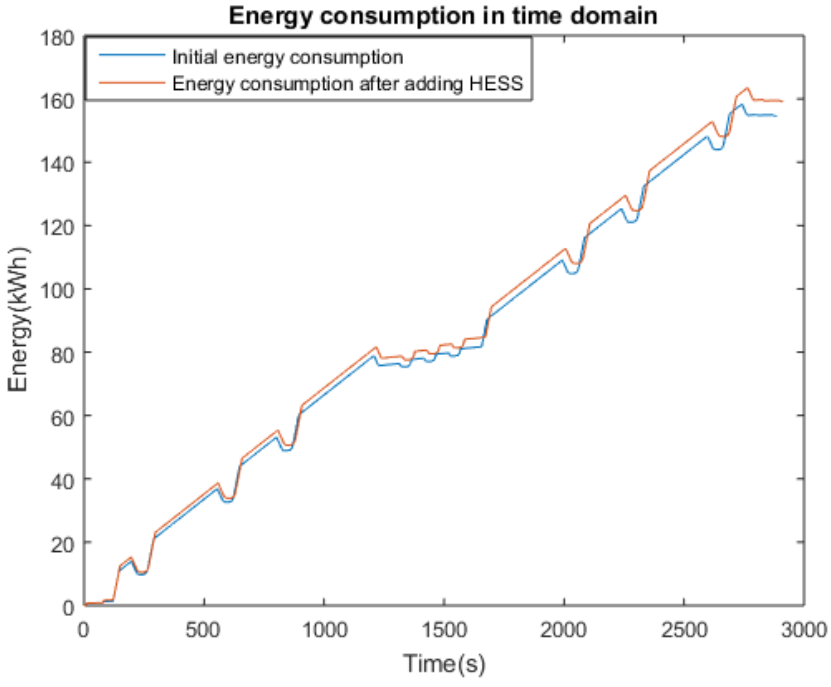
Energy consumption in time domain
Initial energy consumption
Energy consumption after adding HESS
Energy(kWh)
Time(s)
0
20
40
60
80
100
120
140
160
180
0
500
1000
1500
2000
2500
3000

(c)

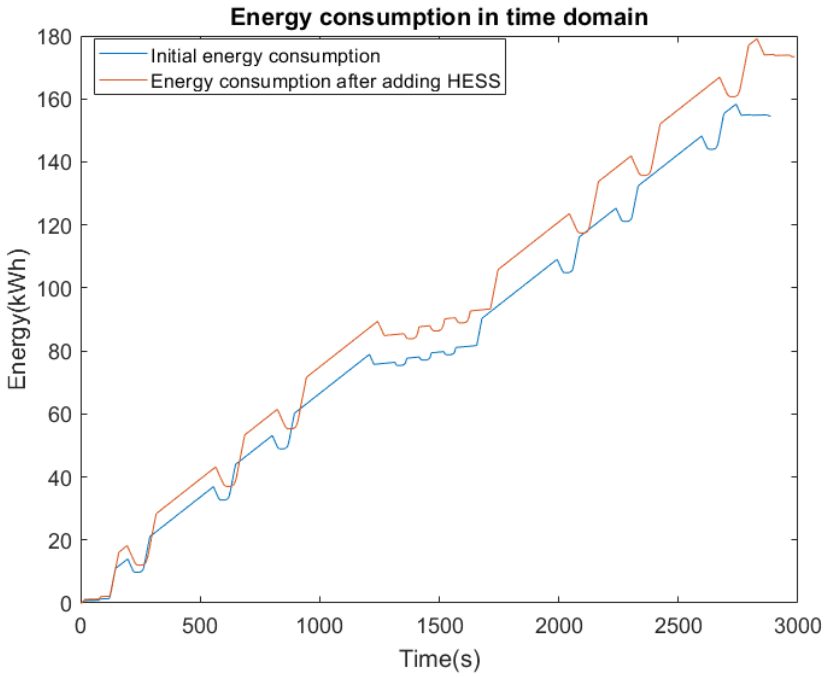
Energy consumption in time domain
Initial energy consumption
Energy consumption after adding HESS
Energy(kWh)
Time(s)
0
20
40
60
80
100
120
140
160
180
0
500
1000
1500
2000
2500
3000

(d)

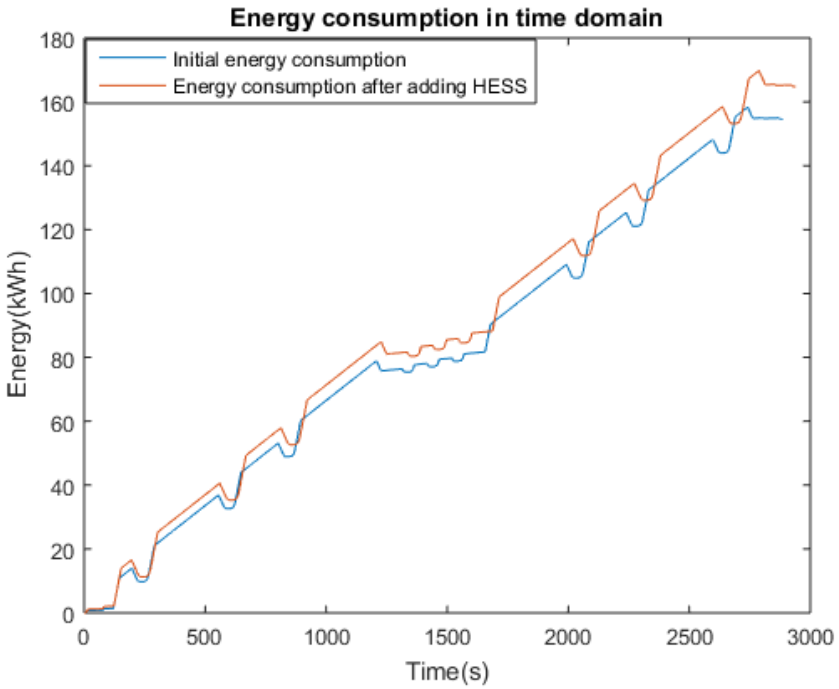
Energy consumption in time domain
Initial energy consumption
Energy consumption after adding HESS
Energy(kWh)
Time(s)
0
20
40
60
80
100
120
140
160
180
0
500
1000
1500
2000
2500
3000

(e)

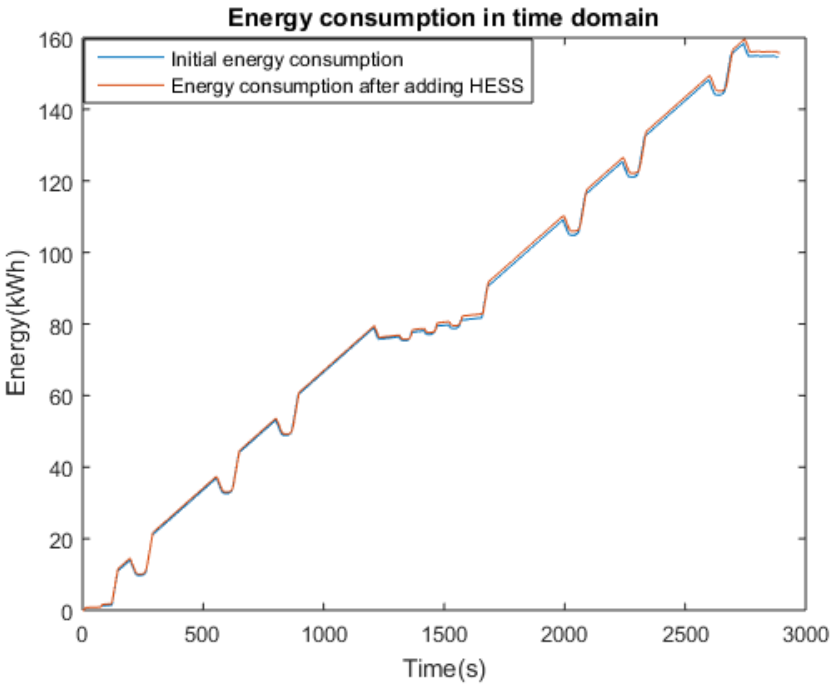
Energy consumption in time domain
Initial energy consumption
Energy consumption after adding HESS
Energy(kWh)
Time(s)
0
20
40
60
80
100
120
140
160
0
500
1000
1500
2000
2500
3000

(f)

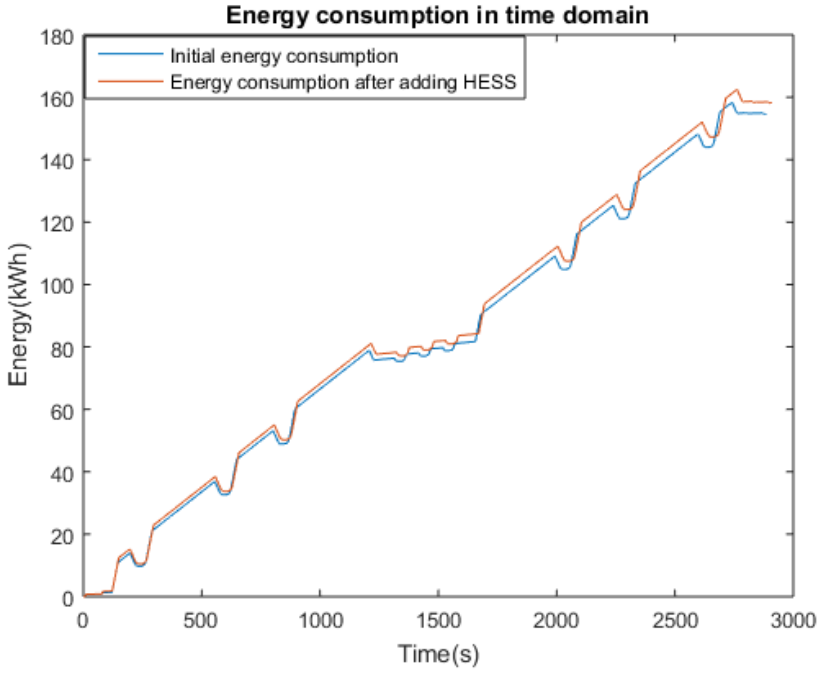
Energy consumption in time domain
Initial energy consumption
Energy consumption after adding HESS
Energy(kWh)
Time(s)
0
20
40
60
80
100
120
140
160
180
0
500
1000
1500
2000
2500
3000

(g)

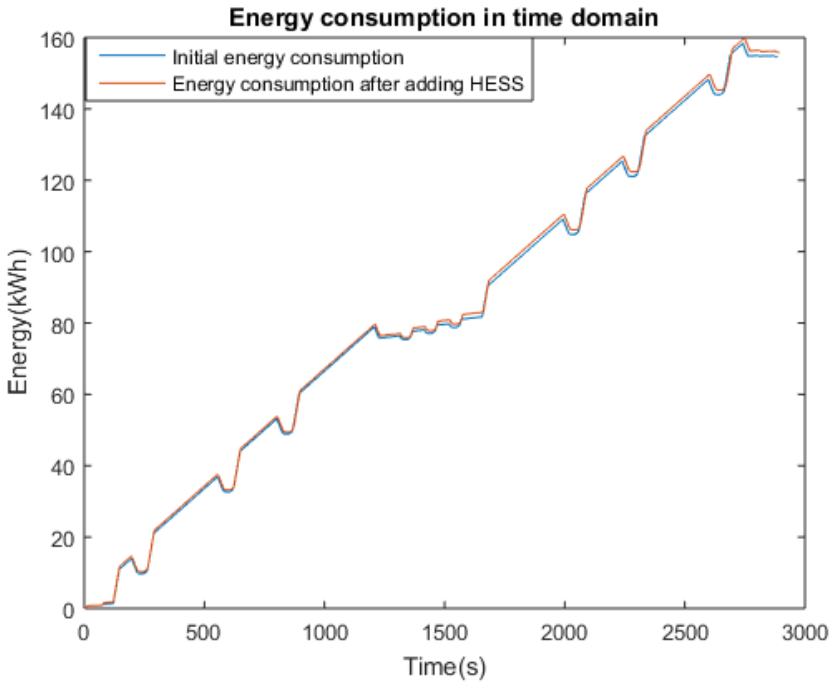

(h)

Figure 4.4.29. Energy consumption before and after adding the ESS/HESS for
(a) Battery-only Scenario
(b) Supercapacitor-only Scenario
(c) Optimised HESS (without C-rate constraint)
(d) Optimised HESS (with C-rate constraint)
(e) Optimised HESS (charging: SOC<1% Scenario)
(f) Optimised HESS (charging: SOC<100% Scenario)
(g) Optimised HESS (charging: cruising-only Scenario)
(h) Optimised HESS (charging: acceleration-only scenario)

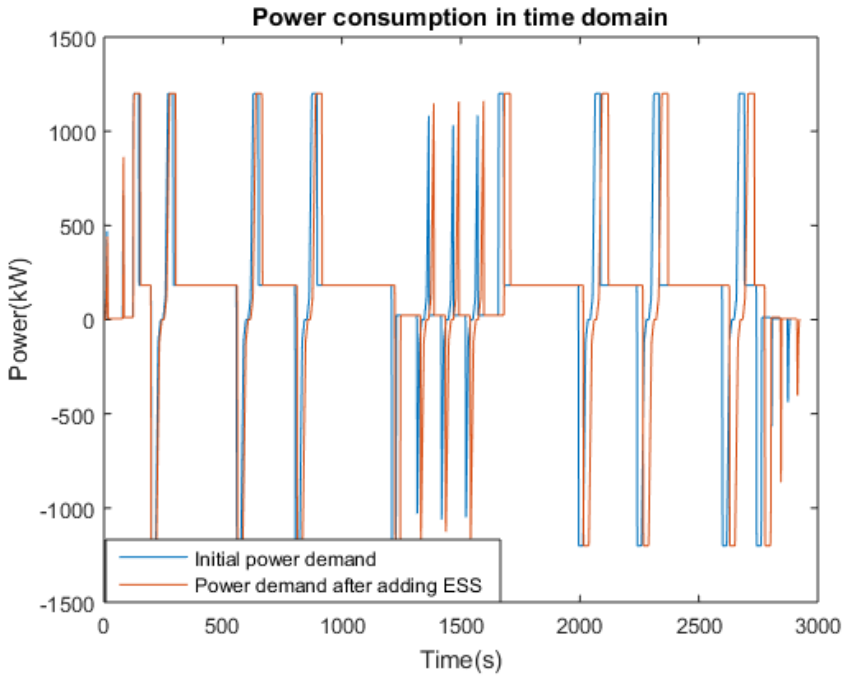
Power consumption in time domain
Power(kW)
Time(s)
Initial power demand
Power demand after adding ESS
1500
1000
500
0
-500
-1000
-1500
0
500
1000
1500
2000
2500
3000

(a)

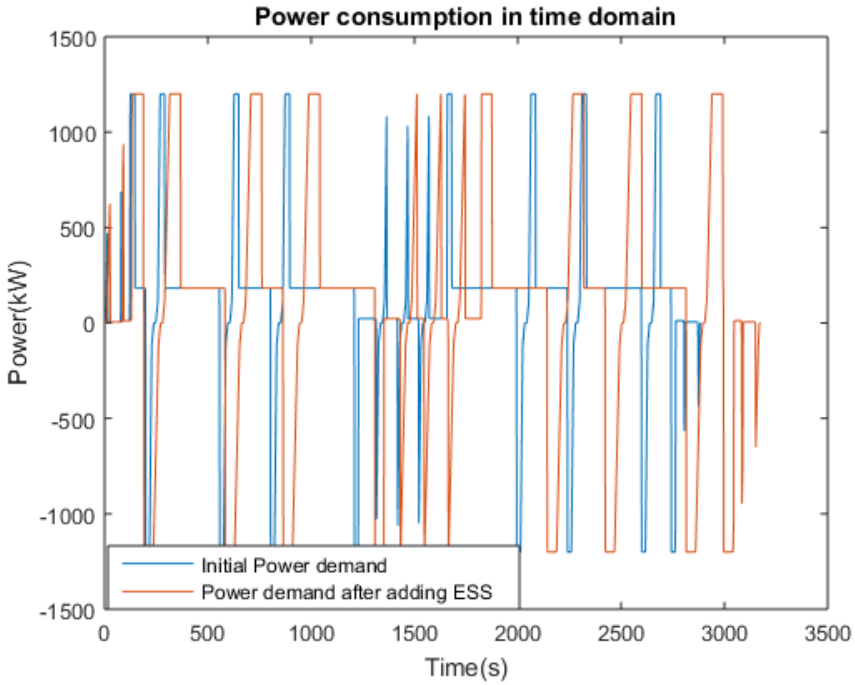
Power consumption in time domain
Power(kW)
Time(s)
Initial Power demand
Power demand after adding ESS
1500
1000
500
0
-500
-1000
-1500
0
500
1000
1500
2000
2500
3000
3500

(b)

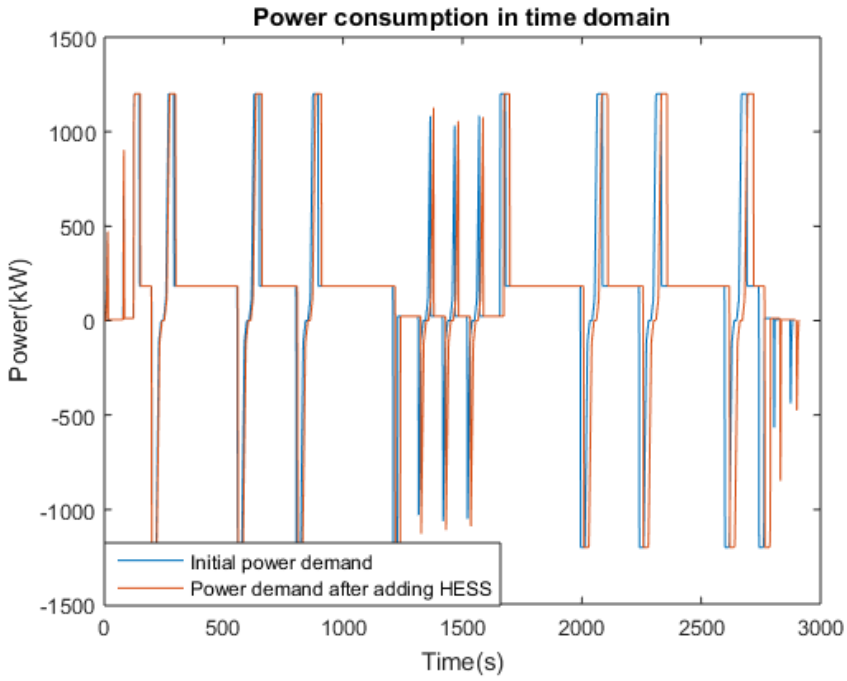
Power consumption in time domain
Power(kW)
Time(s)
Initial power demand
Power demand after adding HESS
1500
1000
500
0
-500
-1000
-1500
0
500
1000
1500
2000
2500
3000

(c)

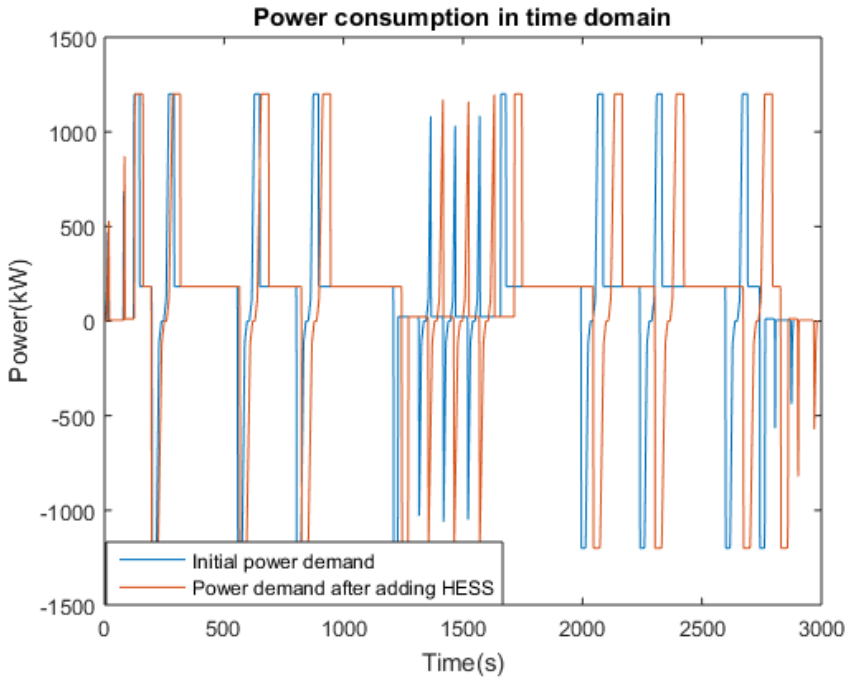
Power consumption in time domain
Power(kW)
Time(s)
Initial power demand
Power demand after adding HESS
1500
1000
500
0
-500
-1000
-1500
0
500
1000
1500
2000
2500
3000

(d)

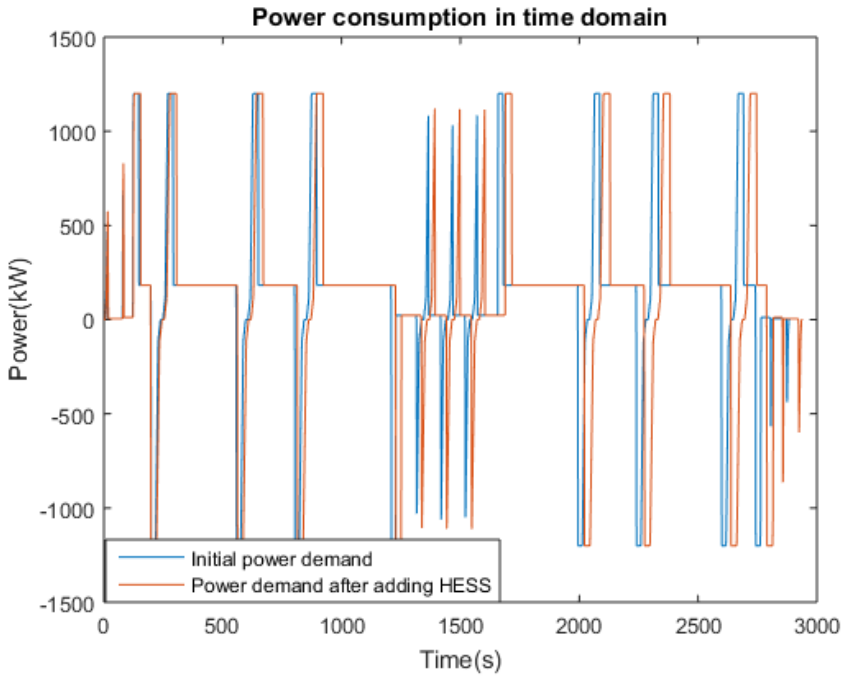
Power consumption in time domain
Power(kW)
Time(s)
Initial power demand
Power demand after adding HESS
1500
1000
500
0
-500
-1000
-1500
0
500
1000
1500
2000
2500
3000

(e)

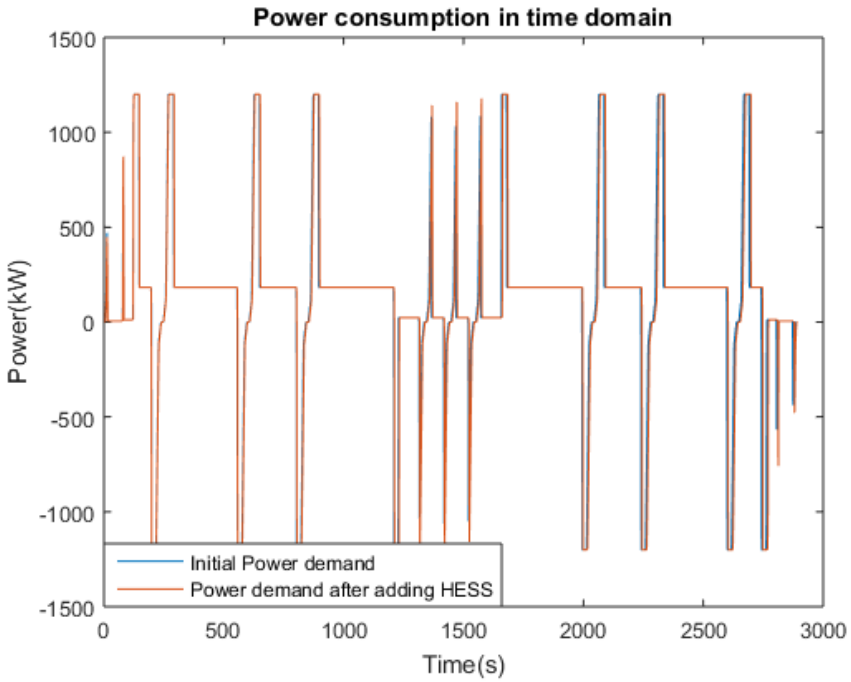
Power consumption in time domain
Power(kW)
Time(s)
Initial Power demand
Power demand after adding HESS
1500
1000
500
0
-500
-1000
-1500
0
500
1000
1500
2000
2500
3000

(f)

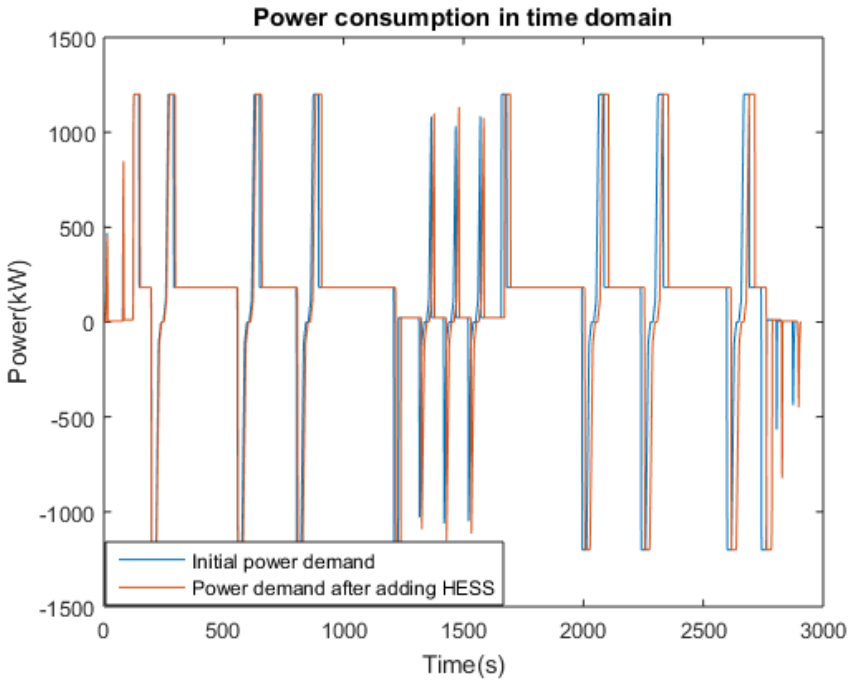
Power consumption in time domain
Power(kW)
Time(s)
Initial power demand
Power demand after adding HESS
1500
1000
500
0
-500
-1000
-1500
0
500
1000
1500
2000
2500
3000

(g)

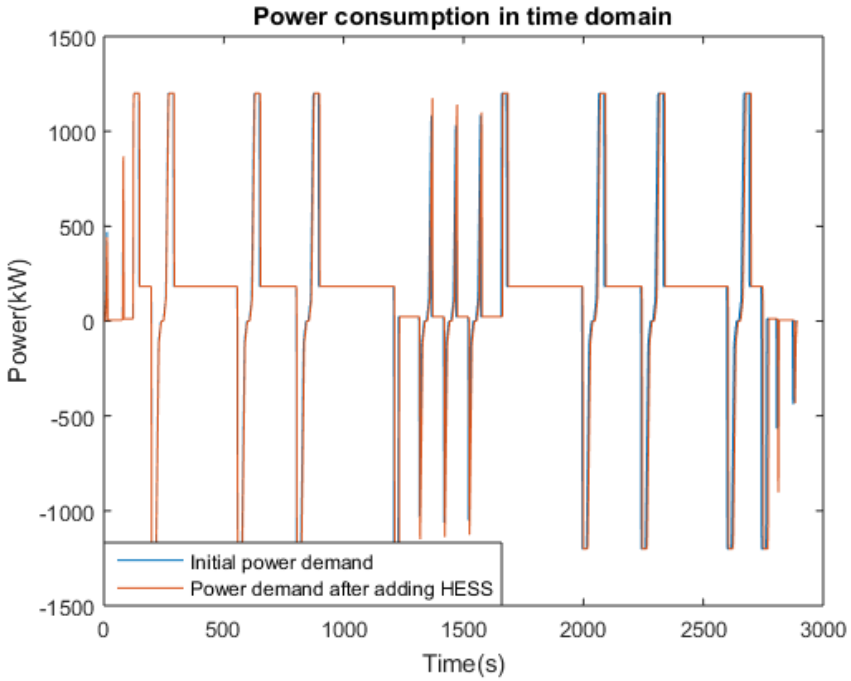
Power consumption in time domain
Power(kW)
Time(s)
Initial power demand
Power demand after adding HESS
1500
1000
500
0
-500
-1000
-1500
0
500
1000
1500
2000
2500
3000

(h)

Figure 4.4.30. Power demand before and after adding the ESS/HESS for
(a) Battery-only Scenario
(b) Supercapacitor-only Scenario
(c) Optimised HESS (without C-rate constraint)
(d) Optimised HESS (with C-rate constraint)
(e) Optimised HESS (charging: SOC<1% Scenario)
(f) Optimised HESS (charging: SOC<100% Scenario)
(g) Optimised HESS (charging: cruising-only Scenario)
(h) Optimised HESS (charging: acceleration-only scenario)

4.5. Summary

In this chapter, first a case study was introduced. The route and vehicle data for an EMU to run running a 750V DC line were determined and the traction was simulated in STS in order to find out the energy and power requirement of the journey to be supplied by the HESS.

First, the first part of the proposed methodology was applied to this case study in order to evaluate the integration of battery and supercapacitor in an HESS. It was seen that with regard to the energy demand, decreasing and increasing the number of battery modules and supercapacitor modules by 25%, respectively, resulted in an increase in the total weight and volume of the HESS by about 40t and about 3.2m^3. Regarding the power demand, decrease and increase in the number of battery modules and supercapacitor modules by 25%, respectively, resulted in an increase in the total weight and volume of the HESS by about 4.3t and 2.86m^3. It was seen that with 607 battery modules and 23 supercapacitor modules (Scenario 2), the supercapacitor pack did not have enough energy to meet the demands. When the battery pack compensated and charged the supercapacitor pack in order to solve the issue, it used 0.9% and 0.65% of its of its saved energy, respectively. Regarding the effect of the change in the C-rate of the battery pack on the total size of the HESS, every time that one supercapacitor module

was removed, the total weight and volume decreased by 0.061t (61kg) and 0.0054m^3 (5400cm^3), respectively.

In the second phase, a combination of the Frequency Analysis method and Brute Force optimisation was applied to the case study in order to achieve an optimal HESS with the objective function of the minimum size of the HESS. In the first optimal HESS, 125 battery modules and 190 supercapacitor modules were achieved resulting in the total size of 15.09t and 2.87m^3. After imposing the C-rate constraint to the energy-based sized supercapacitor pack, it was seen that the supercapacitor pack could not perform as expected and the number of supercapacitor modules had to increase to 855 which the made the size of the HESS 55.65t and 6.54m^3. The battery pack was then used as an energy supply to charge the supercapacitor pack during the journey based on the energy left in the supercapacitor pack and also the mode of traction. It was seen that amongst four charging scenarios, the scenario when the battery pack charged the supercapacitor pack whenever the supercapacitor pack's SOC went below 100% resulted in the lowest weight and volume (3.8t and 1.86m^3). Amongst all eight scenarios in this phase, including battery-only and supercapacitor-only ESSs, optimal HESSs in normal mode and optimal HESSs with charging procedure, the charging scenario with SOC<100% had the lowest weight and therefore, the lowest energy consumption increase, which was 1.2kWh (0.77%). On the other hand, the supercapacitor-only scenario with the highest weight of storage system increased the energy consumption the most to 209.6kWh (35.57%).

Chapter 5
Case Study 2: Tram Line

5.1. Introduction

In order to check the continuity of validation, the proposed methodology should be applied to another case study with different characteristics to the previous one (non-electrified line). For the second case study in this project, a tram line was chosen and the data used in this case study are based on the Edinburgh Tram line. This tram line is already electrified; an electric tram runs on an electrified tramway equipped with 750 V DC Overhead Line Equipment (OLE). However, the proposed methodology was applied to this case study to determine the applicability of the proposed methodology on trams.

As for Case Study 1, the real timetable is considered for this case study. All the proposed approaches introduced in Chapter 3 are applied to this case study too and the Evaluation, Sizing and Charging Phases are applied to this tram line.

5.2. Case study Familiarisation

5.2.1. Route Data

In this tram line, there are 15 stations. A one-way journey is 13.78km long, which makes the return journey 27.56km. The maximum speed in this journey is 70km/h. The line is somewhat hilly line and hence the gradient is variable throughout the journey. The dwell time in the real timetable is 30 seconds for all stations. Table 5.2.1 indicates the route data for this case study.

Table 5.2.1. Route data of case study 2

Parameter	Amount
Stations	15
Distance (km)	13.78
Maximum Speed (km/h)	70
Gradient	Variable
Dwell time (s)	30

5.2.2. Vehicle Data

As mentioned above, the tram running on this line is an electrified one (which is indicated in Figure 5.2.1) and, for this project, it is assumed that the HESS is sized to be installed above the tram to provide the energy required for the whole journey. Therefore, the tram does not have to use the overhead electrification.

Figure 5.2.1. Edinburgh tram

The tram has seven coaches which rest on four bogies. Key features of this tram are shown in Table 5.2.2.

Table 5.2.2. Vehicle data of Case Study 2

Property	**Data**
Tram length (m)	42.85
Laden weight (t)	80.46
Tractive effort (kN)	105.34
Maximum power (including auxiliary loads) (kW)	904
Maximum speed (km/h)	70
Davis coefficients	A = 1.0848, B = 0.007819, C = 0.0006205
Rotary allowance	0.07

5.2.3. Traction Simulation

The same as the previous case study, the first step is to simulate the train traction in STS in MATLAB. Figure 5.2.2 indicates the changes of some parameters of traction during the journey.

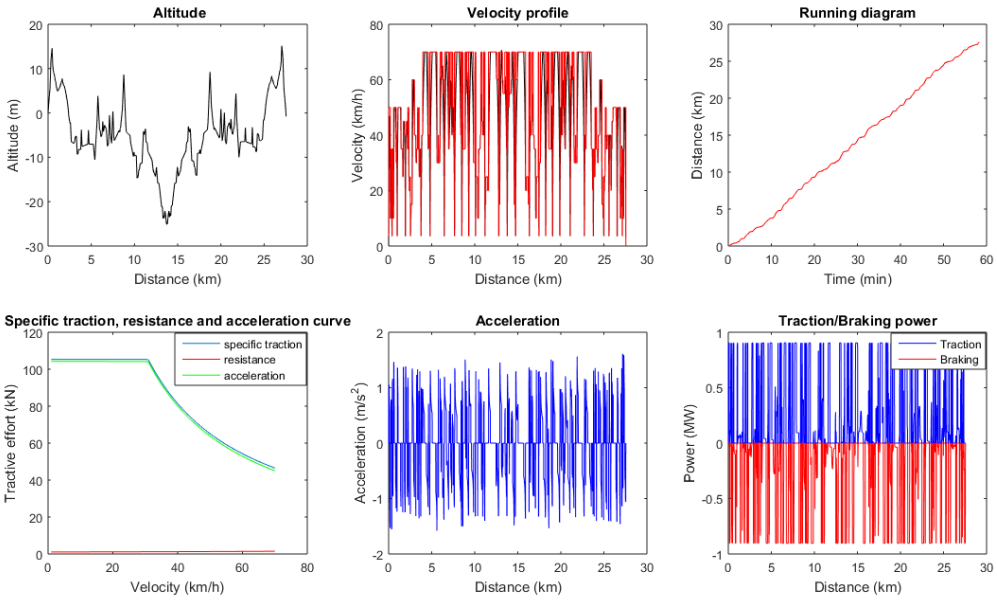

Figure 5.2.2. Altitude, Velocity profile, Running diagram, Specific traction, resistance and acceleration, Acceleration and Traction/Braking power of the simulated route

The upper left figure shows the altitude versus distance, and it can be seen that this parameter changes during the journey, from +15.15m to -25.05m. The upper middle figure is the velocity profile, showing the maximum velocity of 70km/h. The upper right panel shows running diagram which indicates that the train travels 27.56km in 58.35 minutes. The bottom left and the bottom middle figures show the tractive effort and the change of the acceleration of the tram, respectively, during the journey. The bottom right figure indicates power versus time, with 0.904MW (904kW) for both traction and braking. As the power requirement is one of the two key features that should be extracted from the traction simulation, Figure 5.2.3 shows the inclusive Power/Time result for this case study.

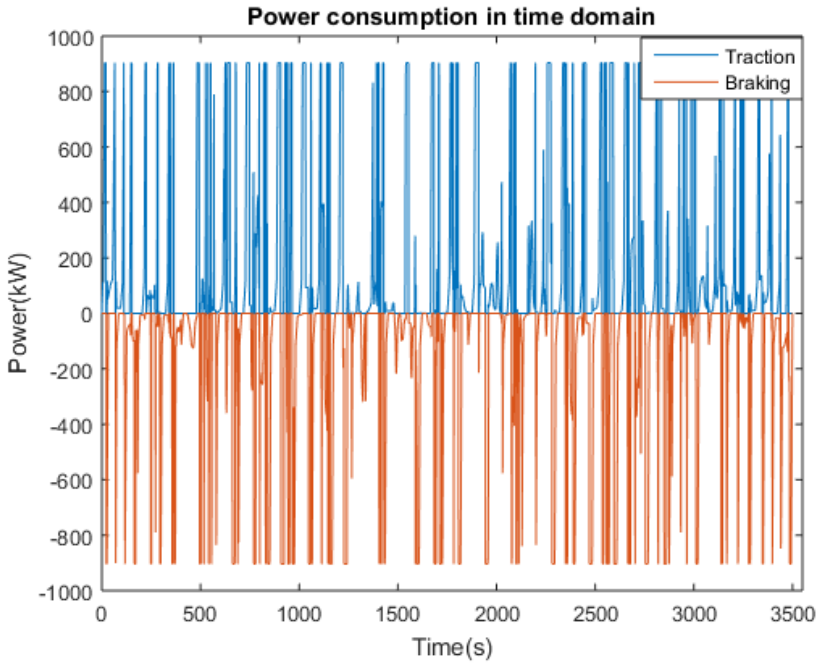

Figure 5.2.3. Power consumption in time domain

Due to the constant changes of velocity and gradient during the journey, several accelerations and brakings are observed in the figure. The HESS needs to be sized in a way to provide 904kW of power.

Energy consumption is the other crucial parameter that is required from the train simulation. Energy/Time is indicated in Figure 5.2.4, which shows that the train requires 112.6kWh in 3501 seconds (58.35 minutes) of journey time. It can be seen that the train absorbs energy whenever it brakes. In order for the HESS to meet the total energy demand for this case study, it should have 112.6kWh of stored energy.

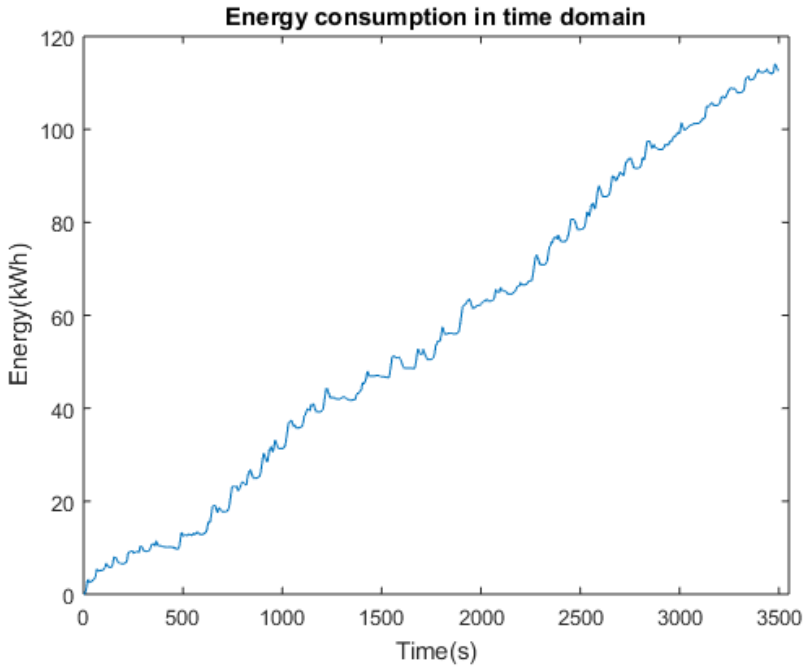

Figure 5.2.4. Energy consumption in time domain

5.3. Applying the 'Evaluation' Phase to the Case Study

As for the previous case study, this section evaluates the use of battery and supercapacitor together in an HESS as well as the impacts of the energy densities and power densities of both storage devices on the total size of the HESS. The first stage is to apply Case 1 of the evaluation tests, five scenarios, (Section 3.2.2.1) to this case study. The HESS is sized for five combinations of batteries and supercapacitors based on the energy demand and power demand obtained in the previous section. The same as the previous case study, the characteristics of 24V 60Ah Altairnano battery modules, shown in Table 4.3.1, and 125V Heavy Transportation Maxwell supercapacitor Modules, shown in

Table *4.3.2*, are considered.

Figure 5.3.1 indicates the total weight and volume of the HESS when it comes to supplying energy. The figures show that from Scenarios 1 to 5, as the number of battery modules increases and the number of supercapacitor modules decreases, both the weight and volume of the HESS increase. It can be seen that every time the battery pack provides 25% less energy and the supercapacitor pack provides 25% more energy, the weight and volume of the HESS increase by about 28.9t and 2.3m^3, respectively.

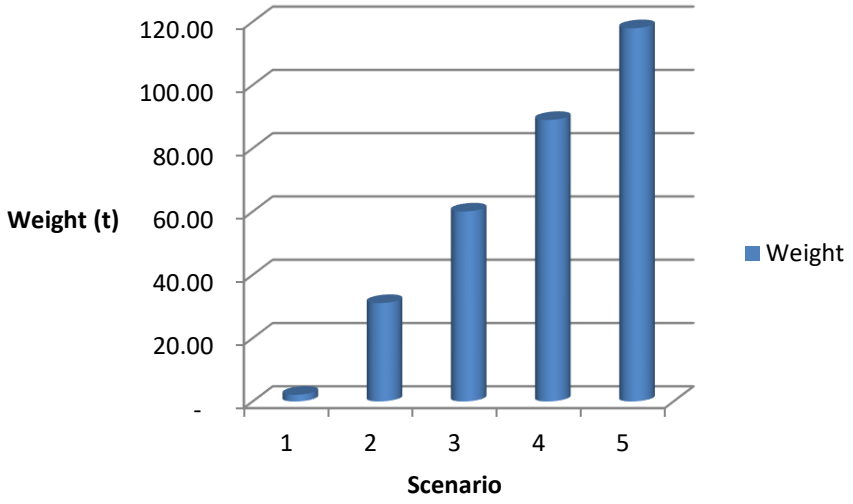

(a)

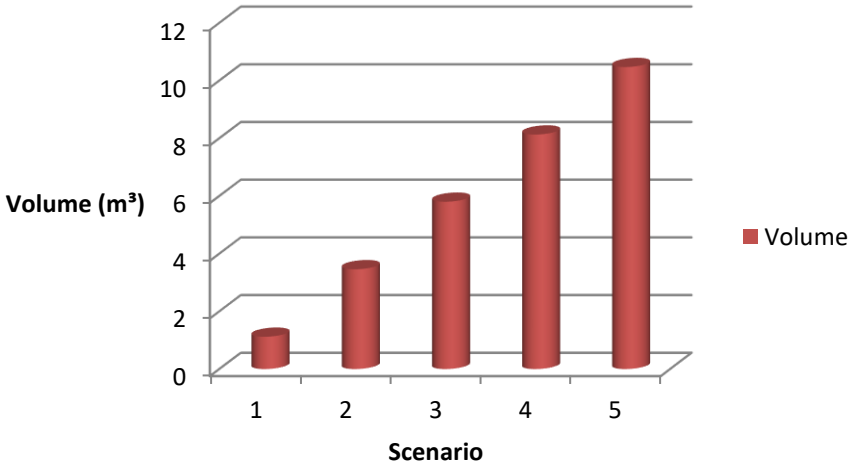

(b)

Figure 5.3.1. (a) Total weight of the HESS for 5 scenarios to meet the energy demand,
(b) Total volume of the HESS for 5 scenarios to meet the energy demand

Now combinations are considered to meet the power demand. Figure 5.3.2 shows the weight and volume of the HESS for this case.

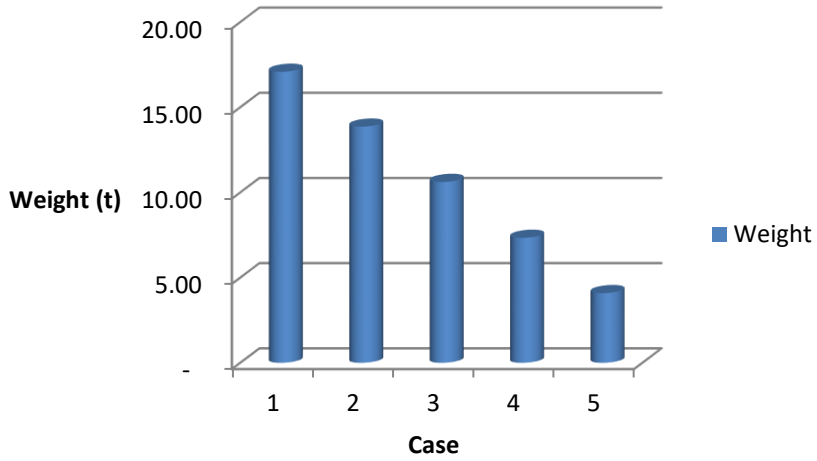

(a)

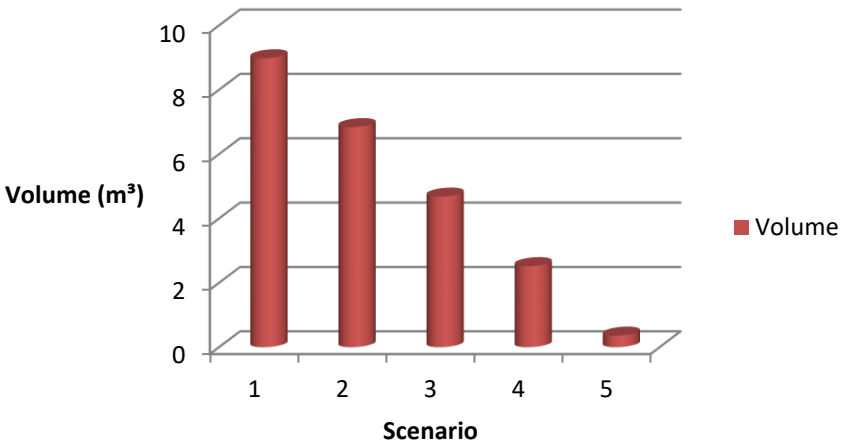

(b)

Figure 5.3.2. (a) Total weight of the HESS for 5 scenarios to meet the power demand,
(b) Total volume of the HESS for 5 scenarios to meet the power demand

From the figures, it can be seen that every time the battery pack and the supercapacitor pack are in charge of providing 25% less power and 25% more power, respectively, the weight decreases by about 3.25t and the volume decreases by about 2.16m^3.

Among all five scenarios, the battery-only ESS has the smallest size when it comes to the energy supply and the largest size regarding supplying the power demand. For the supercapacitor-only ESS, it is vice versa: it is largest when it is in charge of meeting the total energy demand and smallest when it has to meet the required power.

Now Case 2 of the evaluation tests, 25 scenarios (Section 3.2.2.1) should be applied to this case study. Figure 5.3.3 indicates both the weight and volume of the HESS for all 25 scenarios.

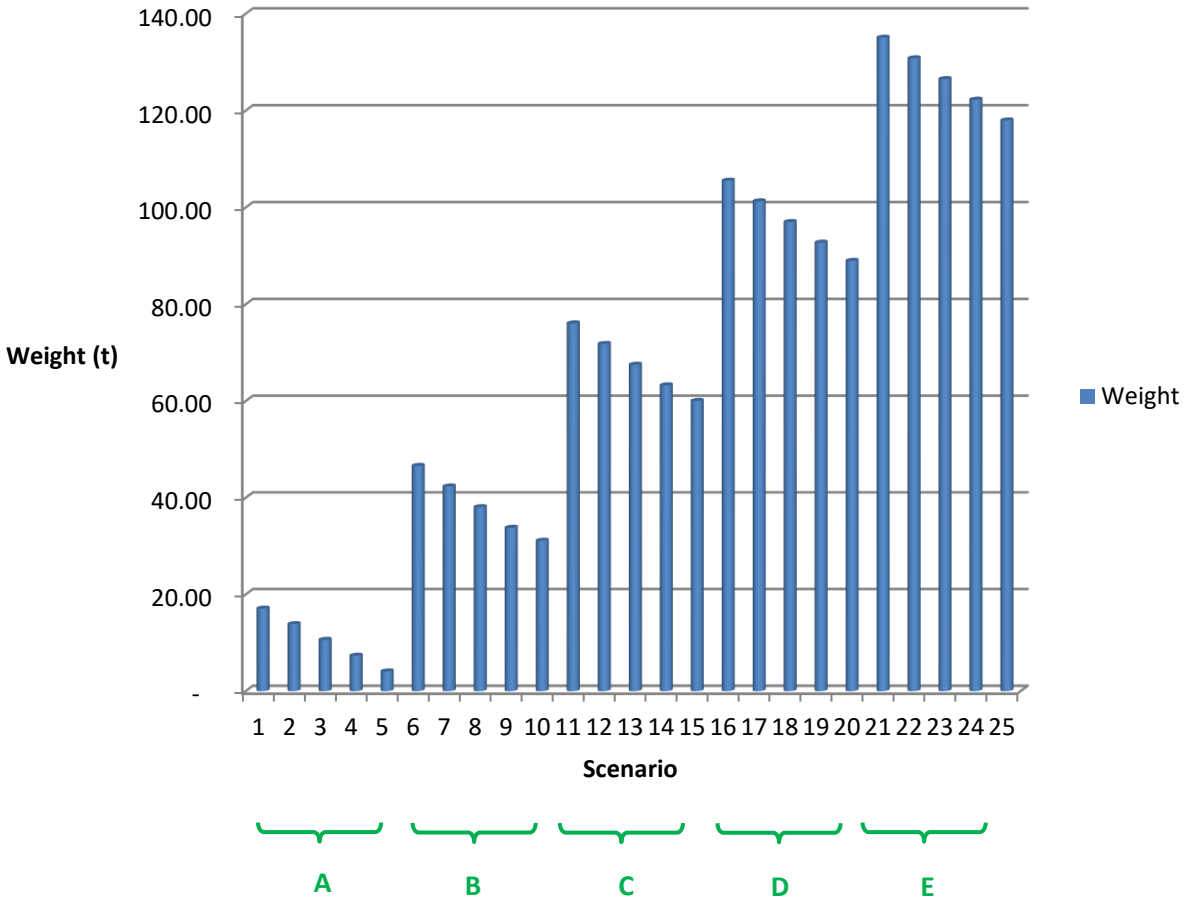
140.00
120.00
100.00
80.00
60.00
40.00
20.00
-
Weight (t)
1 2 3 4 5 6 7 8 9 10 11 12 13 14 15 16 17 18 19 20 21 22 23 24 25
Scenario
Weight
A
B
C
D
E

(a)

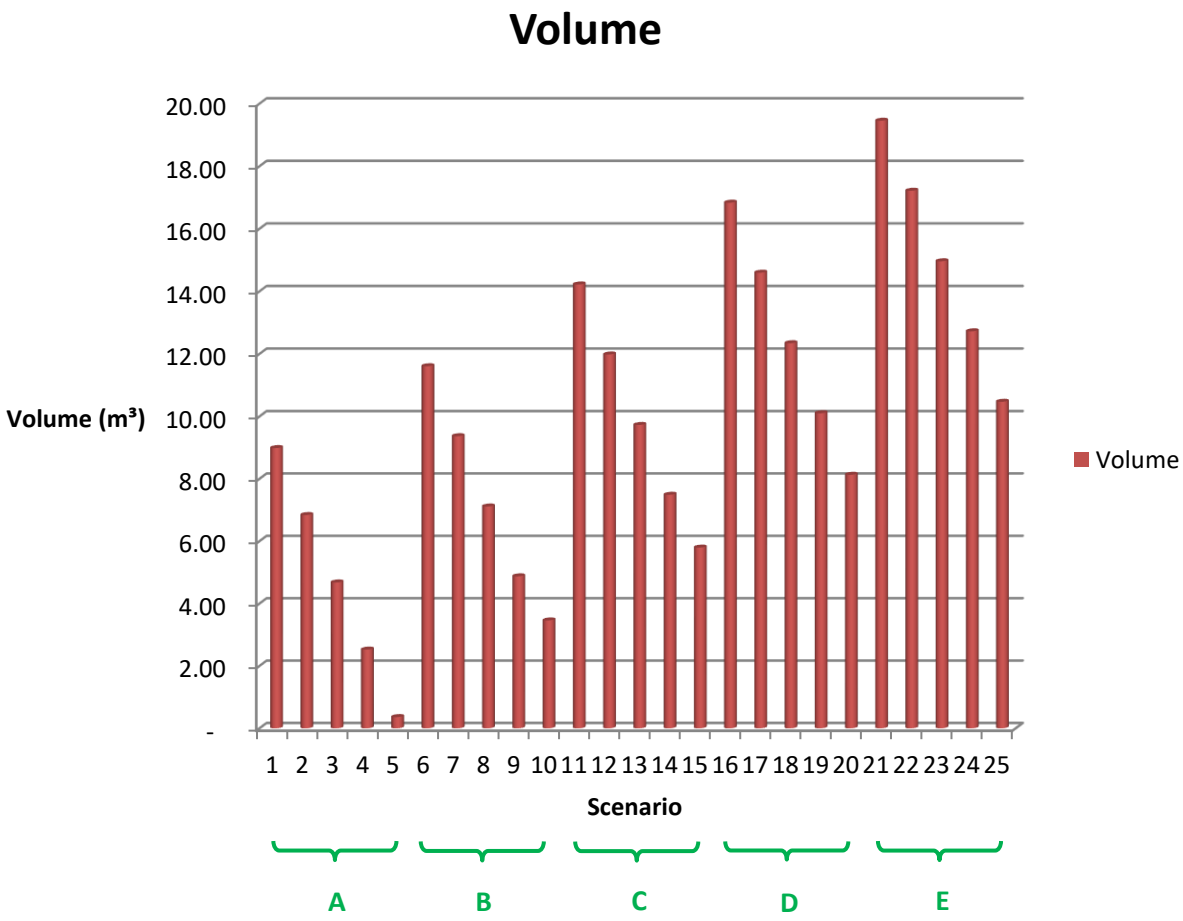

(b)

Figure 5.3.3. (a) Total weight of the HESS for 25 scenarios
(b) Total volume of the HESS for 25 scenarios

From Group A to E, the power demand percentage stays constant, the battery pack provides less energy and the supercapacitor pack provides more energy. It can be seen that every time the battery pack is in charge of supplying 25% less of the total energy demand and the supercapacitor pack needs to provide 25% more energy, the total weight and volume of the HESS increase by about 28.9t and 2.3m^3, respectively. In each individual group, from the first scenario to the fifth one, the energy percentage stays constant and both packs need to meet different percentages of the power demand. It can be seen that from one scenario to the next,

where the battery pack meets 25% less of the power demand and the supercapacitor pack meets 25% more of the power demand, the weight and volume of the HESS decrease by about 3.25t and 2.16m^3, respectively.

Now the sized HESS in Scenario 2 is selected as an example to evaluate its performance. Table 5.3.1 indicate the details of the sized HESS including battery pack and supercapacitor pack in Scenario 2.

Table 5.3.1. Results of sizing HESS in Scenario 2

	Battery pack	Supercapacitor pack
Energy-based module number	76	0
Power-based module number	458	17
Higher number of modules	458	17
Power supply (kW)	679.1	224.9
Weight (t)	12.83	1.03
Total weight of the HESS (t)	13.86	
Volume (m^3)	6.74	0.09
Total volume of the HESS (m^3)	6.83	

Figure 5.3.4 indicates how the sized HESS in Scenario 2 meets the total power demand in this case study. It is obvious that, as for the previous case study, the supercapacitor pack does not have enough energy to meet the percentage of the power demand for which it is responsible. Again, the battery pack needs to discharge more than its 1 C-rate (which is 679.1kW) to compensate for the supercapacitor pack and hence, to help the HESS meet the peak power

requirement. The changes of the SOC of both the battery pack and supercapacitor pack in Scenario 2 are shown in Figure 5.3.5.

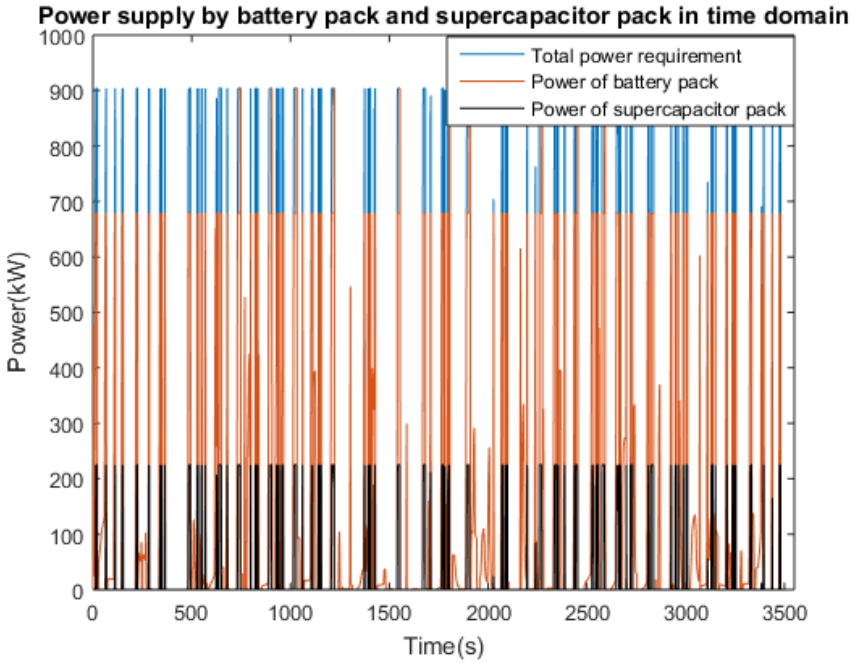

Figure 5.3.4. HESS supplying power demand in time domain for Scenario 2

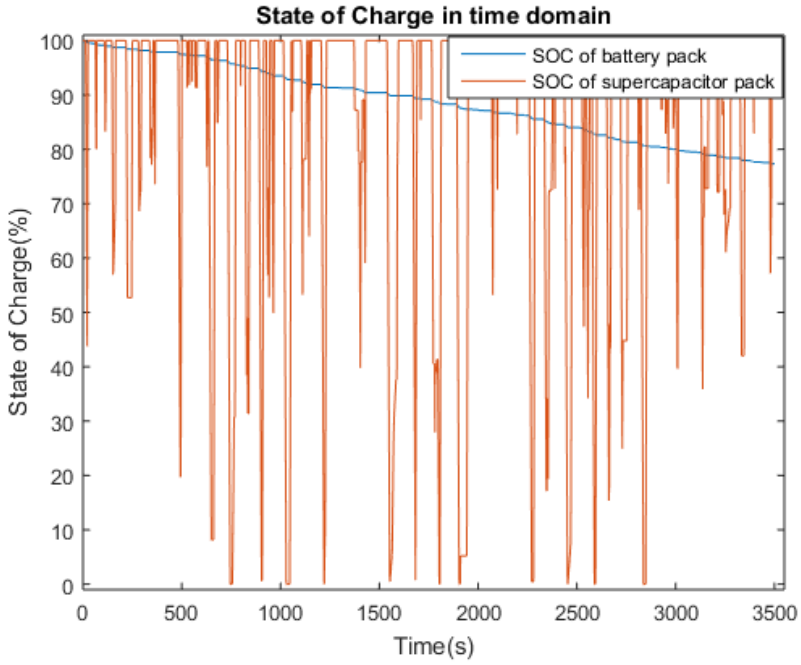

Figure 5.3.5. SOC changes of battery pack and supercapacitor pack in time domain for Scenario 2

From the figure it can be seen that the supercapacitor pack becomes empty during accelerations and it charges by the regen energy whenever the train brakes. The braking energy is enough to fully charge the supercapacitor pack, but this energy is not enough to fulfil the energy required from the supercapacitor pack in acceleration modes. Although the battery pack discharges more than its 1 C-rate to support the supercapacitor pack, it only uses 22.68% of the energy stored in it and 77.32% of this energy is left unused at the end of the journey.

As for the methods proposed in the previous case study in Section 4.3, in order to not force the battery pack to discharge more than its power limit, one solution is to increase the number of supercapacitor modules so that the supercapacitor pack has enough energy to meet the required peak power. For Scenario 2 in this case study, if there are 5 more supercapacitor modules (a total of 22 supercapacitor modules in the supercapacitor pack), this pack is able to perform properly. Figure 5.3.6 indicates how the new HESS with 22 supercapacitor modules supplies the required power and how both packs perform as expected.

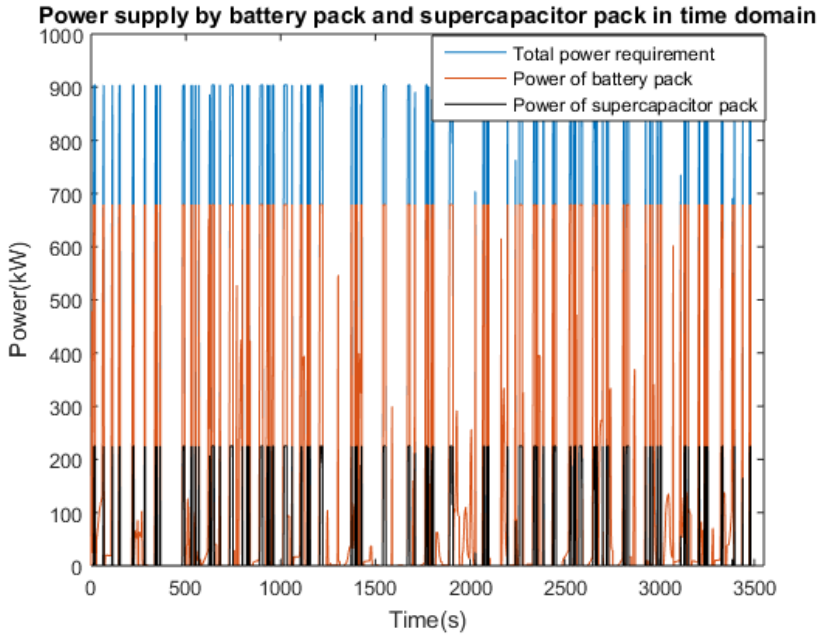

Figure 5.3.6. HESS supplying power demand in time domain for Scenario 2, increased number of supercapacitor modules

The change in the stored energy in both battery pack and supercapacitor pack after increasing the number of supercapacitor modules in shown in Figure 5.3.7.

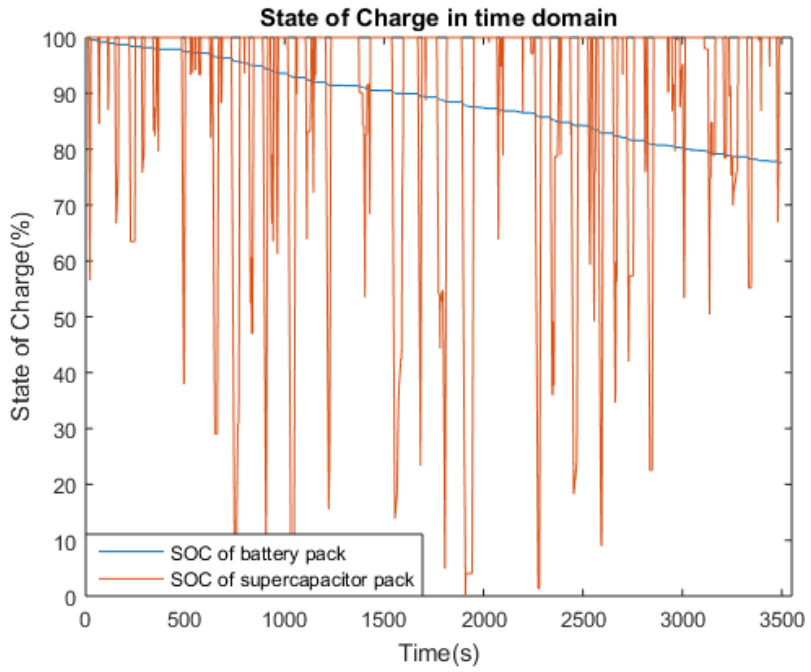

Figure 5.3.7. SOC changes of battery pack and supercapacitor pack in time domain for Scenario 2, increased number of supercapacitor modules

Here, the battery pack is responsible only for its percentage of meeting the power demand and uses 22.43% of its stored energy, having 77.57% energy left at the end of the journey at 3501s. This means that if the supercapacitor pack does not have enough energy, the battery pack needs to spend 0.25% (1.7kW) of its stored energy to compensate for the supercapacitor pack.

As mentioned in Section 4.3, another method to tackle this problem is to get the battery pack to charge the supercapacitor pack. Whenever the supercapacitor pack's SOC goes below 1%, the battery pack charges the supercapacitor pack. Figure 5.3.8 indicates how both packs meet the percentages of the power demand that they are in charge of meeting, when the battery pack charges the supercapacitor pack.

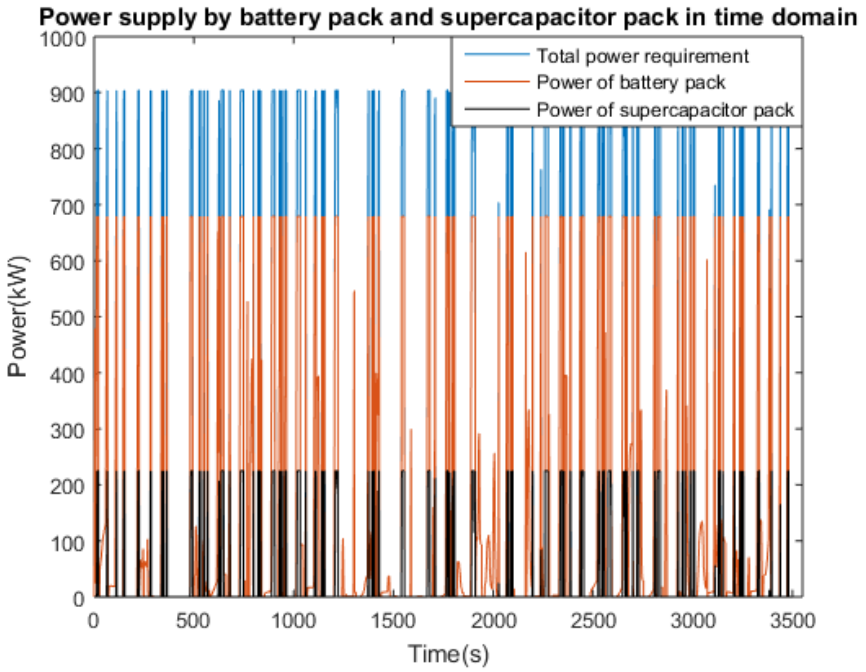

Figure 5.3.8. HESS supplying power demand in time domain for Scenario 2, battery pack charging supercapacitor pack

Figure 5.3.9 shows the changes of the SOC of both packs when the battery pack charges the supercapacitor pack. Whenever the supercapacitor pack's SOC goes below 1%, the battery pack charges the supercapacitor pack. In this solution, the battery pack has 77.49% of its stored energy left. This means the battery pack needs to provide 0.08% (0.54kW) of its stored energy to charge the supercapacitor pack, which is 0.17% (1.16kW) lower than when the battery pack compensates for the supercapacitor pack. Here, as for the previous case study, for seven scenarios (Scenarios 2, 3, 4, 5, 10, 15 and 20) the supercapacitor pack does not have enough energy to meet the required power demand for which it is responsible.

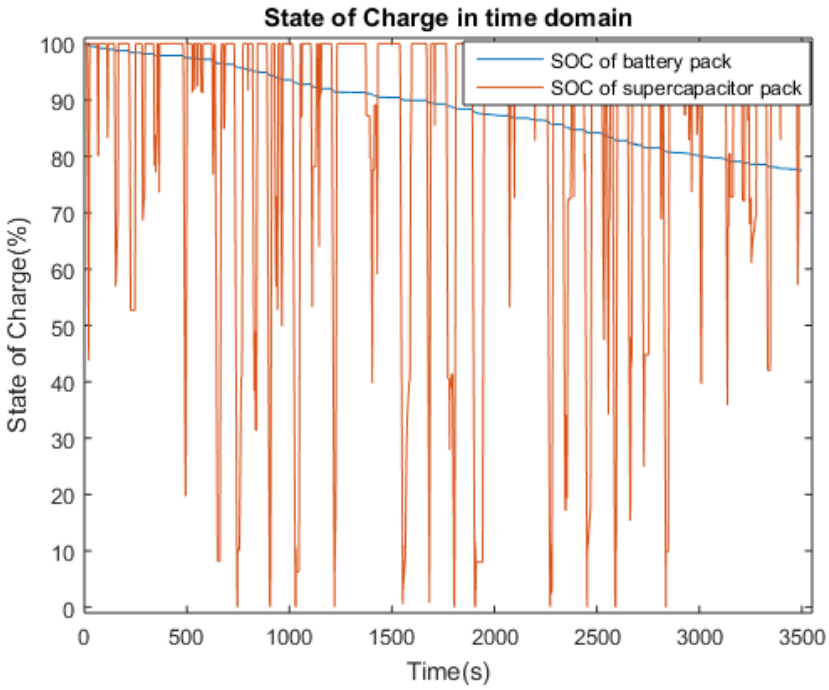

Figure 5.3.9. SOC changes of battery pack and supercapacitor pack in time domain for Scenario 2, battery pack charging supercapacitor pack

Figure 5.3.10 indicates the total weight and volume of the HESS for each proposed solution: the battery pack compensating for the supercapacitor pack, increasing the number of supercapacitor modules and, finally, the battery pack charging supercapacitor pack. It is obvious that the total size of the HESS stays unchanged when the battery pack either compensates for or charges the supercapacitor pack and by increasing the number of supercapacitor modules in the supercapacitor pack, the total size of the HESS increases. The scenarios for which these solutions are proposed are shown with green circles. From the figure, it can be seen that greatest size difference happens in Scenario 5, where increasing the number of supercapacitor modules adds 71.98t and 7.32m^3 to the weight and volume of the HESS, respectively. The orange line indicates the mass of the train, which is 80.46t.

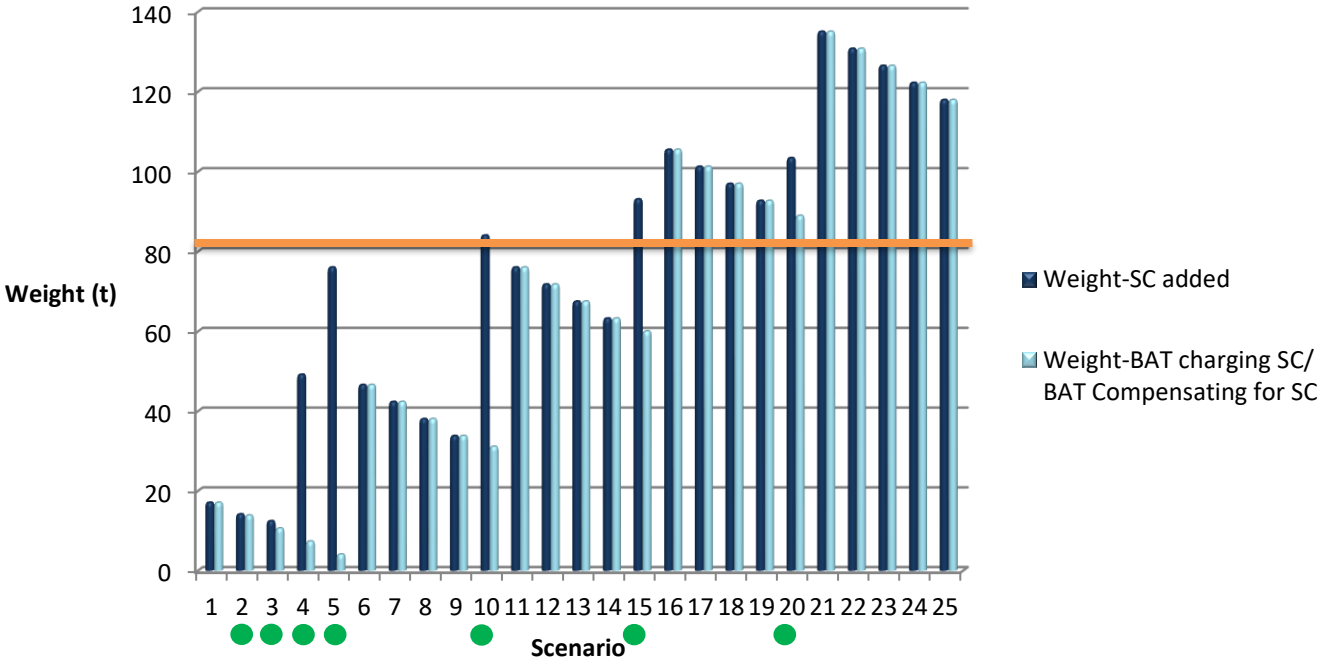

(a)

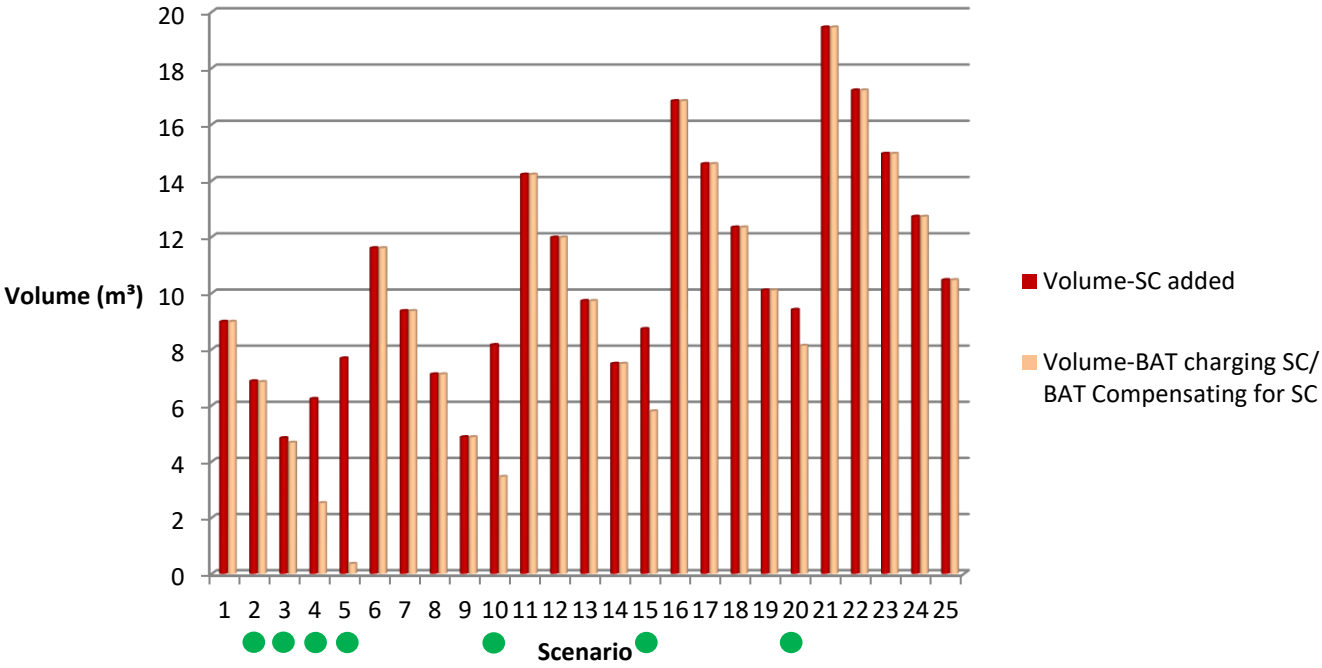

(b)

Figure 5.3.10. (a) Total weight of the HESS for 25 scenarios for 3 solutions
(b) total volume of the HESS for 25 scenarios for 3 solutions

The last evaluation test in this phase is to assess a change of the C-rate of the battery on the total size of the HESS as well as on the rate of change of the SOCs for both battery and supercapacitor. By applying the procedure mentioned in Section 3.2.2.2 to this case study, the total weight and volume of the HESS can be achieved for 1 C-rate, 2 C-rate, 3 C-rate, 4 C-rate and 5 C-rate. Figure 5.3.11 indicates the total weight and volume of the HESS for the mentioned C-rates.

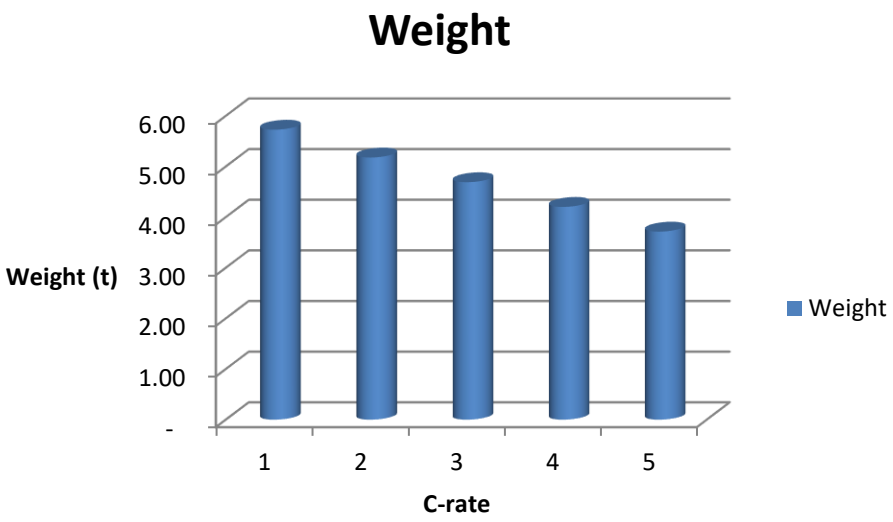

(a)

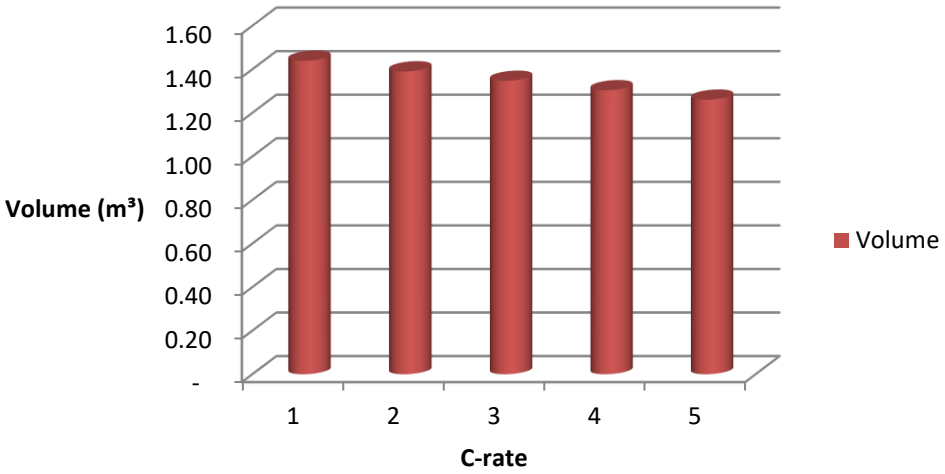

(b)

Figure 5.3.11. (a) Total weight of the HESS for C-rates from 1 to 5
(b) Total volume of the HESS for C-rates from 1 to 5

The figures show that by increasing the C-rate of the battery, both the weight and volume of the HESS decrease gradually. Every time that the C-rate of the battery increases by one unit, one supercapacitor module drops out and the total weight and volume of the HESS decrease by 0.061t (61kg) and 0.0054m^3 (5400cm^3), respectively.

Table 5.3.2 indicates the number of battery and supercapacitor modules for each C-rate as well as the power limit of each pack.

Table 5.3.2. Power limit of battery pack and supercapacitor pack for C-rates from 1 to 5

C-rate	Number of battery modules	Power limit of battery pack (kW)	Number of supercapacitor modules	Power limit of supercapacitor pack (kW)
1	76	112.7	59	791.3
2	76	225.4	50	678.6
3	76	338.1	42	565.9

4	76	450.8	34	453.2
5	76	563.5	26	340.5

It is seen that the number of battery modules has stayed constant, but each time the C-rate increases by one unit, eight/nine supercapacitor module drops.

Again, due to the determination of the supercapacitor pack based on the power demand only, it is expected that the supercapacitor pack does not have enough energy to meet the required power demand. Figure 5.3.12 shows the sized HESS in the 1 C-rate Scenario with 76 battery modules and 59 supercapacitor modules supplying the total power demand. It is obvious that the supercapacitor pack cannot meet the required power demand and the battery pack has to compensate for the supercapacitor pack from the beginning of the journey. After about half of the journey, the supercapacitor becomes fully empty and it is the battery pack which supplies the total power demand until the end of the journey.

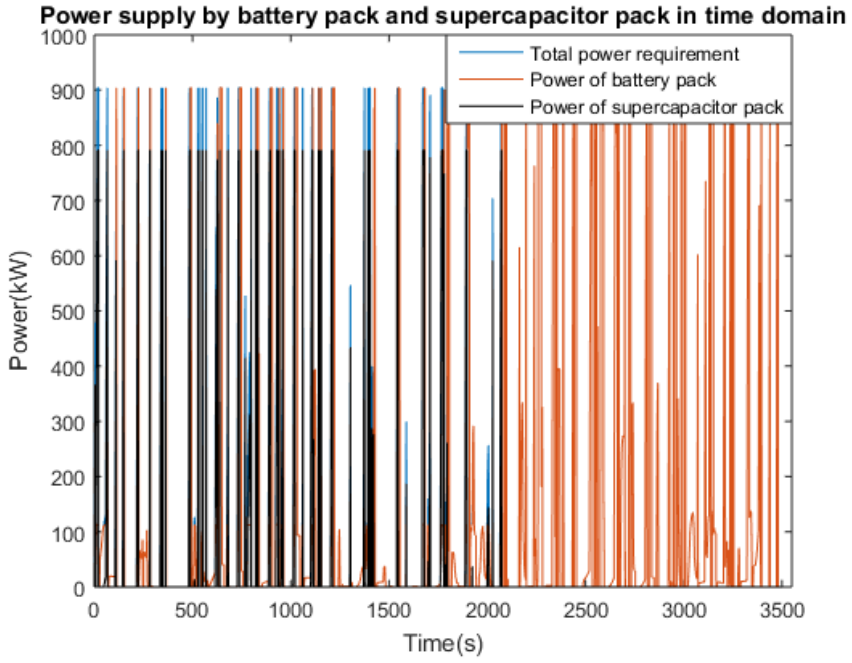

Figure 5.3.12. HESS supplying power demand in time domain for 1 C-rate

The scenario indicated in Figure 5.3.13, is complementary of that in Figure 5.3.12.

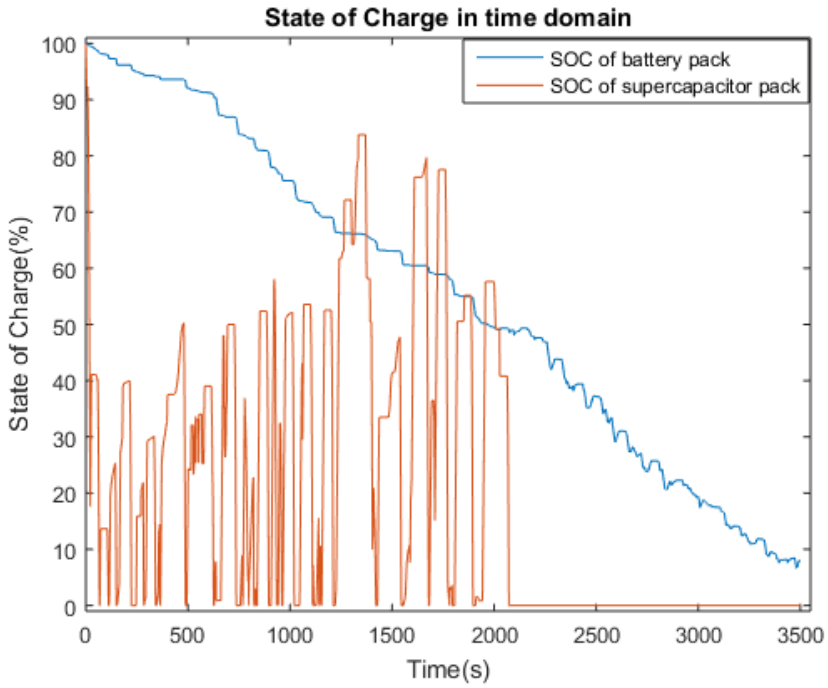

Figure 5.3.13. SOC changes of battery pack and supercapacitor pack in time domain for 1 C-rate

This figure shows that when the energy stored in the battery pack goes below 50% and the battery pack starts to absorb regen energy instead of the supercapacitor pack, the supercapacitor pack stays fully empty until the end of the journey.

As mentioned before, to tackle this issue, the battery pack can charge the supercapacitor pack. Figure 5.3.14 shows the performance of the HESS in meeting the total power demand for C-rates of 1 to 5, when the battery pack charges the supercapacitor pack whenever the supercapacitor pack's SOC goes below 1%. It can be seen that in all five scenarios, the supercapacitor pack is able to meet the given percentage of the power demand, and the battery pack does not have to discharge more than its given C-rate to meet the total power demand. In the figures, it can be seen that by increasing the C-rate of the battery, the power limit of the battery increases and the power demand that the supercapacitor pack has to meet decreases.

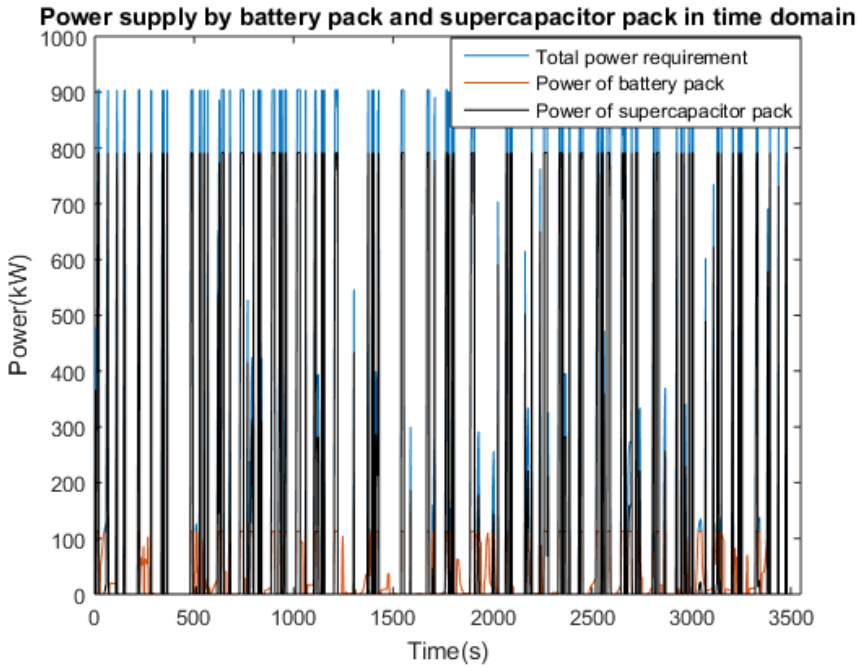
Power supply by battery pack and supercapacitor pack in time domain
Total power requirement
Power of battery pack
Power of supercapacitor pack
Power(kW)
Time(s)
0
100
200
300
400
500
600
700
800
900
1000
0
500
1000
1500
2000
2500
3000
3500

(a)

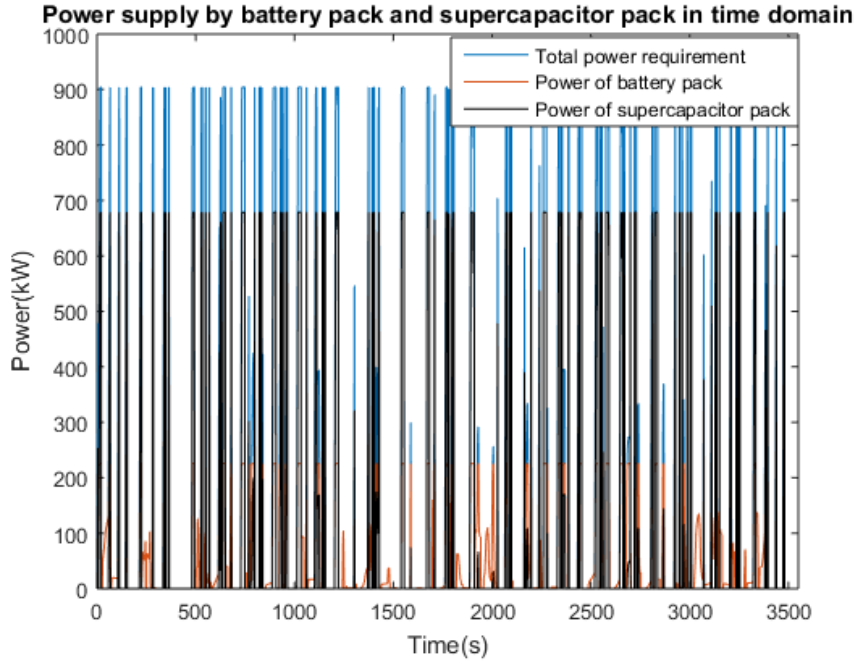
Power supply by battery pack and supercapacitor pack in time domain
Total power requirement
Power of battery pack
Power of supercapacitor pack
Power(kW)
Time(s)
0
100
200
300
400
500
600
700
800
900
1000
0
500
1000
1500
2000
2500
3000
3500

(b)

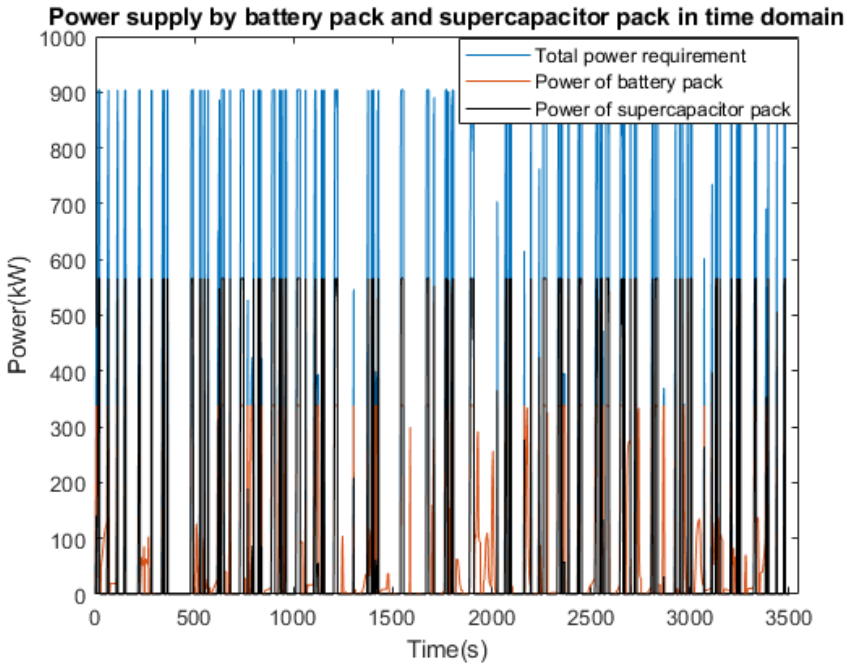
Power supply by battery pack and supercapacitor pack in time domain
Total power requirement
Power of battery pack
Power of supercapacitor pack
Power(kW)
Time(s)
0
100
200
300
400
500
600
700
800
900
1000
0
500
1000
1500
2000
2500
3000
3500

(c)

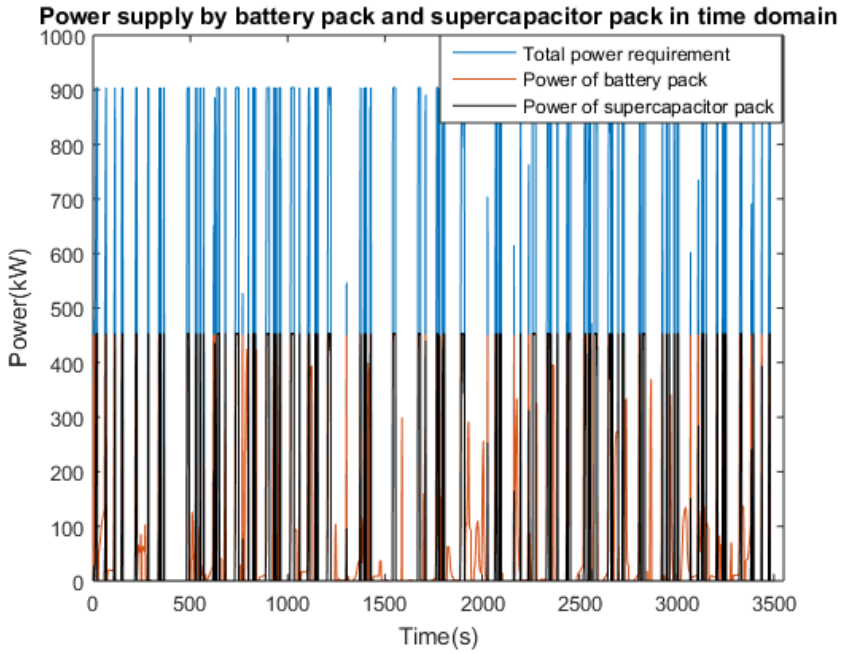
Power supply by battery pack and supercapacitor pack in time domain
Total power requirement
Power of battery pack
Power of supercapacitor pack
Power(kW)
Time(s)
0
100
200
300
400
500
600
700
800
900
1000
0
500
1000
1500
2000
2500
3000
3500

(d)

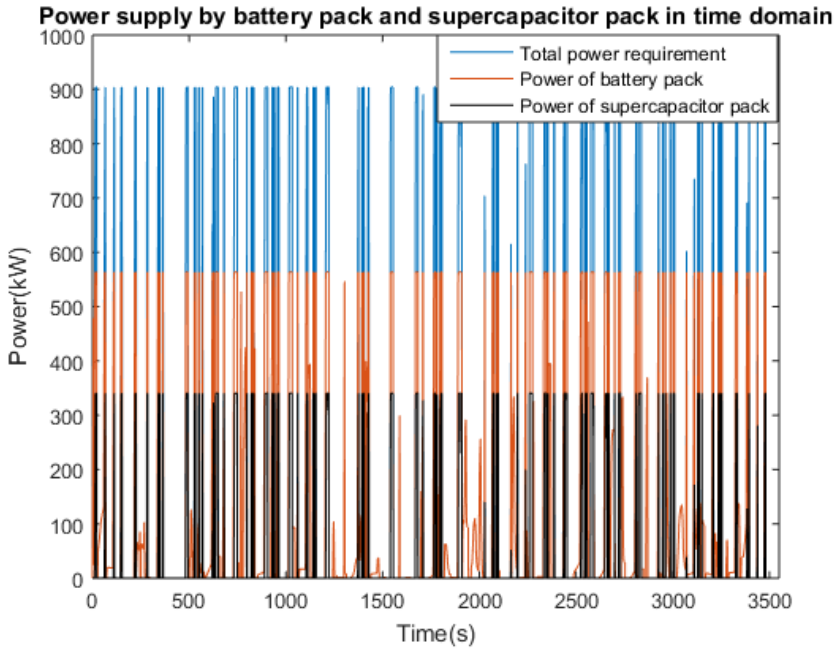

(e)

Figure 5.3.14. HESS supplying power demand in time domain for (a) 1 C-rate
(b) 2 C-rate
(c) 3 C-rate
(d) 4 C-rate
(e) 5 C-rate

Figure 5.3.15 indicates the changes of the SOC of the battery packs at C-rates 1 to 5. As for the previous case study, by increasing the C-rate of the battery, the battery pack discharges more quickly and uses more energy during the journey.

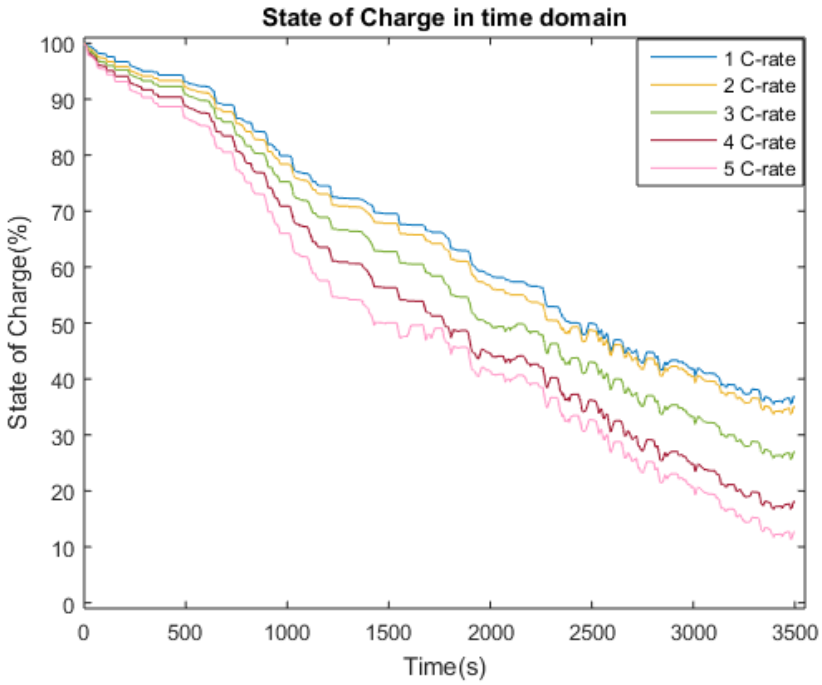

Figure 5.3.15. SOC change of battery pack in time domain for C-rates 1 to 5

Figure 5.3.16 indicates the change of the SOC of both battery pack and supercapacitor pack together, for C-rates from 1 to 5. From the figures it can be deduced that by increasing the C-rate of the battery pack, it discharges more quickly and hence its SOC goes below 50% more quickly. Hence, it starts absorbing regen energy instead of the supercapacitor pack at an earlier stage, which makes the supercapacitor pack stop absorbing the regen energy earlier. The closer look at the charging procedure in figures is provided as well.

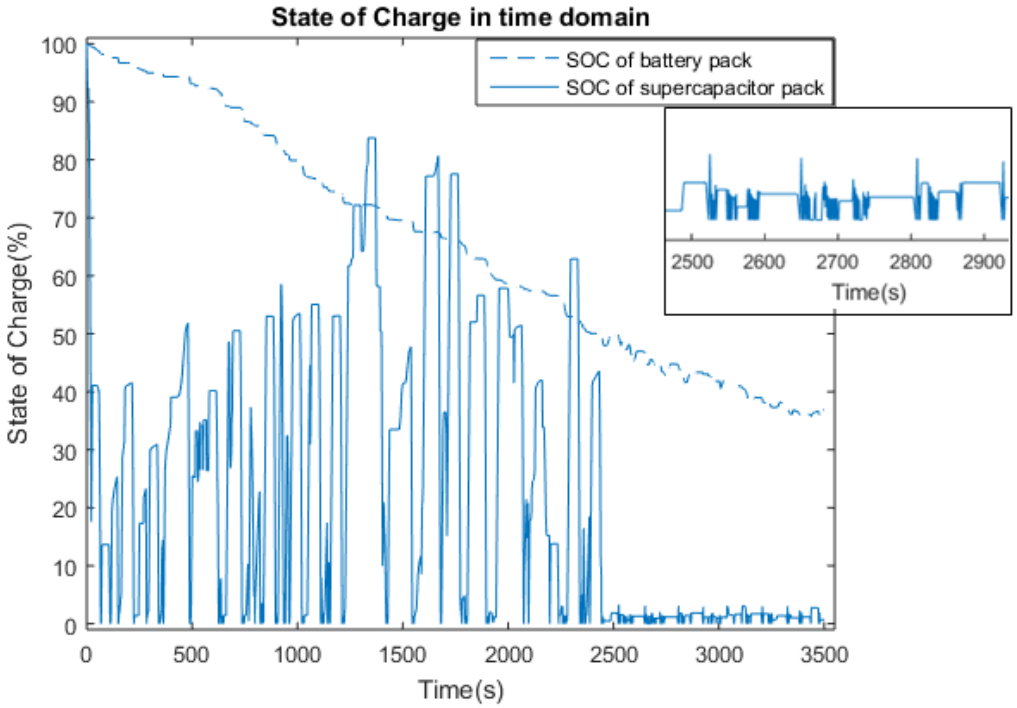
State of Charge in time domain
SOC of battery pack
SOC of supercapacitor pack
State of Charge(%)
Time(s)
0
10
20
30
40
50
60
70
80
90
100
0
500
1000
1500
2000
2500
3000
3500
2500
2600
2700
2800
2900
Time(s)

(a)

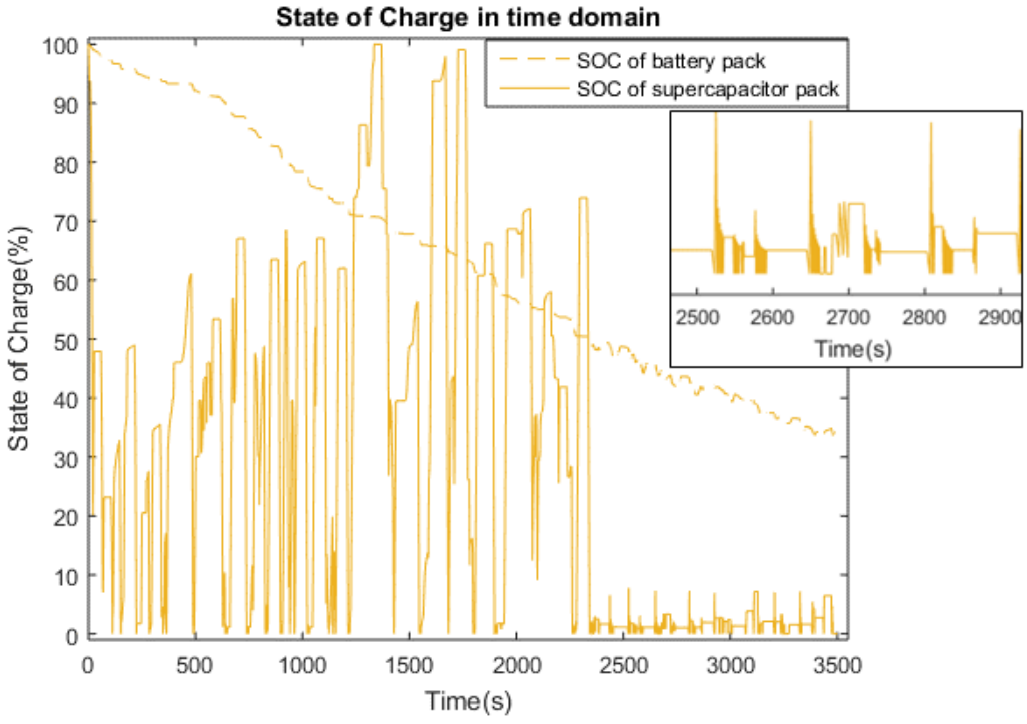
State of Charge in time domain
SOC of battery pack
SOC of supercapacitor pack
State of Charge(%)
Time(s)
0
10
20
30
40
50
60
70
80
90
100
0
500
1000
1500
2000
2500
3000
3500
2500
2600
2700
2800
2900
Time(s)

(b)

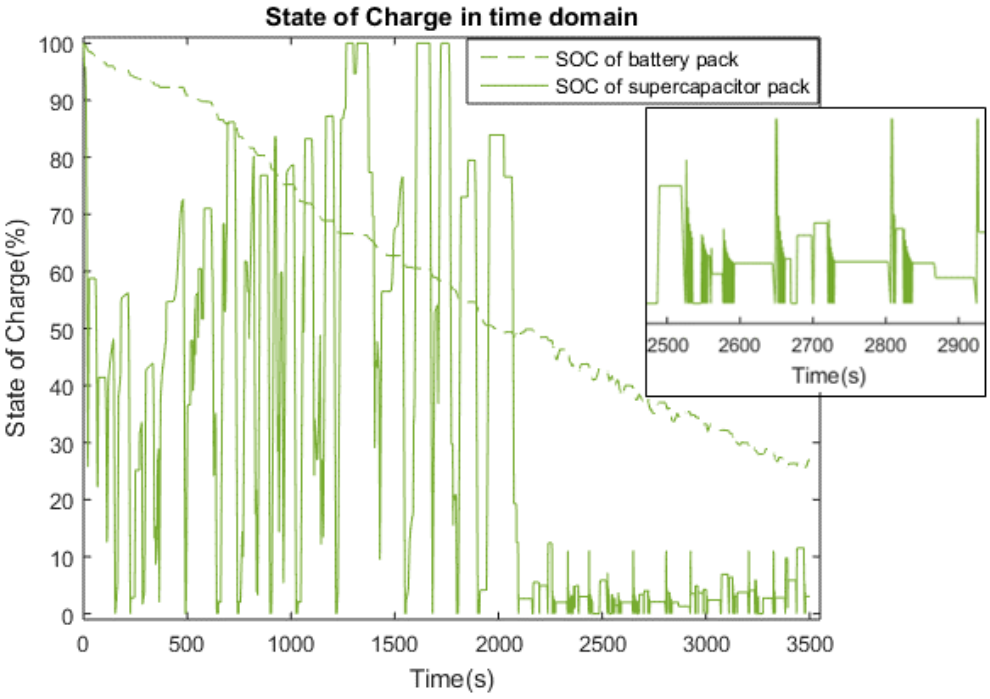
State of Charge in time domain
SOC of battery pack
SOC of supercapacitor pack
State of Charge(%)
Time(s)
0
10
20
30
40
50
60
70
80
90
100
0
500
1000
1500
2000
2500
3000
3500
2500
2600
2700
2800
2900
Time(s)

(c)

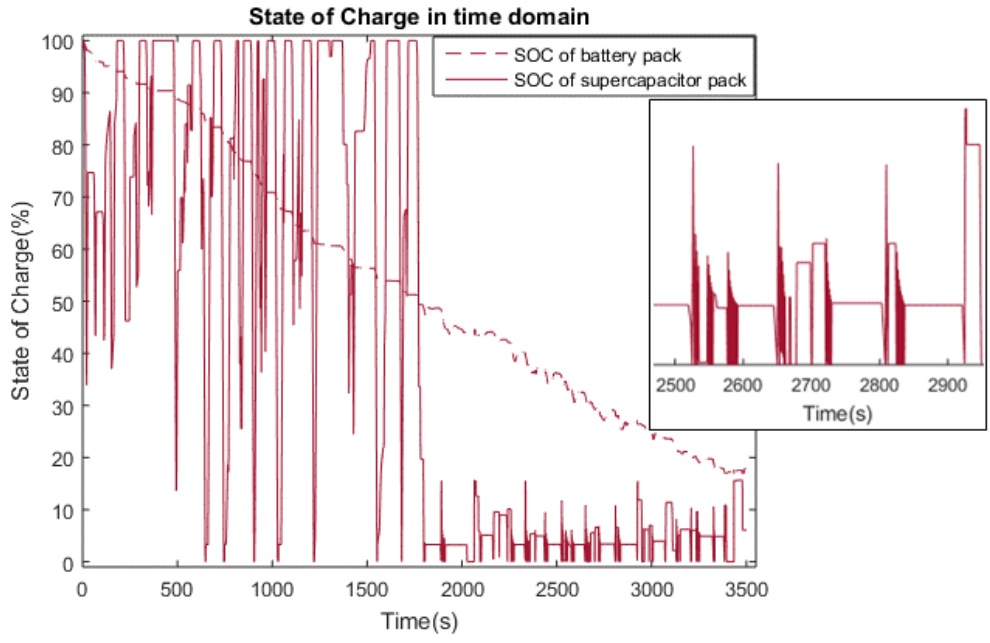
State of Charge in time domain
SOC of battery pack
SOC of supercapacitor pack
State of Charge(%)
Time(s)
0
10
20
30
40
50
60
70
80
90
100
0
500
1000
1500
2000
2500
3000
3500
2500
2600
2700
2800
2900
Time(s)

(d)

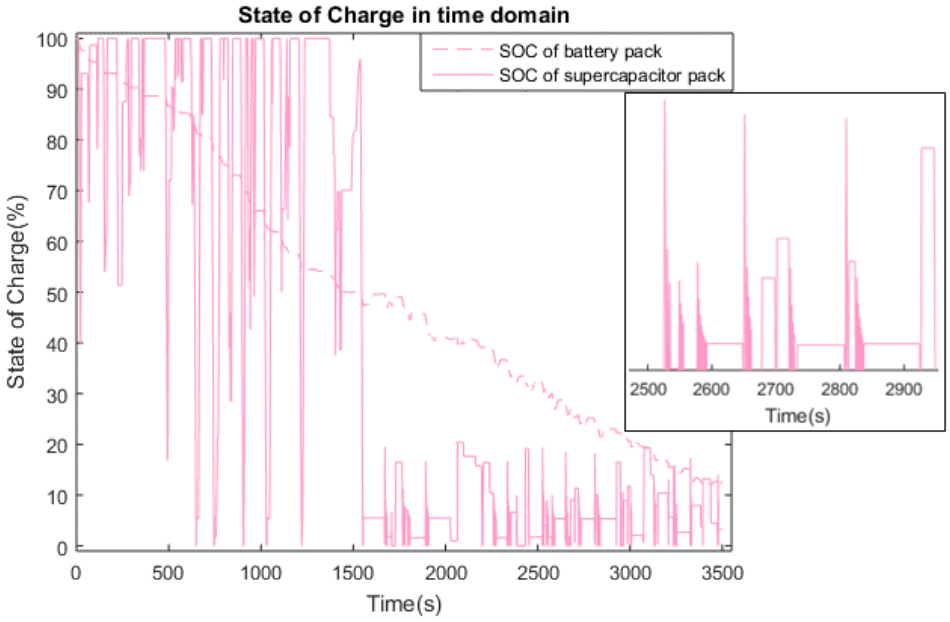

(e)

Figure 5.3.16. SOC changes of battery pack and supercapacitor pack in time domain for (a) 1 C-rate
(b) 2 C-rate
(c) 3 C-rate
(d) 4 C-rate
(e) 5 C-rate

5.4. Applying the 'Sizing' Phase to the Case Study

Now in this phase, an optimal HESS including batteries and supercapacitors should be sized for this case study using the Frequency Analysis method and Brute Force optimisation. As said in 3.3.2, an optimal cut-off frequency needs to be chosen for both low-pass and high-pass filters by the use of Brute Force optimisation to obtain the minimum weight and/or volume for the HESS. Figure 5.4.1 indicates the achieved results from Brute Force optimisation, where the cut-off frequency is indicated versus weight and volume.

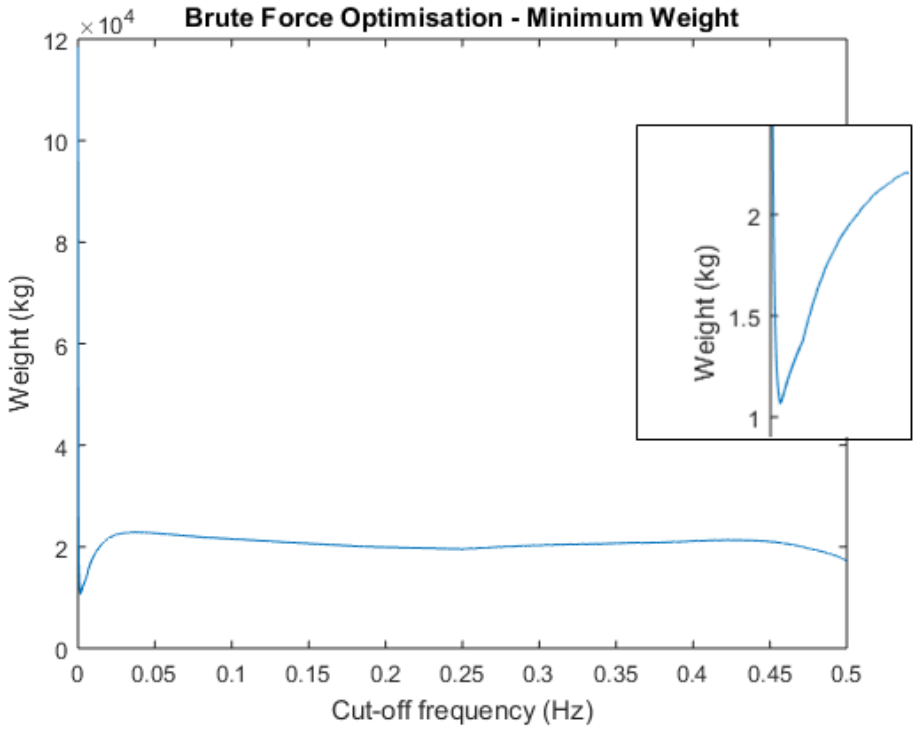

(a)

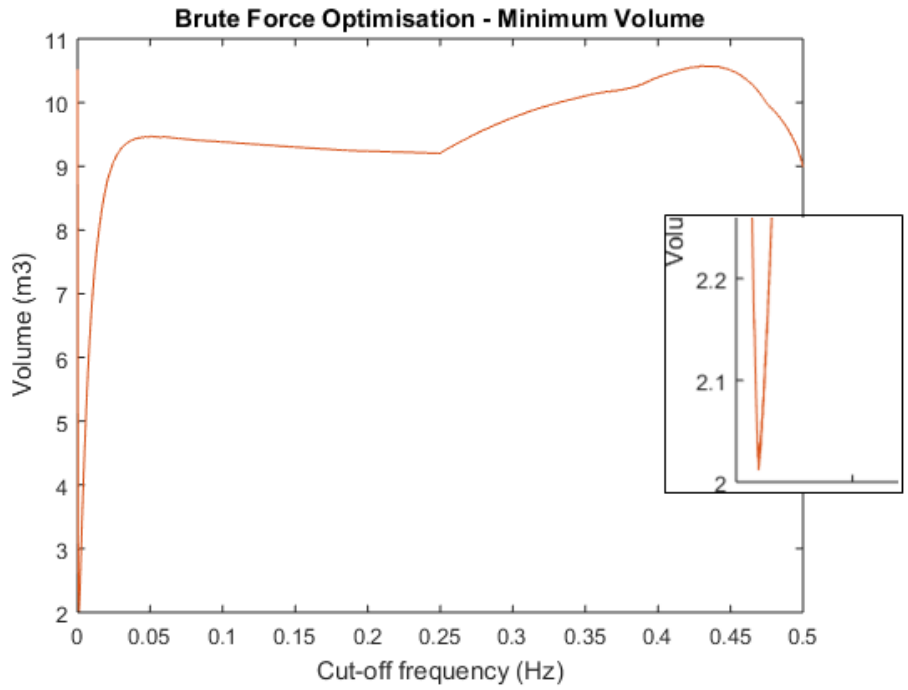

(b)

Figure 5.4.1. Brute Force Optimisation results to achieve minimum (a) weight and (b) volume

As for the previous case study, two optimal cut-off frequencies are determined for this case study after using Brute Force optimisation: one frequency to obtain the minimum weight and one frequency to obtain the minimum volume. Table 5.4.1 indicates the optimal cut-off frequencies obtained a s well as the associated weights and volumes.

Table 5.4.1. Optimal cut-off frequencies

Cut-off frequency (μHz)	Total weight (t)	Total volume (m^3)
1553–1562	10.649	2.26
969–974	12.597	2.01

As mentioned in Section 4.4, the cut-off frequency associated with the minimum weight is chosen. For frequencies between 1553μHz and 1562μHz, the minimum weight of the HESS is achieved: 1553μHz is chosen as the optimal cut-off frequency, where the volume associated with this frequency is 0.25m^3 more than the optimal volume.

Figure 5.4.2 indicates the power demand in the frequency domain and, by applying the low-pass filter with the chosen cut-off frequency, low-pass filtered Power/Frequency can be obtained, as shown in Figure 5.4.3.

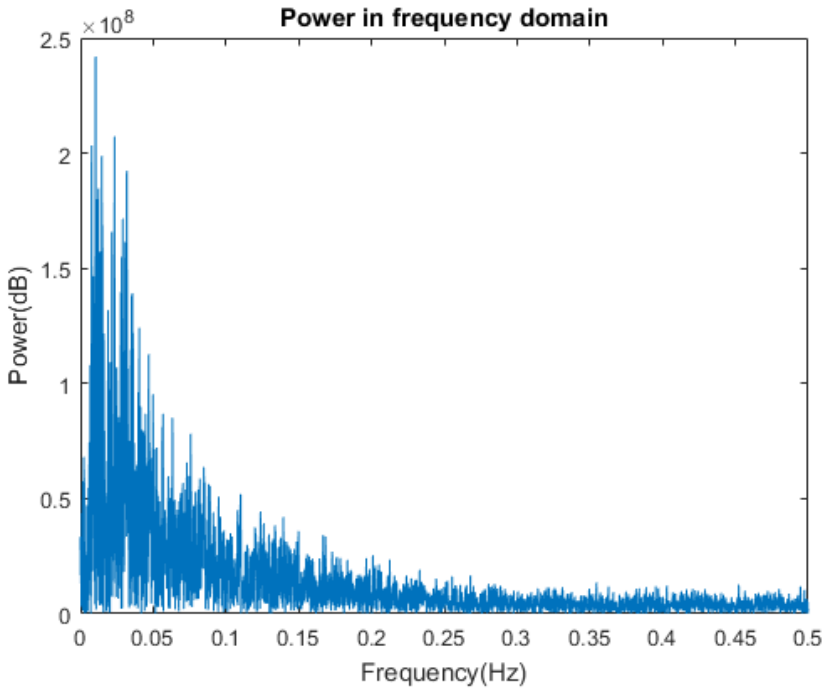

Figure 5.4.2. Power demand in frequency domain

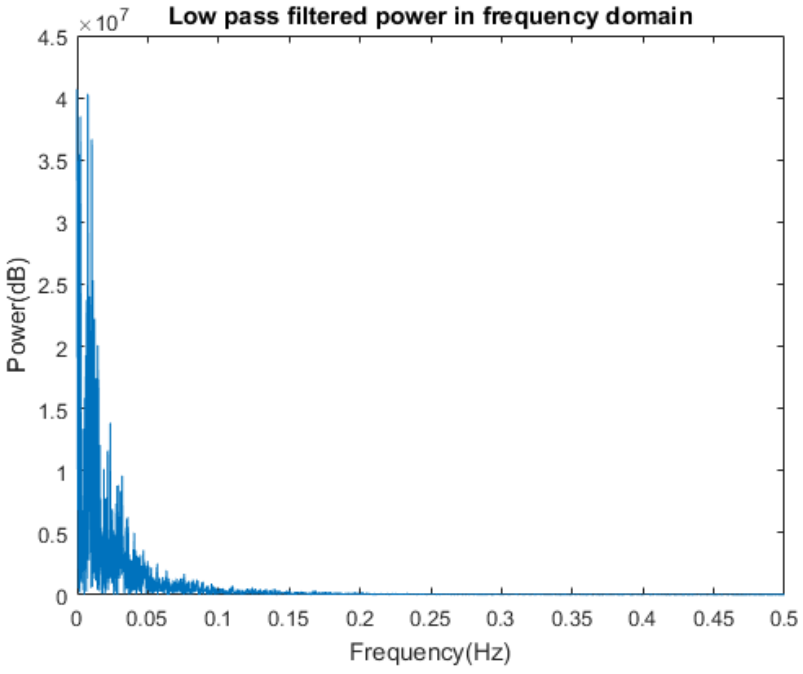

Figure 5.4.3. Low pass-filtered power demand in frequency domain

Low pass-filtered power in the time domain is indicated in Figure 5.4.4 and, by using integration, Figure 5.4.5 can be obtained, which shows low pass-filtered Energy/Time.

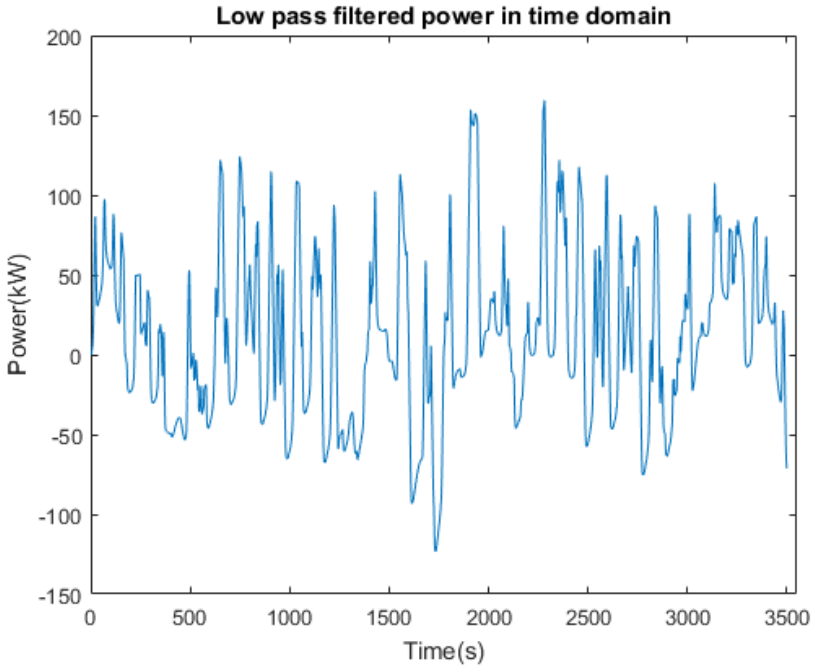

Figure 5.4.4. Low pass-filtered power demand in time domain

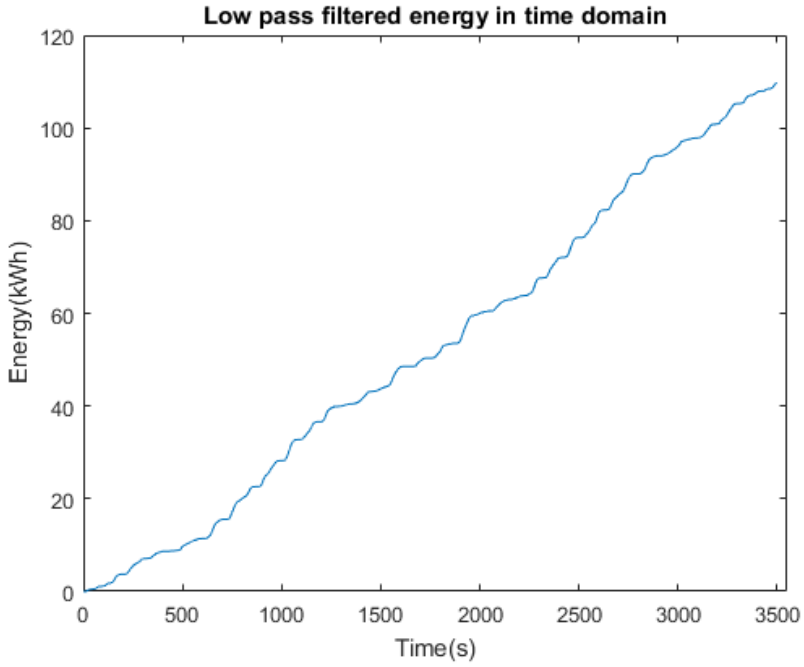

Figure 5.4.5. Low pass-filtered energy demand in time domain

The results obtained from the low-pass filters are used to size the battery pack. By looking at these results and according to the approach mentioned in Section 3.3.1, the battery pack needs to be sized in a way to meet 159.3kW and 109.7kWh. One hundred battery modules are required to meet the power demand and 74 battery modules are required to meet the energy demand; therefore, 108 is chosen as the final number of battery modules. Table 5.4.2 indicates the characteristics of the sized battery pack.

Table 5.4.2. Sized battery pack

Power demand from battery pack (kW)	159.3
Power-based module number	108
Energy demand from battery pack (kWh)	109.7
Energy-based module number	74
Higher number of modules	108
Weight (t)	3.024
Volume (m^3)	1.59

By applying the high-pass filter to the power demand of this case study, the high pass-filtered results can be achieved for the supercapacitor pack. Figure 5.4.6 and Figure 5.4.7 indicate the high pass-filtered power demand in the frequency and time domains, respectively. According to Figure 5.4.7, and by taking the approach mentioned in Section 3.3.1, the supercapacitor pack needs to be sized in a way to provide 1057.4kW. By integrating Figure 5.4.7, the Energy/Time result can be achieved (Figure 5.4.8), which indicates that according to Section 3.3.1, the supercapacitor pack should be in charge of providing 7.3kWh energy. In order to meet the high pass-filtered power and energy demands for which the supercapacitor pack is responsible, 78 supercapacitor modules and 125 supercapacitor modules are required to meet the power demand

and energy demand, respectively. Hence, 125 supercapacitor modules are chosen to be on the safe side.

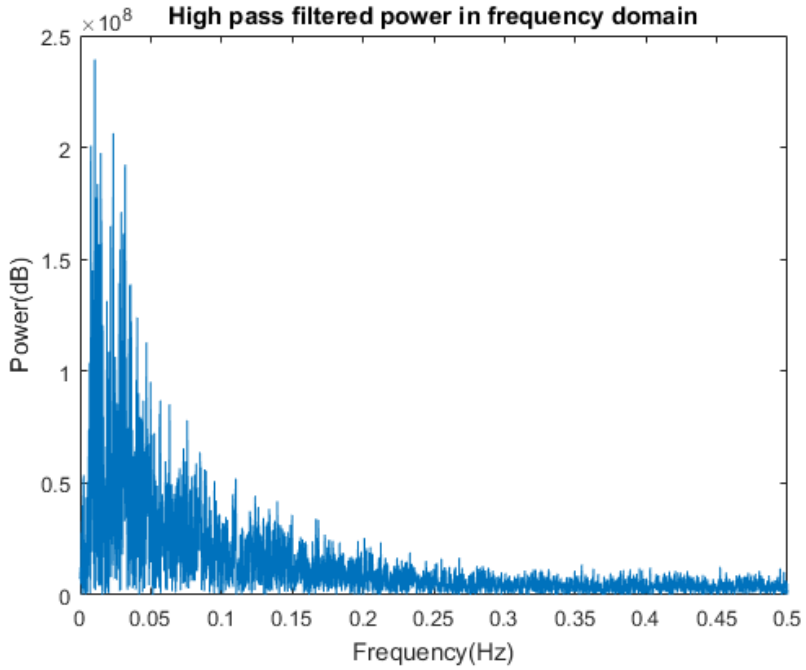

Figure 5.4.6. High pass-filtered power demand in frequency domain

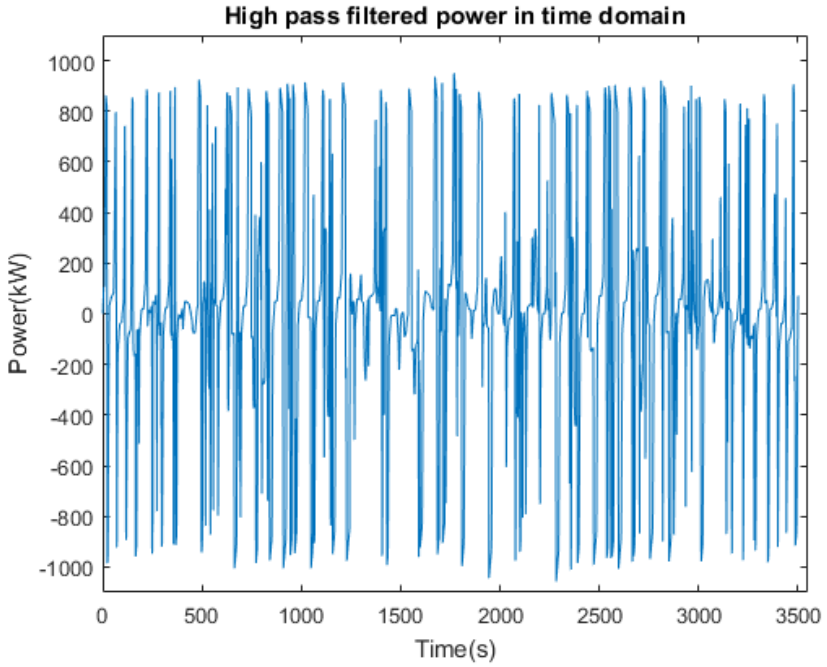

Figure 5.4.7. High pass-filtered power demand in time domain

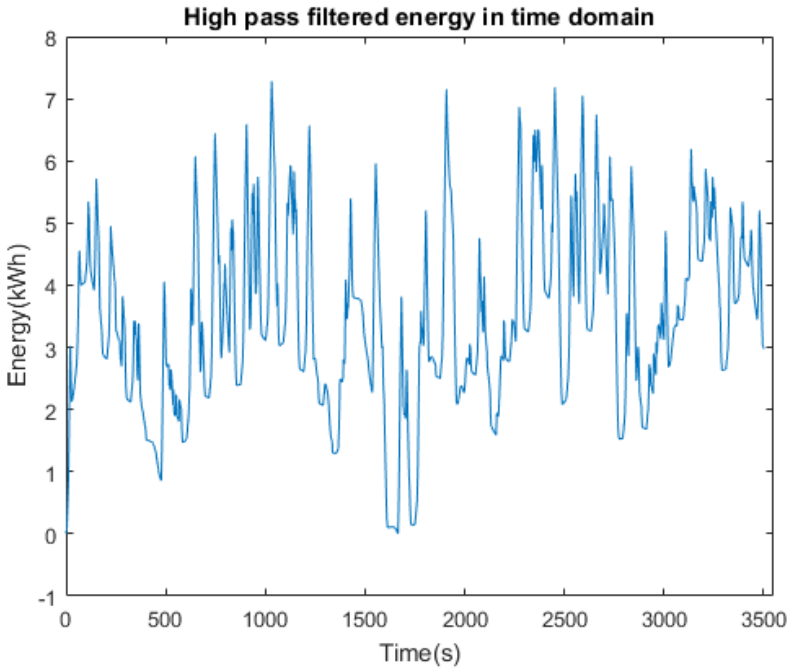

Figure 5.4.8. High pass-filtered energy demand in time domain

Table 5.4.3 shows the characteristics of the sized supercapacitor pack.

Table 5.4.3. Sized supercapacitor pack

Power demand from supercapacitor pack (kW)	1057.4
Power-based module number	78
Energy demand from supercapacitor pack (kWh)	7.3
Energy-based module number	125
Higher number of modules	125
Weight (t)	7625
Volume (m^3)	0.68

Figure 5.4.9 shows the total power demand as well as the low pass-filtered and high pass-filtered power demands in the time domain. The Energy/Time results for the total energy requirements, the low pass-filtered energy demand and the high pass-filtered energy demands are shown in Figure 5.4.10.

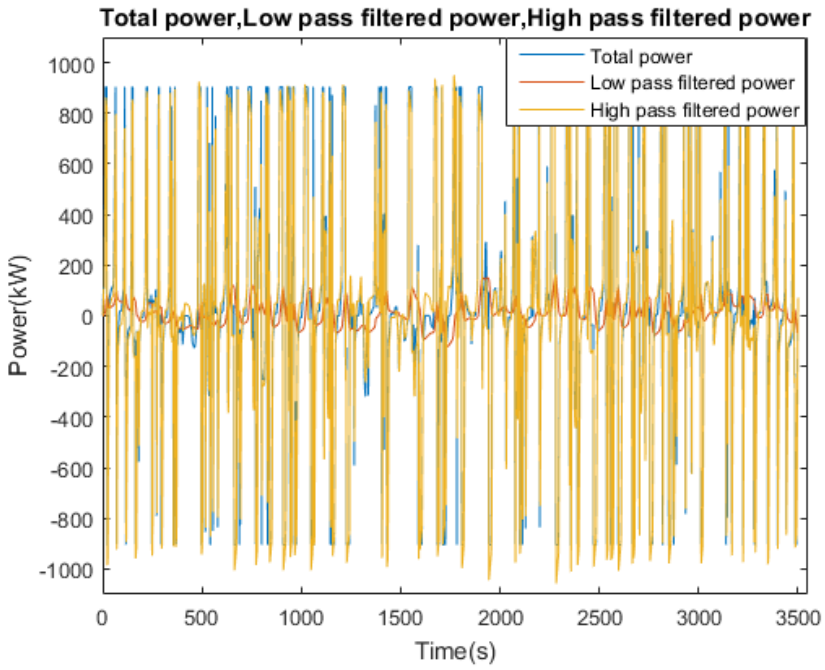

Figure 5.4.9. Total power demand, Low pass-filtered power demand and high pass-filtered power demand in time domain

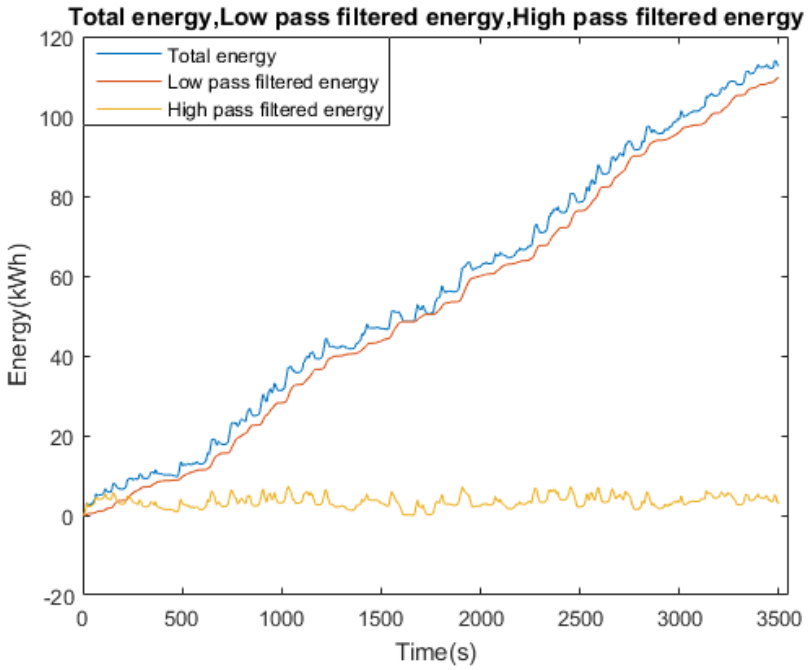

Figure 5.4.10. Total energy demand, Low pass-filtered energy demand and high pass-filtered energy demand in time domain

Figure 5.4.11 indicates the sum of the low pass-filtered and high pass-filtered power demands, and in Figure 5.4.12, the sum of the low pass-filtered and high pass-filtered energy demands is shown. It can be seen that the peak power is 904kW and the energy consumption is 112.6kWh.

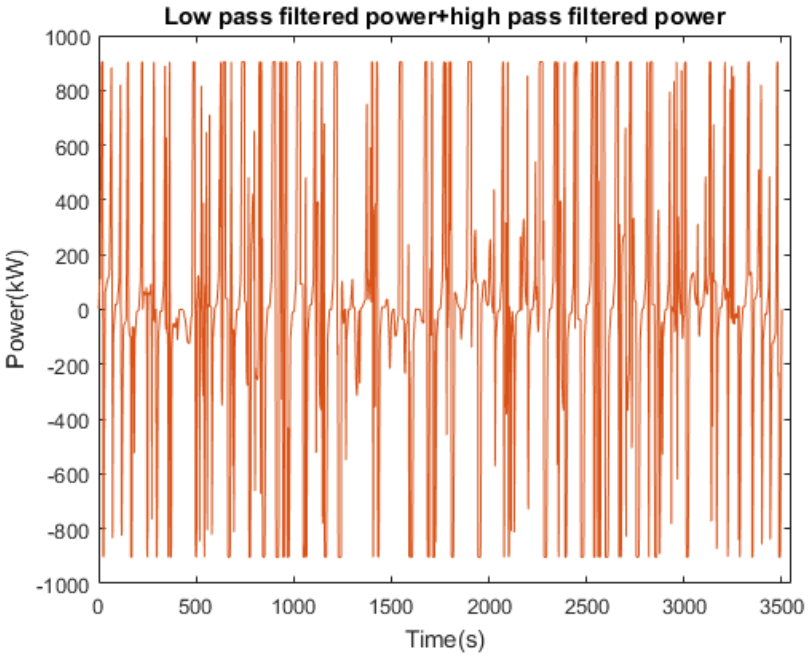

Figure 5.4.11. Sum of low pass-filtered and high pass-filtered power demands

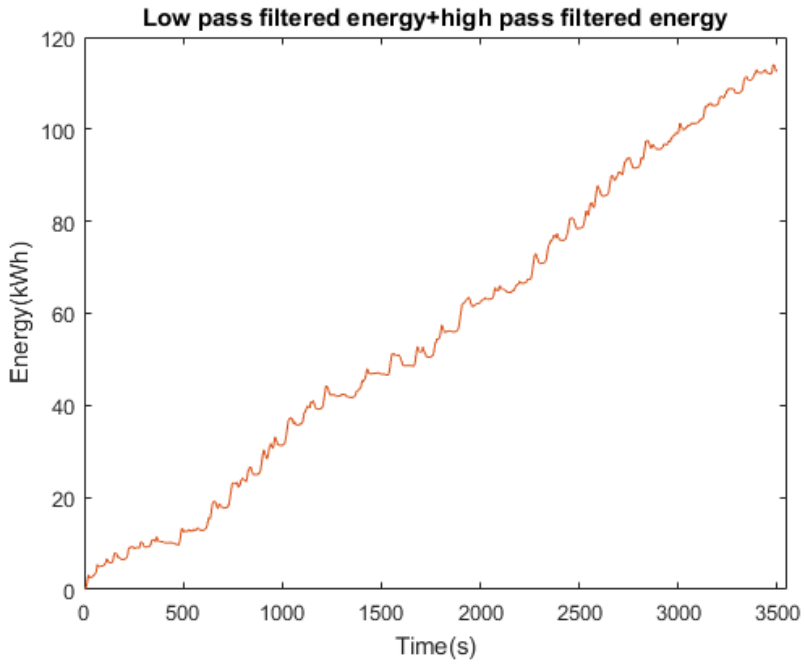

Figure 5.4.12. Sum of low pass-filtered and high pass-filtered power demands

The same as the previous case study, the number of supercapacitor modules are determined based on the energy demand. Now the C-rate constraint should be imposed to the sized supercapacitor pack and the performance of the sized HESS with 108 battery modules and 125 supercapacitor modules with this constraint should be assessed. Figure 5.4.13 and Figure 5.4.14 indicate the performance of the HESS in meeting the power demand and also the changes of the SOC of both packs after imposing the c-rate constraint. It can be seen that the supercapacitor pack cannot meet the required energy and power demand and becomes empty at 2721s, when, the battery pack has to compensate for the supercapacitor pack until the end of the journey.

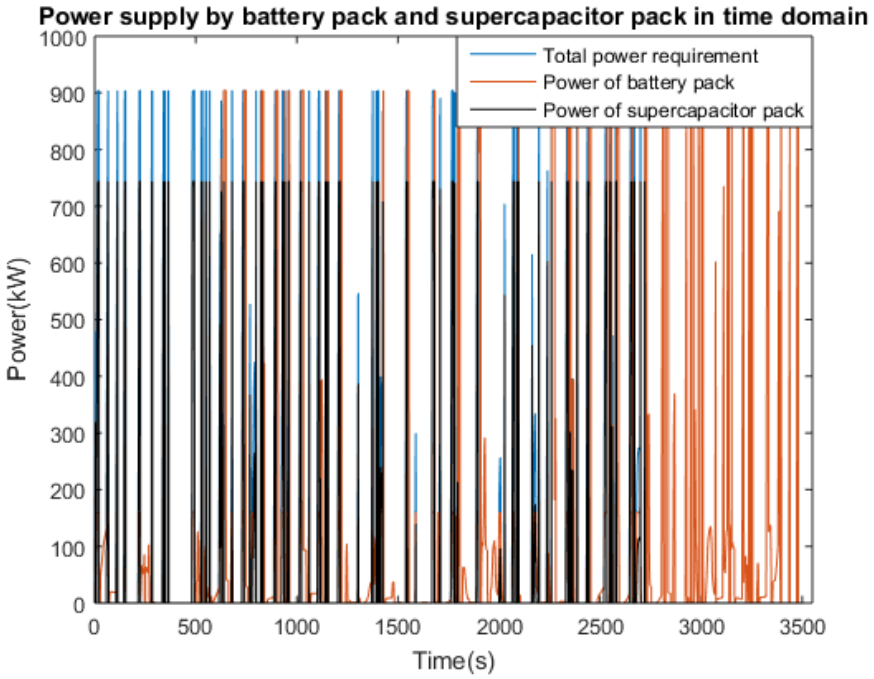

Figure 5.4.13. HESS supplying power demand in time domain
after imposing C-rate constraint

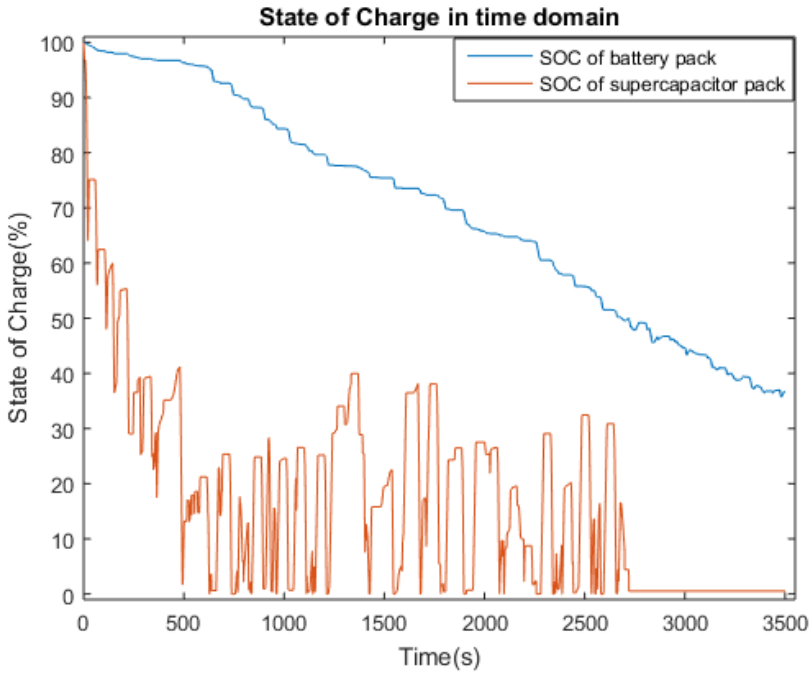

Figure 5.4.14. SOC changes of battery pack and supercapacitor pack in time domain after imposing C-rate constraint

Now the number of supercapacitor modules need to increase in order to be ensured that there are adequate number of supercapacitor modules which do not discharge higher than their typical discharging power, which is 13.6kW. By increasing the number of supercapacitors to 1007, both packs would perform properly without making the supercapacitor modules discharge higher than 13.6kW.

Figure 5.4.15 indicates how the newly-sized battery pack and supercapacitor pack meet the percentages of the power demand that they are responsible for. The changes in the SOC of both packs during the journey are indicated in Figure 5.4.16, where the supercapacitor pack uses 96.65% of its stored energy, but the battery pack uses only 33% of its stored energy and 67% of its energy remains at the end of the journey. The HESS including 108 battery modules and 1007 supercapacitor modules has a size of 64.45t and 7.02m^3.

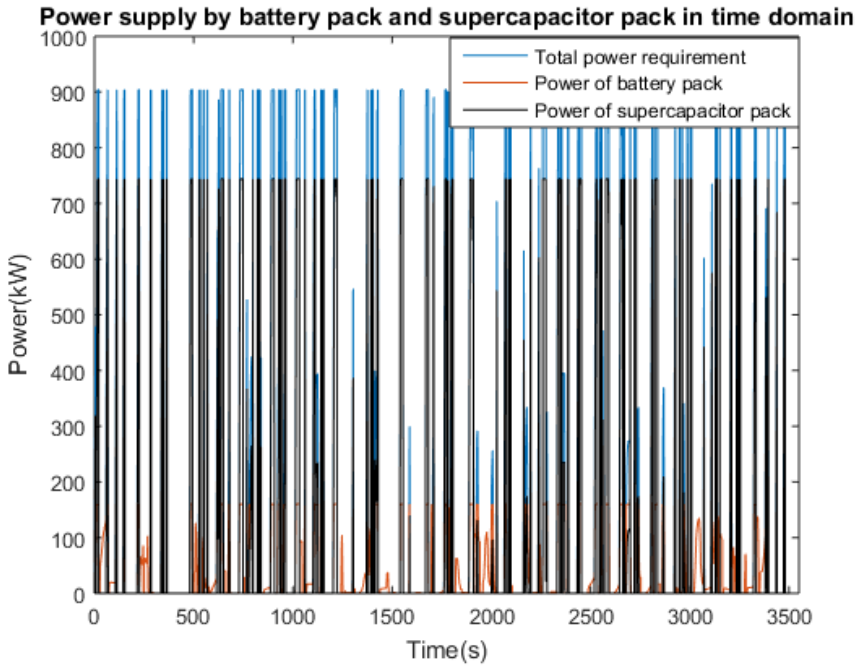

Figure 5.4.15. HESS supplying power demand in time domain
with increased number of supercapacitor modules

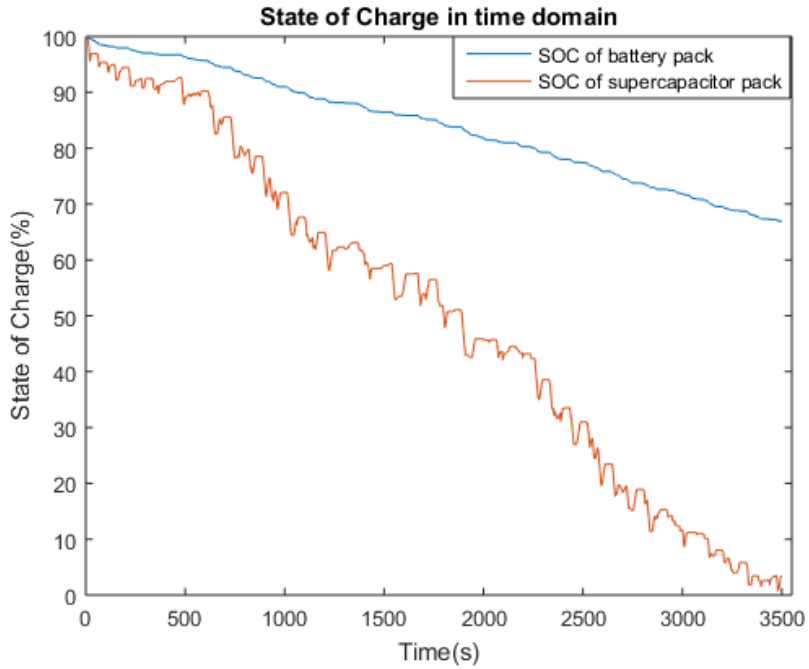

Figure 5.4.16. SOC changes of battery pack and supercapacitor pack in time domain

with increased number of supercapacitor modules

Now the battery pack should be used as an energy supplier to charge the supercapacitor pack during the journey and as for the previous case study, four scenarios are applied to the sized HESS with 108 battery modules and 1007 supercapacitor modules. Brute Force optimisation is employed for each scenario to find out the most optimised number for supercapacitor modules.

The first scenario is charging whenever the supercapacitor pack's SOC goes below 1%. Figure 5.4.17 indicates the result of the Brute Force optimisation where the minimum number of supercapacitor modules without making the supercapacitor pack's SOC become zero is 388 with the minimum SOC of 0.02% during the journey.

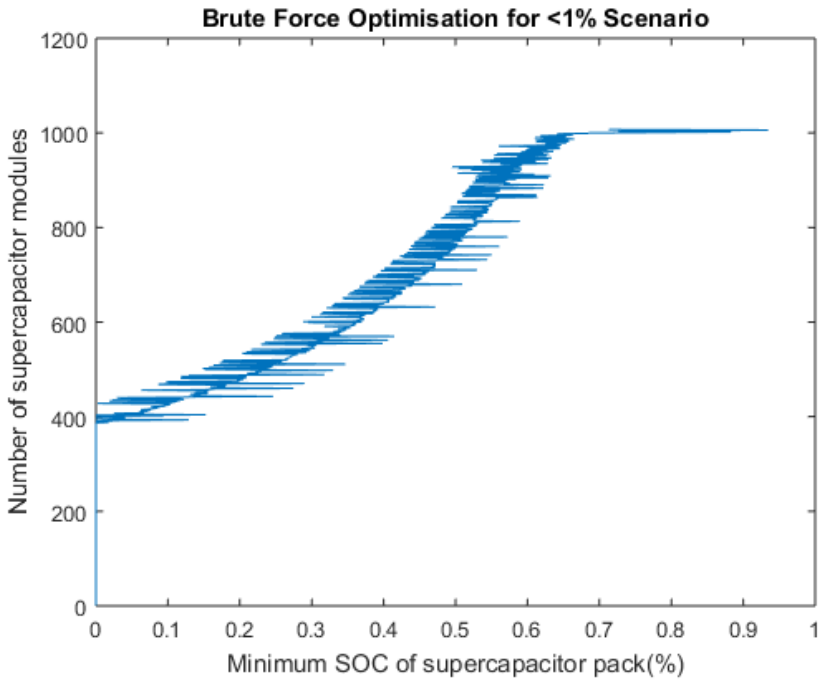

Figure 5.4.17. Brute Force Optimisation for Supercapacitor SOC <1% Scenario

Figure 5.4.18 and Figure 5.4.19 indicate how a sized HESS with 108 battery modules and 388 supercapacitor modules in this charging scenario work. It can be seen that the HESS performs properly. The minimum SOC of the supercapacitor pack is 0.02% during the journey and battery

has 50.02% of its stored energy left unused at the end of the journey. The total weight and volume of this HESS is 26.69t and 3.68m^3, respectively.

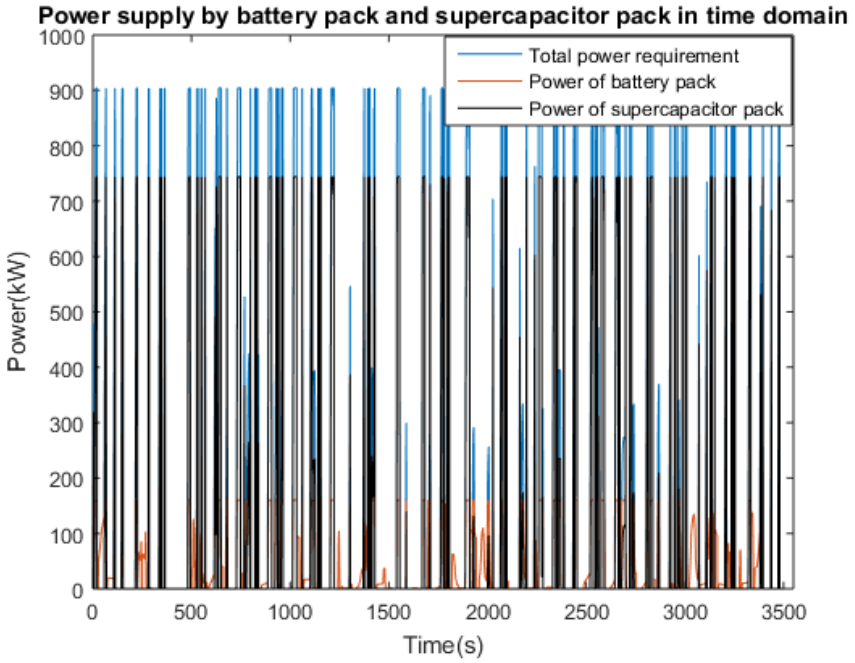

Figure 5.4.18. HESS supplying power demand in time domain,
battery pack charging supercapacitor pack for Supercapacitor SOC <1% Scenario

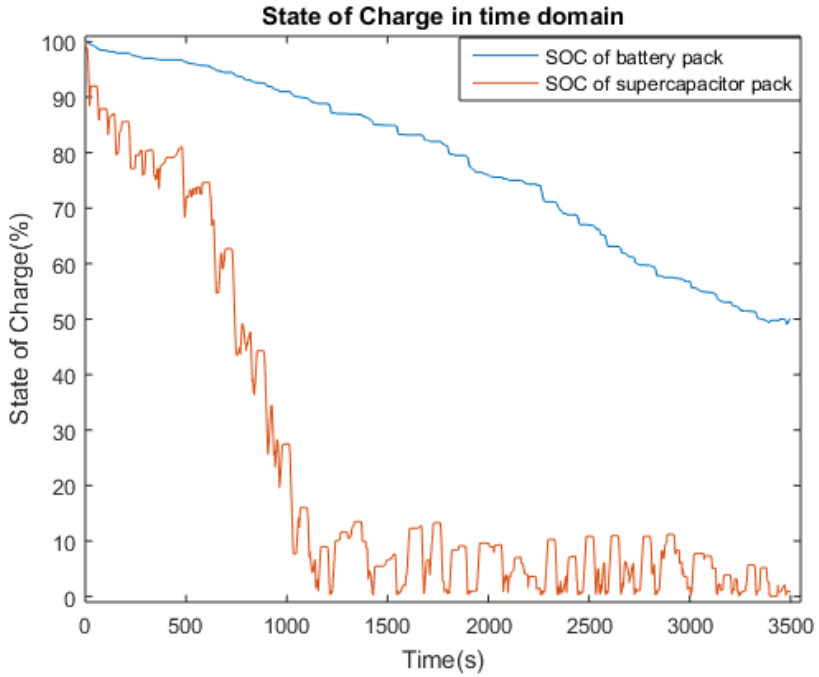

Figure 5.4.19. SOC changes of battery pack and supercapacitor pack in time domain,
battery pack charging supercapacitor pack for Supercapacitor SOC <1% Scenario

The second scenario is to charge the supercapacitor pack whenever its SOC goes below 100%. Figure 5.4.20 indicates the result of the Brute Force optimisation for this scenario, where the optimal number of supercapacitor modules is 4 with the minimum SOC of 0.01% during the journey.

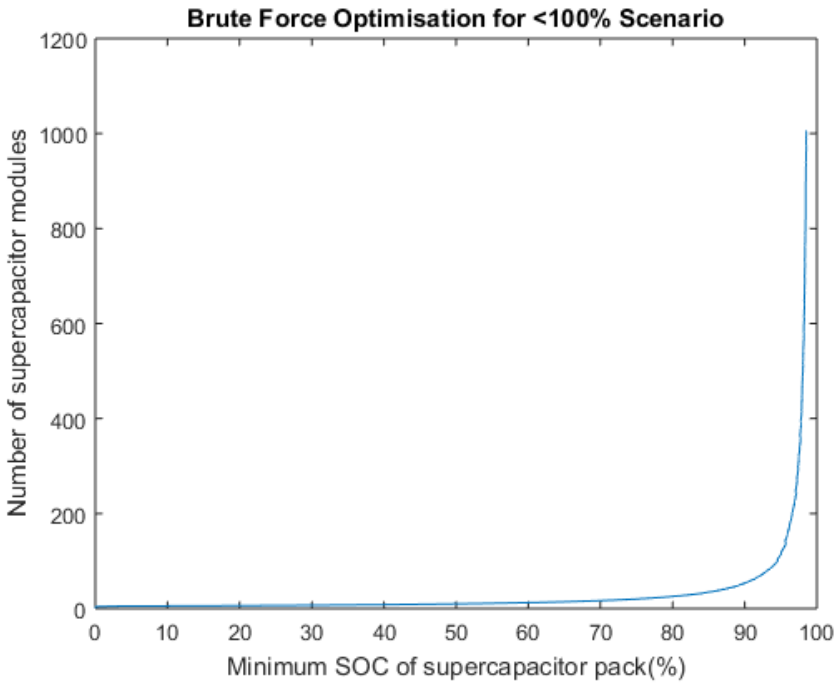

Figure 5.4.20. Brute Force Optimisation for Supercapacitor SOC <100% Scenario

Figure 5.4.21 shows how 108 battery modules and 4 supercapacitor modules meet the power demand during the journey when this scenario is applied to the HESS and Figure 5.4.22 indicates how the SOC of both packs change during the journey; where the minimum SOC of the supercapacitor pack is 0.01% and the energy left in the battery pack at the end of the journey is 26.33%. 108 battery modules and 4 supercapacitor modules make the size of the HESS 3.27t and 1.61m^3.

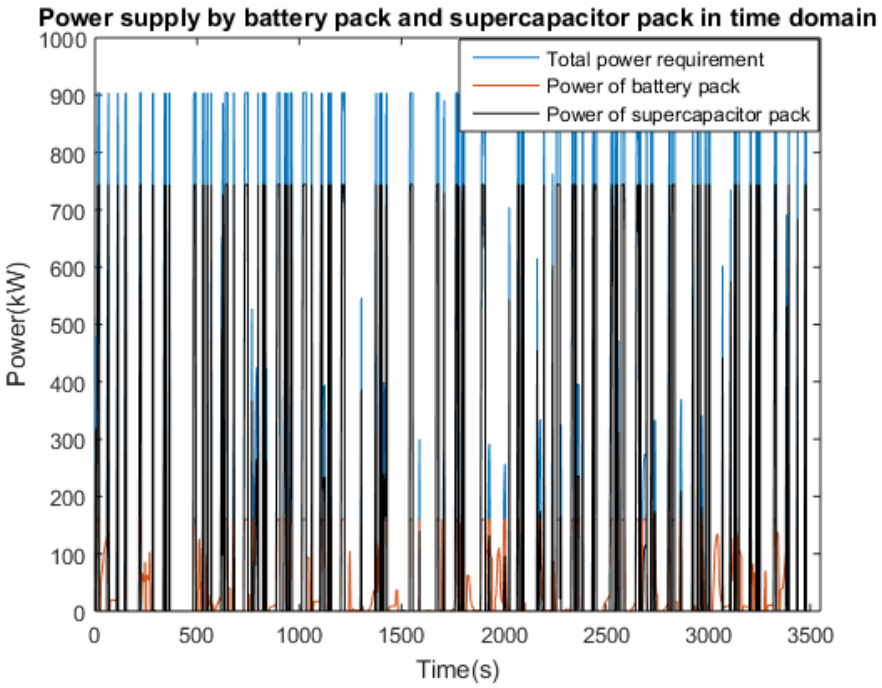

Figure 5.4.21. HESS supplying power demand in time domain,
battery pack charging supercapacitor pack for Supercapacitor SOC <100% Scenario

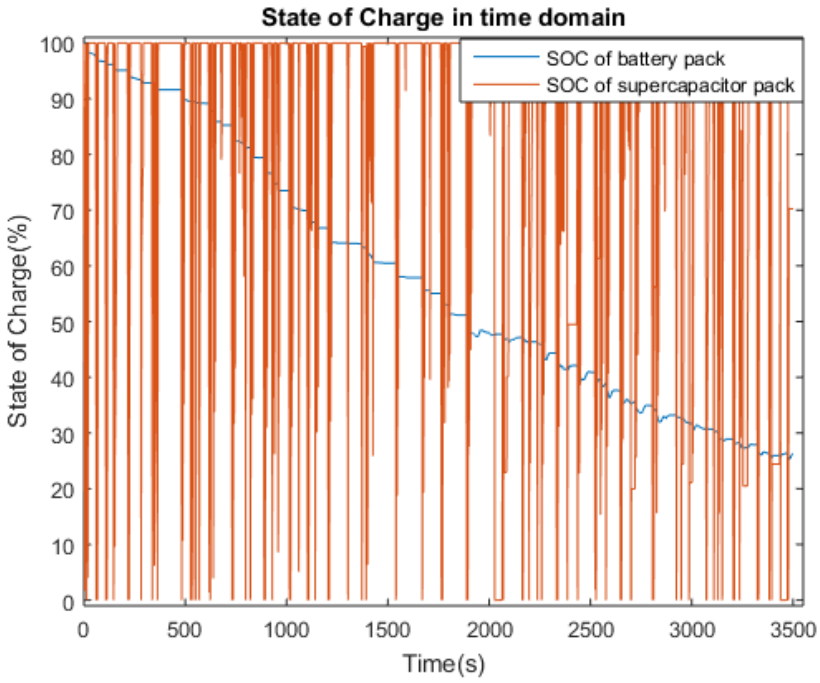

Figure 5.4.22. SOC changes of battery pack and supercapacitor pack in time domain,
battery pack charging supercapacitor pack for Supercapacitor SOC <100% Scenario

The next scenario is to get the battery pack to charge the supercapacitor pack in cruising modes only. Figure 5.4.23 shows the result of the Brute Force optimisation, where the most optimal number of supercapacitor modules is found as 327 and the minimum SOC of the supercapacitor pack is 0.14%.

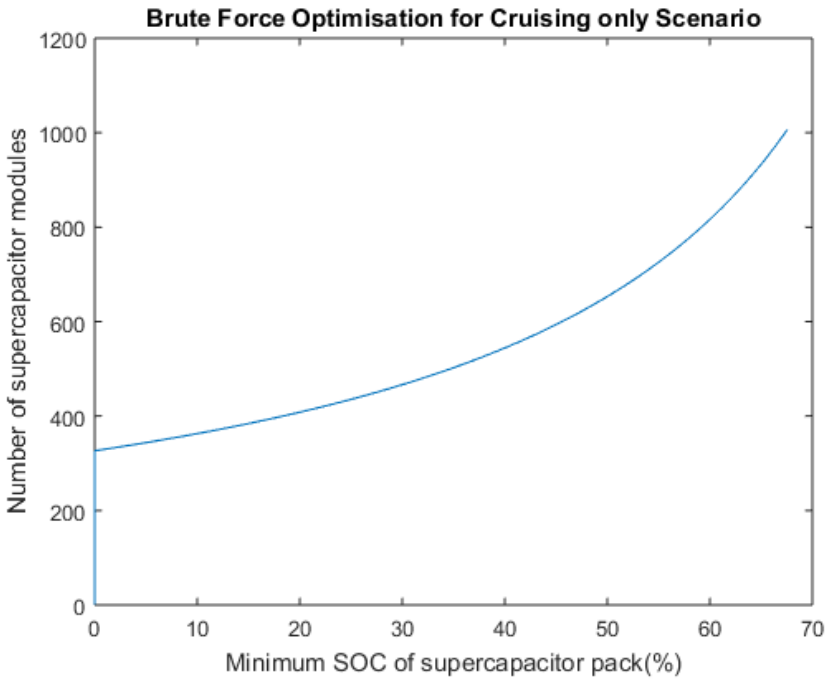

Figure 5.4.23. Brute Force Optimisation for Cruising Scenario

The performance of the sized HESS with 108 battery modules and 327 supercapacitor modules is indicated in Figure 5.4.24 and Figure 5.4.25; where the sized HESS with 22.97t weight and 3.35m^3 volume can meet the required energy and power demand properly and the energy left at the end of the journey for the battery pack is 43.33%.

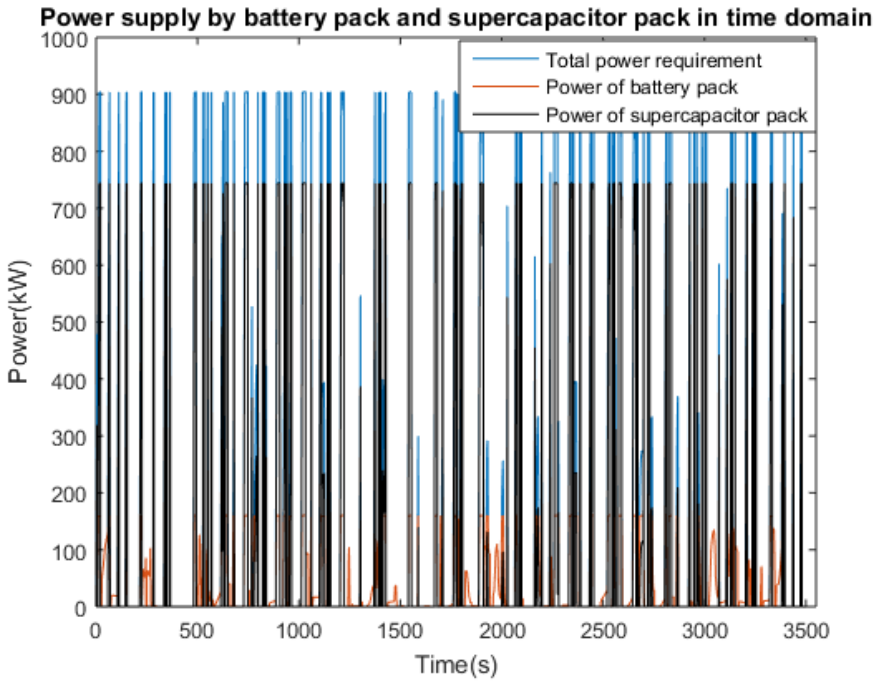

Figure 5.4.24. HESS supplying power demand in time domain, battery pack charging supercapacitor pack for Cruising Scenario

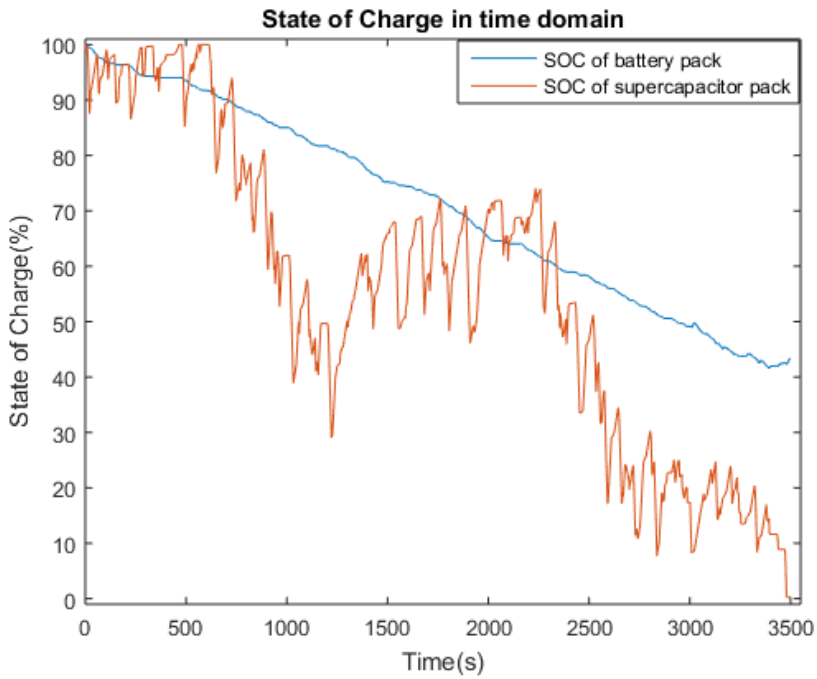

Figure 5.4.25. SOC changes of battery pack and supercapacitor pack in time domain, battery pack charging supercapacitor pack for Cruising Scenario

The final scenario is to charge the supercapacitor pack in acceleration modes only. The result of the Brute Force optimisation for this scenario is indicated in Figure 5.4.26 where the optimal number is achieved as 15 with the minimum SOC of 0.01%.

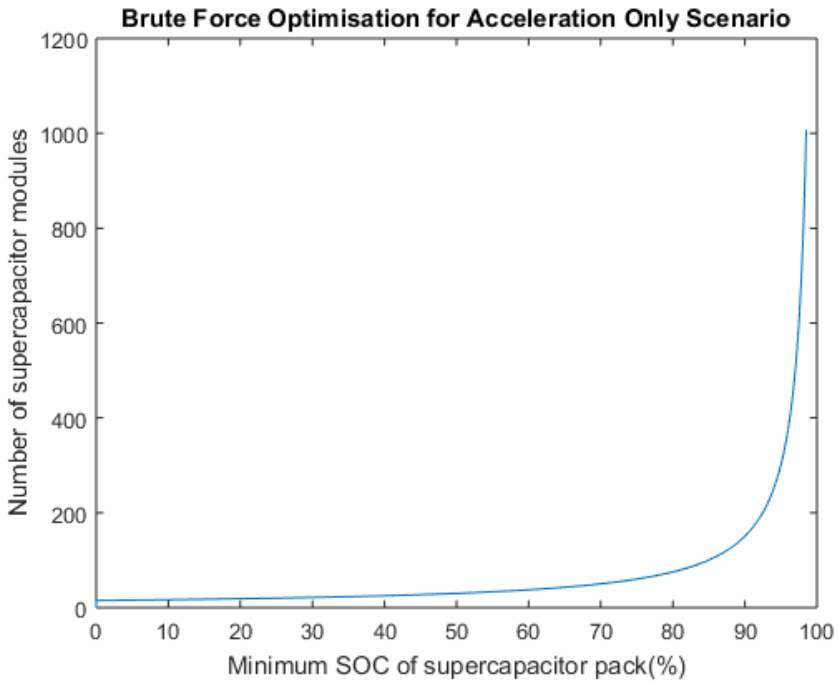

Figure 5.4.26. Brute Force Optimisation for Acceleration Scenario

The 108 battery modules and 15 supercapacitor modules make the size of the HESS 3.94t and 1.67m^3. Figure 5.4.27 and Figure 5.4.28 indicate the performance of the sized HESS in this scenario, where the energy left in the battery pack at the end of the journey is 50.47%.

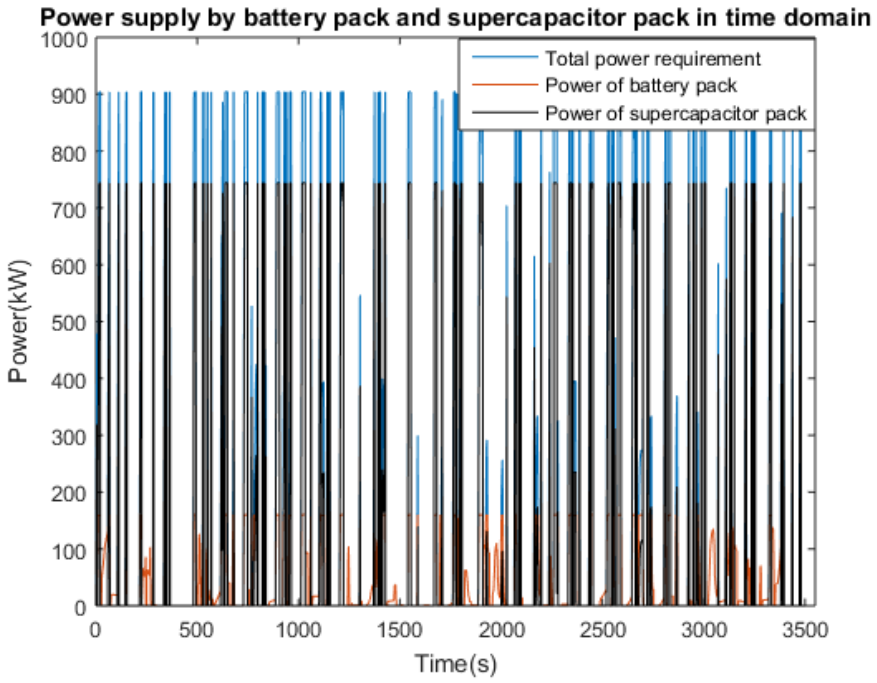

Figure 5.4.27. HESS supplying power demand in time domain,
battery pack charging supercapacitor pack for Acceleration Scenario

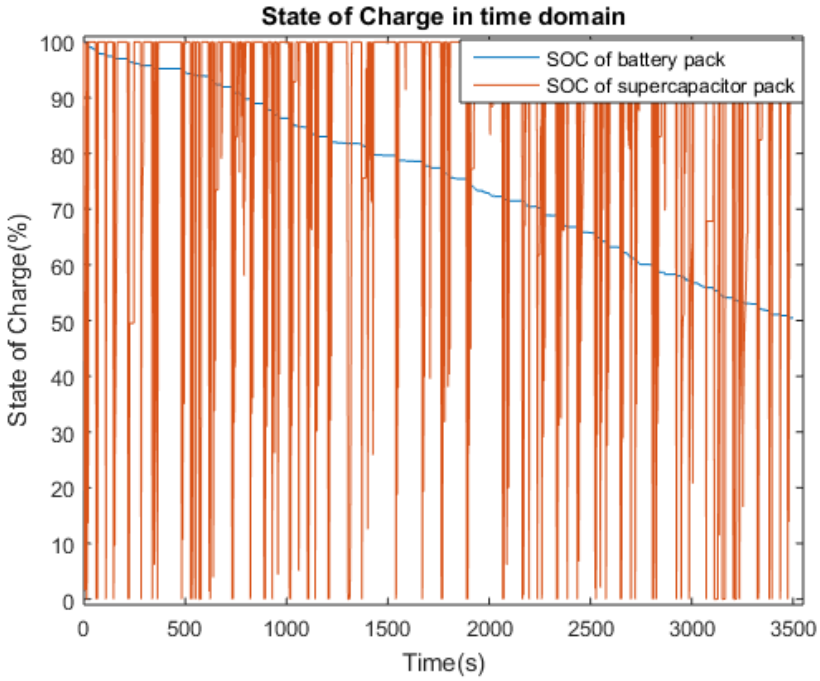

Figure 5.4.28. SOC changes of battery pack and supercapacitor pack in time domain,
battery pack charging supercapacitor pack for Acceleration Scenario

Now the sized ESSs and HESSs in this phase should be compared. Table 5.4.4 indicates the number of modules and sizes of the battery-only and supercapacitor-only ESSs as well as the optimally sized HESSs. It can be seen that the size of the supercapacitor-only scenario is the biggest, with 117t and 10.47m^3 and the size of the optimised HESS in SOC<100% Scenario is the smallest with 3.27t and 1.61m^3. Regarding the optimally-sized HESSs, three out of six scenarios, the HESS with C-rate constraint, the HESS with SOC<1% charging Scenario and the HESS with charging in cruising Scenario have higher weights and volumes than the battery-only scenario. Amongst charging scenarios, the same as the previous case study, SOC<100% Scenario resulted in the lowest weight and volume and SOC<1% Scenario resulted in the highest weight and volume. Moreover, the charging in acceleration only Scenario has lower size than charging in cruising only Scenario.

Now the total energy consumption and peak power demand of the traction after adding the eight sized ESSs/HESSs to the mass of the train should be analysed. Figure 5.4.29 and Figure 5.4.30 indicate the energy consumption and peak power demand for all eight scenarios before and after adding the ESS/HESS. The initial energy consumption of the traction was 112.6kWh. It is obvious that the greater the weight of the HESS is, the more the energy consumption will be. Hence, the lowest energy consumption increase is for the SOC<100% charging Scenario (with the smallest weight of the HESS) with 3.27% increase and the highest increase in the energy consumption is for the supercapacitor only Scenario (with the biggest weight of the HESS) with 65.9% increase. From the figures it can be seen that the higher the energy consumption, the longer the journey time. As for the previous study, the peak power demand has not changed after adding the HESS since this parameter is considered constant for the tram. The new energy and power demands as well as the increase in demands after adding ESSs/HESSs are captured in Table 5.4.4 as well.

Table 5.4.4. Comparing battery-only ESS, supercapacitor-only ESS and optimiesd HESSs

	Battery-only ESS	Supercapacitor-only ESS	Optimised HESS (no C-rate constraint)	Optimised HESS (with C-rate constraint)	Optimised HESS (charging: SOC<1% Scenario)	Optimised HESS (charging: SOC<100% Scenario)	Optimised HESS (charging: in cruising only Scenario)	Optimised HESS (charging: in acceleration only Scenario)
Number of battery modules	610	-	108	108	108	108	108	108
Number of supercapacitor modules	-	1934	125	1007	388	4	327	15
Total weight (t)	17.08	117.97	10.65	64.45	26.69	3.27	22.97	3.94
Total volume (m^3)	8.97	10.44	2.26	7.02	3.68	1.61	3.35	1.67
Total energy consumption after adding storage system (kWh)	126.5	186.8	122	163.3	135.8	116.9	133.3	117
Increased energy consumption (%)	12.34	65.9	8.35	45.02	20.6	3.82	18.39	3.9
Peak power demand after adding storage system (kW)	904	904	904	904	904	904	904	904

Increased peak power demand (%)	0	0	0	0	0	0	0	0

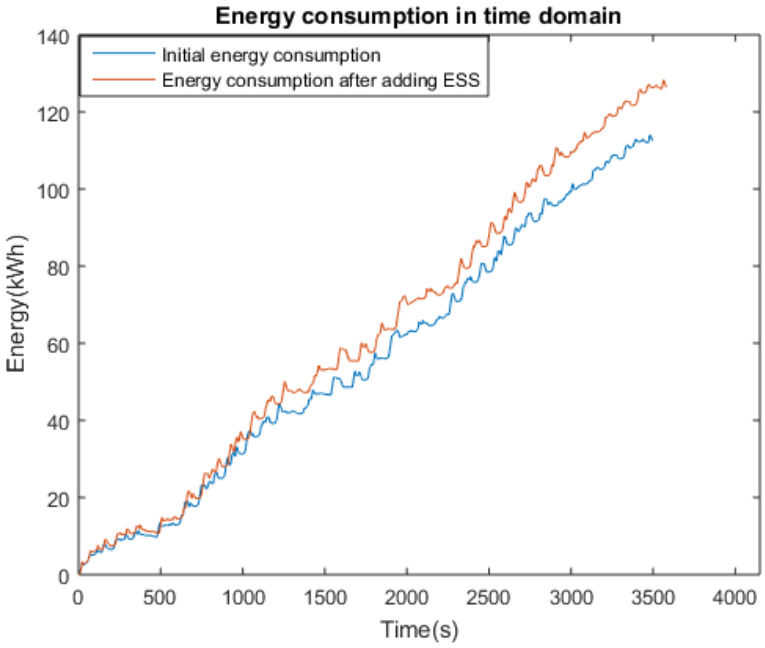

(a)

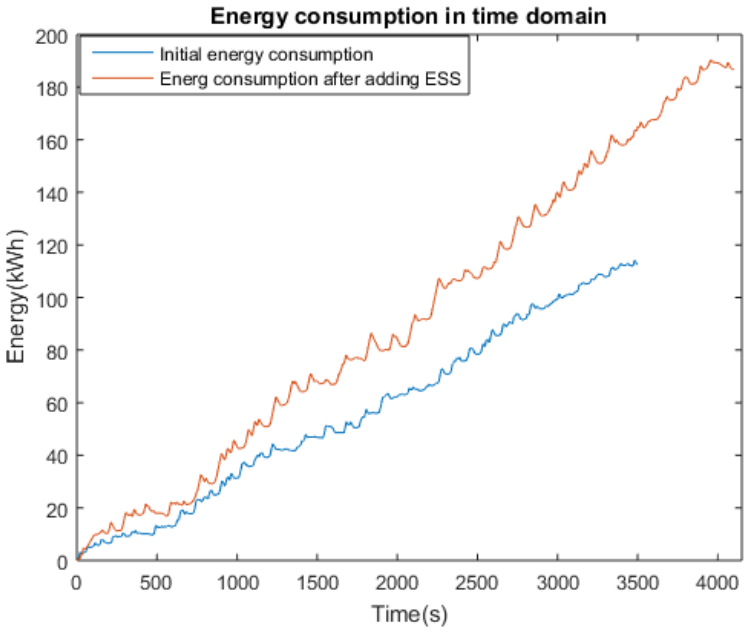

(b)

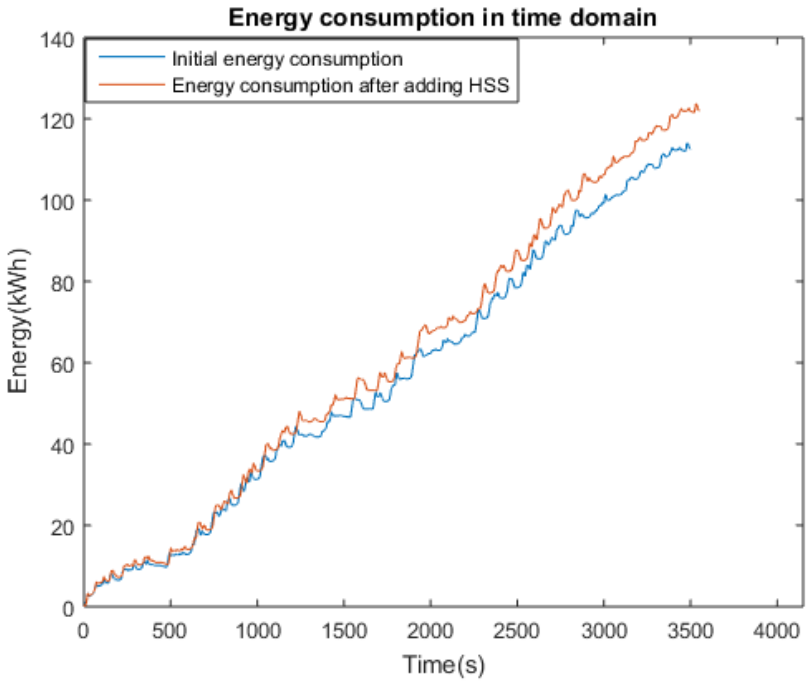
Energy consumption in time domain
Initial energy consumption
Energy consumption after adding HSS
Energy(kWh)
Time(s)
0
20
40
60
80
100
120
140
0
500
1000
1500
2000
2500
3000
3500
4000

(c)

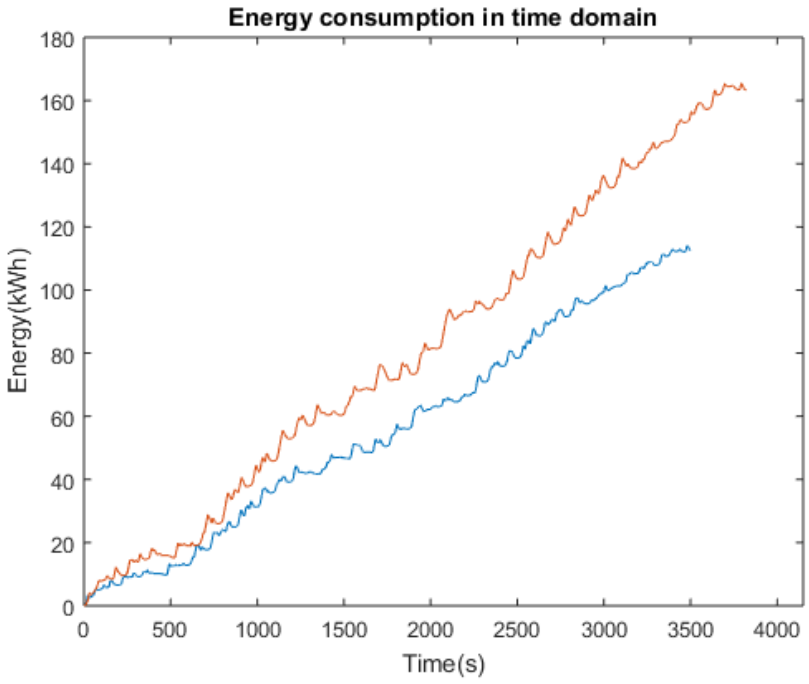
Energy consumption in time domain
Energy(kWh)
Time(s)
0
20
40
60
80
100
120
140
160
180
0
500
1000
1500
2000
2500
3000
3500
4000

(d)

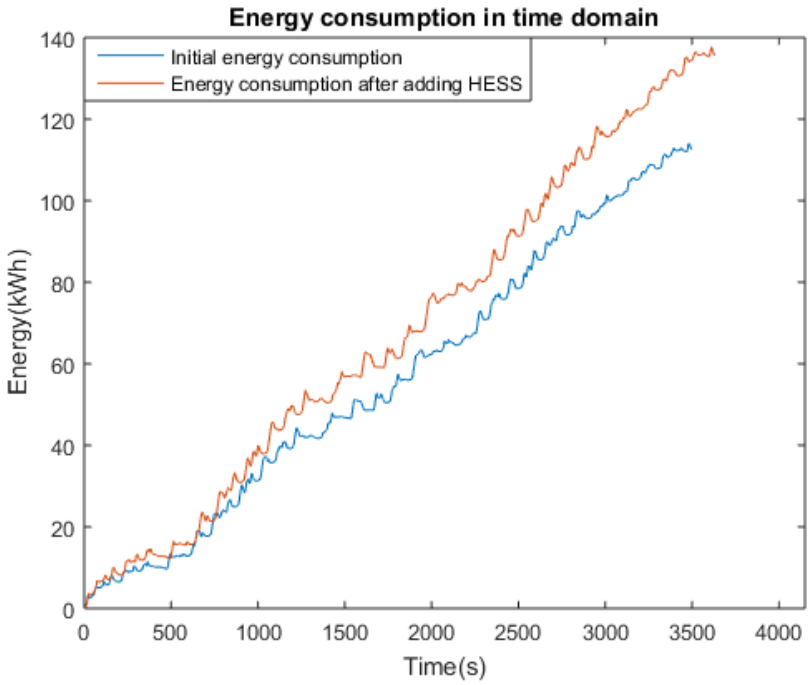
Energy consumption in time domain
Initial energy consumption
Energy consumption after adding HESS
Energy(kWh)
Time(s)
0
20
40
60
80
100
120
140
0
500
1000
1500
2000
2500
3000
3500
4000

(e)

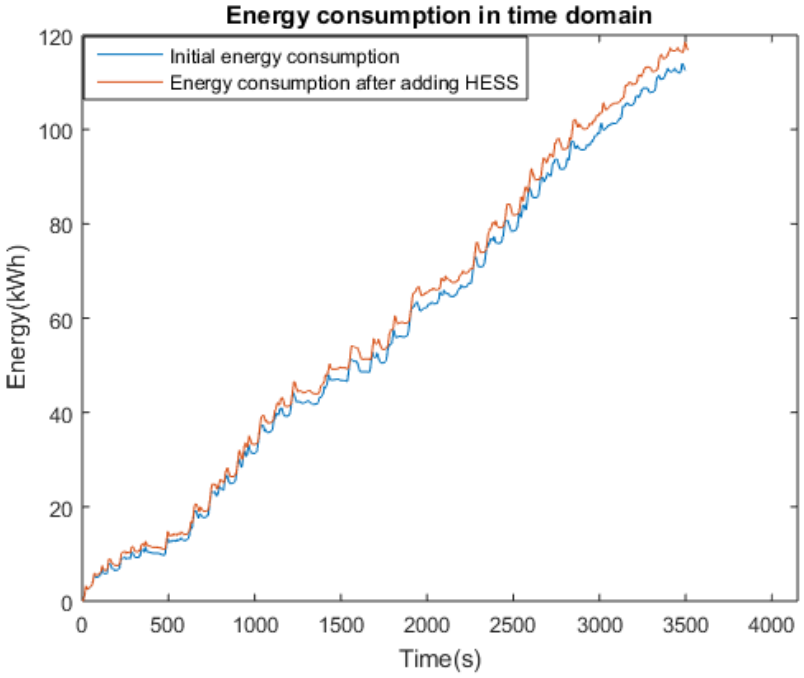
Energy consumption in time domain
Initial energy consumption
Energy consumption after adding HESS
Energy(kWh)
Time(s)
0
20
40
60
80
100
120
0
500
1000
1500
2000
2500
3000
3500
4000

(f)

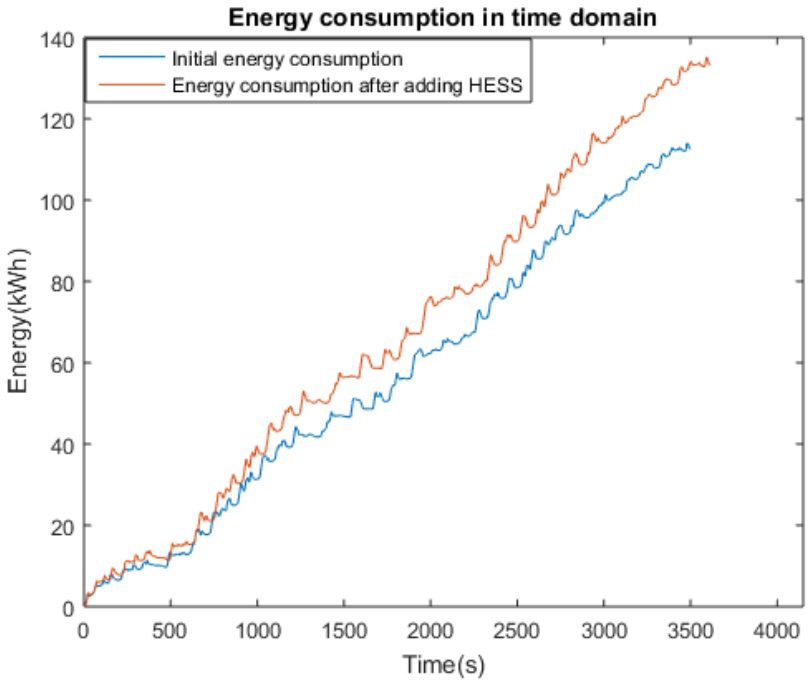

(g)

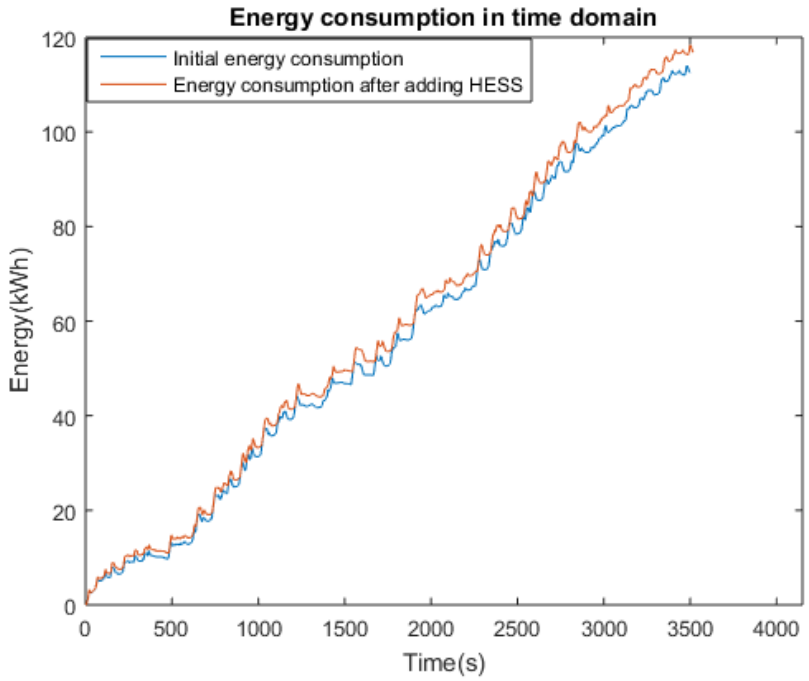

(h)

Figure 5.4.29. Energy consumption before and after adding the ESS/HESS for
(a) Battery-only Scenario
(b) Supercapacitor-only Scenario
(c) Optimised HESS (without C-rate constraint)
(d) Optimised HESS (with C-rate constraint)
(e) Optimised HESS (charging: SOC<1% Scenario)
(f) Optimised HESS (charging: SOC<100% Scenario)

(g) Optimised HESS (charging: cruising-only Scenario)
(h) Optimised HESS (charging: acceleration-only scenario)

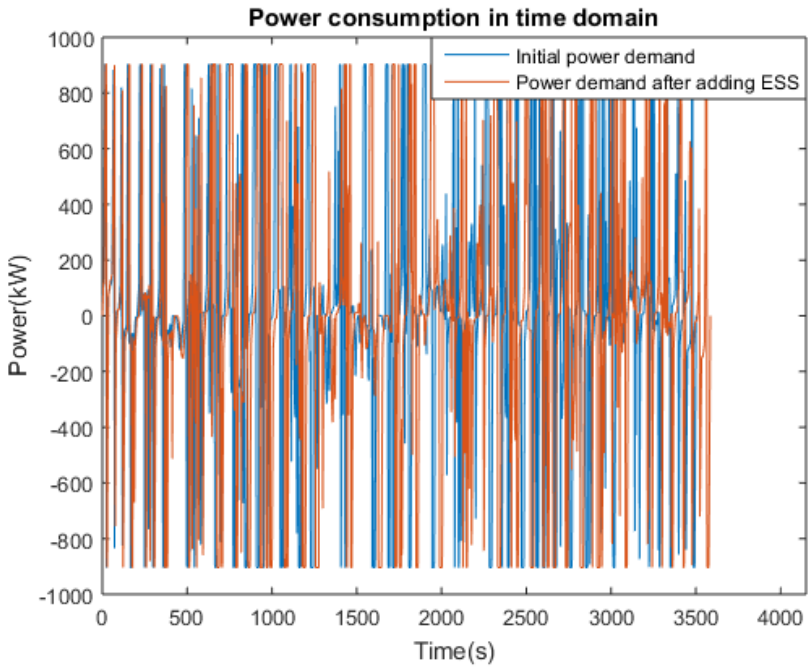

(a)

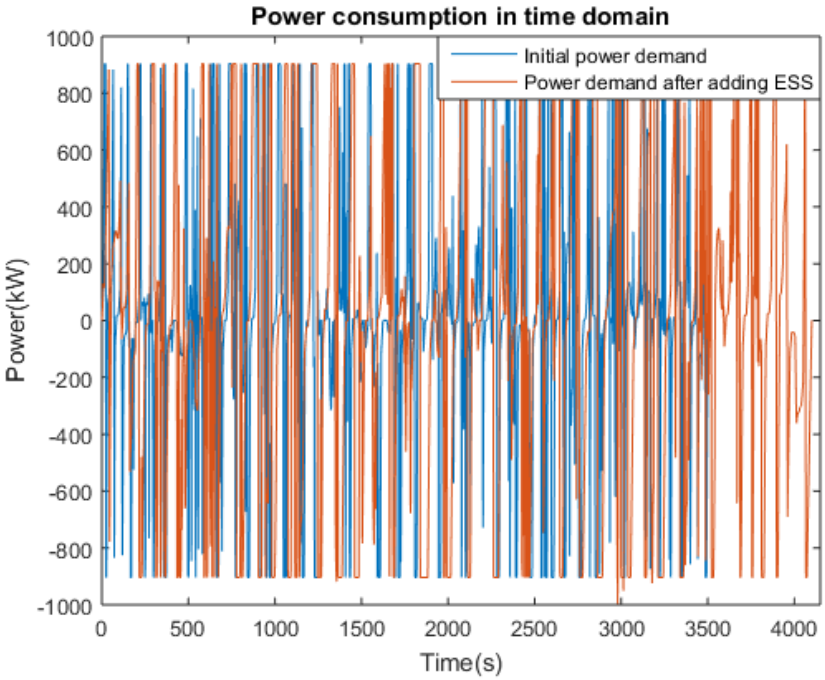

(b)

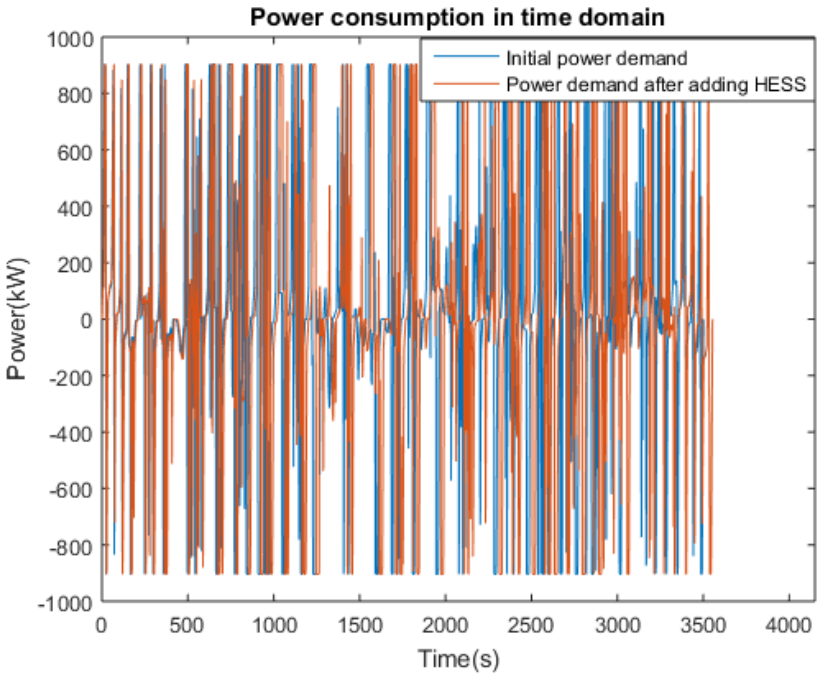
Power consumption in time domain
Initial power demand
Power demand after adding HESS
Power(kW)
Time(s)
1000
800
600
400
200
0
-200
-400
-600
-800
-1000
0
500
1000
1500
2000
2500
3000
3500
4000

(c)

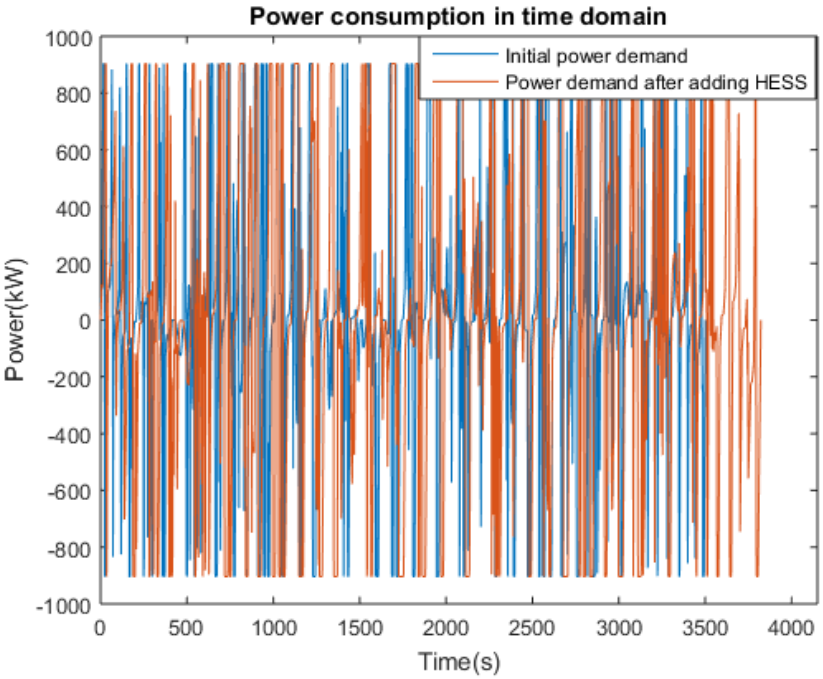
Power consumption in time domain
Initial power demand
Power demand after adding HESS
Power(kW)
Time(s)
1000
800
600
400
200
0
-200
-400
-600
-800
-1000
0
500
1000
1500
2000
2500
3000
3500
4000

(d)

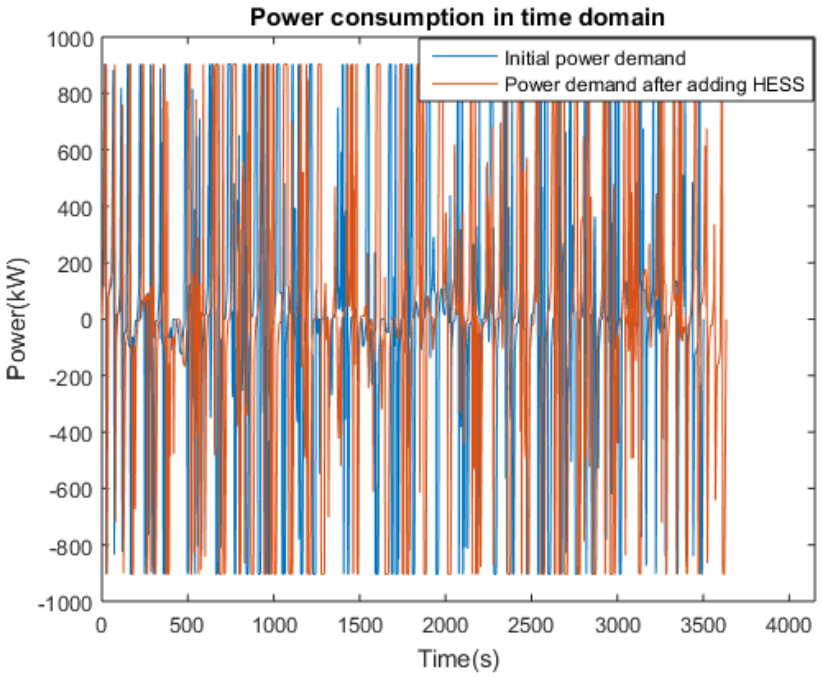
Power consumption in time domain
Initial power demand
Power demand after adding HESS
Power(kW)
Time(s)
1000
800
600
400
200
0
-200
-400
-600
-800
-1000
0
500
1000
1500
2000
2500
3000
3500
4000

(e)

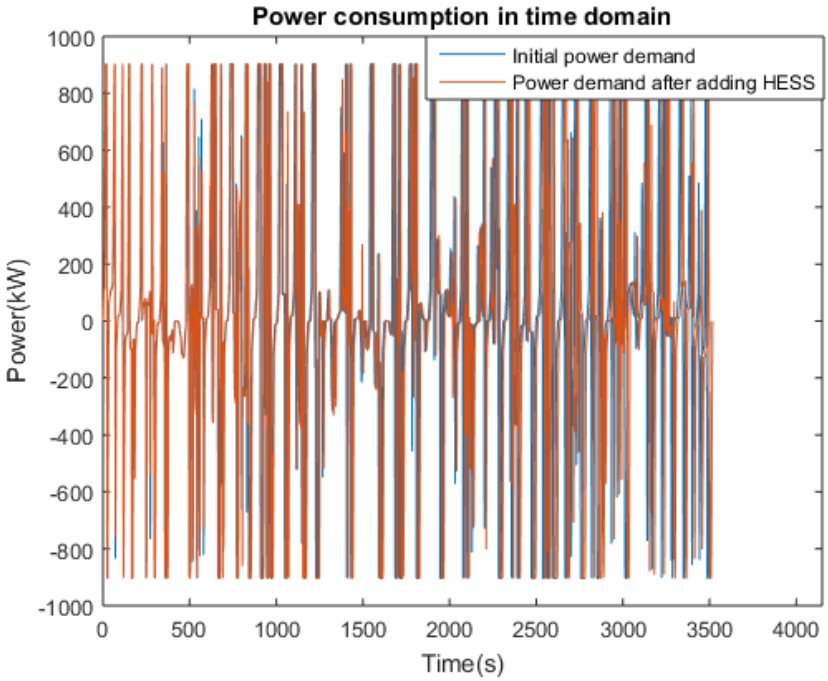
Power consumption in time domain
Initial power demand
Power demand after adding HESS
Power(kW)
Time(s)
1000
800
600
400
200
0
-200
-400
-600
-800
-1000
0
500
1000
1500
2000
2500
3000
3500
4000

(f)

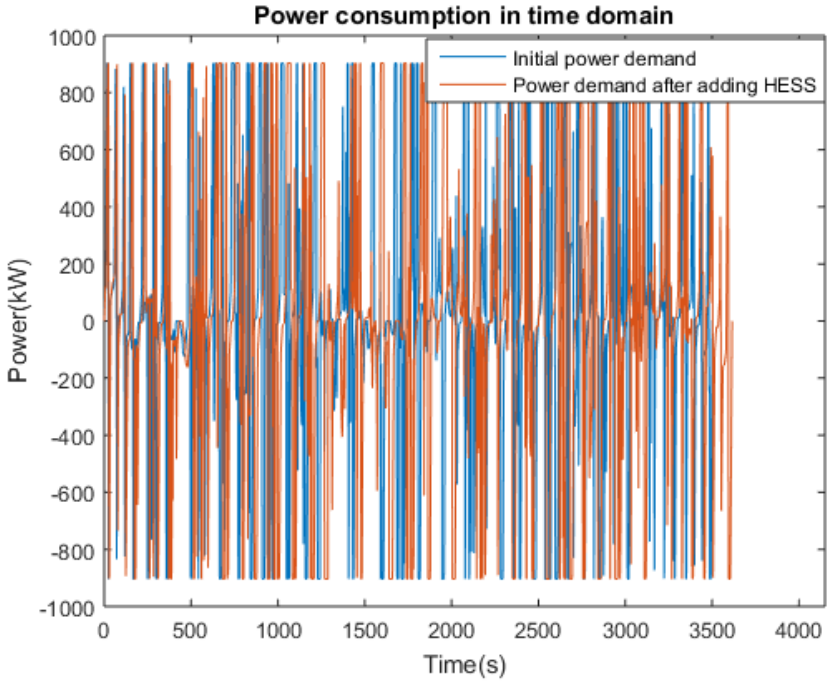

(g)

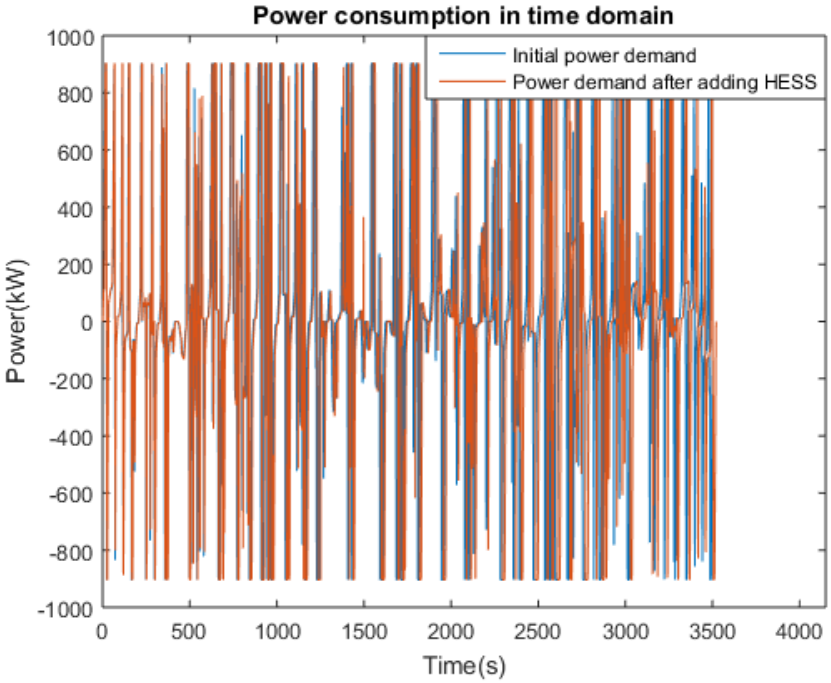

(h)

Figure 5.4.30. Power demand before and after adding the ESS/HESS for
(a) Battery-only Scenario
(b) Supercapacitor-only Scenario
(c) Optimised HESS (without C-rate constraint)
(d) Optimised HESS (with C-rate constraint)

(e) Optimised HESS (charging: SOC<1% Scenario)
(f) Optimised HESS (charging: SOC<100% Scenario)
(g) Optimised HESS (charging: cruising-only Scenario)
(h) Optimised HESS (charging: acceleration-only scenario)

5.5. Summary

This chapter indicated how the proposed methodologies work when they are applied to a different railway application. As the second case study for this project, a tram running on a 750V DC OLE was considered. As in the previous case study, the traction of the tram running on this line was simulated in STS to determine how much energy and power the on-board HESS needs to provide.

The experiments proposed in the methodology were applied to the case study in order to 1) evaluate the influence of the energy density and power density of both the battery and supercapacitor on the total size of the HESS, and 2) observe the effect of a change in the C-rate of the battery on the size and performance of the HESS. Decreasing and increasing the number of battery modules and supercapacitor modules by 25%, respectively, resulted in an increase in the total size of the HESS by about 28.9t and 2.3m^3 regarding the energy demand and a decrease in the total size by about 3.25t and 2.16m^3 with regard to the power demand. With 458 battery modules and 17 supercapacitor modules in Scenario 2, the supercapacitor pack could not perform properly. The battery pack used 0.25% and 0.08% of its stored energy to compensate and charge the supercapacitor pack, respectively. By increasing the C-rate of the battery, every time that one supercapacitor module was removed, the total weight and volume of the HESS decreased by 0.061t (61kg) and 0.0054m^3 (5400cm^3), respectively.

The optimal HESS to meet the required energy and power demand for this case study was sized using the Frequency Analysis method and Brute Force optimisation. In the first optimal HESS, 108 battery modules and 125 supercapacitor modules were determined, the size of the HESS became 10.65t and 2.26m^3 and the energy consumption after adding this HESS to the mas of the train increased by 8.35%. After imposing the C-rate constraint to the sized supercapacitor pack, the supercapacitor pack could not meet the required energy and power demand and the number of supercapacitors had to increase to 1007 modules, which made the total size of the HESS 64.45t and 7.02m^3 and increased the total energy consumption by 45.02%. Charging scenarios were proposed alongside Brute Force optimisation in order to get the battery pack to charge the supercapacitor pack during the journey. The SOC<1% Scenario resulted in the highest size of the HESS amongst four proposed charging scenarios with 108 battery modules and 388 supercapacitor modules. The SOC<100% Scenario resulted in the lowest size of the HESS amongst four charging scenarios and amongst all sized ESSs/HESSs in this phase, with 3.27t weight energy consumption increase of 3.82%. The biggest size of the ESS/HESS and consequently, the highest energy consumption increase, amongst all eight scenarios was for the supercapacitor-only ESS with 117.97t and 65.9% energy consumption increase.

Chapter 6
Discussion

6.1. Introduction

This chapter discusses the results obtained from Chapter 4 and Chapter 5 for the proposed phases to evaluate, size and charge the HESS. This chapter indicates the applicability of the proposed methodologies for both railway applications used as case studies.

First, the obtained results are analysed and compared to what was expected based on the literature, where available, and the proposed hypothesis. Following this, logical reasoning is proposed for the results.

6.2. Evaluation of an HESS including Batteries and Supercapacitors

The first set of results which were obtained in this phase were related to five scenarios where battery and supercapacitor modules were used to meet the energy demand and power demand separately. As mentioned in Section 2.4.3, a battery has higher energy density compared to a supercapacitor. This means that for the same energy requirement, fewer battery modules are required. It is the other way around when it comes to supplying the power demand and with the same amount of power, fewer supercapacitor modules are required. The results from both case studies showed that the supercapacitor-only ESS while supporting the energy demand was much larger than the battery-only ESS while supporting the power demand. This means that it

is easier for the battery to support the power demand than for the supercapacitor to support the energy demand.

In the next set of results, the energy demand and power demand were integrated, and 25 scenarios were obtained. The results indicated that decreasing the number of battery modules and increasing the number of supercapacitor modules regarding the energy demand affects the total size of the HESS much more than to when the number of battery modules decreases and the number of supercapacitor modules increases regarding the power demand. Again, as claimed in the five-scenario experiment, this indicates that it is harder for the supercapacitor to meet the energy demand than for the battery to meet the power demand. This is because the ratio of battery and supercapacitor energy densities is much higher than the ratio of battery and supercapacitor power densities.

In order to assess the proposed experiments, the performance of sized HESSs in all 25 scenarios in both case studies was evaluated. In some combinations, the percentage of energy/power demand that either the battery or supercapacitor was in charge of meeting was 0%, and either the battery or supercapacitor was in charge of meeting only one demand. This was the case in Scenarios 2, 3, 4, 5, 10, 15 and 20 in both case studies and created issues where the sized HESSs did not perform properly. In Scenarios 2, 3 and 4, the battery pack was in charge of meeting the whole energy demand and hence the supercapacitor pack was only responsible for meeting the required percentage of the power demand. This meant determination of the supercapacitor pack was based only on the power demand. In Scenarios 10, 15 and 20, it is the other way around: the whole power demand was to be supplied by the supercapacitor pack and therefore the battery pack was sized based only on the energy demand. Again, as said before, the higher number of modules for the battery is chosen based on the power demand, and sizing the battery pack based only on the energy demand results in a battery pack with a small number of battery

modules which does not provide adequate energy for the journey. This means that the supercapacitor pack has to have more energy than it actually has, to compensate for the battery pack. Finally, the reason for the issue which happened in Scenario 5 was a combination of the two issues mentioned above.

In order to solve this issue for the above-mentioned scenarios, three solutions were given: the battery pack compensating for the supercapacitor pack, adding more supercapacitor modules and the battery pack charging the supercapacitor pack. It was obvious that adding supercapacitor modules adds to the total weight and volume of the HESS: this conflicts with one of the objectives of this project which is minimising the total size of the HESS. Moreover, it was seen that because the battery pack was determined based on the power demand, a lot of the saved energy in this pack was left unused at the end of the journey. Considering these two facts, it is more efficient to get the battery pack's help to solve the issue. Among the two proposed solutions with the battery pack's help, getting this pack to compensate for the supercapacitor pack makes the battery pack discharge at more than its 1 C-rate, which is in conflict with what is considered in Section 3.2.3.1, not discharging the battery pack at more than its 1 C-rate. It was seen that the battery pack uses more energy to compensate for the supercapacitor pack than to charge. This is because in the compensation scenario, the battery pack discharges at a C-rate higher than 1 and hence discharges more energy. This was the same for both case studies.

The next experiment in this phase of the project was changing the C-rate of the battery to evaluate its effects on the size and performance of the HESS. In this experiment, the size of the HESS was dependent on the number of supercapacitor modules since the number of batter modules stayed constant and changing the C-rate of the batteries affected the number of supercapacitor modules.

6.3. Sizing the HESS in the Frequency Domain

In this phase of the project, optimal HESSs including batteries and supercapacitors were sized for both case studies by employing the Frequency Analysis method and Brute Force optimisation. It was seen that in both case studies, the determined power from the high-pass filter which had to be supplied by the supercapacitor pack was more than the total power demand required from the HESS. This is because of the overshoots and undershoots in the high-pass filter, as expected and mentioned in 3.3.1. Although there is overshoot in the high-pass filter, it should be noted that the low-pass filter are high-pass filters' complement and the summing low pass-filtered and high pass-filtered results indicated that the low-pass filters in both case studies have compensated for the existing overshoots and undershoots in the high-pass filters. Therefore, both the battery pack and supercapacitor pack were designed based on the results obtained from the filters.

After imposing the C-rate constraint to the energy based-sized supercapacitor pack, it was seen that the sized supercapacitor pack was not able to meet the required energy and power demand and the number of supercapacitor modules had to increase to achieve the target. This indicates that while sizing an storage system in frequency domain, if there is a limit in the discharging power of a storage device and this is not considered in the body of the energy-based calculations the same as the power-based calculations, there is a risk that the sized pack discharges higher than its allowed discharging power and the storage system is not able to perform properly.

It was seen that in both case studies, a part of the stored energy in the battery pack was left unused at the end of the journey. The achieved results demonstrate that sizing based on the energy demand, if C-rate constraint is considered in the body of energy-based calculations, gives a more accurate result than sizing based on the power demand and the energy demand is

the key demand to be met during the journey. However, the HESS should have enough energy to meet the peak power demand meaning that a great amount of energy should be available in a short period of time. That is why the power demand is considered in sizing the HESS. Considering an adequate number of battery modules to meet the power demand and sticking to not discharging battery modules at more than their 1 C-rates resulted in an amount of unused energy in the battery pack at the end of the journey. As showed in this project, the energy left unused in the battery pack can be used to charge the supercapacitor pack during the journey. There can be other potential uses for this unused energy, such as transferring the energy to the wayside energy storage systems installed by the line and using that energy for other trains, or sending the unused energy back to the substation, or using the energy for low power loads at the stations; such as lighting or Passenger Announcements systems.

Regarding getting the batteries to charge the supercapacitors during the journey, two criteria and two scenarios for each criteria were considered. Amongst four scenarios proposed for the battery pack to size the supercapacitor pack during the journey, getting the batteries to charge the supercapacitors whenever the supercapacitor pack's SOC goes below 100% resulted in the lowest number of supercapacitor modules and hence, the lowest size of the HESS. This is because this scenario means the battery pack continuously charges the supercapacitor pack during the journey, in both acceleration and cruising modes, and supercapacitors can charge by a live energy supply throughout the journey. Hence, the number of supercapacitor modules can be optimized the most. On the other hand, for three other scenarios, the charging procedure happens only in intervals during the journey and not always. Amongst these three scenarios, SOC<1% scenario resulted in the least optimised number as the supercapacitors charge only when they need energy and when they are about to become empty. Charging only in acceleration modes resulted in a more optimised number of supercapacitor modules compared

to the scenario when charging happened in cruising mode. This is because the supercapacitor pack is not used in cruising modes and charging can happen only once until it becomes full, but in acceleration modes the supercapacitor pack continuously charges and discharges and more energy from the battery pack can be received.

6.4. Summary

This chapter first gave a summary of the results achieved in two phases of the project. The results were then discussed, compared to the expectations where feasible and then logical reasoning was used to analyse the results. The results were those obtained from applying the proposed methodology in Chapter 3 to the considered case studies, as indicated in Chapter 4 and Chapter 5. In this chapter, some results were completely aligned with both the literature and methodology. These results were referred to the literature and were analysed. For most of the results, there was no literature to compare them with and they were only expected when the methodology was proposed. For these results, logical reasoning was given.

Chapter 7
Conclusion and Future Works

7.1. Conclusion

This thesis proposed the integration of batteries and supercapacitors in an HESS installed on board independently powered trains. This integration was first evaluated and then methods were proposed to optimally size and charge the HESS.

Chapter 2 studied the fundamentals of train performance and traction systems. ESSs and HESSs with different energy storage devices were discussed and the sizing methods to be used for HESSs were studied. This chapter reviewed the literature on power system applications as well as railway applications that have proposed the combination of batteries and supercapacitors and employed sizing methods to optimally size HESSs. This chapter also discussed the optimisation methods that are employed for railway applications and also the economic aspects of on-board systems versus electrification. Based on investigation and analysis of the literature, the detailed objectives for evaluating, sizing and charging an HESS including batteries and supercapacitors were presented in the hypothesis.

In Chapter 3, the methodology was proposed, considering the objectives of the thesis (reduction in energy consumption, cost and CO_2 emissions). Twenty-five scenarios were introduced to compare the sizes of the HESSs and to observe the influence of the energy and power densities of the batteries and supercapacitors on the total size of the HESS. In addition, this phase proposed observing the effect of a change in the battery C-rate on the total size of the HESS. The next phase of this chapter proposed the combination of FFT and Brute Force optimisation

in order to optimally size the HESS, with the objective function of weight and volume minimisation. Finally, two criteria and two scenarios for each criteria were proposed alongside Brute Force optimisation in order to have the battery pack to charge the supercapacitor pack during the journey.

In order to validate the methodology, the proposed approaches were applied to a non-electrified line and a tram line in Chapter 4 and Chapter 5 (Results Chapters), respectively. Chapter 6 (Discussion Chapter) discussed the results achieved in these chapters. It was seen that in both case studies, the combination of batteries and supercapacitors can result in smaller storage system. This approach indicated the effects of both the energy density and power density of the batteries and supercapacitors on the total size of the HESS. The results in this phase also showed that an increase in battery C-rate leads to a decrease in the total size of the HESS, but it makes the battery discharge quicker.

In the mentioned chapters, the results of the sizing phase indicated that the HESS sized using FFT and Brute Force optimisation could not meet both energy and power requirements during the journey when the C-rate constraint was imposed on the energy based-sized pack. Moreover, the results indicated that getting batteries to charge supercapacitors continuously during the journey can lead to the most optimised HESS with the lowest size. At the end of this phase, the battery-only and supercapacitor-only ESSs and all six optimised HESSs were compared together in terms of the final numbers of energy storage devices, the total sizes of the ESSs/HESSs and the total energy consumption and peak power demand after installing the on-board ESSs/HESSs. The results showed that in both case studies, supercapacitor-only ESS was larger than battery-only ESS and all HESSs and was the worst-case regarding the energy consumption increase amongst all eight scenarios. For Case Study One, HESS with C-rate constraint and HESS with SOC<1% charging scenario, and for Case Study Two, the two

mentioned scenarios as well as the HESS with charging in cruising Scenario had bigger sizes than battery-only Scenario. The HESS with SOC<100% charging Scenario was the lightest and resulted in the lowest energy consumption increase.

From the results achieved in Chapter 4 and Chapter 5Chapter 5 and the following discussion in Chapter 6, it can be deduced that the hypothesis proposed at the beginning of this thesis in Section 2.5 is validated. The energy and power densities of both batteries and supercapacitors as well as the battery C-rate have a remarkable influence on the total size of the HESS. The combination of FFT and Brute Force optimisation can be employed to optimally size an HESS; however, because the C-rate constraint is not generally considered in the body of energy-based calculations, there is a risk that the energy based-sized pack is not capable of meeting the required energy and power demand if the typical discharging power of the device is of a great importance. Finally, batteries can be used to charge supercapacitors during the journey.

7.2. Main Contributions

7.2.1. Evaluation of an HESS Including Batteries and Supercapacitors

This phase of the proposed hypothesis indicates the great influence of the energy density and power density of both batteries and supercapacitors on the total size of the HESS. It shows that combining batteries and supercapacitor in an HESS for an independently powered train targeting size minimisation is a more efficient idea compared to battery-only and supercapacitor-only ESSs. This becomes more important when discharging batteries at higher C-rates is not desirable. This approach indicates that due to the strong influence of the energy and power densities of batteries and supercapacitors, if the HESS is not optimally sized, the

total weight and volume can increase to tens of tonnes and a few cubic metres, respectively. Moreover, the HESS not working properly in some scenarios signifies the importance of considering both energy demand and power demand simultaneously when sizing an HESS. Regarding the battery C-rate, although a higher C-rate decreases the total weight and volume of the HESS, it makes the batteries discharge quicker which, in the long term, harms the batteries and shortens their life. Regarding the solution that suggested the battery pack charging the supercapacitor pack, this can be used not only when the supercapacitor pack does not have adequate energy to meet the demands, but also if something goes wrong with some supercapacitor modules during the journey and the supercapacitor pack is not able to perform as expected. This method can be used as a temporary fix until the problem is solved.

7.2.2. Sizing the HESS in the Frequency Domain

This phase of the proposed hypothesis indicates that although the Butterworth filter is a maximally flat filter, overshoots and undershoots that happen in acceleration and braking modes in the high pass- filtered results can make the results differ to what was expected. However, using both low-pass and high-pass filters together, which are complementary filters, solves the problem and the low-pass filter can fully compensate for the overshoots and undershoots in the high pass-filtered results. The approach in this phase shows that the battery pack did not use all its stored energy during the journey. This means that for the Frequency Analysis method using FFT, even if an optimisation method is employed alongside to determine the optimal numbers of battery modules and supercapacitor modules, the battery pack does not use all its stored energy until the end of the journey because it is sized based on the power demand. This phase indicates that should there is a limit in the discharging power of a storage device, the typical discharging power should be considered as a constraint in energy-based calculations in the

procedure of sizing, otherwise there is a risk for the energy based-sized storage system not to be able to perform properly. In this phase, it was seen that if batteries are used as energy suppliers to charge supercapacitors during the journey, the number of supercapacitor module and consequently, the total size of the HESS can decrease.

7.3. Recommendations for Future Research

Based on the studies in this thesis, the following recommendations and research topics are proposed for future studies:

- For sizing the HESS in the frequency domain, other methods such as DFT or Wavelet transform could be utilised and the results could be compared the ones obtained from FFT in this thesis.
- Other types of FIR and IIR filters with different values could be employed to size the HESS in the frequency domain. The results achieved from different filters could be compared and analysed.
- In order to design the filters more accurately when employing Butterworth filters, considerations could be taken into account to remove the overshoots and undershoots in the high-pass filter.
- When using FFT to size an HESS, measures need to be taken to size the battery pack more accurately. Other optimisation methods could be employed alongside the main optimisation problem, or an average of the number of energy-based battery modules and power-based battery modules could be chosen.
- C-rate constraint could be considered in the body of energy-based calculations in the procedure of sizing in order to be ensured that the energy based-sized pack does not discharge higher than its typical C-rate.

- Economic analysis could be carried out to compare the energy consumption and, consequent costs between these scenarios: 1) sizing the battery pack based on the power demand while not discharging batteries at more than their 1 C-rate which leads to an oversized battery pack; 2) sizing the battery pack based on the energy demand and discharging batteries at their highest possible C-rate, which leads to a quicker battery replacement.

Appendix A

Publications

Journal papers below have been submitted and are under review:

[1] D. Servatian, C. Roberts and S. Hillmansen, "Evaluation of using battery and supercapacitor in a HESS for an IPEMU regarding weight and volume," *Part F: Journal of Rail and Rapid Transit.*

[2] D. Servatian, C. Roberts and S. Hillmansen, "Optimal Sizing of an HESS for an IPEMU by Employing Frequency Analysis," *IEEE Transactions on Vehicular Technology*

References

[1] European Parliament, "Reducing CO2 emissions from transport," 2015.

[2] A. M. C. Egenhofer, V. Rizos, A. Behrens, J. Núñez-Ferrer, A. Hassel and M. Elkerbout, "Towards an effective EU framework for road transport and GHG emissions," *CEPS Special Report*, vol. 141, 2016.

[3] CER and UIC, "Rail Transport and Environment (FACTS AND FIGURES)," 2015.

[4] CER and UIC, "Moving Towards Sustainable Mobility: A Strategy for 2030 and Beyond For the European Railway Sector," 2015.

[5] J. Baker. "Goodbye diesel: what does the phase-out mean for UK rail innovation?" https://www.railway-technology.com/features/goodbye-diesel-phase-mean-uk-rail-innovation/ (accessed 16 December, 2019).

[6] S. M. M. Gazafrudi, A. T. Langerudy, E. F. Fuchs, and K. Al-Haddad, "Power Quality Issues in Railway Electrification: A Comprehensive Perspective," *IEEE Transactions on Industrial Electronics*, vol. 62, no. 5, pp. 3081-3090, 2015.

[7] Wikipedia. "Railway electrification in Great Britain." https://en.wikipedia.org/wiki/Railway_electrification_in_Great_Britain (accessed 2 February, 2019).

[8] L. Sharpe, "Rail partners collaborate to test feasibility of battery-powered trains," *Engineering and Technology Magazine*, 2013.

[9] Committee on Climate Change, "Reducing UK emissions: 2018 Progress Report to Parliament," 2018.

[10] Kable. "Independently Powered Electrical Multiple Unit, Essex, United Kingdom." http://www.railway-technology.com/projects/independently-powered-electric-multiple-unit-ipemu-essex/ (accessed 3 February, 2019).

[11] C. Twort and S. Barret, "Batteries included," *IMechE Seminar 3rd December: Rail Technical Strategy: Determining Our Industry's Future,* 2015. London: Networkrail and Bombardier.

[12] M. Ogasa, "Application of Energy Storage Technologies for Electric Railway Vehicles-Examples with Hybrid Electric Railway Vehicles," *IEEJ Transactions on Electrical and Electronic Engineering,* vol. 5, no. 3, pp. 304-311, 2010.

[13] J. Pringle, "OCS-free Light Rail Vehicle Technology." Parsons.

[14] CAF Power and Automation, "On Board Energy Storage System." District of Columbia Department of Transportation.

[15] Railwaygazette. "LFX-300 Ameritram hybrid streetcar unveiled in Charlotte." https://www.railwaygazette.com/news/single-view/view/hybrid-streetcar-unveiled-in-charlotte.html (accessed 5 February, 2019).

[16] S. Heimbach, "Hybrid trams in Doha: For a cleaner ride without overhead lines," 2015. Munich: Siemesn AG.

[17] Railway Technology Magazine. "Birmingham to introduce UK's first battery-operated trams." http://www.railtechnologymagazine.com/Rail-News/birmingham-to-introduce-uks-first-battery-operated-trams- (accessed 4 February, 2019).

[18] L. Cheng, P. Acuna, S. Wei, J. Fletcher, W. Wang, and J. Jiang, "Fast-Swap Charging: An Improved Operation Mode For Catenary-Free Light Rail Networks," *IEEE Transactions on Vehicular Technology*, vol. 67, no. 4, pp. 2912-2920, 2018. IEEE.

[19] Y. Geng, Z. Yang, and F. Lin, "Design and Control for Catenary Charged Light Rail Vehicle Based on Wireless Power Transfer and Hybrid Energy Storage System," *IEEE Transactions on Power Electronics*, 2020. IEEE.

[20] J. Yang, X. Xu, Y. Peng, J. Zhang, and P. Song, "Modeling and optimal energy management strategy for a catenary-battery-ultracapacitor based hybrid tramway," *Energy*, vol. 183, pp. 1123-1135, 2019. Elsevier.

[21] Metro Report. "Midland Metro tram sent for catenary-free conversion." https://www.metro-report.com/news/single-view/view/midland-metro-tram-sent-for-catenary-free-conversion.html (accessed 14 February, 2019).

[22] Railwaygazette. "Battery train enters passenger service." http://www.railwaygazette.com/news/traction-rolling-stock/single-view/view/battery-train-enters-passenger-service.html (accessed 21 July, 2016).

[23] Y. Wang, Z. Yang, F. Lin, X. An, H. Zhou, and X. Fang, "A Hybrid Energy Management Strategy based on Line Prediction and Condition Analysis for the Hybrid Energy Storage System of Tram," *IEEE Transactions on Industry Applications*, 2020. IEEE.

[24] T. Ratniyomchai, P. Tricoli, and S. Hillmansen, "Recent developments and applications of energy storage devices in electrified railways," *IET Electrical Systems in Transportation*, vol. 4, no. 1, pp. 9-20, 2014.

[25] S. de la Torre, A. J. Sanchez-Racero, J. A. Aguado, M. Reyes, and O. Martianez, "Optimal Sizing of Energy Storage for Regenerative Braking in Electric Railway Systems," *IEEE Transactions on Power Systems,* vol. 30, no. 3, pp. 1492-1500, 2015.

[26] J. A. Aguado, A. J. Sanchez Racero, and S. de la Torre, "Optimal Operation of Electric Railways With Renewable Energy and Electric Storage Systems," *IEEE Transactions on Smart Grid,* vol. 9, no. 2, pp. 993-1001, 2018.

[27] V. I. Herrera, H. Gaztanaga, A. Milo, A. Saez-de-Ibarra, I. Etxeberria-Otadui, and T. Nieva, "Optimal Energy Management and Sizing of a Battery--Supercapacitor-Based Light Rail Vehicle With a Multiobjective Approach," *IEEE Transactions on Industry Applications,* vol. 52, no. 4, pp. 3367-3377, 2016.

[28] G. Graber, V. Galdi, V. Calderaro, and A. Piccolo, "Sizing and Energy Management of On-Board Hybrid Energy Storage Systems in Urban Rail Transit," 2016. IEEE.

[29] H. Moghbeli, H. Hajisadeghian, and M. Asadi, "Design and Simulation of Hybrid Electrical Energy Storage (HEES) for Esfahan Urban Railway to Store Regenerative Braking Energy," 2016. IEEE.

[30] L. Cheng, P. Acuna, R. P. Aguilera, J. Jiang, J. Flecther, and C. Baier, "Model Predictive Control for Energy Management of a Hybrid Energy Storage System in Light Rail Vehicles," 2017. IEEE.

[31] V. I. Herrera, H. Gaztanga, A. Milo, T. Nieva, and I. Etxeberria-Otadui, "Optimal Operation Mode Control and Sizing of a Battery-Supercapacitor Based Tramway," presented at the 2015 IEEE Vehicle Power and Propulsion Conference (VPPC), Montreal, QC, Canada, 2015.

[32] Y. Wang, Z. Yang, and F. Lin, "Collaborative optimization of energy management strategy and sizing for the hybrid storage system of tram," presented at the 2017 IEEE Transportation Electrification Conference and Expo, Asia-Pacific (ITEC Asia-Pacific), Harbin, China, 7-10 August 2017, 2017.

[33] R. E. Araujo, R. de Castro, C. Pinto, P. Melo, and D. Freitas, "Combined Sizing and Energy Management in EVs With Batteries and Supercapacitors," *IEEE Transactions on Vehicular Technology*, vol. 63, no. 7, pp. 3062-3076, 2014.

[34] T.Mesbahi, N. Rizoug, P. Bartholomeüs, and P. L. Moigne, "A New Energy Management Strategy of a Battery/Supercapacitor Hybrid Energy Storage System for Electric Vehicular Applications," presented at the 7th IET International Conference on Power Electronics, Machines and Drives (PEMD 2014), Manchester, UK, 8-10 April 2014, 2014.

[35] Y. Liu, W. Du, L. Xiao, H. Wang, S. Bu, and J. Cao, "Sizing a Hybrid Energy Storage System for Maintaining Power Balance of an Isolated System With High Penetration of Wind Generation," *IEEE Transactions on Power Systems*, vol. 31, no. 4, pp. 3267-3275, 2016.

[36] R. Sadoun, N. Rizoug, P. Bartholomeüs, B. Barbedette, and P. L. Moigne, "Influence of the drive cycles on the sizing of hybrid storage system Battery-Supercapacitor supplying an electric vehicle," presented at the IECON 2011 - 37th Annual Conference of the IEEE Industrial Electronics Society, Melbourne, VIC, Australia, 7-10 November 2011, 2011.

[37] R. Sadoun, N. Rizoug, P. Bartholomeüs, B. Barbedette, and P. L. Moigne, "Optimal Sizing of Hybrid Supply for Electric Vehicle Using Li-ion Battery and Supercapacitor,"

presented at the 2011 IEEE Vehicle Power and Propulsion Conference, Chicago, IL, USA, 6-9 September 2011, 2011.

[38] P. Saenger, N. Devillers, K. Deschinkel, M.-C. Pera, R. Couturier, and F. Gustin, "Optimization of Electrical Energy Storage System Sizing for an Accurate Energy Management in an Aircraft," *IEEE Transactions on Vehicular Technology,* vol. 66, no. 7, pp. 5572-5583, 2017.

[39] S. M. Vaca, C. Patsios, and P. Taylor, "Enhancing Frequency Response of Wind Farms using Hybrid Energy Storage Systems," presented at the 2016 IEEE International Conference on Renewable Energy Research and Applications (ICRERA), Birmingham, UK, 20-23 November 2016, 2016.

[40] H. Babazadeh, W. Gao, J. Lin, and L. Cheng, "Sizing of Battery and Supercapacitor in a Hybrid Energy Storage System for Wind Turbines," presented at the PES T&D 2012, Orlando, FL, USA, 7-10 May 2012, 2012.

[41] A. González-Gil, R. Palacin, and P. Batty, "Sustainable urban rail systems: Strategies and technologies for optimal management of regenerative braking energy," *Energy Conversion and Management,* vol. 75, pp. 374-388, 2013.

[42] A. González-Gil, R. Palacin, P. Batty, and J. Powell, "A systems approach to reduce urban rail energy consumption," *Energy Conversion and Management,* vol. 80, p. 16, 2014. Elsevier.

[43] Hitachi, "Energy consumption and traffic volume of railway traffic systems and Hitachi's energy saving efforts," 2012, vol. 61.

Appendix A

[44] Q. Jianwei, S. Pengfei, W. Qingyuan, and F. Xiaoyun, "Optimization for high-speed train operation considering driving strategies and time table," in *CCC*, CCC, 2013, pp. 8167-8171.

[45] S. Hillmansen, "Sustainable traction drives," presented at the 2009 4th IET professional Development Course on Railway Electrification Infrastructure and Systems, London, UK, 2009.

[46] R. J. Hill, "Electric railway traction-Part 1: Electric traction and DC traction motor Drives," *Power Engineering Journal*, pp. 47-56, 1994. IEE.

[47] S. Lu, S. Hillmansen, and T. K. Ho, "Single-Train Trajectory Optimization," *IEEE Transactions on Intelligent Transportation Systems*, vol. 14, no. 2, pp. 743-750, 2013.

[48] M. Toussaint, "Some notes on gradient descent," Berlin, Lecture Notes 2012.

[49] A. Lejeune, R. Chevrier, and J. Rodriguez, "Improving an evolutionary multi-objective approach for optimizing railway energy consumption," *Procedia-Social and Behavioural Sciences*, vol. 48, pp. 3124-3133, 2012.

[50] R. Chevrier, "An Evolutionary Multi-objective Approach for Speed Tuning Optimization with Energy Saving in Railway Management," presented at the 13th IEEE International Conference on Intelligent Transportation Systems, Portugal, 19-22 September 2010, 2010.

[51] N. Zhao, "Railway Traffic Flow Optimization with Differing Control Systems," Doctor of Philosophy, University of Birmingham, Birmingham, 2013.

[52] Y. V. Bokharnikov, A. M. Tobias, and C. Roberts, "Optimal driving strategy for traction energy saving on DC suburban railways," *IET Electric Power Applications,* vol. 1, no. 5, pp. 675-682, 2007.

[53] N. Zhao, C. Roberts, and S. Hillmansen, "A Multiple Train Trajectory Optimization to Minimize Energy Consumption and Delay," *IEEE Transactions on Intelligent Transportation Systems,* vol. 99, pp. 1-10, 2014.

[54] Cecube. "Class 60 001 “steadfast”: First British Freight Locomotive with Creep Adhesion Control " http://www.cecube.co.uk/simulation/simulation.htm (accessed 14 July, 2014).

[55] I. A. Hansen and J. Pachi, "Railway Timetable and Traffic," Hamburg, 2008.

[56] J. Jong and E. Chang, "Models for Estimating Energy Consumption of Electric Trains," *Journal of the Eastern Asia Society for Transportation Studies,* vol. 6, pp. 278-291, 2005.

[57] G. J. Hull, "Simulation of Energy Efficiency Improvements on Commuter Railways," Master of Philosophy in Railway Systems Engineering, Department of Birmingham Centre for Railway Research and Education, University of Birmingham, Birmingham, 2009.

[58] M. Baohua, J. Wenzheng, and C. Shaokuan, "A Computer-aided Multi-train Simulator for Rail Traffic," presented at the IEEE International Conference on Vehicular Electronics and Safety, Beijing, 13-15 December 2007, 2007.

[59] M. Sjoholm, "Benefits of regenerative braking and eco driving for high-speed trains," Master of Science, Royal Institute of Technology (KTH) Stockhom, 2011.

[60] OpenTrack Railway Technology. "Railway Simulation " OpenTrack. http://www.opentrack.ch/opentrack/opentrack_e/opentrack_e.html (accessed 14 July, 2015).

[61] M. Hata, T. Miyauchi, and A. Oda, "Evaluation Technology for Energy Consumption and Traffic Volume on Railway Traffic Systems and Hitachi's Energy-saving Efforts," 2012, vol. 61.

[62] R. D. White, "DC electrification supply system design," presented at the 7th IET Professional Development Course on Railway Electrification Infrastructure and Systems (REIS 2015), London, UK, 8-11 June 2015, 2018.

[63] R. D. White, "AC 25kV 50 Hz electrification supply design," presented at the 7th IET Professional Development Course on Railway Electrification Infrastructure and Systems (REIS 2015), London, UK, 8-11 June 2015, 2018.

[64] Z. Tian, "System Energy Optimisation Strategies for DC Railway Traction Power Networks," Doctor of Philosophy, Department of Electronic, Electrical and Systems Engineering, University of Birmingham, Birmingham, 2017.

[65] R. J. Hill, "Electric railway traction. Part 3. Traction power supplies," *Power Engineering Journal,* vol. 8, no. 6, pp. 275-286, 1994. IET.

[66] F. Schmid and C. J. Goodman, "Electric railway systems in common use," presented at the 6th IET Professional Development Course on Railway Electrification Infrastructure and Systems (REIS 2013), London, UK, 3-6 June 2013, 2013.

[67] C. J. Goodman, "Overview of Electric Railway Systems and the Calculation of Train Performance," presented at the IET Professional Development Course on Electric Traction Systems, London, UK, 2010.

[68] PASADENA Water&Power, "AB 2514 Energy Storage Systems Evaluation," City of Pasadena, 2014.

[69] International Electrotechnical Comission (IEC), "Electrical Energy Storage," IEC, Geneva, 2011.

[70] R. Barrero, X. Tackeon, and J. V. Mierlo, "Stationary or onboard energy storage systems for energy consumption reduction in a metro network," in *IMechE: Rail and Rapid Transit*, 2010, vol. 224, no. F:J, pp. 207-225.

[71] M. Steiner and J. Scholten, "Energy Storage on hoard of DC fed railway vehicles PESC 2004 Conference in Aachen, Germany," presented at the 35lh Annual lEEE Power Electronics Specialists Conference, Aachen, Germany, 2004.

[72] M. Khodaparastan, O. Dutta, and A. Mohamed, "Wayside Energy Storage System for Peak Demand Reduction in Electric Rail Systems," presented at the 2018 IEEE Industry Applications Society Annual Meeting (IAS), Portland, OR, USA, 23-27 September 2018, 2018.

[73] D. G. Vutetakis, "Batteries," in *Digital Avionics Handbook*, C. R. Spitzer, U. Ferrell, and T. Ferrell Eds., Third ed. Washington: CRC Press, 2015, ch. 26, pp. 26-1 - 26-22.

[74] Gears Educational Systems. LLC, "Battery Basics: Research, Test, Measure, Analyse, and Select the Optimal Battery," Hanover Massachusetts, 2009.

Appendix A

[75] A. Joseph and M. Shahidehpour, "Battery Storage Systems in Electric Power Systems," presented at the 2006 IEEE Power Engineering Society General Meeting, Montreal, Quebec, 2006.

[76] K. R. Sullivan. "Battery Basics." www.Autoshop101.com (accessed 12 May, 2016).

[77] MIT Electric Vehicle Team, "A Guide to Understanding Battery Specifications," Massachusetts Institute of Technology, Massachusetts, 2008.

[78] B. J. Davidson, I. Gledenning, and A. B. Hart, "Large-scale electrical energy storage," in *IEE Proceedings A - Physical Science, Measurement and Instrumentation, Management and Education - Reviews*, 1980, vol. 127, no. 6: IEE, pp. 345-385.

[79] R. Bussar, M. Lippert, and G. Bounduelle, "Battery Energy Storage for Smart Grid Applications," Brussels, 2013.

[80] M. T. Lawder, B. Suthar, and P. W. C. Northrop, "Battery Energy Storage System (BESS) and battery Management System (BMS) for Grid-Scale Applications " in *Proceedings of the IEEE*, 2014, vol. 102, no. 6: IEEE, pp. 1014-1030.

[81] S. R. Raman, X. D. Xue, and K. W. E. Cheng, "Review of charge equalization schemes for Li-ion battery and super-capacitor energy storage systems," presented at the 2014 International Conference on Advances in Electronics, Computers and Communications (ICAECC), Bangalore, India, 10-11 October 2014, 2014.

[82] H. Takahashi, T. Kato, and T. Ito, "Energy Storage for Traction Power Supply Systems," 2008, vol. 57.

[83] G. Albright, J. Edie, and S. Al-Hallaj, "A Comparison of Lead Acid to Lithium-ion in Stationary Storage Applications," Chicago, 2012.

[84] tech bulletin, "Isco Nickel-Cadmium and Lead-Acid Battery Comparisons," 1994, vol. 1.

[85] S. M. A. S. Bukhari, J. Maqsood, and M. Q. Baig, "Comparison of Characteristics - Lead Acid, Nickel Based, Lead Crystal and Lithium Based Batteries," presented at the 17th UKSIM-AMSS International Conference on Modelling and Simulation, Cambridge, 21 March 2015, 2015.

[86] N. Garimella and N.-K. C. Nair, "Assessment of Battery Energy Storage Systems for Small-Scale Renewable Energy Integration," presented at the TENCON 2009 - 2009 IEEE Region 10 Conference, Singapore, 23-26 January 2009, 2009.

[87] A. H. Fathima and K. Palanisamy, "Battery energy storage applications in wind integrated systems - A review," presented at the 2014 International Conference on Smart Electric Grid (ISEG), Guntur, 19-20 September 2014, 2014.

[88] Battery University. "BU-205: Types of Lithium-ion." Battery University. https://batteryuniversity.com/learn/article/types_of_lithium_ion (accessed 15 February, 2020).

[89] Y. Miao, P. Hynan, A. v. Jouanne, and A. Yokochi, "Current Li-Ion Battery Technologies in Electric Vehicles and Opportunities for Advancements," *Energies*, vol. 12, no. 6, pp. 1074-1094, 2019.

Appendix A

[90] F. Ciccarelly, "Energy management and control strategies for the use of supercapacitors storage technologies in urban railway traction systems," Doctor of Philosophy, University of Naples “Federico II”, Naples, 2014.

[91] M. S. Halper and J. C. Ellenbogen, "Supercapacitors: A Brief Overview," Virginia, 2006.

[92] R. Barrero, J. V. Mierlo, and X. Tackeon, ") Energy Savings in Public Transport," *IEEE Vehicular Techonology Magazine,* vol. 3, no. 3, pp. 26-36, 2008. IEEE.

[93] Wikipedia. "Supercapacitor." Wikipedia. https://en.wikipedia.org/wiki/Supercapacitor (accessed 21 July, 2016).

[94] S. M. Mousavi, F. Faraji, A. Majazi, and K. Al-Haddad, "A comprehensive review of Flywheel Energy Storage System technology," *Renewable and Sustainable Energy Reviews,* vol. 67, pp. 477-490, 2017. Elsevier.

[95] R. Service. "Suzuki Swift Supercharger kit Powertrain Parts R's Inc." https://www.rsrs.jp/en/powertrain/flywheel.html (accessed 15 February, 2020).

[96] L. Chen, Y. Liu, A. B. Arsoy, P. F. Ribeiro, M. Steurer, and M. R. Iravani, "Detailed modeling of superconducting magnetic energy storage (SMES) system," *IEEE Transactions on Power Delivery*, vol. 21, no. 2, pp. 699-710, 2006. IEEE.

[97] P. Nikolaidis and A. Poullikkas, "A comparative review of electrical energy storage systems for better sustainability," *Journal of Power Technologies,* vol. 97, no. 3, pp. 220-245, 2017. IHE.

[98] N. H. Jafri and S. Gupta, "An overview of Fuel Cells application in transportation," presented at the 2016 IEEE Transportation Electrification Conference and Expo, Asia-Pacific (ITEC Asia-Pacific), Busan, South Korea, 2016.

[99] S. V. M. Guaitolini and J. F.Fardin, "Fuel Cells: History (Short Remind), Principles of Operation, Main Features, and Applications," in *Advances in Renewable Energies and Power Technologies*, vol. 2: Biomass, Fuel Cells, Geothermal Energies, and Smart Grids, S. V.M.Guaitolini and J. F.Fardin Eds. Amsterdam, Oxford, Cambridge: Elsevier, 2018, ch. 3, pp. 123-150.

[100] E. Condliffe, "Duel Cells: Hope for the Future," *Journal of Young Investigators*, vol. 5, no. 7, 2002.

[101] M. Streichfuss and Andreas Schwilling. "Accelerating the decarbonisation of rail." Railwaygazette. https://www.railwaygazette.com/in-depth/accelerating-the-decarbonisation-of-rail/55086.article (accessed 16 February, 2020).

[102] I. Staffell *et al.*, "The role of hydrogen and fuel cells in the global energy system," *Energy and Environmental Science*, no. 2, pp. 463-491, 2019.

[103] Z. B. A. Mat, Madya, Y. B. Kar, S. H. B. A. Hassan, and N. A. B. Talik, "Proton exchange membrane (PEM) and solid oxide (SOFC) fuel cell based vehicles-a review," presented at the 2017 2nd IEEE International Conference on Intelligent Transportation Engineering (ICITE), Singapore, Singapore, 1-3 September 2017, 2017.

[104] L. White and A. Oleksiewicz. "Fuel Cells." publish.illinois.edu. https://publish.illinois.edu/fuel-cells/benefits-and-disadvantages/ (accessed 16 February, 2020).

[105] F. S. Garcia, A. A. Ferreira, and J. A. Pomilio, "Control Strategy for Battery-Ultracapacitor Hybrid Energy Storage System," presented at the Twenty-Fourth Annual Power Electronics Conference and Exposition, Washington, DC, 15-19 February 2009, 2009.

[106] F. Ju, Q. Zhang, and W. Deng, "Review of Structures and Control of Battery-Supercapacitor Hybrid Energy Storage System for Electric Vehicles," presented at the 2014 IEEE International Conference on Automation, Science and Engineering (CASE), Taipei, 18-22 August 2014, 2014.

[107] A. Thakur and L. M. Saini, "A Voltage and State of Charge Control Technique for Battery-Supercapacitor Hybrid Energy Storage System for Standalone Photovoltaic Application," presented at the 2015 International Conference on Energy, Power and Environment: Towards Sustainable Growth (ICEPE), Shillong, India, 12-13 June 2015, 2016.

[108] I. Chotia and S. Chowdhury, "Battery storage and hybrid battery supercapacitor storage systems: A comparative critical review," presented at the 2015 IEEE Innovative Smart Grid Technologies - Asia (ISGT ASIA), Bangkok, Thailand, 3-6 November 2015, 2016.

[109] C. Gao, J. Zhao, J. Wu, and X. Hao, "Optimal Fuzzy Logic Based Energy Management Strategy of Battery/Supercapacitor Hybrid Energy Storage System for Electric Vehicles," presented at the 2016 12th World Congress on Intelligent Control and Automation (WCICA), Guilin, China, 12-15 June 12-15 2016, 2016.

[110] F. Ongaro, S. Saggini, and P. Mattavelli, "Li-Ion Battery-Supercapacitor Hybrid Storage System for a Long Lifetime, Photovoltaic-Based Wireless Sensor Network," *IEEE Transactions on Power Electronics,* vol. 27, no. 9, pp. 3944-3952, 2012.

[111] A. Lahyani, P. Venet, and A. Troudi, "Design of Power Sharing System Between Supercapacitors and Battery in an Uninterruptible Power Supply," presented at the 2011 IEEE 33rd International Telecommunications Energy Conference (INTELEC), Amsterdam, Netherlands, 9-13 October 2011, 2011.

[112] J. P. Trovão, P. G. Pereirinha, and F. Machado, "Hybrid electric excursion ships power supply system based on a multiple energy storage system," *IET Electrical Systems in Transportation*, vol. 6, no. 3, pp. 190-201, 2016. IET.

[113] K. L. D. Koker, G. Crevecoeur, B. Meersman, M. Vantorre, and L. Vandevelde, "Energy Storage System for Off-grid Testing of a Wave Energy Converter," presented at the 2016 IEEE International Energy Conference (ENERGYCON), Leuven, Belgium, 4-8 April 2016, 2016.

[114] S. R., A. Bolonne, and D. P. Chandima, "Sizing an Energy System for Hybrid Li-Ion Battery-Supercapacitor RTG Cranes Based on State Machine Energy Controller," *IEEE Access* vol. 7, pp. 71209 - 71220, 2019. IEEE.

[115] A. Ostadi and M. Kazerani, "A Comparative Analysis of Optimal Sizing of Battery-Only, Ultracapacitor-Only, and Battery–Ultracapacitor Hybrid Energy Storage Systems for a City Bus," *IEEE Transactions on Vehicular Technology*, vol. 64, no. 10, pp. 4449 - 4460, 2014. IEEE.

[116] J. Xiao, L. Bai, F. Li, H. Liang, and C. Wang, "Sizing of Energy Storage and Diesel Generators in an Isolated Microgrid Using Discrete Fourier Transform (DFT)," *IEEE Transactions on Sustainable Energy*, vol. 5, no. 3, pp. 907-916, 2014. IEEE.

[117] Y. Liu, M. Chen, Y. Chen, and L. Chen, "Energy Management of Connected Co-Phase Traction Power System Considering HESS and PV," presented at the 2019 14th IEEE Conference on Industrial Electronics and Applications (ICIEA), Xi'an, China, China, 19-21 June 2019, 2019.

[118] V. I. Herrera, H. Gaztañaga, and T. Nieva, "Optimal Energy Management of a Battery-Supercapacitor based Light Rail Vehicle using Genetic Algorithms," 2015.

[119] A. Ostadi, M. Kazerani, and S.-H. Chen, "Hybrid Energy Storage System (HESS) in vehicular applications: A review on interfacing battery and ultra-capacitor units," presented at the 2013 IEEE Transportation Electrification Conference and Expo (ITEC), Detroit, MI, 16-19 June 2013, 2013.

[120] I. N. Moghaddam and B. Chowdhury, "Optimal sizing of Hybrid Energy Storage Systems to mitigate wind power fluctuations," presented at the 2016 IEEE Power and Energy Society General Meeting (PESGM), Boston, MA, USA, 17-21 July 2016, 2016.

[121] L. Tian, J. Guo, and L. Cheng, "A novel method for energy storage sizing based on time and frequency domain analysis," presented at the 2016 International Conference on Probabilistic Methods Applied to Power Systems (PMAPS), Beijing, China, 16-20 October 2016, 2016.

[122] K. Itani, A. De Bernardinis, Z. Khatir, A. Jammal, and M. Oueidat, "Regenerative Braking Modeling, Control, and Simulation of a Hybrid Energy Storage System for an Electric Vehicle in Extreme Conditions," *IEEE Transactions on Transportation Electrification,* vol. 2, no. 4, pp. 465-479, 2016.

[123] J. Shen, S. Dusmez, and A. Khaligh, "Optimization of Sizing and Battery Cycle Life in Battery/Ultracapacitor Hybrid Energy Storage Systems for Electric Vehicle Applications," *IEEE Transactions on Industrial Informatics,* vol. 10, no. 4, pp. 2112-2121, 2014.

[124] H. H. Eldeeb, A. T. Elsayed, C. R. Lashway, and O. Mohammed, "Hybrid Energy Storage Sizing and Power Splitting Optimization for Plug-In Electric Vehicles," *IEEE Transactions on Industry Applications,* vol. 55, no. 3, pp. 2252 - 2262, 2019. IEEE.

[125] T. yang, "Optimal Sizing of the Hybrid Energy Storage System Aiming at Improving the Penetration of Wind Power," presented at the 2016 IEEE PES Asia-Pacific Power and Energy Engineering Conference (APPEEC), Xi'an, China, 25-28 October 2016, 2016.

[126] S. Sinha and K. K. Mandal, "Optimal Sizing of Battery-Ultracapacitor Hybrid Energy Storage Device in a Standalone Photovoltaic System," presented at the 2018 International Conference On Advances in Communication and Computing Technology (ICACCT), Sangamner, India, 8-9 February 2018, 2018.

[127] S. Sikder, G. Konar, and N. Chakraborty, "Effect of Hybrid Energy Storage on Sizing of PV-Wind Standalone System using Bacteria Foraging Optimization Algorithm," presented at the 2018 20th National Power Systems Conference (NPSC), Tiruchirappalli, India, India, 14-16 December 2018, 2018.

[128] S. Mandal, K. K. Mandal, and M. D. G. Das, "A new improved algorithm for optimal sizing of battery-supercapacitor based hybrid energy storage systems," presented at the 2018 Emerging Trends in Electronic Devices and Computational Techniques (EDCT), Kolkata, India, 8-9 March 2018, 2018.

[129] O. Dutta, M. Saleh, and A. Mohamed, "HESS in DC rail transit system: Optimal sizing and system design," presented at the 2017 IEEE 6th International Conference on Renewable Energy Research and Applications (ICRERA), San Diego, CA, USA, 5-8 November 2017, 2017.

[130] M. Pang, Y. Shi, W. Wang, and X. Yuan, "A method for optimal sizing hybrid energy storage system for smoothing Fluctuations of Wind Power," presented at the 2016 IEEE PES Asia-Pacific Power and Energy Engineering Conference (APPEEC), Xi'an, China, 25-28 October 2016, 2016.

[131] T. Jiang, H. Chen, X. Li, R. Zhang, X. Kou, and F. Li, "Optimal Sizing and Operation Strategy for Hybrid Energy Storage Systems Considering Wind Uncertainty," presented at the 2018 IEEE Power & Energy Society General Meeting (PESGM), Portland, OR, USA, 5-10 Auguest 2018, 2018.

[132] S. Majumder, S. A. Khaparde, A. P. Agalgaonkar, S. Perera, and S. V. K. P. Ciufo, "Hybrid storage system sizing for minimum daily variability injection," presented at the 2019 IEEE Region 10 Symposium (TENSYMP), Kolkata, India, India, 7-9 June 2019, 2020.

[133] A. S. Mir and N. Senroy, "Resource-Mix Variability Mitigation: EWT Based Optimal Sizing/Control of Hybrid Storage System," presented at the 2019 IEEE Power & Energy Society General Meeting (PESGM), Atlanta, GA, USA, USA, 4-8 Auguest 2019, 2020.

[134] R. Yang, D. Qu, Q. Fu, K.-H. Kuo, and D. C. Yu, "An Optimum Design of Hybrid Energy Storage for PV Power Fluctuation Smoothing Based on Frequency Analysis," presented at the 2018 IEEE Power & Energy Society General Meeting (PESGM), Portland, OR, USA, 5-10 Auguest 2018, 2018.

[135] S. Karrari, N. Ludwig, V. Hagenmeyer, and M. Noe, "A Method for Sizing Centralised Energy Storage Systems Using Standard Patterns," presented at the 2019 IEEE Milan PowerTech, Milan, Italy, Italy, 23-27 June 2019, 2019.

[136] A. Tani, M. B. Camara, and B. Dakyo, "Energy Management Based on Frequency Approach for Hybrid Electric Vehicle Applications: Fuel-Cell/Lithium-Battery and Ultracapacitors," *IEEE Transactions on Vehicular Technology*, vol. 61, no. 8, pp. 3375-3386, 2012. IEEE.

[137] L. Sun, K. Feng, C. Chapman, and N. Zhang, "An Adaptive Power-Split Strategy for Battery–Supercapacitor Powertrain—Design, Simulation, and Experiment," *IEEE Transactions on Power Electronics*, vol. 32, no. 12, pp. 9364-9375, 2017. IEEE.

[138] L. Zhang, X. Hu, Z. Wang, F. Sun, J. Deng, and D. G. Dorrell, "Multiobjective Optimal Sizing of Hybrid Energy Storage System for Electric Vehicles," *IEEE Transactions on Vehicular Technology*, vol. 67, no. 2, pp. 1027 - 1035, 2018. IEEE.

[139] R. Liu, L. Xu, F. Liu, Z. Zheng, K. Wang, and Y. Li, "A Novel Architecture of Urban Rail Transit Based on Hybrid Energy Storage Systems Using Droop Control," presented at the 2018 IEEE International Conference on Electrical Systems for Aircraft, Railway, Ship Propulsion and Road Vehicles & International Transpor tation Electrification Conference (ESARS-ITEC), Nottingham, UK, 7-9 November 2018, 2019.

[140] D. O. Akinyele and R. K. Rayudu, "Review of energy storage technologies for sustainable power networks," *Sustainable Energy Technologies and Assessments*, vol. 8, pp. 74-91, 2014. Elsevier.

[141] E. Lai, *Practical Digital Signal Processing for Engineers and Technicians*. Oxford: Elsevier, 2003.

[142] R. Pal, "Comparison of the design of FIR and IIR filters for a given specification and removal of phase distortion from IIR filters," presented at the 2017 International Conference on Advances in Computing, Communication and Control (ICAC3), Mumbai, India, 1-2 December 2017, 2017.

[143] P. Stark, "High-Pass and Low-Pass Filters," in *Electronics 101 Textbook*, 2004, ch. 20, pp. 20-1 - 20-8.

[144] H. Zumbahlen and the engineering staff of Analog Devices, "Analog Filters," in *Linear Circuit Design Handbook*: Elsevier, 2008, ch. 8.

[145] R. C. Burgess, "Filtering of neurophysiologic signals," in *Handbook of Clinical Neurology: basis and Technical Aspects*, vol. 160, L. H. Levin and P. Chauvel Eds., no. 3). Netherlands, United Kingdom, United States: Elsevier, 2019, ch. 4.

[146] D. G. Robertson and J. J. Dowling, "Design and responses of Butterworth and critically damped digital filters," *Journal of Electromyography and Kinesiology*, vol. 13, no. 6, pp. 569-573, 2003. Elsevier.

[147] Green Energy UK. "TIDE Programme." www.greenenergyuk.com (accessed 8 November, 2018).

[148] Z. Chen, J. M. Guerrero, and F. Blaabjerg, "A Review of the State of the Art of Power Electronics for Wind Turbines," *IEE Transactions on Power Electronics*, vol. 24, no. 8, pp. 1859-1875, 2009. IEEE.

[149] P. Jamieson, *Innovation in Wind Turbine Design*, First ed. Chicester: John Wiley and Sons, Ltd, 2011.

[150] G. M. Crawley, *Solar Energy* (World Scientific Series in Current Energy Issues). Singapore: World Scientific, 2016.

[151] Z. Salameh, *Renewable Energy System Design* 1st ed. United States: Elsevier Academic Press, 2014.

[152] A. K. Bansal, R. A. Gupta, and R. Kumar, "Optimization of hybrid PV/wind energy system using Meta Particle Swarm Optimization (MPSO)," presented at the India International Conference on Power Electronics 2010 (IICPE2010), New Delhi, India, 28-30 January 2011, 2011.

[153] R. Belfkira, O. Hajji, C. Nichita, and G. Barakat, "Optimal sizing of stand-alone hybrid wind/PV system with battery storage," presented at the 2007 European Conference on Power Electronics and Applications, Aalborg, Denmark, 2-5 September 2007, 2008.

[154] Altairnano. "24V 70Ah Battery Module." Altairnano. https://altairnano.com/products/battery-module/ (accessed 15 February, 2020).

[155] "125V Heavy Transportation Module." Maxwell. https://www.maxwell.com/images/documents/125V_Module_datasheet.pdf (accessed 15 February, 2020).

[156] Gaia Wind Ltd. "Gaia-Wind 133-11kW Data Sheet." Gaia Wind Ltd. https://www.sustainableenergysystems.co.uk/wp-content/uploads/2015/06/Gaia-Wind-133-11kW-Datasheet.pdf (accessed 11 July, 2018).

Appendix A

[157] LG Ltd. "NeON® R Prime." LG. https://www.lg.com/uk/business/neon-r-prime (accessed 16 July, 2018).

[158] M. Stables, "Small wind turbine feasibility study," Burscough Renewable Energy Community Group, UK, 5 September 2014.

[159] N. U. Church, "Wind Assessment Report Supplement ", Hanska, 2018.

[160] The Energy Manager's Accosication, "Solar PV: Buyer's Guide ", London, 2018.

[161] National Statistics, Department for Business, Energy & Industrial Strategy, " Digest of United Kingdom Energy Statistics 2019 ", London, 2018.

[162] X. Fu, D. Yu and J. Zhou, ey al., "Inorganic and organic hybrid solid electrolytes for lithium-ion batteries," *CrystEngComm*, vol. 23, 2016.

[163] M. Allan. "Hydrogen cars: How the fuel cell works, where the UK's filling stations are and how expensive they are to run" https://www.sussexexpress.co.uk/lifestyle/cars/hydrogen-cars-how-fuel-cell-works-where-uks-filling-stations-are-and-how-expensive-they-are-run-1386285 (accessed 19 August, 2020).

[164] D. Servatian "Optimisation of Railway Vehicle Trajectories to Reduce Energy Consumption" Master of Science, University of Birmingham, Birmingham, 2015.

[165] C. Schellenberg, J. Lohan and L. Dimache, "Comparison of metaheuristic optimisation methods for grid-edge technology that leverages heat pumps and thermal energy storage, " *Renewable and Sustainable Energy Reviews*, Vol. 131, pp. 1-13, 2020. Elsevier.

[166] S. Vadi , S, Padmanaban and R. Bayindir 3 et al., "A Review on Optimization and Control Methods Used to Provide Transient Stability in Microgrids, " *energies*, pp. 1-20, 2019. MDPI.

[167] P.M. Fernandez, I.V. Sanchís and V. Yepes, et al. "A review of modelling and optimisation methods applied to railways energy consumption, " *Journal of Cleaner Production*, Vol. 222, pp. 153-162, 2019. Elsevier.

[168] Y. Cui, Z. Geng and Q. Zhu, et al. "Review: Multi-objective optimization methods and application in energy saving, " *Energy*, Vol. 125, pp. 681-704, 2017. Elsevier.

[169] D. Meegahawatte, "A Design Method For Specifying Power Sources for Hybrid Power Systems," Doctor of Philosophy, Department of Electronic, Electrical and Systems Engineering, University of Birmingham, Birmingham, 2010.

[170] B. Fan, "Railway Traffic Rescheduling Approaches to Minimise Delays in Disturbed Conditions," Doctor of Philosophy, Department of Electronic, Electrical and Systems Engineering, University of Birmingham, Birmingham, 2012.

[171] Network Rail, "Tration Decarbonisation Network Strategy: Interim Programme Business Case," UK: Network Rail, 31 July 2020.

[172] RSSB, "T1145 - Options for Traction Energy Decarbonisation in Rail," UK: RSSB, 12 June 2019.

[173] RSSB, "Future Costs for Hydrogen and Battery Power for Traction," UK: RSSB, August 2020.

[174] T. Harþarika, J. Bockoa and K. Masláková, "Frequency analysis of acoustic signal using the Fast Fourier Transformation in MATLAB," *Procedia Engineering,* Vol. 48, pp. 199-204, 2012. Elsevier.

[175] B. Guo, S. Song and A. Ghalambor, et al., "An Introduction to Condition-Based Maintenance, " In *Offshore Pipelines, Design, Installation, and Maintenance,* pp. 257-297, 2014. Elsevier.

[176] J. Roberts, "Signals and Systems, Analysis Using Transform Methods and MATLAB", 2003. Singapore: Mc-Graw Hill Education.